Myeloid cell regulation by CD200 signalling in atherosclerosis

Christina Kassiteridi

Kennedy Institute of Rheumatology

&

Wolfson College



A thesis submitted for the degree of Doctor of Philosophy in
Molecular and Cellular Medicine

University of Oxford

Michaelmas Term 2016

Declaration

This thesis comprises results produced solely by myself. Some studies were carried out with the help of members from the laboratory and are indicated in the Materials and Methods section. The work was carried out at the Kennedy Institute of Rheumatology, Nuffield Department of Orthopaedics, Rheumatology and Musculoskeletal Sciences, University of Oxford.

Abstract

Myeloid cell regulation by CD200-CD200R signalling

Christina Kassiteridi

Kennedy Institute of Rheumatology, University of Oxford
Submitted for the degree of D.Phil in Molecular and Cellular Medicine
Michaelmas Term 2016

Atherosclerosis, the major risk factor for cardiovascular disease and the leading cause of death worldwide, is a multifactorial chronic inflammatory disease. Deletion of CD200 *in vivo* increases myeloid cell numbers and activation resulting in enhanced susceptibility to autoimmune diseases and infection. However, the importance of CD200 in atherosclerosis development is still unknown. To understand the role of CD200 signalling, both the effect of CD200 deletion and provision were assessed in a murine model of atherosclerosis.

Firstly, the role of CD200R ligation was examined in a murine model of carotid injury. Apolipoprotein E deficient (ApoE -/-) mice underwent surgery for placement of a perivascular collar and were treated with 10mg/kg of a CD200-Fc fusion protein. Three weeks post injury, carotid arteries were removed and neointima formation was assessed. CD200-Fc fusion protein treatment attenuated neointima development and increased M2 anti-inflammatory macrophage accumulation.

Secondly, CD200-deficient (CD200-/-) mice were crossed with ApoE-/- mice. CD200 deficiency accelerated advanced atherosclerotic lesion formation in the aortic roots, as shown by the morphometric measurement of aortic root atherosclerotic lesion development. Moreover, CD200 regulated hypercholesterolemia-induced monocytosis, as its deletion increased the numbers of CCR2-expressing Ly6C^{hi} monocytes in the blood and in the plaques. To further understand the mechanism of CD200-mediated monocytosis in the plaques, the role of the haematopoietic system was assessed by flow cytometry and *in vitro* culture systems. CD200 deficiency was shown to regulate GM-CSF-mediated myelopoiesis. CD200 does not only affect myeloid cells in the blood, but also in the spleen and in the aorta. In the plaques, CD200 deficiency skewed the phenotype of macrophages towards iNOS+CD86+MHCII+ inflammatory macrophages and enhanced CD4+ T cell activation. Therefore, CD200 regulates macrophage phenotypes and possibly their

antigen presenting abilities at advanced stages of atherosclerosis. Finally, a highly multiparametric technique (CyTOF) enabled the detection of CD200 predominantly in stromal cells in the plaques suggesting a key role for stromal-immune cell interactions in CD200-mediated athero-protection.

Collectively, these findings identify a new role for CD200 expression in modulating myeloid cell function and phenotype in advanced stages of atherosclerosis.

Acknowledgements

I would like to thank all the people who helped me during my DPhil studies. First and foremost, I would like to thank my primary supervisor, Prof. Claudia Monaco, for giving me the opportunity to develop this research project. I really appreciate her guidance and counsel, and especially her continuous enthusiasm about science, which has motivated me during the course of this project. I am also grateful for having had the opportunity to communicate my work at major international conferences, where I had the opportunity to meet other experts in this field and broaden my horizons. I would also like to thank my secondary supervisor, Prof. Keith Channon, for his valuable advice during the laboratory meetings and his significant scientific input during my studies. I am very grateful to Dr. Jennifer Cole for teaching me various techniques in the laboratory, and for supervising me particularly during the first years of my studies. I would like to acknowledge Michael Goddard for teaching me to work with laboratory animals and assisting me in my experiments. To Inhye Park, Natacha Zanin, Trish Green, and Andreas Edsfeldt and everyone in the Monaco group for their support and assistance but most importantly for being such great colleagues and friends. I would also like to acknowledge Parisa Amjadi and Jonathan Webber for their help in flow cytometry; David Ahern, Monica Rodriguez Mercado and Dina Danso-Abeam for assisting me with CyTOF; Dr Serafim Kyriakidis for his advice and support; everyone in the Kennedy Institute of Rheumatology for their assistance and support over the last 4 years.

Finally, I would like to give a big thank you to my family, which includes my parents, my brother and my fiancé, Paris. Were it not for their love and unfailing support this journey would not have been possible.

Table of Contents

Declaration ..... **i**

Abstract ..... **ii**

Acknowledgements ..... **iv**

List of Figures ..... **viii**

List of Tables ..... **x**

List of abbreviations ..... **xi**

Chapter 1 Introduction **1**

1.1 Atherosclerosis **2**

1.1.1 The normal arterial wall 4

1.1.2 The role of stromal cells in the normal vessel wall and in atherosclerosis 4

1.1.3 Extracellular matrix in arterial physiology and disease 6

1.1.4 Histological lesion classification 7

1.1.5 Lipid accumulation in atherosclerosis 10

1.2 Murine models of atherosclerosis **12**

1.2.1. ApoE-/- mice 12

1.2.2 LDLR-/- mice 13

1.2.3 Murine models of neointima formation 13

1.4 The inflammatory nature of atherosclerosis **14**

1.4.1 Innate immune system 16

1.4.2 Adaptive immune system 17

1.5 Myeloid cells **20**

1.5.1 Ontogeny 21

1.5.2 Nomenclature 24

1.6 The role of myeloid cells in atherosclerosis **28**

1.6.1 Monocyte recruitment in atherosclerosis 28

1.6.2 Inflammatory macrophages in atherosclerosis 29

1.6.3 Arterial DC subsets 31

1.6.4 Neutrophils in atherosclerosis 32

1.7 Myeloid activating and inhibitory receptors **32**

1.7.1 ITIM-bearing inhibitory receptors 33

1.7.2 ITAM- bearing activating receptors 35

1.8 CD200-CD200R: a myeloid inhibitory regulator **36**

1.8.1 Molecular analysis of the CD200-CD200R pathway: unraveling a cell-cell interaction 36

1.8.2 The CD200R family: Why do multiple isoforms exist? 38

1.8.3 CD200-mediated immunoregulation: Evidence from disease models 38

1.9 Aims and rationale **42**

Chapter 2 Materials and Methods **43**

2.1 Reagents **44**

2.1.1 Primary antibodies 44

2.1.2 Secondary antibodies 48

2.1.3 List of buffers and solutions 48

2.2 Maintenance of animals **49**

2.2.1. Generation of ApoE-/-CD200-/- mice 49

2.2.2 Genotyping 51

2.2.3 Perivascular collar-induced injury 53
2.3 Tissue preparation 54
2.4 Histology 56
2.4.1 Oil Red O staining 56
2.4.2 Carotid lesion quantification: Elastin Van Gieson staining 56
2.4.3 Immunohistochemistry 57
2.4.4 Haematoxylin and eosin staining 59
2.4.5 Masson Trichrome staining 60
2.5 Image analysis and quantification 60
2.6 Flow cytometry of murine tissues 61
2.6.1 Optimising conditions for enzymatic digestion of mouse aorta 62
2.7 Single-cell mass cytometry (CyTOF) 66
2.7.1 Antibody conjugation 66
2.7.2 Mass cytometry staining 67
2.8 Analysis of murine serum cholesterol 68
2.9 *In vitro* cell culture 68
2.9.1 *In vitro* differentiation and stimulation of bone-marrow derived myeloid cells 68
2.10 Statistical analysis 69

Chapter 3 The effects of a CD200-Fc fusion protein in atherosclerosis 70
3.1 Introduction 71
3.2 Results 72
3.2.1 CD200-Fc treatment reduces neointima formation in a perivascular collar model 72
3.2.2 CD200-Fc treatment increases lesional M2 macrophage accumulation 74
3.2.3 CD200-Fc treatment does not affect CD11c expression 78
3.2.4 CD200-Fc treatment does not affect cellular proliferation, necrosis or collagen content but increases lipid content 79
3.2.5 CD200-Fc treatment does not affect myeloid populations in the aorta but increases F4/80+ macrophages in the spleen 86
3.2.6 CD200R treatment inhibits IFN-γ but increases LPS or IL-4/IL-13 mediated IL-6 production in M-CSF treated myeloid cells *in vitro* 89
3.3 Discussion 91

Chapter 4 CD200 deficiency promotes the development of advanced atherosclerotic lesions 94
4.1 Introduction 95
4.2 Results 96
4.2.1 CD200 deficiency does not affect the body weight of ApoE-/-mice 96
4.2.2 CD200 deficiency does not affect serum cholesterol levels 96
4.2.3 CD200 deficiency increases the lesion size in 27-week old ApoE-/- mice 97
4.2.4 CD200 deficiency affects lesion phenotype in 27-week old ApoE-/- mice 99
4.2.5 CD200 deficiency enhances arterial myeloid cell accumulation in 27-week old ApoE-/- mice 102
4.2.6 The effect of CD200 deficiency in secondary organs 110
4.2.7 CD200 deficiency increases inflammatory blood monocytes in 27-week old ApoE-/- mice 113
4.3 Discussion 117

Chapter 5 High dimensional analysis unravels a role for CD200 in athero-inflammation 121

5.1 Introduction **122**
5.2 Results **123**
5.2.1 Immune cell composition in the aorta of ApoE-/-CD200-/- mice 123
5.2.2 Proliferating arterial iNOS+ macrophages are increased in the aorta of ApoE-/-CD200-/- mice 127
5.2.3 CD4+T cells are expanded in the aorta of ApoE-/-CD200-/- mice 130
5.2.4 CD200 deficiency increases arterial CCR2+ monocytes in ApoE-/- mice 132
5.2.5 CD200 deficiency affects immune cells in secondary organs 133
5.2.6 CD200 and CD200R expression *in vivo* and *in vitro* 135
5.3 Discussion **140**

Chapter 6 CD200 regulates GM-CSF mediated myelopoiesis during atherosclerosis **144**
6.2 Results **147**
6.2.1 CD200 deficiency affects macrophage regulation in response to GM-CSF *in vitro* 147
6.2.2 CD200 deficiency significantly expands HSCs in the BM of ApoE-/- mice 155
6.3 Discussion **163**

Chapter 7 Final discussion **168**
7.1 Hypothesis of the study **169**
7.2 Key findings of the study **170**
7.2.1 CD200 mediates hypercholesterolemia-induced monocytosis 172
7.2.2 CD200 regulates the balance of inflammatory M1-M2 macrophages 175
7.2.3 CD200-CD200R: A role for stromal-immune cell interactions in atherosclerosis 177
7.3 Final conclusions **178**
References **180**
Appendices **204**

List of Figures

Figure 1.1 Atherosclerotic plaques (white shading) develop in distinct locations in the arterial vasculature. 3
Figure 1.2 Classification of plaque progression according to (Stary et al., 1995). 9
Figure 1.3 The progression of atherosclerosis. 16
Figure 1.4 Innate and adaptive immunity. 20
Figure 1.5 Hierarchical structure of HSCs. 24
Figure 1.6 Classification of myeloid cells. 27
Figure 2.1 Breeding strategy to generate ApoE-/-CD200-/- mice. 50
Figure 2.2 Screening for ApoE and CD200 deficiency. 52
Figure 2.3 Surgical placement of a perivascular collar on a mouse carotid. 54
Figure 2.4 Optimisation of staining with an antibody against CD200. 58
Figure 2.5 Optimisation of staining with antibodies against CD200R, CD11c and ki-67 59
Figure 2.6 Addition of elastase to the standard enzyme mix does not affect leucocyte yield or viability. 64
Figure 2.7 Halving the elastase concentration does not affect cell viability or cell yield 65
Figure 2.8 One hour incubation of murine aortas with an enzyme cocktail gives optimal cell yield and viability. 66
Figure 3.1 The weights of the ApoE-/- mice treated with IgG control or CD200-Fc during the three-week treatment. 73
Figure 3.2 CD200-Fc fusion protein treatment inhibits collar induced carotid atherosclerosis in ApoE-/- mice. 74
Figure 3.3 CD200-Fc fusion protein increases lesional CD68+ macrophage content in a perivascular carotid collar model in ApoE-/- mice. 75
Figure 3.4 CD200-Fc fusion protein treatment increases lesional CD206+ macrophage content in a perivascular carotid collar injury model in ApoE-/- mice. 76
Figure 3.5 CD200-Fc fusion protein treatment does not significantly affect the lesional iNOS+ macrophage content in arterial injury. 77
Figure 3.6 CD200-Fc fusion protein treatment does not significantly affect the lesional CD11c expression. 78
Figure 3.7 CD200-Fc fusion protein treatment does not significantly affect the necrosis in a perivascular carotid collar injury model in ApoE-/- mice. 80
Figure 3.8 CD200-Fc fusion protein treatment does not affect the collagen content within the lesions in a perivascular carotid collar model in ApoE-/- mice. 81
Figure 3.9 CD200-Fc fusion protein treatment affects the lipid content within the lesions in a perivascular carotid collar model in ApoE-/- mice. 82
Figure 3.10 CD200-Fc fusion protein treatment does not significantly affect cellular ki-67+ content within the lesions in a perivascular carotid collar model in ApoE-/- mice. 83
Figure 3.11 CD200-Fc fusion protein treatment does not significantly affect lesional CD200+ content in a perivascular carotid collar model in ApoE-/- mice. 84
Figure 3.12 CD200-Fc fusion protein treatment does not significantly affect the lesional CD200R+ cell content in a perivascular carotid collar model in ApoE-/- mice. 85
Figure 3.13 Gating strategy applied to detect myeloid cells in the spleen of CD200-Fc-treated ApoE-/- mice. 87

Figure 3.14 CD200-Fc treatment increases the number of macrophages in the spleen but has no effect on myeloid cells in the aorta and lymph nodes in ApoE-/- mice. 88
Figure 3.15 IL-6 secretion in GM-CSF and M-CSF treated myeloid cells following an agonistic CD200R antibody treatment. 90
Figure 4.1 Weights of male ApoE-/- and ApoE-/-CD200-/- mice at 15, 20 or 27 weeks of age on chow diet. 96
Figure 4.2 CD200 deficiency increases atherogenesis in 27-week old ApoE-/- mice. 99
Figure 4.3 CD200 deficiency increases lesional macrophage infiltration in 27-week old ApoE-/- mice. 100
Figure 4.4 CD200 deficiency increases necrotic core size in 27-week old ApoE-/- mice. 101
Figure 4.5 CD200 deficiency decreases SMC content within aortic root lesions in 27-week old ApoE-/- mice. 102
Figure 4.6 Gating strategy for macrophages and DCs in the aorta of ApoE-/- and ApoE-/-CD200-/- mice at 27 weeks of age. 105
Figure 4.7 Increased numbers of F4/80+ macrophages and $CD11c^{+}MHCII^{+}$ DCs in the aorta of ApoE-/-CD200-/- mice. 106
Figure 4.8 CD103+ DCs are increased in the aorta of ApoE-/-CD200-/- mice. 107
Figure 4.9 Splenic macrophages in ApoE-/- and ApoE-/-CD200-/- mice. 112
Figure 4.10 Lymph node macrophages in ApoE-/- and ApoE-/-CD200-/- mice. 113
Figure 4.11 The numbers of monocytes and neutrophils in the blood and BM of ApoE-/- and ApoE-/-CD200-/- mice. 115
Figure 4.12 Monocytes and neutrophils in the blood of ApoE-/- and ApoE-/-CD200-/- mice. 116
Figure 5.1 Schematic diagram of experimental design showing the time-course of low- and high-cholesterol feeding in ApoE-/- mice. 122
Figure 5.2 Immune and stromal cell composition of the aorta of ApoE-/- and ApoE-/-CD200-/- mice. 125
Figure 5.3 Macrophage subsets within the aortic wall of ApoE-/- and ApoE-/-CD200-/- mice. 130
Figure 5.4 T cell subsets within the aortic wall of ApoE-/- and ApoE-/-CD200-/- mice. 131
Figure 5.5 CCR2+ and CX3CR1+ monocytes within the aortic wall of ApoE-/- and ApoE-/-CD200-/- mice. 133
Figure 5.6 Immune cell composition of the spleen and lymph nodes of ApoE-/- and ApoE-/-CD200-/- mice. 135
Figure 5.7 The expression of CD200 and CD200R *in vivo* and *in vitro*. 138
Figure 6.1 CD200 deficiency affects macrophage regulation *in vitro*. 152
Figure 6.2 CD200R expression in *in vitro* differentiated myeloid populations in ApoE-/- and ApoE-/-CD200-/- mice. 154
Figure 6.3 Stimulation with agonistic CD200R antibody does not affect pSTAT6 expression *in vitro*. 155
Figure 6.4 Gating strategy for HSCs progenitors in the BM of ApoE-/- mice. 156
Figure 6.5 CD200 deficiency increases HSCs in the BM but not in the spleen of ApoE-/- mice. 159
Figure 6.6 CD200 and CD200R expression on BM HSCs in ApoE-/- mice. 160
Figure 6.7 The effect of CD200 deficiency on monocytes and neutrophils in the BM and blood of ApoE-/- mice. 162
Figure 7.1 The proposed model of CD200 in myeloid function in advanced atherosclerotic lesions. 179

List of Tables

Table 1-1 Macrophage subsets in atherosclerosis.....30
Table 1-2 Arterial DC subsets.....32
Table 1-3 Manipulation of the CD200-CD200R pathway in mouse disease models. .40
Table 2-1 Primary antibodies used in experiments.....44
Table 2-2 Secondary antibodies and labels used in experiments.....48
Table 2-3 Buffers and solutions used in experiments.....48
Table 2-4 Sequences of primers used for genotyping.....52
Table 2-5 PCR master mixes for genotyping ApoE and CD200.....52
Table 2-6 Parameters for reverse transcription PCR of genotyping assays.....53
Table 2-7 Biologic reagents used for the fusion protein experiments.....54
Table 2-8 Halving the concentration of collagenase XI does not affect the effect of elastase on cell viability and yield.....65
Table 4-1 Serum cholesterol levels in ApoE-/- and ApoE-/-CD200-/- mice at 27 weeks of age.....97
Table 4-2 The number of macrophages, cDCs, CD11b+cDCs and CD103+cDCs expressed as percentages of CD45+ cells and absolute numbers, in the aorta of ApoE-/- and ApoE-/-CD200-/- mice at 15, 20 and 27 weeks of age.....108
Table 4-3 The numbers of arterial macrophages, characterised by additional markers (such as CD64 and MerTK) and expressed as percentages of single cells, CD45+ cells and absolute numbers in the aorta of ApoE-/- and ApoE-/-CD200-/- mice at 27 weeks of age.....109
Table 4-4 Numbers of macrophages in the spleen and lymph nodes, expressed as percentages of CD45+ cells and as absolute numbers of ApoE-/- and ApoE-/-CD200-/- mice at 15, 20 and 27 weeks.....111
Table 4-5 The numbers of monocytes and neutrophils in the blood and BM of ApoE-/- and ApoE-/-CD200-/- mice at 15, 20 and 27 weeks of age.....114
Table 5-1 The numbers of ECs, SMCs, T cells, B cells, NK cells, mast cells, basophils, pDCs, monocytes, neutrophils, macrophages and cDCs in the aortic wall of ApoE-/- and ApoE-/-CD200-/- mice.....126
Table 5-2 CD200 expression (mean) on T cells, B cells, NK cells, neutrophils, monocytes, macrophages/DCs, pDCs, SMCs and ECs in the aorta, spleen and lymph nodes in ApoE-/- mice.....136
Table 5-3 CD200R expression (mean) on T cells, B cells, NK cells, neutrophils, monocytes, macrophages/DCs, pDCs, SMCs and ECs in the aorta, spleen and lymph nodes in ApoE-/- mice.....137
Table 6-1 Numbers of HSCs, including LSKs, MPPs, LT-HSCs, GMPs, CMPs and MEPs, expressed as percentages of single cells and absolute numbers, in the BM of ApoE-/- and ApoE-/-CD200-/- mice fed a HFD for 12 weeks.....157

List of abbreviations

ABC	Adenosine triphosphate-binding cassette t
ABCG-1	Adenosine triphosphate- binding cassette subfamily G member 1
ANOVA	Analysis of variance
ApoB	Apolipoprotein B
ApoE	Apolipoprotein E
ATM	Adipose tissue macrophage
BM	Bone marrow
BSA	Bovine serum albumin
CAD	Coronary artery disease
CCR	C-C chemokine receptor
CD	Cluster of differentiation
cDC	Classical/conventional dendritic cell
CDP	Common dendritic cell precursor
CIA	Collagen induced arthritis
CLP	Common lymphoid progenitor
CLR	C-type lectin receptor
cMoP	Common monocyte progenitor
CNS	Central nervous system
CTD	Connective tissue diseases
CX3CL	C-X3—C motif chemokine ligand
CX3CR	C-X3-C- motif chemokine receptor
DAMP	Damage associated molecular pattern
DAP12	DNAX activation protein of 12kDa
DC	Dendritic cell
DC-SIGN	Dendritic cell-specific intercellular adhesion molecule-3-grabbing non-integrin
DCIR	Dendritic cell immunoreceptor
Dok	Downstream of tyrosine kinase
EC	Endothelial cell
ECM	Extracellular matrix
EEL	External elastic lamina
EMP	Erythro-myeloid progenitors
ERK	Extracellular signal–regulated kinase
FcεRI	Fc epsilon receptor
Flt3	Fms related tyrosine kinase 3
G-CSF	Granulocyte-colony stimulating factor
GAG	Glycosaminoglycans
GM-CSF	Granulocyte macrophage colony stimulating factor
HDL	High -density lipoprotein
HFD	High fat diet
HLA	Human leukocyte antigen
HMGB	High mobility group box
HSC	Haematopoietic stem cell
ICAM-1	Intercellular adhesion molecule 1
IEL	Internal elastic lamina
IFN	Interferon

IgSR	Immunoglobulin superfamily receptor
IL	Interleukin
IMR	Intima/media ratio
iNOS	Inducible nitric oxide synthase
IRF	Interferon regulatory factor
ITAM	Immunoreceptor tyrosine-based activation motif
ITIM	Immunoreceptor tyrosine-based inhibition motif
JNK	C-Jun N-terminal kinase
KLF	Krüppel-like factor
LDL	Low density lipoprotein
LDLR	Low density lipoprotein receptor
LPS	Lipopolysaccharide
LT-HSC	Long term haematopoietic stem cell
Ly6C	Lymphocyte antigen 6C
MAPK	Mitogen-activated protein kinase
MCP	Monocyte chemoattractant protein
MCSF	Macrophage-colony stimulating factor
MDP	Macrophage-dendritic cell precursor
MEF	Mouse embryonic fibroblast
MEK	MAPK/Erk kinase
MEP	Megakaryocyte-erythrocyte progenitor
MerTK	C-mer proto-oncogene tyrosine kinase
MHC	Major histocompatibility complex
MIF	Macrophage migration inhibitory factor
mmLDL	Minimally modified low density lipoprotein
MMP	Matrix metalloproteinase
mo-DC	Monocyte-derived dendritic cell
MPP	Multipotent progenitor
MPS	Mononuclear phagocyte system
MyD88	Myeloid differentiation primary-response protein 88
NF- κB	Nuclear factor kappa light polypeptide gene enhancer in B cells
NK	Natural killer
NKT	Natural killer T cell
NO	Nitric oxide
ORO	Oil Red O
oxLDL	Oxidised low density lipoprotein
PALN	Para-aortic lymph node
PAMP	Pathogen associated molecular pattern
PBS	Phosphate buffered saline
PCR	Polymerase chain reaction
pDC	Plasmacytoid dendritic cell
PDCA-1	Plasmacytoid dendritic cell antigen 1
PDGF	Platelet derived growth factor
PECAM-1	Platelet endothelial cell adhesion molecule 1
PFA	Paraformaldehyde
PI3K	Phosphoinositide 3-kinase
PPAR	Peroxisome proliferator-activated receptor
PRR	Pattern recognition receptor
RA	Rheumatoid arthritis
RAGE	Receptor for advanced glycation endproducts

RBC	Red blood cell
RNA	Ribonucleic acid
ROR	Retinoid-related orphan receptor
SEM	Standard error of the mean
SHIP	SH2-domain-containing inositol polyphosphate 5' phosphatase
SHP	Src homology region 2 domain-containing phosphatase
Siglec	Sialic acid binding immunoglobulin-like lectin
SILN	Subiliac lymph node
SLE	Systemic lupus erythematous
SMC	Smooth muscle cell
SOCS	Suppressor of cytokine signalling
STAT	Signal transducers and activators of transcription
TCFA	Thin-cap fibroatheroma
TE	Toxoplasma encephalitis
TGF	Transforming growth factor
Th	T helper cell
Tip-DC	TNF-iNOS-producing DCs
TLR	Toll-like receptor
TNF	Tumour necrosis factor
Treg	Regulatory T cell
TREM	Triggering receptor expressed on myeloid cells
VCAM-1	Vascular cell adhesion molecule 1
VEGF	Vascular endothelial growth factor

Chapter 1 Introduction

Chapter 1: Introduction

1.1 Atherosclerosis

Atherosclerosis derives its name from the Greek words “athere’ meaning gruel and “sclerosis” meaning hardening. It is a multi-factorial inflammatory disease that is characterised by the interplay of lipids, inflammatory cells and connective tissue components and it is the underlying cause of heart attacks, stroke and death worldwide (Wong, 2014).

The prevalence of atherosclerosis increases with age. At the age of 65 years and older, atherosclerotic plaques in the carotid arteries are detectable in 75% of men and 62% of women (O'Leary et al., 1992). However, fatty streaks have also been detected in infants and young adults (Imakita et al., 2001).

Focal development of lesions has been observed at branch points or curvatures, where blood flow is disturbed and therefore exerts proatherogenic low or oscillatory shear stress (Caro et al., 1971, Zarins et al., 1983). Non laminar flow promotes changes in endothelial regulation, leucocyte adhesion and cytoskeletal arrangements, and ultimately leads to the formation of an atherosclerotic plaque (Cheng et al., 2006). Atherosclerotic plaques can form in several locations of the arterial tree including: the carotid arteries, the coronary arteries, the aortic artery, the iliac arteries and the femoral arteries (Figure 1.1). The location of the lesion contributes to distinct clinical manifestations of the disease. For example, plaques in coronary arteries lead to myocardial infarction or ischemia, plaques in carotid arteries lead to a stroke while plaques in iliac or femoral arteries result in critical limb ischemia (Bentzon et al.,

2014).

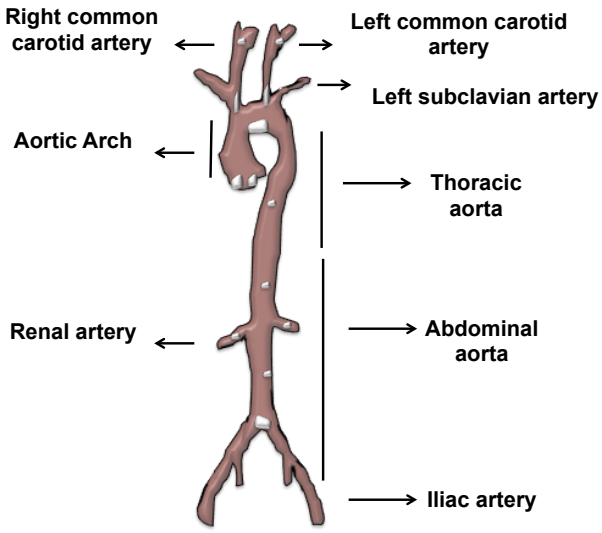


Figure 1.1 Atherosclerotic plaques (white shading) develop in distinct locations in the arterial vasculature.

Several major risk factors are linked to cardiovascular disease. These include hypercholesterolemia, hypertension, insulin resistance, obesity smoking and family history (Wong, 2014). Additionally, increased incidence of cardiovascular disease associates with patients suffering from inflammatory connective tissue diseases (CTD) like systemic lupus erythematosus (SLE) and rheumatoid arthritis (RA) (Alenghat, 2016). Examples of current treatments for cardiovascular disease that confer a prognostic benefit include cholesterol-lowering drugs (statins), aspirin that is used for platelet inhibition and β-blockers, which are used as antihypertensive agents and for myocardial protection from ischemia.

1.1.1 The normal arterial wall

Normal arteries (except for the pulmonary artery) function to supply the organs with oxygen. Normal arteries consist of three layers: the intima, media and adventitia.

a) The **intima** is the innermost layer of the vessel wall, which mainly consists of endothelial cells (ECs) and is rich in laminin, fibronectin, type IV collagen, glycoproteins and proteoglycans. In humans, the intima of the healthy artery is mainly populated by smooth muscle cells (SMCs) (Lum and Malik, 1994).

b) The **media** is separated from the intima by an internal elastic lamina (IEL) and mainly contains SMCs, fibronectin, proteoglycans and type I/III/V collagens (Wolinsky and Glagov, 1967).

c) The **adventitia** is the outermost layer of the vessel wall and is separated from the media by an external elastic lamina (EEL). The adventitia is composed of fibroblasts, macrophages, type I/III collagens and elastin (Coen et al., 2011, Chelladurai et al., 2012).

1.1.2 The role of stromal cells in the normal vessel wall and in atherosclerosis

The vascular **endothelium** is much more than a barrier between the blood and the subendothelial tissues; it is an active organ, which maintains vascular homeostasis. The phenotype of ECs differs among the various regions of the arterial vasculature. Linear vessels with laminar flow and high shear stress do not develop lesions and present an atheroprotective endothelial phenotype. However, curves and branch-points display low shear stress and high oscillatory shear index and have an atherosclerosis-prone endothelial phenotype. In particular, ECs located in

atherosclerosis-prone regions display a cyboidal morphology, impaired endothelial barrier function, higher rates of cell turnover and cellular senescence (Chistiakov et al., 2015, Buchanan et al., 2014). At the molecular level, the nuclear factor kappa-light-chain-enhancer of activated B cells (NF-κB) pathway is activated, causing the increased expression of vascular cell adhesion molecule 1 (VCAM-1) (Cybulsky and Gimbrone, 1991, Nakashima et al., 1998) and toll-like receptor 2 (TLR2) (Mullick et al., 2008, Monaco et al., 2009), thus promoting monocyte entry into the intima of the artery. Additionally, endothelial dysfunction has been associated with impaired endothelium-dependent vasodilation, which is mediated by nitrogen oxide (NO) (Koo et al., 2013, Tabas et al., 2015). In contrast, the athero-protective EC phenotype is characterised by gene expression of Krüppel-like Factor (KLF) - 2 and - 4, which are activated by the MEK5/ERK5/MEF2 signalling cascade (Parmar et al., 2006, Villarreal et al., 2010).

Vascular **SMCs** are highly specialised cells whose principal function is to control the vessel tone. They synthesise large amounts of extracellular matrix (ECM) proteins, mainly collagen I and III (Amento et al., 1991).

In atherosclerosis, SMCs switch their phenotype from contractile to synthetic; they migrate from the media to the intima and have higher proliferative ability.

Although SMCs are generally considered as plaque stabilisers because they produce fibrous tissue, they can also uptake lipids, express CD68 and finally form foam cells (Gomez and Owens, 2012, Andreeva et al., 1997).

SMC/monocyte interaction has also been documented as SMCs can express adhesion molecules such as VCAM-1 and intercellular adhesion molecule 1 (ICAM-1). SMCs can also inhibit monocyte apoptosis *in vitro* (Cai et al., 2004b, Cai et al., 2004a).

SMCs produce various cytokines such as platelet-derived growth factor (PDGF), transforming growth factor beta (TGF-β), macrophage migration inhibitory factor (MIF), interferon gamma (IFN-γ), interleukin 6 (IL-6) and monocyte chemoattractant protein-1 (MCP-1) (Inoue et al., 2002, Raines and Ferri, 2005, Wilcox et al., 1988, Moses et al., 1990).

1.1.3 Extracellular matrix in arterial physiology and disease

The ECM is composed of several biological components including collagens, elastin and proteoglycans.

Collagens represent 60% of the total protein content of atherosclerotic plaques. They consist of a unique triple-helical structure of three polypeptide α chains, each having a gly-x-y repeating sequence. Collagens can be divided into classes such as fibril-forming collagens (types I-III, V, and XI), network-forming collagens (types VIII and X), facit collagens (types IX, XII, XIV, XVI, and XIX), beaded filaments collagen (type VI), collagen of anchoring fibrils (type VII) and collagens with a transmembrane domain (types XIII and XVII) (Prockop and Kivirikko, 1995).

Collagen determines plaque stability, as it is an important component of the fibrous cap (see section 1.1.4 for details on fibrous cap formation) (type I, III, IV and V). Collagens (type I, III, IV and V) also have binding activities to oxidised low-density lipoprotein (oxLDL). Type I and III collagens have been detected during all stages of atherosclerotic lesion development (Katsuda et al., 1992).

Collagen is mainly synthesised by SMCs. The release of matrix metalloproteinases (MMPs) by inflammatory cells, such as macrophages, degrade collagen and lead to

apoptosis of intimal SMCs, causing further reduction of collagen content and thinning of the protective fibrous cap (Hiraga et al., 2000).

Elastin is an extracellular matrix protein that contributes to the elasticity of vessels. Its gene encodes a protein of 60-70kDa called tropoelastin. Tropoelastin contains hydrophobic domains rich in glycine, valine, proline, and alanine and hydrophilic lysine/alanine-rich regions. Elastin is mainly produced by SMCs and can be degraded by elastases (Debelle and Tamburro, 1999, Krettek et al., 2003).

Proteoglycans consist of proteins that are attached to glycosaminoglycan (GAG) chains. There are two types of proteoglycans: large proteoglycans that interact with hyaluronan such as versican and aggrecan and small leucine-rich proteoglycans. They are responsible for the subendothelial retention of LDL in the vessel wall. Murine studies have shown that expression of proteoglycan-binding-defective apoB100 attenuates the development of atherosclerosis (Anber et al., 1996, Camejo et al., 1993, Skalen et al., 2002). In humans, the earliest progressive lesions consist of an ECM rich in proteoglycans (Virmani et al., 2000, Nakashima et al., 2008).

1.1.4 Histological lesion classification

Stary et al. classified atherosclerosis progression into different stages: type I, II (fatty streaks), III (intermediate), IV (atheroma), V (fibroatheroma) and VI (complicated) (Stary et al., 1995) (Figure 1.2).

Type I is the initial lesion which is characterised by the modification of EC function due to conditions such as hyperlipidemia, hypertension, oxidative stress and inflammation, resulting in the deposition of plasma LDL in the intima. The lesion contains lipoproteins and leucocytes. As a consequence of this subendothelial lipid

retention, LDL particles are trapped in the intima and are susceptible to oxidation, ultimately causing endothelial activation and dysfunction. The uptake of oxLDL by myeloid cells converts macrophages into foam cells, a typical feature of the fatty streaks observed in type II lesions. Type III lesions are characterised by extracellular lipid droplets, which disrupt the integrity of SMCs. Extracellular lipids accumulate and form a lipid core in the musculoelastic layer of eccentric adaptive thickening, which characterises atheroma or type IV lesions. Type V lesions are characterised by the formation of a fibrous cap, which is a protective layer against the lumen formed by SMCs and ECM proteins. Type V lesions can be further subdivided into: Type Va lesions or fibroatheromas which contain a lipid core, type Vb lesions, that have their lipid core calcified and type Vc lesions, that do not have a lipid core or the lipid core is minimal. The development of type IV and V lesions into haemorrhage or thrombosis is classified as type VI lesions, which are often referred to as complicated lesions (Stary et al., 1995) (Figure 1.2).

However, this paradigm of atherosclerosis classification was re-examined mainly due to its inability to capture erosion and calcified nodules as clinical aetiologies that, in addition to plaque rupture, lead to thrombus formation (Virmani et al., 2000). Therefore, the I-IV types of lesion progression were replaced by the terms fatty streaks or intimal xanthomas, (adaptive and pathological) intimal thickening and fibrous cap atheroma. **Intimal xanthomas** are lesions primarily composed of lipid-laden macrophages (Virmani et al., 2000). These lesions do not always become atherosclerotic and have been shown to regress in young individuals (Velican and Velican, 1980).

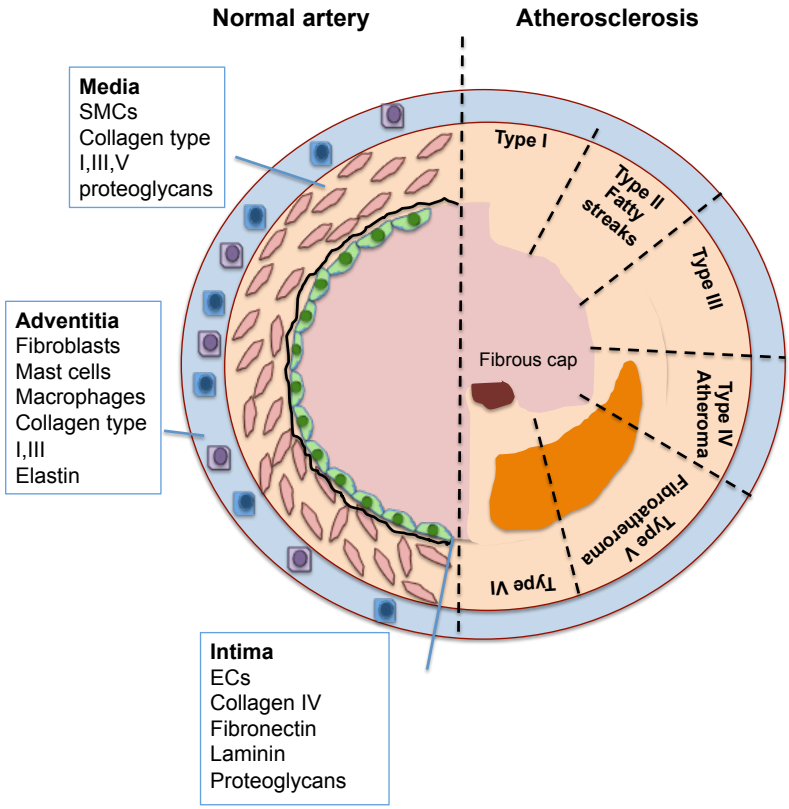


Figure 1.2 Classification of plaque progression according to (Stary et al., 1995). The normal artery consists of three layers: the intima, media and adventitia. Lesion progression can be classified into types I, II, III, IV (or atheroma), V (or fibroatheroma) and VI (or complicated lesions).

Progressive atherosclerotic plaques that are characterised by SMC proliferation in an ECM rich in proteoglycans and extracellular lipid accumulation are termed **pathological intimal thickening**. Fibrous cap atheromas are progressive lesions that have a necrotic core (generated by macrophage infiltration), which is surrounded by a fibrous cap. Fibrous cap atheroma type can either be **thin cap fibroatheromas (TCFAs)**, which have a <65μm thick fibrous cap and are more likely to rupture, or **fibrocalcific plaques** which are heavily calcified lipid-rich lesions that contain few inflammatory cells and SMCs (Virmani et al., 2000).

Progressive atherosclerotic lesions can often lead to thrombi formation through three processes: plaque rupture, plaque erosion or calcified nodules. Plaque ruptures consist

of a necrotic cap and a disturbed fibrous cap. Plaque erosion is identified when a thrombosed artery fails to show fibrous cap rupture. Often, the endothelium is damaged or absent at the site of thrombosis. Interestingly, 35% of lesions with thrombi failed to show rupture among 200 cases of sudden coronary death. Calcified nodules; when fibrous cap disruption is associated with eruptive, dense, calcified nodules, are a rare cause of thrombosis (Virmani et al., 2000).

1.1.5 Lipid accumulation in atherosclerosis

Hyperlipidaemia has long been considered a risk factor for the initiation of atherosclerosis. The lipid theory of atherosclerosis was firstly suggested by Antitschkow (Anitschkow et al., 1964, 1983) and then by Goldstein (Goldstein et al., 1976) who discovered the LDL receptor (LDLR). The lipid theory was then revised by Tabas (Tabas et al., 1993) who proposed the theory of "response to lipoprotein retention", highlighting a key role for the binding of lipoprotein, LDL, to the matrix components of the arterial subendothelium.

LDL is a lipoprotein that functions to transport cholesterol in the blood. In humans, there are five different groups of lipoproteins: High-density lipoproteins (HDL), LDL, intermediate density lipoproteins (IDL), very low density lipoproteins (VLDL) and chylomicrons. Chylomicrons transport dietary lipids from the intestines while VLDL and HDL transport endogenous lipids. Each LDL molecule contains a single apolipoprotein-B (ApoB) molecule. VLDL is synthesised by the liver and is converted into LDL by lipases. LDL is taken up by LDL receptors, which recognise the N-terminal domain of Apo B-100 (Goldstein and Brown, 2009, Fogelstrand and Boren, 2012).

Lipoproteins enter the endothelial wall by endocytosis or transcytosis and some are retained in the intima by proteoglycans. When retained in the subendothelial space, LDL is prone to oxidative modification by myeloperoxidases and reactive nitrogen species and therefore converts into minimally modified LDL (mmLDL) and to oxLDL (Furnkranz et al., 2005). LDL can be hydrolysed in lysosomes to free cholesterol and triglycerides (Brown et al., 2000). Free cholesterol can then be transported out of the cell (reverse cholesterol transport) by adenosine triphosphate-binding cassette (ABC) transporters such as adenosine triphosphate-binding cassette transporter 1 (ABCA-1) and adenosine triphosphate-binding cassette sub-family G member 1 (ABCG-1) or stored as lipid droplets. Mouse models with genetic deletion of both ABCA-1 and ABCG-1 display impaired cholesterol efflux and accelerated atherosclerosis (Yvan-Charvet et al., 2007, Yvan-Charvet et al., 2008).

Retention of oxLDL is considered to be an important initiating factor of atherogenesis. OxLDL increases the expression of selectins and adhesion molecules such as VCAM-1 by ECs promoting monocyte recruitment (Gebuhrer et al., 1995, Nakashima et al., 1998) and also facilitates the migration and entry of monocytes into the intima of the arterial wall by inducing the expression of chemotactic molecules such as MCP-1. Interestingly, C-C chemokine receptor 2 (CCR2), the receptor for MCP-1, is upregulated on monocytes in hypercholesterolemic patients (Han et al., 1999). Additionally, oxLDL triggers ECs and SMCs to express monocytic maturation factors such as macrophage colony-stimulating factor (M-CSF) (Rajavashisth et al., 1990), thus, affecting the differentiation of macrophages. Modified-LDL can be taken up by macrophages via scavenger receptors, such as CD36, leading to foam cell formation, a key feature of the atherosclerotic process (Brown et al., 2000).

1.2 Murine models of atherosclerosis

Over the last decade the mouse has become the predominant species used for cardiovascular research due to its several advantages over other species such as ease of genetic manipulation, its small size, fast breeding cycles and lower maintenance costs. In terms of cardiovascular research, the mouse heart appears to have remarkable similarities to the human heart in terms of its anatomy, development and maturation.

Transgenic and knockout mouse models are extensively used to understand the pathogenesis of atherosclerosis. Several examples include transgenic mice (e.g. apolipoprotein mutants, ApoB, apolipoprotein B mRNA editing enzyme, catalytic polypeptide 1 (ApoBEC-1), apolipoprotein B100 (ApoB100), apolipoprotein E (ApoE) mutants expressing human ApoE2 and ApoE3-Leiden isoforms, apolipoprotein CIII (ApoCIII) or gene-targeted mouse models, such as the ApoE knockout (ApoE-/-) and LDL receptor knockout (LDLR-/-) mice (Daugherty, 2002).

1.2.1. ApoE-/- mice

ApoE is a glycoprotein that is mainly produced in the liver and brain. It is a structural component of all lipoproteins except LDL. It is considered to play a role in cholesterol homeostasis because it functions as a high-affinity ligand for receptors that clear chylomicrons, including LDLR.

Targeted inactivation of the ApoE gene was performed simultaneously in two separate laboratories (Piedrahita et al., 1992, Plump et al., 1992). ApoE-/- mice are hypercholesterolemic even when fed a chow diet. The earliest lesion development occurs in these mice at 5-6 weeks of age, when monocytes adhere to the aortic

endothelium. Lesions develop into intermediate lesions containing foam cells and SMCs (around 15 weeks of age) and ultimately into fibrous plaques (around 20 weeks of age) (Nakashima et al., 1994, Reddick et al., 1994). As in humans, lesions develop at specific sites throughout the aortic tree, particularly at curved and branched areas of low shear stress (Nakashima et al., 1994). However, spontaneous plaque rupture, which is a common complication of the human coronary artery, has not been observed in these mice. Lesion development is accelerated by feeding the mice a Western diet, which contains 21% fat, 0.15% cholesterol and no cholate and supposedly replicates the fast-food diet of the western developed world (Meir and Leitersdorf, 2004).

1.2.2 LDLR-/- mice

LDLR plays an important role in regulating the levels of serum cholesterol as it can remove cholesterol-rich IDL and LDL from the circulation. LDLR-/- mice, a mouse model of familial hypercholesterolemia, were developed in 1993 (Ishibashi et al., 1993). These mice have modest hypercholesterolemia compared with ApoE-/- mice when fed a normal chow diet but they are hyper-responsive to high fat and high cholesterol diets.

1.2.3 Murine models of neointima formation

In addition to transgenic and knock out mouse models, arterial injuries are another type of mouse model for studying atherosclerosis. The first arterial injury model in mice was developed by Lindner *et al.,* in 1993 and used a wire to induce injury (Lindner et al., 1993).

To date several arterial injury models have been developed including the wire injury model, electric injury and arterial remodelling models (carotid artery ligation and the perivascular collar) (Xu, 2004). The wire-injury model involves a flexible wire which is introduced in the common carotid artery and leads to endothelial denudation, damage to medial SMCs and induces a neointimal response three weeks after the injury (Lindner et al., 1993). Electric injury model involves an electric current, which is passed through femoral or carotid arteries and destroys the endothelium, medial SMCs and adventitial fibroblasts and results in severe thrombosis within two to three weeks (Carmeliet et al., 1997). The carotid artery ligation model is a model of arterial injury whereby the blood flow is severely reduced by ligating the common carotid artery near the bifurcation and results in a great loss of SMCs (Kumar et al., 1997). The perivascular collar model involves the placement of a hollow polyethylene tube and induces neointima formation in the carotid artery within three weeks. The endothelium is not directly removed and there is minimal thrombosis and SMC damage (Booth et al., 1989, Kockx et al., 1992).

1.4 The inflammatory nature of atherosclerosis

Inflammatory responses are vital components of the immune system that restore tissue homeostasis after tissue injury or infection. Inflammatory responses that persist for an extended time-course lead to chronic inflammation, which contributes to many human diseases such as RA and atherosclerosis (Libby et al., 2002).

It has long been known that many inflammatory cells, including macrophages (Libby and Hansson, 1991) and lymphocytes (Hansson et al., 1989) and proinflammatory

mediators such as cytokines (TNF) (Barath et al., 1990) and chemokines (MCP-1) (Yla-Herttuala et al., 1991) can be detected in atherosclerotic lesions. Nevertheless, atherosclerosis was only first referred to as "an inflammatory disease" by Russell Ross in 1999 (Ross, 1999).

The pathogenesis of atherosclerosis involves the interplay between mechanical stimuli, ECM remodelling, immune cells and inflammatory mediators. Subendothelial retention and subsequent oxidative modification of lipoproteins (described above) triggers an inflammatory cascade. When the endothelial monolayer becomes inflamed it releases chemokines and stimulates monocyte entry into the arterial wall (Tabas et al., 2015). Infiltration of inflammatory cells such as macrophages contributes to the production of proinflammatory cytokines, chemokines and degradative enzymes; MMPs. Lymphocytes can also join macrophages in the intima and produce cytokines contributing to the migration and proliferation of SMCs thus causing further damage. Inflammatory mediators can also degrade collagen, a fundamental component of the ECM. Apoptosis of lipid-laden macrophages (foam cells) generates the necrotic core contributing to plaque vulnerability (Figure 1.3) (Tabas et al., 2015, Libby et al., 2014).

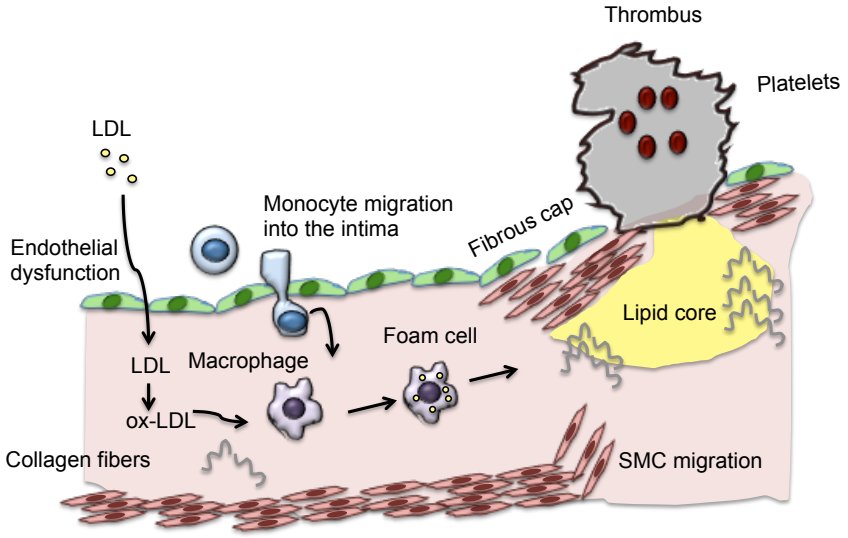


Figure 1.3 The progression of atherosclerosis. Atherosclerosis is initiated by the adhesion of blood monocytes to the activated endothelium and their migration into the intima of the artery. Myeloid cells then accumulate and uptake lipids leading to the formation of foam cells. Lesion progression involves the migration of SMCs into the intima of the artery and the formation of the lipid core. Eventually, plaque vulnerability is increased due to calcification of the lipid core, platelet activation and thrombus formation.

1.4.1 Innate immune system

The innate immune system recognises pathogens and destroys them within minutes of infection. It consists of cellular components such as macrophages, dendritic cells (DCs), neutrophils, natural killer (NK) cells, mast cells and humoral components such as cytokines and the complement system (Figure 1.4).

The first lines of defence against pathogens are epithelial surfaces such as the skin, respiratory and genitals tracts. If the epithelial barrier is breached by microorganisms, innate defence mechanisms destroy them without harming the host, by recognising molecular patterns, such as lipopolysaccharides (LPS), that are absent in the host and by stimulating inflammatory responses and phagocytosis.

If the pathogen overcomes the first line of defence, it next encounters the complement system, which is a series of proteins produced in the liver. They normally circulate in the blood in an inactive form, but become activated after infection. The complement

system becomes activated through three pathways: the classical (initiated by antibody complexes), lectin (initiated by mannose-binding lectin) and alternative (initiated by C3 component which then binds to microbial surfaces) pathways. The complement system ultimately leads to cell lysis, inflammatory responses and opsonisation (a process whereby a microbe is ingested by a phagocyte) (Chaplin, 2003).

Pattern recognition receptors (PRRs) are expressed by innate immune cells and can recognise pathogen constituents including pathogen-associated molecular patterns (PAMPs), such as LPS, or damage-associated molecular patterns (DAMPs), such as high mobility group box 1 (HMGB1). One of the most important family members of the PRRs are toll-like receptors (TLRs). TLR1, TLR2, TLR4, TLR5, TLR6 and TLR11 are found in the extracellular space while TLR3, TLR7, TLR8, TLR9 and the murine TLR13 are intracellular. Each TLR specifically binds to certain ligands (Akira et al., 2006).

The different members of the TLR family have a different functional role in atherosclerosis development. For example, atherosclerosis-prone mice deficient in TLR2 (Mullick et al., 2005) or TLR4 (Michelsen et al., 2004) exhibit a decrease in atherosclerosis development while TLR3 (Cole et al., 2011) and TLR7 (Salagianni et al., 2012) deficiency exacerbates atherosclerosis.

1.4.2 Adaptive immune system

Unlike the innate immune system, the adaptive immune system produces a slower response and depends on the specificity of lymphocytes to the antigen. There are two types of lymphocytes: T- and B- cells.

T cells can react directly with a foreign antigen while B cells produce antibodies, called immunoglobulins (Figure 1.4). Over the last 15 years research has been intensively focussed on the role of T cells in atherosclerosis, as highly activated T cells have been found in atherosclerotic plaques (Hansson et al., 1989, Frostegard et al., 1999). T cells can differentiate into diverse subsets, depending on the tissue microenvironment. CD4+ T cells can be broadly divided into type 1 T helper (Th1), type 2 T helper (Th2), regulatory T (Treg), T helper 17 (Th17) and follicular helper T (Tfh) cells. Th1 cells are considered to be proatherogenic, as they can secrete several proinflammatory cytokines such as TNF-α and IFN-γ (Zhou et al., 1998, Frostegard et al., 1999). The production of IL-12 by plaque macrophages and DCs contributes to Th1 differentiation (Lee et al., 1999, Uyemura et al., 1996). CD40-CD40 ligand (CD40L) interactions also play a role in Th1 differentiation and disruption of this pathway inhibits lesion development and drives the development of a "stable" plaque phenotype (Lutgens et al., 2007). Th2 cells produce IL-4, IL-5, IL-9, and IL-13 cytokines, contribute to antibody production by B cells and are considered as antagonists of the proatherogenic Th1 cells (Xu et al., 1998, Zhou et al., 1998). Tregs develop in the thymus, and are characterised by the expression of CD4, CD25 and Foxp3. The CD28-CD80/CD86 pathway is essential for the maintenance of Tregs. Additionally, several studies have reported that IL-10 (Caligiuri et al., 2003) or TGF-β (Gojova et al., 2003) can induce Tregs and contribute to atheroprotective effects (Mor et al., 2007, Ait-Oufella et al., 2006). Th17 cells produce IL-17, IL-21 and IL-22 and they have an important role in defence against bacteria and fungi (Milner et al., 2010). Studies have reported both antiatherogenic (Taleb et al., 2009) and proatherogenic (Smith et al., 2010, van Es et al., 2009) functions for Th17 cells. CD8+T cells have been detected in human and murine atherosclerotic plaques (Xu et

al., 1990). Several studies have shown that CD8+T cells exert proatherogenic effects through controlling monopoiesis (Cochain et al., 2015) but also through cytotoxic and proinflammatory effects directed by granzyme B, perforin, and TNF-α expression (Kyaw et al., 2013). Finally, natural killer T (NKT) cells bind glycolipid antigens and exert a proatherogenic role (Tse et al., 2013, Subramanian et al., 2013, Chaudhry et al., 2011, Ait-Oufella et al., 2006).

B cells can be mainly divided into two subsets based on their developmental pathway: the B1 and B2 cells. B2 cells, which represent the vast majority of B cells, are bone marrow (BM) derived and include follicular as well as marginal zone B cells. B1 cells, which can be further divided into B1a and B1b based on their surface marker expression, seem to be a developmentally and functionally distinct subset that is localised primarily in the peritoneal and pleural cavities. B cells are believed to play a role in atherosclerosis development through antibody production, antigen presentation and via production of cytokines (such as IL-10) (Simelyte et al., 2008, Tsiantoulas et al., 2014). There is evidence for both pro (Ait-Oufella et al., 2010, Kyaw et al., 2010, Sage et al., 2012) and antiatherogenic (Major et al., 2002, Dimayuga et al., 2002, Strom et al., 2015) roles for B cells in atherosclerosis.

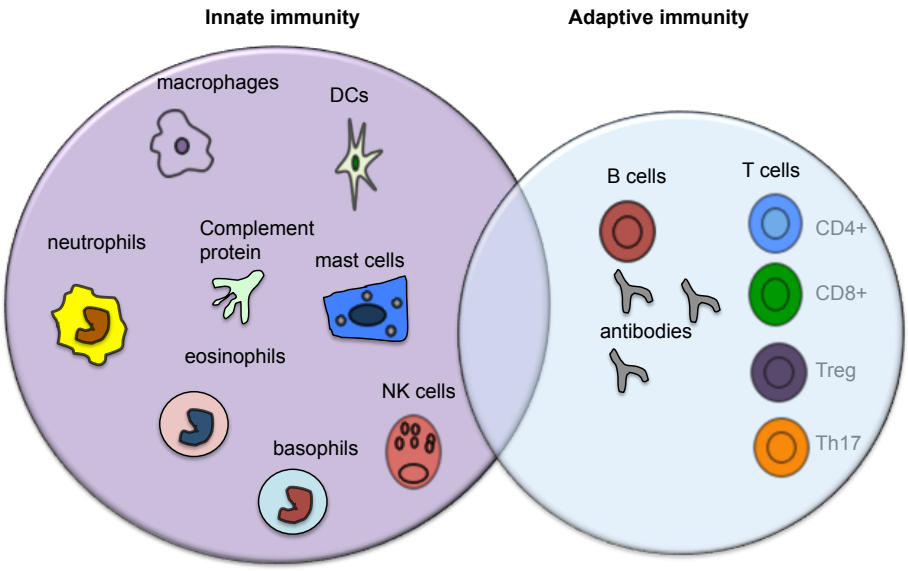


Figure 1.4 Innate and adaptive immunity. Innate immunity consists of cellular and humoral components such as macrophages, DCs, granulocytes, mast cells, NK cells and complement proteins. The adaptive immune system consists of B and T lymphocytes.

1.5 Myeloid cells

The mononuclear phagocyte system (MPS) can be categorised into monocytes, macrophages and DCs, which have distinct ontogenic, functional and phenotypic features.

Monocytes are a conserved population of leucocytes that are present across all vertebrate species. There are two main murine monocyte subsets: lymphocyte antigen 6C (Ly6C) ^{hi} and Ly6C^{lo}. These populations can be distinguished by the surface expression of CCR2 and CX3C chemokine receptor 1 (CX3CR1). In humans, CD14+ and CD14^{lo} CD16+ monocytes are the equivalent of murine Ly6C^{hi} and Ly6C^{lo} monocytes respectively. Ly6C^{hi} monocytes are the "classical monocytes" that are recruited to sites of inflammation and give rise to macrophages and DCs while Ly6C^{lo} monocytes are resident cells that possibly differentiate from Ly6C^{hi} monocytes and

are responsible for endothelial integrity (Ginhoux and Jung, 2014, Geissmann et al., 2010, Jakubzick et al., 2013, Jung et al., 2000, Geissmann et al., 2003).

Macrophages are phagocytic cells that were discovered by Metchnikoff in 1884. Macrophages express PRRs on their surface and can induce a range of inflammatory cytokines (Stefater et al., 2011).

DCs are the immune cells that link innate and adaptive immunity. DCs were identified by Steinman in 1973 (Steinman and Cohn, 1973). They are known as antigen presenting cells that can migrate to lymph nodes and interact with lymphocytes (Inaba et al., 1998, Allan et al., 2006).

1.5.1 Ontogeny

Monocytes arise in the fetal liver and in the BM and their development depends on the growth factors M-CSF and granulocyte-macrophage colony-stimulating factor (GM-CSF) (Hamilton, 2008). Monopoiesis can also occur in the murine spleen (Kim, 2010, Robbins et al., 2012). Mice deficient in M-CSF or its receptor exhibit monocytopenia (leukopenia which is associated with monocyte deficiency) (Dai et al., 2002, Wiktor-Jedrzejczak and Gordon, 1996). Monocytes are also generated in the BM by haematopoietic stem cells (HSCs) via monocyte-dendritic progenitors (MDPs) and common monocyte progenitor (cMoP) intermediates as described in detail in section 1.5.1.1 (Fogg et al., 2006, Hettinger et al., 2013).

Macrophages and DCs were considered to solely derive from monocytes. However this concept has been recently challenged as monocyte contribution to the tissue macrophage population has been proven to be minimal in the steady state and tissue resident macrophages can in fact be derived embryonically and can self maintain by proliferation (Ginhoux and Jung, 2014, Ginhoux et al., 2010).

Macrophages can derive not only from the BM but also from the yolk sac and the fetal liver. The majority of tissue macrophages are seeded before birth independently of monocytes while monocytes contribute to macrophage numbers during inflammatory conditions. Embryonic macrophages can arise from primitive and definitive haematopoiesis. Primitive haematopoiesis occurs in the yolk sac at embryonic day 7 (E7) and generates the erythro-myeloid progenitors (EMPs), which are phenotypically defined as c-kit+CD41+ cells. The yolk sac macrophages, then, emerge at E9. Definitive haematopoiesis occurs in the fetal liver at E10.5 and gives rise to HSCs. At E12.5 -13.5 fetal liver monocytes migrate to the blood and then to tissues and dilute the already existing population of yolk sac macrophages in various tissues such as the heart. In terms of their transcriptional regulation, yolk-sac macrophages depend on PU.1 and are independent of MYB. Thus, with the exception of microglia, which arise exclusively from yolk-sac macrophages and Langerhans cells, which originate both from yolk sac macrophages and fetal liver monocytes, all other tissue macrophages derive from definitive haematopoiesis (Jenkins et al., 2011, Hashimoto et al., 2013, Ginhoux and Jung, 2014, Kassiteridi and Monaco, 2015, Takahashi et al., 1989, Takahashi and Naito, 1993, Ginhoux et al., 2010).

DCs can derive from cMoPs and common DC progenitors (CDPs) progenitors (see section 1.5.1.1). DC lineage is heterogeneous and consists of developmentally and functionally distinct subsets: classical DCs (cDCs), monocyte-derived DCs (mo-DCs) and plasmacytoid DCs (pDCs). Tyrosine kinase 3 (Flt3) is the key cytokine that controls the development of all DC subsets (Guilliams et al., 2014, Onai et al., 2007, Waskow et al., 2008).

1.5.1.1 Postnatal haematopoiesis: the classical HSC hierarchy

After birth, the BM becomes the main site of definitive haematopoiesis and this relies on HSCs. In brief, the hierarchy of HSCs is as follows: The Lin−Sca-1+c-Kit+ (LSK) population is enriched by CD34- long-term HSCs (LT-HSCs) that have long-term self-renewal ability or CD34+ short-term HSCs (ST-HSCs) or multipotent progenitors (MPPs), which sustain haematopoiesis only in the short term (Morrison and Weissman, 1994). Further downstream, common lymphoid progenitors (CLPs) upregulate IL-7R and can be identified as IL-7Ra+c-Kit^{lo}Lin-Sca-1^{lo} cells that possess clonogenic T, B, and NK cell potential lineage (Peschon et al., 1994, Iwasaki and Akashi, 2007).

The common myeloid progenitors (CMPs) are IL-7Ra- but CD16/32^{lo} CD34+ and can differentiate into the CD16/32+CD34+ granulocyte-macrophage progenitors (GMPs) and the CD16/32^{lo} CD34^{lo} megakaryocyte-erythroid progenitors (MEPs). The CMPs can give rise to all types of myeloid colonies, whereas the GMPs or the MEPs produce only granulocytes and myeloid cells or megakaryocyte erythrocyte lineage cells, respectively (Figure 1.5) (Akashi et al., 2000).

Within GMPs, there are CD11b-Ly6C-CD117+CD115+CD135+MDPs that can differentiate into macrophages and monocytes via the Lin-CD11b-Ly6C+CD115+ CD135- CoMPs or into DCs via Lin-CD11b-Ly6C+CD115- CDPs. The differentiation of monocytes, macrophages and DCs can be controlled by several cytokines such as GM-CSF, IL-3 and M-CSF. DCs have not only a myeloid but also a lymphoid progeny (common lymphoid progenitors, CLPs) (Figure 1.5-1.6) (Onai et al., 2013, Onai et al., 2007).

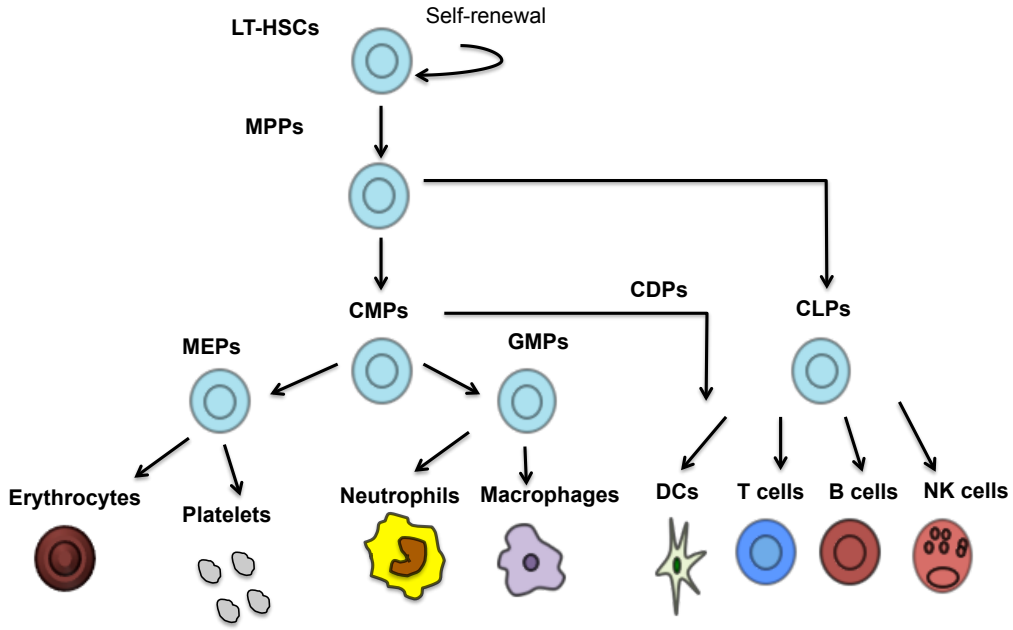


Figure 1.5 Hierarchical structure of HSCs. HSCs initially differentiate into multipotent progenitors (MPPs) with no self-renewal ability, which in turn give rise to common lymphoid progenitors (CLPs) and common myeloid progenitors (CMPs). CMPs can then differentiate into megakaryocyte/erythrocyte progenitors (MEPs) and granulocyte/macrophage progenitors (GMPs).

1.5.2 Nomenclature

Macrophages and DCs are highly heterogeneous populations, which were historically grouped together due to their common monocytic origin. However, myeloid nomenclature has been proven to be complex. Advanced technology, including the use of flow cytometry, has created further confusion. For example, due to the functional and phenotypic complexity of the MPS, categorising myeloid cells solely on the basis of the surface expression of several markers, including CD11c, MHCII and F4/80 expression is poor (Guilliams et al., 2014). Several DC subsets have been identified in lymphoid and non-lymphoid tissues based on their phenotypic characteristics such as TNF- inducible nitric oxide synthase (iNOS)-producing DCs (TIP-DCs), CD103+DCs, CD11c+DCs and CD11b+DCs creating many concerns about misconnections between laboratories (Kassiteridi and Monaco, 2015, Merad et

al., 2013, Miller et al., 2012, Sorg et al., 1999, Guilliams et al., 2014). Recent studies have revealed that macrophages and DCs have a unique transcriptional signature in various organs. In terms of phenotypic features of myeloid cells, co-staining of the surface markers MerTK and CD64 has been reported to better distinguish murine tissue macrophages from DCs than, for example staining for F4/80 and CD11c (Gautier et al., 2012).

Interestingly, Guilliams *et al.,* have recently proposed a unified nomenclature of myeloid cells based on their origin (level one nomenclature) and their location/phenotype/function (level two nomenclature) (Guilliams et al., 2014). Based on their origin, mononuclear phagocytes are divided into: **macrophages** (they have embryonic origin), **monocyte-derived cells (MCs)** (they derive from monocyte precursors: MDPs and cMoPs) and finally **DCs** (they derive from CDPs) (see section 1.5.1.1) (Figure 1.6).

Using this nomenclature, a macrophage is classified as any mononuclear phagocyte of embryonic origin. This group includes liver-resident Kupffer cells, microglia, alveolar macrophages and Langerhans cells.

Concerning DCs, it was proposed that DCs that originate from CDPs should be categorised into cDC1s, cDC2s and pDCs based on their developmental pathway and their transcriptional regulation. cDC1s are the CD8α+ and CD103+ DCs and are BATF3- dependent while cDC2s are the CD11b+ and CD172a+ DCs which are IRF4-dependent. In contrast to cDCs, pDCs are E2-2- dependent and produce high levels of type I IFN (Guilliams et al., 2014, Onai et al., 2007, Waskow et al., 2008). Besides gene-expression, cellular origin and transcription factor profiles, functional characteristics are also important and illustrated in level two of the nomenclature. For

example, cDC2s can be further divided in subpopulations based on their ability to exert Notch2-dependent Th2 or KLF4-dependent Th17 responses (Satpathy et al., 2013, Tussiwand et al., 2015).

Finally, monocyte-derived cells include monocyte-derived macrophages and monocyte-derived DCs such as TIP-DCs (Guilliams et al., 2014). This group also includes the *in vitro* generated DCs and macrophages. Monocytes that are cultured with GM-CSF give rise to DC-like cells, known as mo-DCs. Monocytes cultured with M-CSF gives rise to macrophage-like cells. These macrophages can be further polarised into classically-activated M1 macrophages when stimulated with IFN-γ and LPS or alternatively-activated M2 macrophages when stimulated with IL-4 and IL-13 (Guilliams et al., 2014).

Thus, distinguishing myeloid cells based only on limited phenotypic criteria is not enough. Their ontogeny, developmental pathways and transcriptional control should also be evaluated to improve our understanding of their biology. Novel technologies, such as mass cytometry (CyTOF) could delineate tissue specific myeloid compositions (Becher et al., 2014).

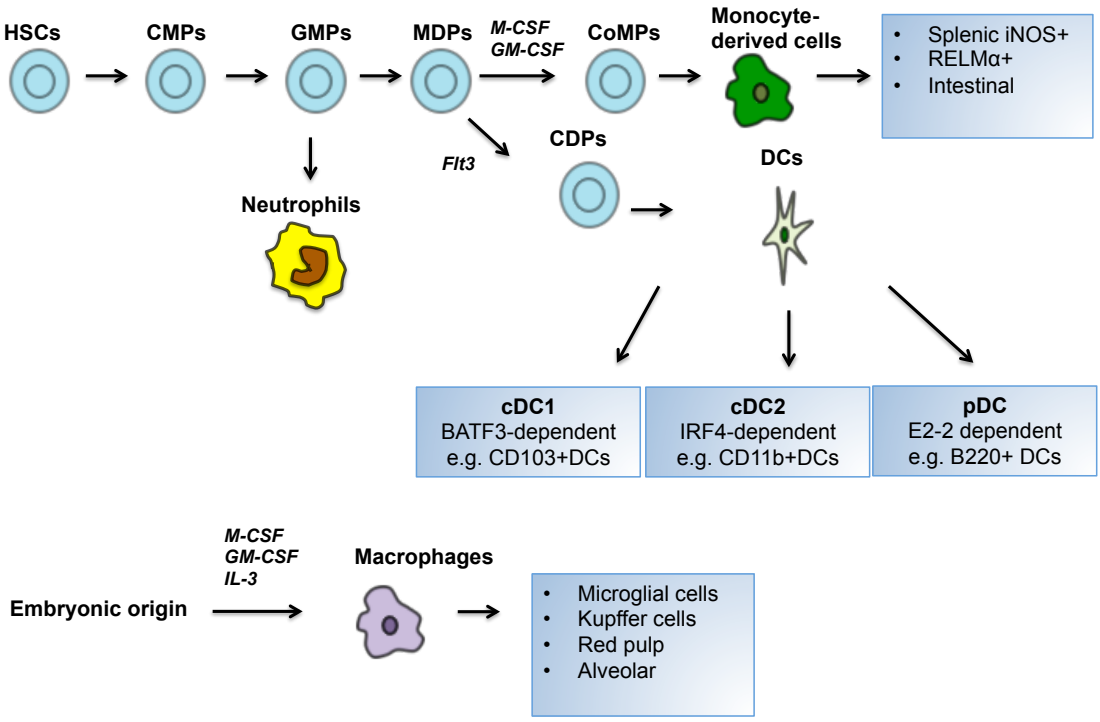


Figure 1.6 Classification of myeloid cells. Based on their origin, mononuclear phagocytes are divided into: macrophages (they have embryonic origin), monocyte-derived cells (they derive from monocyte precursors: MDPs and cMoPs) and finally DCs (they derive from CDPs). DCs can be further divided into cDC1s, cDC2s and pDCs based on their developmental pathway and transcriptional regulation.

1.6 The role of myeloid cells in atherosclerosis

1.6.1 Monocyte recruitment in atherosclerosis

Monocyte recruitment is one of the early stages in the initiation of atherosclerosis. Swirski *et al.,* showed that hyperlipidemia in ApoE-/- mice expands Ly6C^{hi} monocytes whilst leaving Ly6C^{lo} monocytes unaffected (Swirski et al., 2007).

Monocyte recruitment is mediated by chemokines, integrins and selectins. Ly6C^{hi} monocytes, which represent 90% of plaque monocytes, depend on CCR2 for their release from the BM (Swirski et al., 2007, Combadiere et al., 2008, Tsou et al., 2007), while CX3CR1 is important for the survival of Ly6C^{lo} monocytes. Ly6C^{lo} monocytes utilise CCR5 to enter the plaques (Tacke et al., 2007). Interestingly, combined inhibition of CCL2, CX3CR1 and CCR5 results in reduced monocytosis and atherosclerosis (Combadiere et al., 2008). Additionally, both CX3CL1 and CX3CR1 deficiency decreases the amount of blood Ly6C^{lo} monocytes while introducing the Bcl2 trangene restores the monocyte reduction and atherogenesis in mice (Landsman et al., 2009).

Disruption of cell adhesion molecules such as ICAM-1, VCAM-1, P-selectin or E-selectin results in reduced monocyte recruitment and lesion formation (Cybulsky et al., 2001, Nageh et al., 1997).

Monocytes differentiate into macrophages under the influence of M-CSF. Osteopetrotic mice, which lack M-CSF, are characterised by reduced lesion size and decreased circulating monocytes (Qiao et al., 1997).

1.6.2 Inflammatory macrophages in atherosclerosis

The versatility of monocyte-derived subsets of macrophages stems from their ability to modify their behaviour in response to microenvironmental cues (Table 1.1).

According to the classic macrophage activation paradigm suggested by Mantovani *et al.,* macrophages can be subdivided into the proatherogenic M1 and the anti-inflammatory M2 macrophages. M1 polarisation depends on IFN-γ and TNF-α cytokine production while M-CSF and IL-4 drive macrophages into the M2 phenotype (Martinez and Gordon, 2014, Mantovani et al., 2005). Additionally, peroxisome proliferator-activated receptor (PPAR) -γ activation can drive M2 differentiation in human atherosclerotic lesions (Bouhlel et al., 2007). However, the classification of macrophages has been recently revisited by Guilliams *et al.,* who categorised the M1 and M2 *in vitro* differentiated macrophages into the MC group (see section 1.5.2) (Guilliams et al., 2014). Interestingly, a link between macrophage polarisation and the stability of the coronary atherosclerotic plaque has been reported. For example, plaques from symptomatic patients mainly consist of M1 macrophages while M2 macrophages are the predominant myeloid population in plaques from asymptomatic patients (Cho et al., 2013). Apart from M1 and M2 macrophages other myeloid subsets, named Mox, M4 and Mhem, have been identified. In particular, Kadl *et al.,* found that an oxidised phospholipid-rich microenvironment shifts myeloid cells into an Mox phenotype, which display dysregulated phagocytic ability (Kadl et al., 2010). Another study showed the presence of another poorly phagocytic myeloid phenotype that was induced by M-CSF/CXCL4 *in vitro* and termed them M4 macrophages (Gleissner et al., 2010). Finally, Mhem cells derive from the *in vitro* treatment of human-derived monocytes with hapto-hemoglobin complexes or oxidised red blood cells. They express high levels of CD163 and low levels of human

leukocyte antigen-antigen D related (HLA-DR) (Boyle et al., 2009). Studies in LDLR-/- mice have shown that the murine aortic myeloid compartment contains 39% M1, 21% M2 and 45% Mox cells. M1, M2 and Mox phenotypic polarisation is reversible; polarisation towards M4 cells is irreversible (Ley et al., 2011, Kassiteridi and Monaco, 2015).

An important factor for better understanding of the biology of myeloid cells in atherosclerosis is their origin. It has recently been shown that resident plaque macrophages accumulate due to *in situ* proliferation and inhibiting macrophage proliferation supresses' plaque inflammation (Robbins et al., 2013, Ensan et al., 2016, Tang et al., 2015, Klapproth et al., 2016). Therefore, understanding the developmental pathways of macrophages would be of interest.

Table 1-1 Macrophage subsets in atherosclerosis. Table adapted from (Kassiteridi and Monaco, 2015).

Subsets	**Resident macrophages**	**Inflammatory macrophages or MCs**				
	e.g. liver Kupffer cells, microglia, peritoneal, lung, splenic red pulp (Davies et al., 2013a)	M1 (Mantovani et al., 2005)	M2 (Mantovani et al., 2005)	Mox (Kadl et al., 2010)	M4 (Gleissner et al., 2010)	Mhem (Boyle et al., 2009)
Activation	Mild zymosan peritonitis, (Davies et al., 2011, Davies et al., 2013a) influenza infection (Lauder et al., 2011), helminth infection (IL-4) (Allen and Wynn, 2011)	IFN-γ, LPS, GM-CSF	IL-4, IL-13	oxLDL	CXCL4	Hemorrhage
Markers		iNOS, MHCII, IL-1β, IL-6, IL-8, IL-12 and TNF-α	Arginase I, CD206, IL-10	HO-1, TXNRD 1, VEGF	MMP7, S100-A8, IL-6, reduced CD163 expression	CD163

Function	Erythrocyte clearance, degradation of erythroid nuclei, apoptotic cell clearance (Davies et al., 2013a)	Proinflammatory, proteolysis	Anti-inflammatory, wound healing/repair, fibroblast recruitment, efferocytosis	Unknown	Pro-inflammatory	Anti-inflammatory
Transcriptional regulation	PU.1 (yolk sack-derived), Myb (Haematopoietic stem cell derived) (Davies et al., 2013a)	NFκB, NLRP3, SOCS3 (Leitinger and Schulman, 2013)	PPARγ, KLF4, NR4A, IRF4, RELMa, SOCS2, Chia, CHI3L1; CHI3L2, CHI3L3, CXCL13, CCL12, CCL24, STAT6 (Leitinger and Schulman, 2013, Sharma et al., 2012)	NRF2 (Collins et al., 2012)	Unknown (Leitinger and Schulman, 2013)	NRF2 (Boyle et al., 2011)

1.6.3 Arterial DC subsets

Various vascular DC subsets have been described in the aorta of healthy and atherosclerotic mice (Table 1.2). Choi *et al.,* observed two major aortic CD11c+MHCII+ DCs populations in the aorta of a normal C57BL/6 mouse: CD103-CD11b+F4/80+ and CD103+CD11b-F4/80- DCs based on their developmental pathway. Arterial CD11b+DCs are M-CSF dependent and can be additionally phenotypically described by the expression of CX3CR1, CD14 and dendritic cell-specific intercellular adhesion molecule-3-grabbing non-integrin (DC-SIGN) while CD103+DCs depend on the Flt3-Flt3l signalling pathway and have an atheroprotective role (Choi et al., 2011). Busch *et al.,* identified an additional DC subset of CD103-CD11b+F4/80- DCs (Busch et al., 2014). Another study identified a proatherogenic CCL17+ DC population, which expresses CD11b but lacks CD115 or

F4/80 expression (Weber et al., 2011). Finally, the role of pDCs is controversial in atherosclerosis development, as both pro and anti-inflammatory roles for pDCs have been suggested (Niessner et al., 2006, Daissormont et al., 2011). Despite recent advances, the diversity and biology of arterial DCs needs better understanding.

Table 1-2 Arterial DC subsets. Table adapted from (Kassiteridi and Monaco, 2015).

DC subsets	CD11b+cDCs	CD103+cDCs	CCL17+cDCs	pDCs
Cell surface expression	CX3CR1, CD11b, F4/80, CD14, DC-SIGN, Sirp-α, CD64	CD103 and CD135 (Choi et al., 2011)	CD11b, MHCII, CD40, CD80, and CD86 (Weber et al., 2011)	PDCA-1, Siglec-H and only low levels of CD11c and MHCII

1.6.4 Neutrophils in atherosclerosis

Compared to the other inflammatory cell populations, the role of granulocytes, including basophils eosinophils and neutrophils, in atherosclerosis has not been extensively studied. Recent evidence suggests that neutrophils are able to eliminate intracellular pathogens but also communicate with immune or non-immune cells by releasing inflammatory mediators or by direct cell-cell contact (Mayadas et al., 2014). Neutrophil infiltration has been observed both in the intima and adventitia of atherosclerosis-prone mice, while treatment with an anti-Ly6G antibody that depletes neutrophils, decreases lesion size in ApoE-/- mice (Rotzius et al., 2010).

1.7 Myeloid activating and inhibitory receptors

Inflammatory responses are balanced through activating and inhibitory receptors that are expressed on various cell types, including myeloid cells.

1.7.1 ITIM-bearing inhibitory receptors

The expression of inhibitory receptors by myeloid cells has been reported by various studies. These receptors can be divided into two groups: the immunoglobulin (Ig) superfamily receptors (IgSR), which include immunoglobulin-like transcripts (ILTs), signal-regulatory proteins (SIRPs), leukocyte-associated immunoglobulin-like receptor 1 (LAIR-1) and the C-type lectin inhibitory receptors such as dendritic cell immunoreceptor (DCIR) and Ly49Q. The structure of IgSRs is characterised by an extracellular single V-type Ig-like domain. Both types of receptors can downregulate immune cell activity via the immunoreceptor tyrosine-based inhibitory motif (ITIM) motif located in the cytoplasmic domain. ITIMs share a sequence of 6 amino acids (V/I) XYXX (L/V)), where X denotes any amino acid. Upon ligand engagement, ITIMs become phosphorylated and recruit tyrosine phosphatases: SH2 domain-containing inositol-5'-phosphatase (SHIP)-1 or -2 (Steevels and Meyaard, 2011).

Several ITIM-bearing receptors expressed by myeloid cells are described below:

a) **SIRP** family: The SIRP family consists of Sirp-α, Sirp-β and Sirp-γ. Sirp-α binds to CD47 (also known as integrin-associated protein) and inhibits myeloid cells though the Src homology region 2 domain-containing phosphatase (SHP) 1 and 2 (Kharitonenkov et al., 1997). Additionally, CD47-/- red blood cells are rapidly cleared by splenic macrophages, indicating that the ligation of Sirp-α by CD47 might play a role in macrophage phagocytic ability (Oldenborg et al., 2000).

b) **PILRs** (Paired immunoglobulin-like receptors): The PILR family consists of PILR-α and PILR-β. PILR- α (FDF03) is an inhibitory receptor that binds CD99 and inhibits human macrophages and DCs (Fournier et al., 2000, Mousseau et al., 2000).

c) **ILT** family: 8 of the 10 ILT receptors have an ITIM motif in their cytoplasmic domains. The majority of ILT receptors are expressed on monocytes, macrophages and DCs, although their expression on neutrophils, basophils and eosinophils and B lymphocytes has also been described (Nakajima et al., 1999, Samaridis and Colonna, 1997). ILT2 binds human MHCI and inhibits macrophage activation during viral infection (Cosman et al., 1997).

d) **C-type lectins**: Several C-type lectin inhibitory receptors can affect DC function. For example, deficiency of DCIR expands DCs and exacerbates collagen-induced arthritis (CIA) (Bates et al., 1999, Fujikado et al., 2008). Ly49Q, another C-type lectin inhibitor, inhibits neutrophils and TLR9 signalling in pDCs (Sasawatari et al., 2010, Tai et al., 2008, Toyama-Sorimachi et al., 2004).

e) **LAIR-1** (also known as CD305) is expressed on monocytes, macrophages and DCs and binds to collagen (Meyaard, 2008, Lebbink et al., 2007). Recent evidence suggests that LAIR-1 inhibits GM-CSF-dependent survival of leukemia cells in a calcium and AKT1/protein kinase B α (PKBα) dependent manner (Zocchi et al., 2001).

f) **Siglecs** (Sialic-acid-binding immunoglobulin-like lectins): Siglec-3 (also known as CD33), 5, 7, 8 and 9 are inhibitory receptors that are expressed on myeloid cells. A

crosslinking Siglec-3 antibody can suppress the proliferation of CD34+ myelomonocytic cell precursors *in vitro* (Vitale et al., 1999, Vitale et al., 2001).

1.7.1.1 Other myeloid inhibitory receptors

A unique myeloid inhibitory mechanism has been recently demonstrated in the case of CD200-CD200R signalling, which does not depend on an ITIM motif but instead contains a NPXY motif (see section 1.8).

1.7.2 ITAM- bearing activating receptors

Besides myeloid inhibitory signals mediated by ITIM-bearing receptors, evidence suggests that immunoreceptor tyrosine-based activation motif (ITAM, YXXLX6–8YXXL in single-letter amino acid code) -mediated signalling can elicit myeloid cell activation under certain conditions (Unkeless and Jin, 1997). These motifs are present in adaptor molecules such as DNAX activation protein 12 (DAP12) (Wu et al., 2000). Several ITAM-bearing receptors which are expressed by myeloid cells are ILT1, ILT7 (Nakajima et al., 1999), triggering receptor expressed on myeloid cells (TREM) 1 and 2 (Daws et al., 2001), CMRF35A2 (GREEN ET AL., 1998), Sirp-β (Tomasello et al., 2000), PILR-β. (Mousseau et al., 2000) and CLEC-5A (Watson et al., 2011).

1.8 CD200-CD200R: a myeloid inhibitory regulator

1.8.1 Molecular analysis of the CD200-CD200R pathway: unraveling a cell-cell interaction

Rat CD200 (originally referred to as OX-2) was first characterised as a 41-47kDa cell surface glycoprotein in 1982 (Barclay and Ward, 1982), that has a wide distribution on several cell types including thymocytes, activated T cells, B cells, ECs, follicular DCs, neurons and cells in reproductive organs (Hoek et al., 2000) and also in murine keratinocytes (Rosenblum et al., 2004b). CD200 contains two immunoglobulin superfamily (IgSF) domains, a single transmembrane region and a short cytoplasmic domain, a type of structure that is common in proteins that are capable of mediating cell-cell interactions (Barclay and Ward, 1982, Clark et al., 1985). Using techniques to detect low affinity binding (whereby a fusion protein bearing the extracellular domains of CD200 was constructed), a receptor for CD200 was found: the CD200R or CD200R1 (Wright et al., 2000). Like CD200, CD200R has two IgSF domains but has a longer cytoplasmic domain (67 amino acids compared with 19 in CD200) suggesting that it can signal (Wright, Immunity 2000). The genes of both human CD200 and its receptor are closely linked on chromosome 3, suggesting that they are closely related (Douglas et al., 1988). CD200R is mainly expressed by myeloid cells.

The CD200-CD200R axis has recently attracted interest due to its ability to inhibit myeloid cell activation. Although the exact mechanism has not been delineated, CD200-CD200R mediated inhibition is thought to occur not in an ITIM-dependent manner but via the phosphorylation of the NPXY motif located in the cytoplasmic tail of CD200R. This in turn results in the phosphorylation of the downstream of tyrosine kinase (Dok) proteins, Dok-1 and Dok-2 and finally inhibits the Ras/Mitogen-

activated protein kinase (MAPK) pathways (Zhang et al., 2004, Mihrshahi et al., 2009, Mihrshahi and Brown, 2010). The role of Dok-1 and Dok-2 in CD200-CD200R signalling has been further described by Mihrshahi and Brown who suggested that Dok-1 recruits less RasGAP than Dok-2 and that Dok-2 phosphorylation precedes Dok-1 phosphorylation. Following CD200-CD200R interaction, Dok-2 phosphorylation recruits the adaptor molecule Nck, while Dok-1 phosphorylation recruits CrkL. The authors concluded that Dok-1 acts as a negative regulator of Dok-2-mediating CD200R signalling through CrkL (Mihrshahi and Brown, 2010). Although CD200R has high levels of glycosylation, Hatherley and Barclay showed that the GFCC' face of the CD200R N-terminal domain is free of glycosylation, and is possibly the binding site (Hatherley and Barclay, 2004). The actual affinity of the interaction between CD200 and CD200R is low (~2.5 μM) as many other cell: cell interactions in the immune system (van der Merwe and Barclay, 1996).

Barclay suggested that the CD200-CD200R interaction and CD47- Sirp-α (see section 1.7.1) fall in the same category of receptor pairs that allow the fine-tuning of myeloid cells. Interaction between CD47 and Sirp-α downregulates myeloid cells through SHP1 and SHP2 (see section 1.7.1). However, the CD200-CD200R interaction is simpler because CD200 cannot signal itself, as it contains a short cytoplasmic domain (Kharitonenkov et al., 1997, Barclay et al., 2002). The CD200 gene is structurally linked to co-stimulatory molecules, CD80 and CD86 that bind the activating receptor CD28 and the inhibitory receptor CD152, respectively (Borriello et al., 1997). Therefore, studies to identify the role of CD200 as a co-stimulatory molecule are needed.

1.8.2 The CD200R family: Why do multiple isoforms exist?

Besides CD200R/CD200R1, alternate CD200Rs have been found, including murine CD200R2-5 and human CD200R1-2. Unlike CD200R1, alternate CD200Rs might function as activating receptors because they have a short cytoplasmic tail and are thought to signal via adaptor molecules such as DAP12 (Wright et al., 2003). The expression of CD200R2 and CD200R3 has been detected in mast cells and basophils in several studies (Voehringer et al., 2004, Kojima et al., 2007). Gorczynski *et al.,* suggested a role for CD200R2 in inducing tolerogenic DCs which drive Treg development (Gorczynski et al., 2008). Although, the ligands for alternate CD200Rs are unknown, one study suggested that CD200 is not only a ligand for CD200R1 but also for alternate CD200Rs (Gorczynski et al., 2004), but another group have proposed that CD200 is an exclusive ligand for CD200R1 (Wright et al., 2003, Hatherley et al., 2005). Further studies are needed to clarify these conflicting results.

Many viral homologues of CD200 have been found, including homologues in Betaherpeviridae, Gammaherpesviridae and Poxviridae, suggesting survival benefits for the virus to downregulate immune responses through CD200R1 signalling (Afonso et al., 2002). Thus one plausible explanation for the origin of alternate CD200Rs is that they evolved as activating receptors to override the pathogen-induced inhibitory responses mediated by CD200R1.

1.8.3 CD200-mediated immunoregulation: Evidence from disease models

The role of the CD200-CD200R axis has been extensively studied in chronic inflammatory diseases, autoimmunity, infection and cancer. Many techniques have evolved to allow manipulation of the CD200-CD200R pathway and to help

understand its role in immunoregulation (Table 1.3).

The first CD200-/- mice were reported by Hoek *et al.,* (Hoek et al., 2000) and showed increased myeloid activation, measured by staining with antibodies against CD11b, F4/80, CD68, iNOS, CD45 or DAP12 (myeloid activator protein, see section 1.7.2). CD200-/- mice appeared to have enlarged splenic red pulp area and MOMA (monocyte/macrophage)-1+ metallophilic zone and enlarged mesenteric lymph nodes. The same study found that CD200-/- mice showed accelerated microglial response after neuronal damage, and that the mice were also susceptible to experimental autoimmune encephalomyelitis (EAE) and CIA (Hoek et al., 2000). The authors concluded that these effects were probably due to deregulation of myeloid pathways and were unrelated to T cell activation (Hoek et al., 2000). Today, there is a growing body of data on the detrimental effects of CD200 deficiency in inflammatory responses in mouse models of CIA, EAE, experimental autoimmune uveoretinitis (EAU), SLE and influenza virus infection (see Table 1.3). CD200-/- mice have increased bone density, suggesting a role for CD200 in osteoclastogenesis (Cui et al., 2007). CD200/BTLA deletions have been suggested as a prognostic factor in human B-cell precursor acute lymphoblastic leukemia (Ghazavi et al., 2015) and in multiple myeloma (Moreaux et al., 2006). Another study showed that the CD200 mRNA was decreased in the hippocampus of rats with increasing age (Frank et al., 2006). Additionally, deficiency in CD200 and CD200R levels has been reported in human elderly brains affected by Alzheimer's disease, which could be responsible for the chronic inflammatory responses associated with the disease (Walker et al., 2009).

On the other hand, CD200-Fc or agonistic CD200-R antibody treatment has beneficial effects in animal models of autoimmunity and chronic inflammation (see Table 1.3).

Administration of a CD200-Fc has been shown to reduce the severity of CIA and down regulates gene expression of proinflammatory mediators including, TNF-α, IL-1β and MMP13 (Gorczynski et al., 2001).

Mice deficient in CD200R have increased severity of arthritis while no differences in T cells have been observed (Simelyte et al., 2010). Additionally, Boudakov *et al.,* showed that CD200R-/- mice show increased production of TNF-α in response to LPS, and an inability of CD200 to inhibit this inflammatory response (Boudakov et al., 2007).

Table 1-3 Manipulation of the CD200-CD200R pathway in mouse disease models.

Manipulation of CD200/R	Murine disease model	Possible mechanism of effect	References
CD200 deletion	↑CIA		(Hoek et al., 2000)
	↑EAE	↑iNOS ↑CD68+macrophages	(Hoek et al., 2000)
	Facial nerve transection	↑CD11b microglia	(Hoek et al., 2000)
	↑EAU onset	↑CD45+CD11b+ resident microglia and perivascular macrophages ↑NOS2 expression by microglia ↑apoptosis	(Broderick et al., 2002)
	↑EAU onset but ↓ EAU disease incidence at mid and late disease stages	↑splenic CD25+ Treg and IL-10-secreting $CD11b^{+}$ and $CD11c^{lo/-}$ cells ↑Th2 responses in the spleen ↑STAT6 in the spleen and lymph nodes	(Taylor et al., 2005)
	↓Toxoplasma encephalitis (TE)	↑microglia ↑microglia proliferation (ki-67) and activation (iNOS, TNF, MHCI and II) ↓parasite burden	(Deckert et al., 2006)
	Contact hypersensitivity		(Rosenblum et al., 2004a)
	↑sensitivity to influenza infection	↑MHCII, CD80, expression by alveolar macrophages ↑TNF-α, IL-6 responses by alveolar macrophages in	(Snelgrove et al., 2008)

		response to LPS ↑lung CD11c+macrophages ↑macrophages (CD11b+CD11c-), DCs (CD11b-CD11c+), CD4+ and CD8+T cells in the mesenteric lymph nodes	
Blocking CD200R antibodies	↑CIA	↑Synovial inflammation, articular cartilage erosion (as assessed by H&E staining)	(Hoek et al., 2000)
	↑EAU	↑CD45+leucocyte infiltration ↑NOS2 expression	(Banerjee and Dick, 2004)
	SLE	↑anti-CD3/CD28 stimulated CD4+T cell proliferation	(Li et al., 2012)
CD200 overexpression	↑Breast cancer		(Gorczynski et al., 2010)
	↑Cardiac and skin allografts	↓mast cell degranulation ↑Tregs ↓T cell activation	(Gorczynski et al., 2011a, Gorczynski et al., 2013)
CD200R deletion	↑CIA	↑TNF-α, IL-12 No effect on T cell cytokine production	(Simelyte et al., 2010, Boudakov et al., 2007)
CD200Fc	↓CIA	↓proinflammatory mediators such as TNF-α, IL-1β and MMP13	(Simelyte et al., 2008)
		↓serum and PLN (peripheral lymph node) production of IFN-γ and TNF-α ↓production of autoantibody to collagen type II	(Gorczynski et al., 2002)
	↓ EAE	↓CD11b+macrophages	(Liu et al., 2010)
	↓SLE	↓IL-6 and IL-10 production by DCs	(Yin et al., 2016)
		↓Th17 differentiation ↑Treg induction (TGF-β-mediated) ↓DC migration	(Li et al., 2012)
	↓influenza-induced illness	↓CD4+, CD8+T cells (and their TNF and IFN-γ production) in the lungs and bronchoalveolar lavage (BAL) fluid	(Snelgrove et al., 2008)
Agonistic CD200R	↓CIA	↓serum and PLN production of IFN- γ and TNF-α	(Gorczynski et al., 2002)

		↓production of autoantibody to collagen type II	
	↓influenza-induced illness		(Snelgrove et al., 2008)
	↓EAU	↓IFN-γ mediated macrophage activation	(Copland et al., 2007)

1.9 Aims and rationale

Myeloid cells are the dominant cell type in atherosclerotic plaques and the CD200-CD200R axis has been shown to deliver an inhibitory signal to myeloid cells in various chronic inflammatory diseases. I hypothesised that the CD200-CD200R axis has a role in shaping myeloid responses in vascular diseases. In order to validate this, I first studied the role of CD200R agonism in vascular disease by administration of CD200-Fc in a murine perivascular injury model (Chapter 3). Secondly, I assessed the effects of CD200 deficiency in early and advanced stages of atherosclerosis development and on arterial myeloid cell subsets by applying 10-color flow cytometry using an optimised digestion protocol for murine aortic digestion (Chapter 4). I also assessed the role of CD200 deficiency on myeloid and non-myeloid cells and their phenotypic characteristics by applying 36-parameter mass cytometry in various tissues of ApoE-/- mice (Chapter 5). Subsequently, once a role for CD200R in atherosclerosis development and on myeloid cell phenotypes was established, I then assessed the role of CD200-CD200R on myeloid cell differentiation and myelopoiesis (Chapter 6).

Chapter 2 Materials and Methods

Chapter 2: Materials and Methods

2.1 Reagents

2.1.1 Primary antibodies

Table 2-1 Primary antibodies used in experiments. IHC = Immunohistochemistry, IF = Immunofluorescence/Confocal Microscopy, FC = Flow Cytometry, CyTOF=cytometry by time-of-flight, All = All methods listed.

Marker	Clone	Use	Source
ACTA2 155Gb	1A4	CyTOF	Sigma
B220 176Yb	RA3-6B2	CyTOF	FDM
B220 PerCPcy5.5	RA3-6B2	FC	Biolegend
CCR2 163Dy	SA203G11	CyTOF	Biolegend
CCR2 APC	SA203G11	FC	R&D systems
CD103 BV421	2E7	FC	Biolegend
CD117 (c-kit) BV785	2B8	FC	BD Biosciences
CD11b 148Nd	M1/70	CyTOF	FDM
CD11b BV711	M1/70	FC	Biolegend
CD11b PE	M1/70	FC	Biolegend
CD11b PerCP	M1/70	FC	Biolegend
CD11b PerCPcy5.5	M1/70	FC	Biolegend
CD11c	N418	IHC	BD Pharmigen
CD11c 142Nd	N418	CyTOF	FDM
CD11c APC	N418	FC	Biolegend
CD11c APC-Cy7	N418	FC	Biolegend
CD11c BV711	N418	FC	Biolegend
CD11c PerCPcy5.5	N418	FC	Biolegend
CD150 BV605	TC15-12F12.2	FC	Biolegend

CD16/32 APC-Cy7	2.4G2	FC	BD Biosciences
CD169 156Gd	3D6.112	CyTOF	Biolegend
CD19 149Sm	6D5	CyTOF	FDM
CD19 PerCP	6D5	FC	Biolegend
CD200	OX-90	IHC	AbD Serotec
CD200 169Tm	OX-90	CyTOF	Biolegend
CD200 APC	OX-90	FC	Biolegend
CD200R	OX-110	IHC	AbD Serotec
CD200R 171Yb	OX-110	CyTOF	Biolegend
CD200R PE	OX-110	FC	Biolegend
CD206 (MRC-I)	MR5D3	IHC	AbD Serotec
CD206 158Gd	C068C2	CyTOF	Biolegend
CD206 APC	C068C2	FC	Biolegend
CD3 FITC	17A2	FC	Biolegend
CD3 PerCPcy5.5	17A2	FC	Biolegend
CD31 (PECAM-1) 154Sm	390	CyTOF	Biolegend
CD31 (PECAM-1) BV605	390	FC	Biolegend
CD34 FITC	RAM34	FC	eBiosciences
CD4 172Yb	RM4-5	CyTOF	FDM
CD4 BV421	RM4-5	FC	Biolegend
CD4 PerCPcy5.5	RM4-5	FC	Biolegend
CD45 147Sm	30-F11	CyTOF	FDM
CD45 Alexa700	30-F11	FC	Biolegend
CD45 APC	30-F11	FC	Biolegend
CD45 APC-Cy7	30-F11	FC	Biolegend
CD45 BV421	30-F11	FC	Biolegend
CD45 BV605	30-F11	FC	Biolegend
CD45 BV711	30-F11	FC	Biolegend
CD45 FITC	30-F11	FC	Biolegend

CD45 PE	30-F11	FC	Biolegend
CD45 PECy7	30-F11	FC	Biolegend
CD45 PerCP	30-F11	FC	Biolegend
CD45 PerCPcy5.5	30-F11	FC	Biolegend
CD64 151Eu	X54-5/7.1	CyTOF	FDM
CD64 APC	X54-5/7.1	FC	Biolegend
CD68	FA-11	IHC	AbD Serotec
CD68 175Lu	FA-11	CyTOF	Biolegend
CD68 PECy7	FA-11	FC	Biolegend
CD8 BV711	53-6.7	FC	Biolegend
CD86 167Er	PO-3	CyTOF	Biolegend
CD86 FITC	PO-3	FC	Biolegend
CD8a 168Er	53-6.7	CyTOF	FDM
CX3CR1 146Nd	SA011F11	CyTOF	Biolegend
DC-SIGN (CD209) 166Er	22D1	CyTOF	eBiosciences
DC-SIGN (CD209) PE	5H10	FC	Biolegend
ERK/pERK	E10	WB	Cell signalling
ERK1/2 Alexa 647	20A	FC	BD Biosciences
F4/80 159Tb	BM8	CyTOF	FDM
F4/80 BV605	BM8	FC	Biolegend
F4/80 PE	BM8	FC	Biolegend
FcεRIα 144Nd	MAR-1	CyTOF	Biolegend
FcεRIα PerCPcy5.5	MAR-1	FC	Biolegend
Gr-1 PE	RB6-8C5	FC	FDM
Gr-1141Pr	RB6-8C5	CyTOF	Biolegend
IL-4R 143Nd	I015F8	CyTOF	Biolegend
iNOS (NOS2)	Polyclonal	IHC	Abcam
iNOS (NOS2) 161Dy	CXNFT	CyTOF	FDM
Isotype control (Rabbit IgG)	Polyclonal	IHC	Abcam

Isotype control (Rat IgG1)	4639	IHC	AbD Serotec
Isotype control (Rat IgG2a κ)	R35-95	IHC	AbD Serotec
Ki-67	Polyclonal	IHC	Abcam
Ki-67 162Dy	B56	CyTOF	FDM
Ki-67 Pacific Blue	B56	FC	Biolegend
Ly6C 150Nd	HK1.4	CyTOF	FDM
Ly6C PECy7	HK1.4	FC	Biolegend
Ly6G APC	1A8	FC	Biolegend
MerTK 170Er	Polyclonal	CyTOF	R&D
MerTK biotin	Polyclonal	FC	R&D
MerTK PE	108928	FC	R&D
MHCII 174Yb	M5/114.15.2	CyTOF	FDM
MHCII BV421	M5/114.15.2	FC	Biolegend
MHCII FITC	M5/114.15.2	FC	Biolegend
NK1.1 (CD161) 165Ho	PK136	CyTOF	FDM
NKp46 153Eu	29A1.4	CyTOF	FDM
NKp46 PerCPcy5.5	29A1.4	FC	Biolegend
ROR- γ 164Dy	Q21-559	CyTOF	BD Biosciences
Sca-1 Pacific Blue	D7	FC	Biolegend
Siglec H 173Yb	551	CyTOF	Biolegend
SMC α-actin	1A4	IF	Sigma Aldrich
STAT5 Alexa 647	47/Stat5 (pY694)	FC	BD Biosciences
STAT6 Alexa 647	18/P-Stat6	FC	BD Biosciences
TCR γδ 145Nd	GL3	CyTOF	Biolegend
TER-119 PE	TER-119	FC	Biolegend
TER-119 PerCPcy5.5	TER-119	FC	Biolegend

2.1.2 Secondary antibodies

Table 2-2 Secondary antibodies and labels used in experiments. IHC = Immunohistochemistry, FC = Flow Cytometry, CyTOF=cytometry by time-of-flight.

Name of reagent	Reagent type	Use	Source
163Dy APC	Secondary antibody	CyTOF	FDM
Biotinylated Goat Anti-Hamster IgG antibody	Secondary antibody	IHC	AbD Serotec
Biotinylated Rabbit Anti-mouse IgG antibody	Secondary antibody	IHC	AbD Serotec
Biotinylated Rabbit Anti-Rat IgG Antibody	Secondary antibody	IHC	AbD Serotec
Rat Anti-mouse CD16/32	Mouse Fc block	FC	BD Pharmingen
Streptavidin APCy7	Streptavidin	FC	

2.1.3 List of buffers and solutions

Table 2-3 Buffers and solutions used in experiments.

Name of reagent	Composition
10% buffered formalin	100 ml Formaldehyde (37-40%) 900 ml Distilled water 4.0 g NaH2PO4 6.5 g Na2HPO4 (anhydrous)
10x PBS (pH 7.4)	137 mM NaCl, 2.7 mM KCl, 4.3 mM Na2HPO4, 1.47 mM KH2PO4 in H_20
50x TAE	242g Tris-base, 57.1ml Glacial Acetic Acid, 18.6g EDTA in dH_20
FACS buffer	5% w/v foetal calf serum (PAA, UK) in 1x PBS
Foxp3/Transcription factor staining set	Fixation/Permeabilization concentrate (4x) diluted with Fixation/Permeabilization Diluent
IC fixation buffer	Aqueous buffered solution containing 4% v/v paraformaldehyde
Oil red O solution	1% w/v Oil red O in 100% isopropanol
Dextrin solution	1% w/v dextrin
Working solution	3:2 (Oil red O: Dextrin solution)
Red blood cell (RBC) lysis buffer	8.3g/L ammonium chloride in 0.01 M Tris-HCl buffer
Roswell Park Memorial Institute Medium (RPMI) 1640	Contains 2 mM L-glutamine and 71mM sodium chloride (as specified by manufacturer)

2.2 Maintenance of animals

ApoE-/- mice on a C57BL/6 background were purchased from Charles River Laboratories (UK) and bred in-house. Four-week-old mice were weaned and maintained on a normal chow diet.

CD200+/- embryos were received from MERCK. The CD200+/- embryos were put into B6 pseudo-pregnant females; heterozygous F1 (first filial generation) progenies were inter-crossed to obtain CD200-/- mice and screened by polymerase chain reaction (PCR). The ApoE-/-CD200-/- mice developed normally, although on a high fat diet (HFD), they seemed to develop more severe dermatitis compared to ApoE-/-.

In several experiments, normal chow diet was replaced at 8 weeks of age for a duration of 12 weeks, with a cholate-free HFD manufactured by Special Diets Services (Essex, UK), consisting of (w/w) cocoa butter (15%), cholesterol (0.25%), maize starch (10%), casein (20%), sucrose (40.5%), cellulose (5.95%), corn oil (1%), 50% choline chloride (2%), methionine (0.2%) and mineral mixture (5.1%).

All experimental animal procedures were approved by the local ethical review process and performed according to United Kingdom Home Office guidelines.

2.2.1. Generation of ApoE-/-CD200-/- mice

ApoE-/- mice were bred with CD200-/- mice to generate ApoE-/-CD200-/- mice. As the parents of F1 were knockout for one gene and wild type for the other, all the offspring were heterozygous for both genes (ApoE+/-CD200+/-). Mice from the F1 generation were then bred to produce several genotypes. Mice from the F2 generation, that were already double knockout or knockout for ApoE and heterozygous for

CD200, were put together for breeding to increase the chances of producing more double knockout mice, and eventually an entire colony of ApoE-/-CD200-/- mice was produced. Mice that were knockout for ApoE and wild type for CD200 were kept as littermate controls. These mice were maintained as described above (section 2.2) (Figure 2.1).

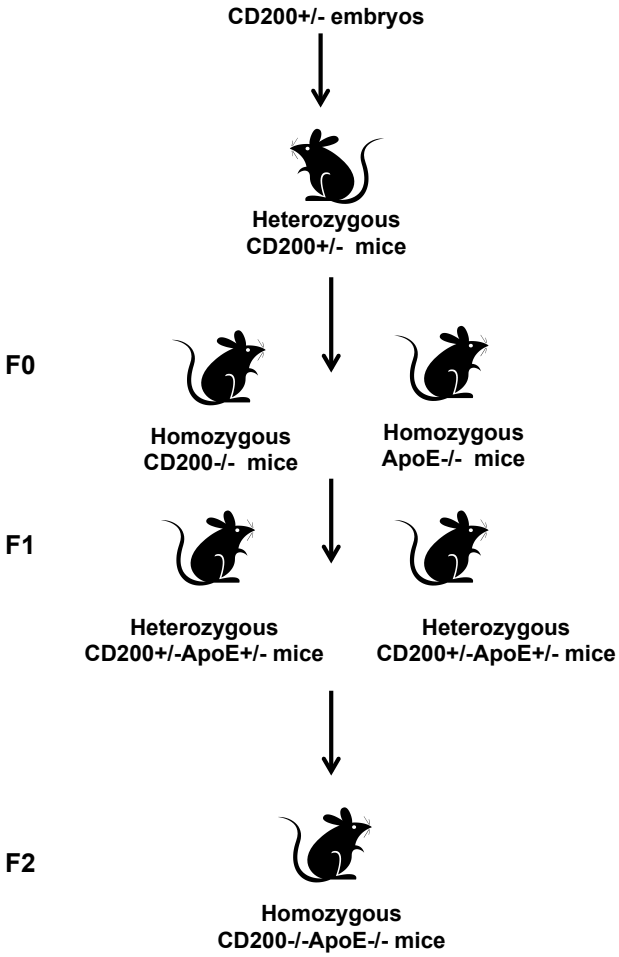


Figure 2.1 Breeding strategy to generate ApoE-/-CD200-/- mice. Heterozygous CD200 mice were rederived and crossed with each other. Homozygous CD200-/- and ApoE-/- mice were then crossed to generate CD200-/-ApoE-/- mice. F-numbers represent the breeding generation.

2.2.2 Genotyping

2.2.2.1 DNA extraction and PCR

Ear tissues were collected into 0.5 ml tubes and DNA was extracted using the REDExtract-N-Amp™ Tissue PCR Kit (Sigma-Aldrich) according to manufacturer's instructions. In brief, 25µl of the extraction solution and 5.25µl of the tissue preparation solution were added to the tissues. After the tubes were vortexed, they were incubated at room temperature for 10 minutes and then at 95^{o}C for 3 minutes. Finally, 25µl of neutralizing solution B was added and the tissues were stored at 4^{o}C. PCR was run according to the REDExtract-N-Amp™ Tissue PCR Kit (Sigma-Aldrich) and then the PCR amplification reaction was run on a DYAD Peltier Thermal Cycler (Bio-Rad, UK). Then, the samples were run on a 1.5% agarose gel at 100 volts and imaged using Molecular Imager Gel Doc XR+ machine and Image Lab software (Bio-Rad, UK). PCR primers, PCR master mix and PCR cycling conditions to screen for CD200, are listed in Tables 2.4-2.6. Homozygous ApoE+/+ mice would produce a band of 200bp; homozygous ApoE-/- mice would produce a 150bp band while heterozygous ApoE+/- mice would produce both the 150bp and the 200bp bands. Homozygous CD200+/+ mice would produce a single band of 1000bp, homozygous CD200-/- would produce a single band of 1300bp while heterozygous CD200+/- mice would produce both the 1300bp and 1000bp bands (Figure 2.2).

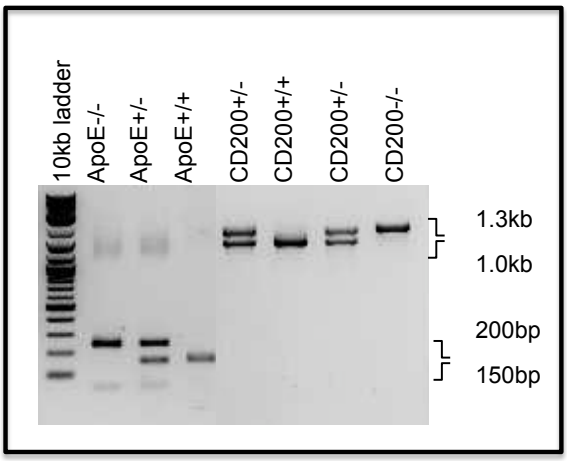


Figure 2.2 Screening for ApoE and CD200 deficiency.

Table 2-4 Sequences of primers used for genotyping.

Gene		Sequence
ApoE	Common	GCCTAGCCGAGGGAGAGCCG
	Wild-type	TGTGACTTGGGAGCTCTGCAGC
	Mutant	GCCGCCCCGACTGCATCT
CD200	Forward primer (FP)	GCCCAGAAATGGTCA-CCTAC
	Reverse primer (RP)	GTAGAAGATCCCTGCATCCAT-CAG

Table 2-5 PCR master mixes for genotyping ApoE and CD200.

ApoE	CD200
REDExtract-N-Amp PCR Reaction Mix 5µl	REDExtract-N-Amp PCR Reaction Mix 5µl
Common primer 1µl	FP primer 1µl
Wild-type primer 1µl	RP primer 1µl
Mutant primer 1µl	Nuclease Free Water 1µl
Tissue extract 2µl	Tissue extract 2µl

Table 2-6 Parameters for reverse transcription PCR of genotyping assays.

Step	ApoE	CD200
Initial denaturation	94°C for 3 minutes	95°C for 5 minutes
Denaturation	94°C for 30 seconds	95°C for 30 seconds
Annealing	60°C for 45 seconds (x30 cycles)	62°C for 30 seconds (x36 cycles)
Extension	72°C for 45 seconds	72°C for 1.3 seconds
Final extension	72°C for 10 minutes	72°C for 6 minutes

2.2.3 Perivascular collar-induced injury

ApoE-/- mice aged 22 weeks were anesthetised with isoflurane and a non-occlusive tygon collar (length: 2.5 mm; internal bore diameter: 510 μm; Cole-Parmer) was placed around the left carotid artery (Figure 2.3). Mice received 10mg/kg of CD200-Fc or control (mouse IgG1 kappa), both provided by Dr Thimothy Zeng, Biogen Idec. Inc. (Table 2.7), intraperitoneally, three times per week for three weeks. Subsequently, mice were euthanised with a barbiturate overdose. Following perfusion with saline, both carotid arteries (the left perivascular collar-treated and the right contralateral artery) were blunt dissected, and placed in optimal cutting temperature (OCT) embedding medium, snap-frozen and stored at -80^{o}C.

Individual animals received appropriate doses of CD200-Fc and IgG control according to their weight. CD200-Fc was received from Biogen in citrate buffer and IgG control in phosphate-buffered saline (PBS) buffer. The dose for each mouse was calculated as follows: (10mg/kg) x weight of the mouse x 9 doses of the drug / concentration of the drug, and then the drugs were diluted into 1mg/ml working stock so that both the CD200-Fc and the IgG control were composed of 16.6% of citrate and 83.3% of PBS to ensure that both reagents were in identical citrate/PBS solution (Table 2.7).

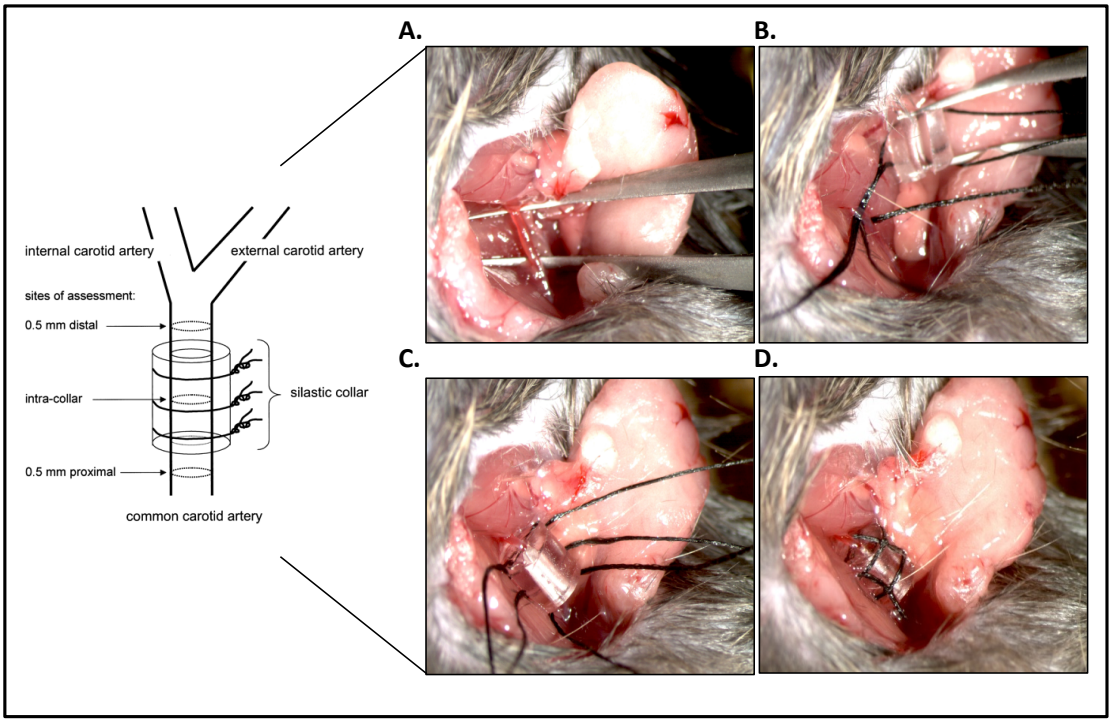


Figure 2.3 Surgical placement of a perivascular collar on a mouse carotid.A) Exposure of left carotid artery B) passing of the ligatures under the vessel C) placement of the collar onto the vessel, and D) securing the collar with ligatures.

Table 2-7 Biologic reagents used for the fusion protein experiments.

Reagent	Stock	Suspension	Final
muCD200-agly muIgG (Biogen Idec Inc.)	6.0mg/ml	20mM citrate 100mM Nacl pH 6	1mg/ml pH 8.3
MOPC-21 (CHO derived) (Biogen Idec Inc.)	3.3mg/ml	PBS (sterile) 310 mOsm pH 7	1mg/ml pH 7

2.3 Tissue preparation

Mice were euthanised with intra-peritoneal (i.p) barbiturate overdose from chow-diet fed ApoE-/- and ApoE-/-CD200-/- mice at 15, 20 and 27 weeks of age and from HFD-fed ApoE-/- and ApoE-/-CD200-/- mice at 20 weeks of age (see section 2.2 for details on animal maintenance). The weights of the mice were recorded and blood

was collected by cardiac puncture. Hearts, aortas and other tissues including kidney, liver and spleen were perfused with 8ml sterile saline via a cannula inserted into the left ventricle (outflow via an incision in the right atrium). Tissues (carotids, hearts) were then frozen in OCT compound and stored at -80°C. In some cases some of the tissues (blood, bones, aorta, spleen and lymph nodes) were used for flow cytometry or CyTOF (see section 2.6 and 2.7) or were snap frozen and stored at -80°C.

In several cases, blood was spun down at 6000 rpm for 30 minutes at 4°C in a Heraeus Primo R centrifuge (Thermo Scientific) in order to separate the serum which was then collected in 100µl aliquots and stored at -80°C.

OCT-embedded tissues were cryosectioned in a CM1860 UV cryostat (Leica, Germany) and the sections were collected on Superfrost Plus Adhesion microscope slides (Thermo Scientific, USA). For aortic roots, five-micrometer cryosections were taken of the aortic root for the entire region of the valve leaflets and every 20^{th} section at 100 µm intervals was stained with Oil red O (ORO) and counterstained with haematoxylin (as described in section 2.4), while other slides were reserved for further staining. For carotid arteries, both the perivascular-collar treated and the contralateral carotid arteries were taken and frozen in OCT. For perivascular-collar treated carotid arteries, five-micrometer sections were collected distal to the collar. Five sections were collected on each slide and an average of 70 slides were collected. The first eight alternate slides were then stained with Accustain elastic stain kit (see section 2.4), while other slides were reserved for further staining. For contralateral arteries, 60 five-micrometer cryosections were collected at 300µm intervals and stored at -20°C or -80°C.

2.4 Histology

2.4.1 Oil Red O staining

Five-micrometer cryosections were taken of the aortic root for the entire region of the valve leaflets. Every 20th section was stained for Oil red O (ORO) to highlight lipid. Cryosections were rinsed in water and then rinsed in 60% isopropanol for 30 seconds before staining with ORO working solution (3 parts 1% Oil Red O in isopropanol solution to 2 parts 1% dextrin in water solution) for 15 minutes. Following washing in water, sections were counterstained with haematoxylin and mounted using Kaiser's Glycergel mounting medium (which was melted at 50°C in a water bath, Merck Millipore, Germany) and the slides were left overnight for the media to harden.

2.4.2 Carotid lesion quantification: Elastin Van Gieson staining

For the collar-treated carotid artery, five-micrometer cryosections were taken of the carotid tissue and were stained with the Elastic Van Gieson stain, according to manufacturer's instructions (Sigma-Aldrich). In brief, slides were fixed with paraformaldehyde (PFA) for 8 minutes and then stained in working elastin solution (consisting of haematoxylin, ferric chloride, iodine solution and deionised water) for 10 minutes. Slides were differentiated in working ferric chloride solution for a maximum of three minutes. Slides were stained with Van Gieson solution for 30 seconds and dehydrated in ethanol and xylene, followed by mounting in Histomount. Slides were left overnight for the media to harden.

2.4.3 Immunohistochemistry

Immunohistochemistry was performed using standard ABC protocols. The slides were fixed in acetone and blocked with 10% normal serum (species of serum was the same as the host species of the secondary antibody). Endogenous avidin and biotin were blocked using undiluted Avidin and Biotin solutions (blocking kit from Vector Laboratories Inc., California, USA). Slides were then incubated with a primary antibody (see Table 2.1). Following a wash in PBS, slides were incubated with a biotinylated secondary antibody (see Table 2.2). After washing, endogenous peroxidase activity in the sections was inactivated using 0.3% hydrogen peroxide (Sigma-Aldrich Inc.). The slides were then incubated with Avidin-Biotin peroxidase complexes (ABC) (Vector's ABC-Elite-Standard Kit for Peroxidase from Vector Laboratories Inc.). Bound peroxidase was detected following incubation of the tissues with DAB solution (3, 3'-diaminobenzidine, Vector Laboratories Inc.) and the cell nuclei were counterstained with haematoxylin. For all primary antibodies used, staining using an appropriate isotype matched control was performed on a consecutive section.

2.4.3.1. Optimising immunohistochemical staining

Carotid sections were stained with antibodies against CD200 (Figure 2.4), CD200R, CD11c and ki-67 (Figure 2.5). Several concentrations were tested and the optimal concentration was found to be 5μg/ml for the antibodies against CD200, CD200R and CD11c, while 1μg/ml was the optimal concentration for the anti-ki-67 antibody. To confirm the specificity of the antibody against CD200, kidneys were harvested from

ApoE-/- and ApoE-/-CD200-/- mice and stained with an antibody for CD200 (Figure 2.4).

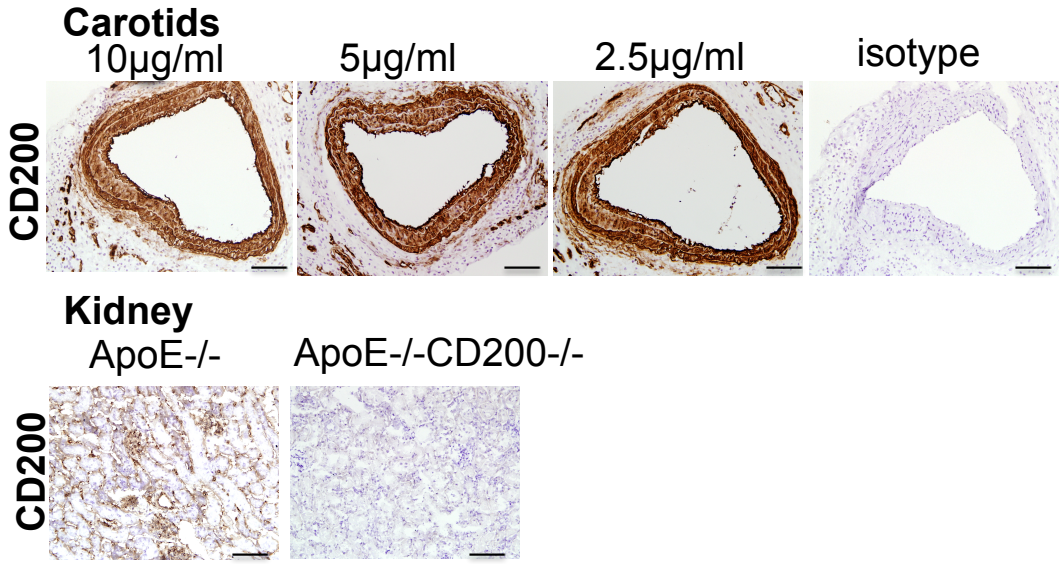


Figure 2.4 Optimisation of staining with an antibody against CD200. Carotid sections were stained with several concentrations with an antibody against CD200. Rat IgG2a is the isotype control for CD200. Scale bars = 100µm.

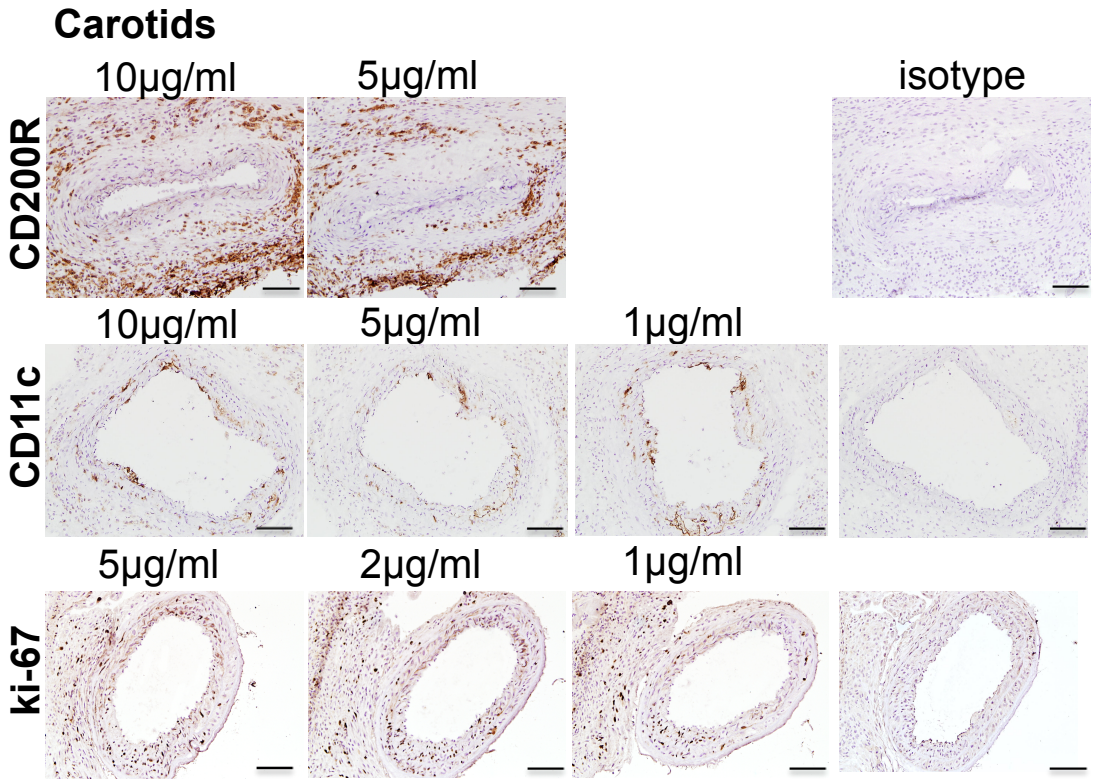


Figure 2.5 Optimisation of staining with antibodies against CD200R, CD11c and ki-67. Carotid sections were stained with several concentrations with an antibody against CD200R, CD11c and ki-67. Rat IgG2a is the isotype control for CD200R. Hamster IgG is the isotype control for CD11c and rabbit IgG is the istype control for ki-67. Scale bars = 100µm.

2.4.4 Haematoxylin and eosin staining

Haematoxylin and eosin (H&E) staining was performed using a Tissue Tek Prisma/Film automated slide stainer (Sakura). Slides were fixed in 10% (vol/vol) buffered formalin for 10 minutes, rinsed in distilled water, and then stained with Harris Hematoxylin for 8 minutes, washed in running tap water for 5 minutes, and differentiated with 0.3% acid alcohol for 2 minutes and rinsed in distilled water. The slides were counterstained with eosin for 2 minutes before being rinsed in distilled water. For necrosis quantification, in the aortic root only areas larger than 3000µm^2 were counted and in the carotid artery only areas larger than 300µm^2 were counted (as described in section 2.5).

2.4.5 Masson Trichrome staining

Staining for collagen in aortic root and carotid artery sections was performed using the Masson Trichrome stain kit from TCS biosciences (UK) according to the manufacturer's instructions. The slides were air dried for 30 minutes, fixed in 10% buffered formalin for 10 minutes and hydrated in distilled water for 5 minutes. The slides were stained with Harris haematoxylin for 8 minutes, washed in running tap water for 5 minutes before being placed Ponceau2R/Acid Fuschin stain (as supplied by the manufacturer) for 5 minutes to give the red colour. The slides were washed in distilled water before being differentiated with phosphotungstic acid (made from 1 part phosphotungstic acid, 1 part phosphomolybdic acid and 2 parts distilled water) for 30 seconds. Following a wash in distilled water, the slides were counterstained in Light Green stain (as supplied by the manufacturer) for 5 minutes, rinsed again in distilled water. Collagen was stained green, cell nuclei were purple and, muscle was red.

2.5 Image analysis and quantification

Images were captured using the Olympus DP Controller software at x10 or x20 magnification to capture entire sections for quantitative analysis. Slides were imaged under identical lighting, microscope and camera conditions and carotid and aortic root sections were coded and analysed blind. The ProgRes CapturePro image analysis software (version 2.5.2.0, Jenoptik, Germany) software was used to quantify the intima:media ratio of elastin-stained sections. The area between the internal and external elastic arteries was taken as the media area and the intimal area was

calculated by subtracting the lumen area from the internal elastic lamina area. The intimal:media ratio (IMR) was then calculated by dividing the intima area by the media area. The IMR measurements were then averaged for each mouse. For necrosis quantification, necrotic areas were considered as H&E-free regions absent of the pink eosin stain and cell nuclei stained by haematoxylin. In the aortic root only areas larger than 3000μm^2 were counted and in the carotid artery only areas larger than 300μm^2 were counted. Clemex software was used to quantify immunopositive areas of immunohistochemically stained sections, by selecting the lesion area and measuring the percentage and size of absolute areas positively stained within the lesion.

2.6 Flow cytometry of murine tissues

Mice were euthanized and several tissues, including spleen, subiliac (SILNs) and para-aortic (PALNs) lymph nodes, bones, blood and aortas, were collected from chow-diet fed ApoE-/- and ApoE-/-CD200-/- mice at 15, 20 and 27 weeks of age and from HFD ApoE-/- and ApoE-/-CD200-/- mice at 20 weeks of age.

For spleen, bones and blood, erythrocytes were lysed with red blood cell (RBC) lysis buffer (Sigma Aldrich). Bones were prepared as described in section 2.9. Single suspensions from spleen and lymph nodes were prepared by mashing the tissues through a 70μm cell strainer.

Aortas, including the aortic arch, thoracic and abdominal portions were incubated with an enzyme cocktail containing 230U/ml collagenase I, 144U/ml collagenase XI, 64U/ml hyalurodinase, 61U/ml DNase, 2mM CaCl2, 1mg/ml soybean trypsin inhibitor (Sigma-Aldrich) in FACs buffer for 1 hour, 2 hours or two 30-minute digestions at 37^{o}C. In some experiments 2.5U/ml or 1.25U/ml of elastase (Sigma-

Aldrich) was added to the digestion mixture. In some experiments, aortas from two mice were pooled. Post-digestion, single cell suspensions were obtained by mashing aortas through a 70μm cell strainer. Aortic digestion cocktail was optimised as described in section 2.6.1.

Next, cells were resuspended in PBS, counted on a hematocytometer and resuspended again in FACs buffer. Fc receptors were blocked by incubation with Fc block for 10-20 minutes. Cells were then incubated with primary antibodies for 40 minutes at 4°C in the dark, washed twice, and if required, incubated with secondary antibodies for an additional 30 minutes. Intracellular staining was performed using cell fixation/permeabilization reagents from eBioscience (see Table 2.1.3). In some cases, cells were additionally stained with the Live/Dead Fixable Dead Cell Stain kit according to manufacturer's instructions (Invitrogen). Data were acquired using Canto LSR flow cytometer (BD) and analysed with Flow Jo software (TreeStar).

2.6.1 Optimising conditions for enzymatic digestion of mouse aorta

Whole aortas were harvested from male ApoE-/- mice aged 25-54 weeks (Figures 2.6A-F). Single cell suspensions were obtained by enzymatic digestion with the standard enzyme mix in the presence or absence of elastase.

An average total cell number of $1.9\pm0.06x10^6$ with an average cell viability of 48% was obtained from the digestion of each pair of aortas with the standard enzyme mix (Figure 2.6A). No significant changes in cell yields were observed in the presence of 2.5U/ml elastase ($1.85\pm0.13x10^6$) compared to the standard enzyme mix. Addition of elastase did not significantly affect the total proportion (58%) or number ($1.0\pm0.1x10^6$) of live cells (Figure 2.6A).

The proportion of total and live CD45+ cells in mouse aorta was then determined. Using the standard enzyme mix, live CD45+ cells comprised 8% of total cells corresponding to $0.16x10^6 \pm 0.06$ cells per a pair of aortas. The addition of elastase did not appear to have a considerable effect on the total and live leucocyte numbers (Figure 2.6D).

Next I assessed whether the number of total cells acquired following digestion with the standard enzyme mix increased with the age of the mice. The average cell number obtained from the aortas of older mice (>34 weeks) was $1.8 \pm 0.08x10^6$, while from younger mice (<34 weeks) it was $2.0 \pm 0.05x10^6$. The average cell viability for older mice was 46% (Figure 2.6B), whereas for younger mice, the average cell viability was 50% (Figure 2.6C). Elastase addition resulted in 62% live cells in older mice (Figure 2.6B), and 53% live cells in younger mice (Figure 2.6C). Similar patterns were observed for CD45+ and live CD45+ cells (Figures 2.6E-F).

Since the addition of 2.5U/ml of elastase to the standard enzymatic mixture did not produce any differences in terms of leucocyte yield or viability, I halved its concentration to examine further whether the balance of enzymes in the mix was important for cell yields (Figures 2.7A-B). However, 1.25U/ml of elastase did not seem to influence the percentage (11%) or number (0.17 ± 0.12 x10^6) of live CD45+ cells (Figure 2.7B). Additionally, an enzymatic mixture containing 2.5U/ml elastase and half dosage of collagenase XI (72U/ml) did not improve cell viability and yield (Table 2.8).

To determine whether length of incubation of mouse aortas with the cocktail of enzymes affects cell yield or viability, cell numbers were compared following incubation of the aortas with the standard enzyme mix for: 1 hour, 2 hours or two 30-minute digestions (in which fresh enzyme mix was added after the first 30-minute

incubation). An incubation time longer than one hour did not enhance cell viability and yield, and appeared to have the reverse effect instead (Figure 2.8).

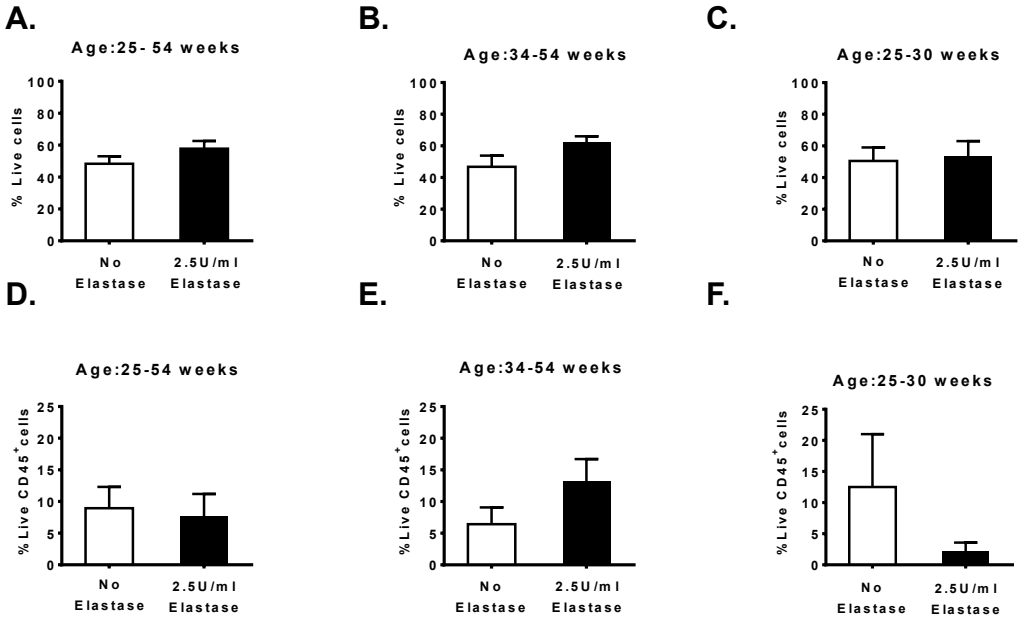


Figure 2.6 Addition of elastase to the standard enzyme mix does not affect leucocyte yield or viability. Whole aortas including aortic arch, abdominal and thoracic portions, were dissected from ApoE-/- mice. Aortas from two mice were pooled and treated with either the standard enzyme mix or standard enzyme mix with 2.5U/ml elastase added at 37^{o}C for 1 hour. Cells were stained with an antibody against CD45 (APC-Cy7) and a live/dead viability dye and analysed on a BD FACSCantoII. (A-C) Percentage of live cells in the aorta of ApoE-/- mice aged 25-54 (A; n=5), >34 (B; n=3) or <34 (C; n=2) weeks digested with standard enzyme mix (No elastase, white bars) or with standard enzyme mix supplemented with elastase (2.5U/ml elastase, black bars) (D-F) Percentage of live CD45+ cells in the aorta of ApoE-/- mice aged 25-54 (D) or >34 (E) or <34 (F) weeks digested with standard enzyme mix (No elastase, white bars) or with standard enzyme mix supplemented with elastase (2.5U/ml elastase, black bars). Bars show mean ± SEM, $p>0.05$, unpaired Student's t-test.

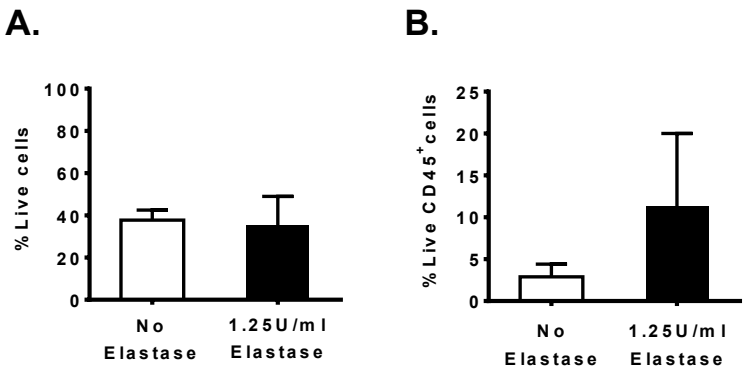


Figure 2.7 Halving the elastase concentration does not affect cell viability or cell yield. Whole aortas were dissected from ApoE-/- mice and treated with either the standard enzyme mix or standard enzyme mix with 1.25U/ml elastase at 37°C for 1 hour. Cells were stained with an antibody against CD45 (APC-Cy7) and a live/dead viability dye and analysed on a BD FACSCantoII. Graphs represent the percentages of (A) live cells and (B) live CD45+ cells in the aorta of ApoE-/- mice aged 25 and 34 weeks digested with standard enzyme mix (No elastase, white bars) or with standard enzyme mix supplemented with elastase (1.25U/ml elastase, black bars). Bars show mean ± SEM, $p>0.05$, n=2, unpaired Student's t-test.

Table 2-8 Halving the concentration of collagenase XI does not affect the effect of elastase on cell viability and yield. Whole aortas were dissected from ApoE-/- mice and treated with either the standard enzyme mix with 2.5U/ml elastase added or a modified standard enzyme mix with 72U/ml collagenase type XI and 2.5U/ml elastase 37°C for 1 hour (n=1). Cells were stained with an antibody against CD45 (PE) and a live/dead viability dye and analysed on a BD FACSCantoII using FlowJo software.

	Collagenase type XI concentration	
	144U/ml	72U/ml
Live cells (%)	51.1	41.6
CD45+cells (%)	16.6	11.3
Live CD45+cells (%)	10.3	5.49
Total number of cells ($x10^6$)	1.9	2.5
CD45+cells ($x10^6$)	0.3154	0.2825
Live CD45+cells ($x10^6$)	0.1957	0.13725

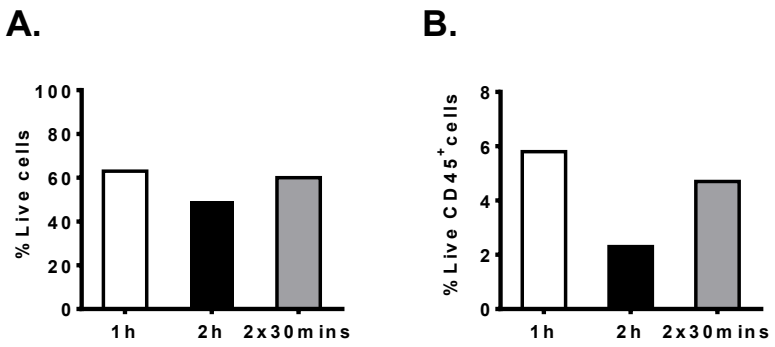


Figure 2.8 One hour incubation of murine aortas with an enzyme cocktail gives optimal cell yield and viability. Whole aortas were treated with the standard enzyme mix at 37°C for 1 hour, 2 hours or for two 30-minute digestion in which the enzymes mix was refreshed after the first 30-minute incubation. Cells were stained with an antibody against CD45 (APC-Cy7) and a live/dead viability dye and analysed on a BD FACSCantoII. Graphs represent the percentage of (A) live cells and (B) Live CD45+ cells are shown after digestion with standard enzyme mix for 1 hour (1h, white bar), 2 hours (2h,black bars) or with two 30-minute digestions (2x30mins, grey bars; n=1).

2.7 Single-cell mass cytometry (CyTOF)

2.7.1 Antibody conjugation

All preconjugated antibodies were purchased from DVS Sciences (Sunnyvale, CA). For other antibodies, conjugation was performed in house according to MAXPAR antibody labelling kit instructions (DVS Sciences). In brief, polymers were pre-loaded with Lanthanide, while antibodies were partially reduced. After Lanthanide-loaded polymers and partially reduced antibodies were purified, the antibodies were conjugated with the polymers. Finally the metal-conjugated antibodies were washed, recovered and stored at 4°C. Following conjugation, the antibodies were titrated for optimum working concentration.

2.7.2 Mass cytometry staining

Following cell preparation as previously described in section 2.6, cells were stained according to DVS staining protocols. In brief, cells were incubated with the Cell-ID Intercalator-103Rh for 15 minutes at room temperature, to discriminate dead from live cells. After cells were washed, they were incubated with Fc block for 10-20 minutes and then with metal-labelled antibodies for surface antigens for 30-40 minutes. The cells were washed, fixed and permeabilised with the Foxp3/Transcription Factor Staining Buffer Set (eBiosciences) according to manufacturer's instructions, and stained with antibodies against intracellular markers for 30 minutes at room temperature. Cells were then washed and stained with Cell-ID Intercalator-Ir overnight. Each sample was washed twice and adjusted to 2.5-5x10^5/ml cell concentration with Maxpar Water and filtered through blue-capped tubes.

In order to minimise cell variability, cells from spleen and lymph nodes were barcoded (meaning that samples from the same genotype were combined and treated as one sample to achieve consistency). For cell barcoding, cells were additionally incubated with barcodes (Pd104, Pd106, Pd108, Pd110) for 30 minutes at room temperature, and all barcoded samples were combined in one tube.

For quality control, EQ calibration beads were mixed with the cells. Samples were analysed on a CyTOF mass cytometer.

Normalised, background-subtracted and debarcoded FCS files were imported into Cytobank for single cell and population gating.

2.8 Analysis of murine serum cholesterol

Serum cholesterol levels from chow-diet fed ApoE-/- and ApoE-/-CD200-/- mice at 27 weeks of age were measured enzymatically using Infinity Total Cholesterol (Thermo Scientific), according to the manufacturer's instructions. In brief, murine serum was diluted by 1:5 and then the serial 1:2 dilutions were performed four times. Next, 200µl of the Infinity Cholesterol reagent (Thermo Scientific) was added to the samples and incubated for 10 minutes at 37^{o}C. A calibration sera (Randox Laboratories) with a known cholesterol concentration was used as a reference. The plate was read on a Multiskan plate reader (Thermo Scientific) at the 540 nm and 640 nm wavelengths.

2.9 *In vitro* cell culture

2.9.1 *In vitro* differentiation and stimulation of bone-marrow derived myeloid cells

ApoE-/- and ApoE-/-CD200-/- bone marrow-derived monocytes were polarised into M1 or M2 macrophages and dendritic cells according to established protocols (Fleetwood et al., 2007). Femurs and tibias were removed from chow-diet fed 15-27 week old mice or HFD -fed 20-week old mice. The surrounding muscle tissue was removed, and the bones were placed in 70% ethanol for one minute, and then moved to serum-free RPMI media (PAA, USA). Each end of the bones were carefully cut using dissecting scissors, and the BM was flushed out by an autoclavable 26G steel needle, attached to a 10ml syringe full of serum free RPMI media, and the cells

suspended in media. The cells were cultured in the presence of RPMI 1640 medium, supplemented with 10% heat-inactivated FCS, 2 mM GlutaMax-1, 100 U/ml penicillin, and 100 mg/ml streptomycin in the presence of M-CSF (100ng/ml) or GM-CSF (20ng/ml) in 90mm^2 bacterial dish for 6-8 days and refreshed every two days or murine Flt3 (200ng/ml) in a 6-well plate for 10 days without disturbing. Both adherent and nonadherent cells were collected. M-CSF-treated cells were stimulated with LPS (100ng/ml), IL-4 and IL-13 (20ng/ml) (M2 polarisation) or IFN-γ (10ng/ml) and LPS (100ng/ml) (M1 polarisation). GM-CSF and Flt-3- treated cells were stimulated with LPS (100ng/ml) for 16 hours.

2.10 Statistical analysis

Statistical analysis was performed using a Student's t-test, Mann-Whitney test or one-way analysis of variance (ANOVA) test with Bonferroni's multiple comparison tests, as appropriate using the GraphPad Prism 6 software. For data that passed a normality test, Student's t tests or one-way ANOVA were used as appropriate. Where data did not pass a normality test, Mann–Whitney U tests or Kruskal–Wallis (ANOVA) tests with Dunn's multiple comparison test were performed. Results were considered statistically significant where p-values were below 0.05.

Chapter 3 The effects of a CD200-Fc fusion protein in atherosclerosis

Chapter 3: The effects of a CD200-Fc fusion protein in atherosclerosis

3.1 Introduction

By administering CD200-Ig fusion proteins and agonistic antibodies to CD200R, the CD200-CD200R pathway has been manipulated for therapeutic purposes in various models of chronic inflammatory disease (Simelyte et al., 2008, Gorczynski et al., 2001, Copland et al., 2007, Liu et al., 2010).

Several groups have documented the beneficial effect of CD200-Fc treatment in collagen-induced arthritis (CIA). Administration of a CD200-Fc has been shown to reduce the severity of CIA and down regulated gene expression of proinflammatory mediators including, tumour necrosis factor (TNF)-α, interleukin (IL)-1β and matrix metalloproteinase (MMP)-13 without affecting the activity of T and B cells in the synovium (Simelyte et al., 2008). Similar results with either CD200-Fc or anti-CD200R treatment have been found by Gorczynski *et al.,* (Gorczynski et al., 2001). Additionally, administration of an anti-CD200R antibody (DX109) suppressed experimental autoimmune uveoretinitis (EAU) by reducing interferon (IFN)-γ mediated macrophage activation (Copland et al., 2007). Administration of CD200-Fc attenuated another autoimmune disease, experimental autoimmune encephalomyelitis (EAE) and diminished CD11b+ macrophage infiltration but did not affect immune T cell responses, indicating a role for innate rather than adaptive immune responses (Liu et al., 2010). Additionally, CD200 agonism has been shown to alleviate the severity of influenza infection (Snelgrove et al., 2008). Herein, I aim to explore the effects of a CD200-Fc protein in a model of carotid arterial injury in hypercholesterolemic mice.

3.2 Results

3.2.1 CD200-Fc treatment reduces neointima formation in a perivascular collar model

To assess the effect of the CD200R-CD200 interaction on vascular disease, I tested the effect of a recombinant fusion protein with murine CD200 extracellular domains attached to a murine IgG1-Fc portion (CD200-Fc), obtained from Biogen Inc, in a well characterised perivascular carotid collar-induced injury model, as described in Materials and Methods. Female ApoE-/- mice were treated intraperitoneally with CD200-Fc or an IgG1 control, three times per week for three weeks. During the three-week treatment, there was a decrease in body weight in IgG but not in CD200-Fc treated mice. However, this was not statistically significant beyond the first week of the treatment (Figure 3.1).

Carotids were snap frozen in optimal cutting temperature (OCT), cryosectioned and stained with Elastin-Van Gieson (EVG) stain (Figure 3.2A). Neointima formation, as assessed by the intima:media ratio (IMR), was decreased in CD200-Fc-treated compared to control-treated mice (0.69 ± 0.07 versus 0.49 ± 0.09, p=0.049) (Figure 3.2B). The intima area was also reduced following CD200-Fc treatment (33598 ± 3566 μm^2) compared to control treatment (27072 ± 3890 μm^2; p=0.23). The media area was unaffected by CD200-Fc treatment (50113 ± 3326 μm^2 versus 56461 ± 3768 μm^2; p=0.22) (Figure 3.2B). No neointima formation was observed in the uninjured contralateral artery.

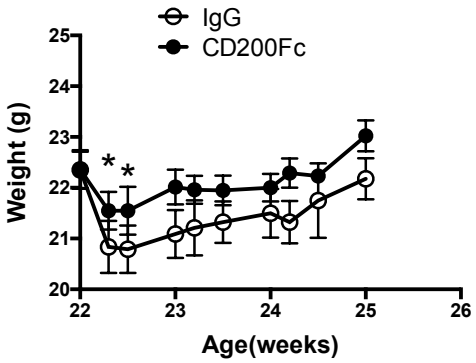


Figure 3.1 The weights of the ApoE-/- mice treated with IgG control or CD200-Fc during the three-week treatment. Female ApoE-/- mice aged 22 weeks were anesthetised with isoflurane and a non-occlusive tygon collar was placed around the left carotid artery. Mice received 10mg/kg of CD200-Fc or control (mouse IgG1 kappa, clone MOPC-21) three times per week for three weeks. Weights were measured in grams, graphs show mean ± SEM, n=8-15, * p <0.05.

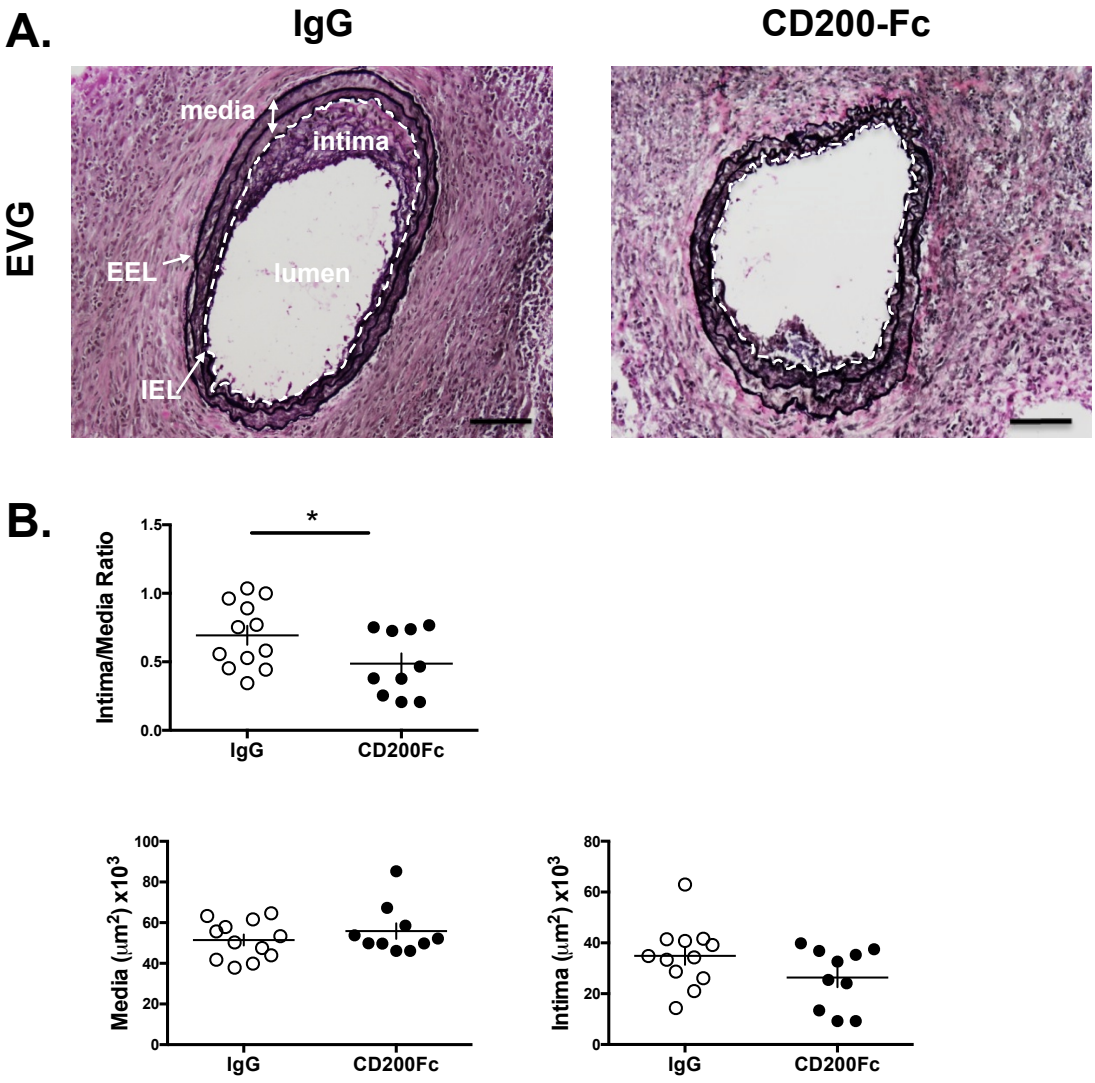


Figure 3.2 CD200-Fc fusion protein treatment inhibits collar induced carotid atherosclerosis in ApoE-/- mice. Female ApoE-/- mice aged 22 weeks were anesthetised with isoflurane and a non-occlusive tygon collar was placed around the left carotid artery. Mice received 10mg/kg of CD200-Fc or control (mouse IgG1 kappa, clone MOPC-21) three times per week for three weeks. Carotids were snap frozen in OCT, cryosectioned and stained with Elastin-Van Gieson stain. Quantification of lesion size was performed using ProgRes CapturePro image analysis software. (A) Representative photomicrographs of carotid artery sections stained with elastin Van Gieson (EVG). Dotted lines show internal elastic lamina (IEL). Scale bars = 100μm. (B) Graphs show intima:media ratio, media and intima area from carotids of IgG (control) or CD200Fc treated ApoE-/- mice. Individual dots represent individual mice. Horizontal line denotes group mean. Graphs show mean ± SEM, n=10-12, unpaired Student's t-test, * $p < 0.05$.

3.2.2 CD200-Fc treatment increases lesional M2 macrophage accumulation

To assess the macrophage content of the lesions, perivascular collar-treated carotid sections were stained with an antibody against CD68, a scavenger receptor that is widely used as a macrophage marker (Figure 3.3A). Interestingly, the lesion area staining positive for CD68 was higher in ApoE-/- mice treated with CD200-Fc compared to control-treated ApoE-/- mice when expressed as a fraction of lesion size (8.5 ± 1.385% versus 18.23 ± 12.82%, p=0.0057) (Figure 3.3B) but not when expressed as an absolute area (3096 ± 734.8 μm^2 versus 5067 ± 1079 μm^2; p=0.13) (Figure 3.3C). The carotid sections were also stained with antibodies against the M2 macrophage marker, CD206 (Figure 3.4A) and the M1 macrophage marker, iNOS (Figure 3.5). CD200-Fc treatment could significantly increase the CD206+ lesional area both when expressed as a fraction of lesion size (1.508 ± 0.3625% versus 3.355 ± 0.7458%, p=0.0327) (Figure 3.4B) and when expressed as an absolute area (443.6 ± 104.7 μm^2 versus 1303 ± 395.6 μm^2, p=0.04) (Figure 3.4C). No change was observed in iNOS+ lesional area (Figure 3.5).

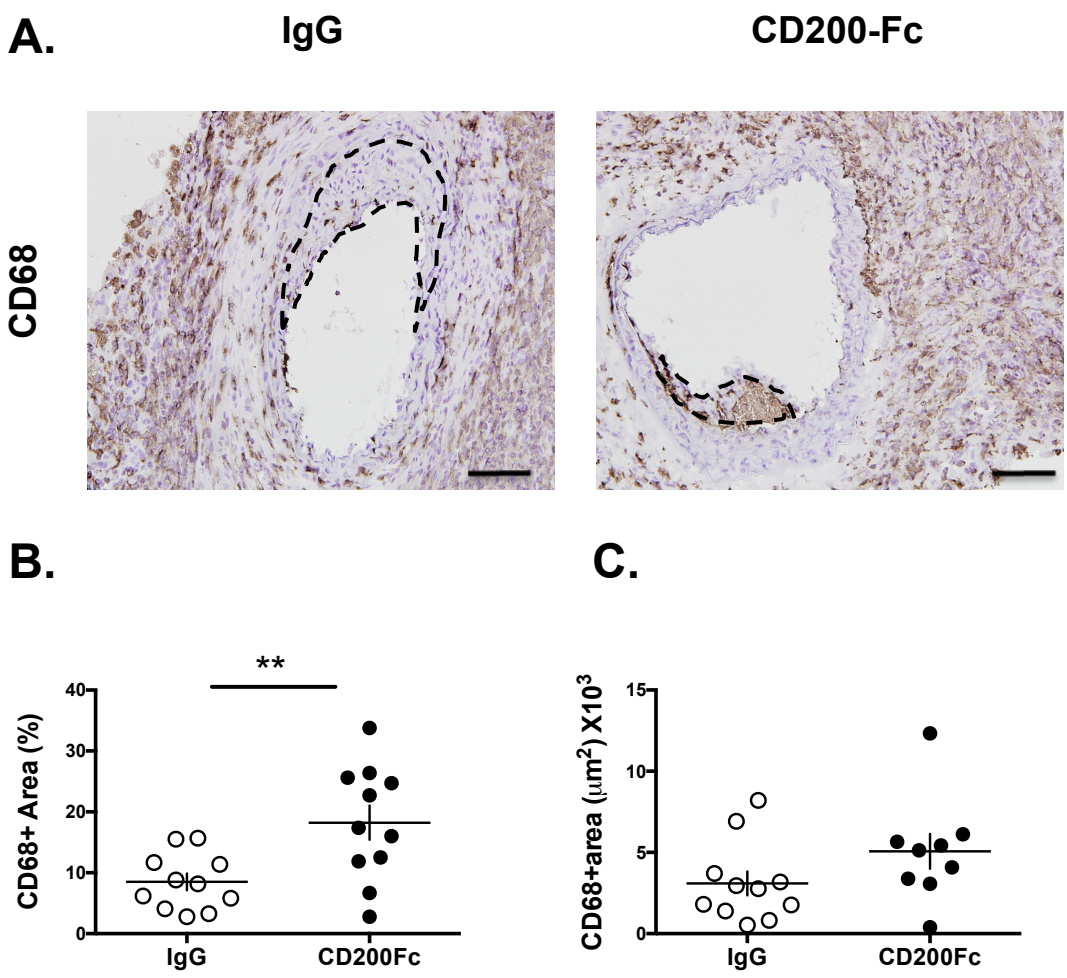


Figure 3.3 CD200-Fc fusion protein increases lesional CD68+ macrophage content in a perivascular carotid collar model in ApoE-/- mice. Female ApoE-/- mice aged 22 weeks were anesthetised with isoflurane and a non-occlusive tygon collar was placed around the left carotid artery. Mice received 10mg/kg of CD200-Fc or control (mouse IgG1 kappa, clone MOPC-21) three times a week for three weeks. Carotids were snap frozen in OCT, cryosectioned and stained with an antibody against the macrophage marker CD68. Quantification was performed using Clemex software. (A) Representative photomicrographs of injured carotid arteries from ApoE-/- mice treated with IgG (control) or CD200-Fc fusion protein stained with an antibody against the macrophage marker CD68 (brown staining) and with haematoxylin to highlight nuclei. Dotted lines show lesional areas. Scale bars = 100μm. Graphs show the (B) percentage and (C) absolute lesion area (μm^2) staining positive for CD68 in IgG- (control) or CD200-Fc-treated injured carotids. Individual dots represent individual mice. Horizontal line denotes group mean. Graphs show mean ± SEM, ** $p<0.01$, n=11, unpaired Student's t-test.

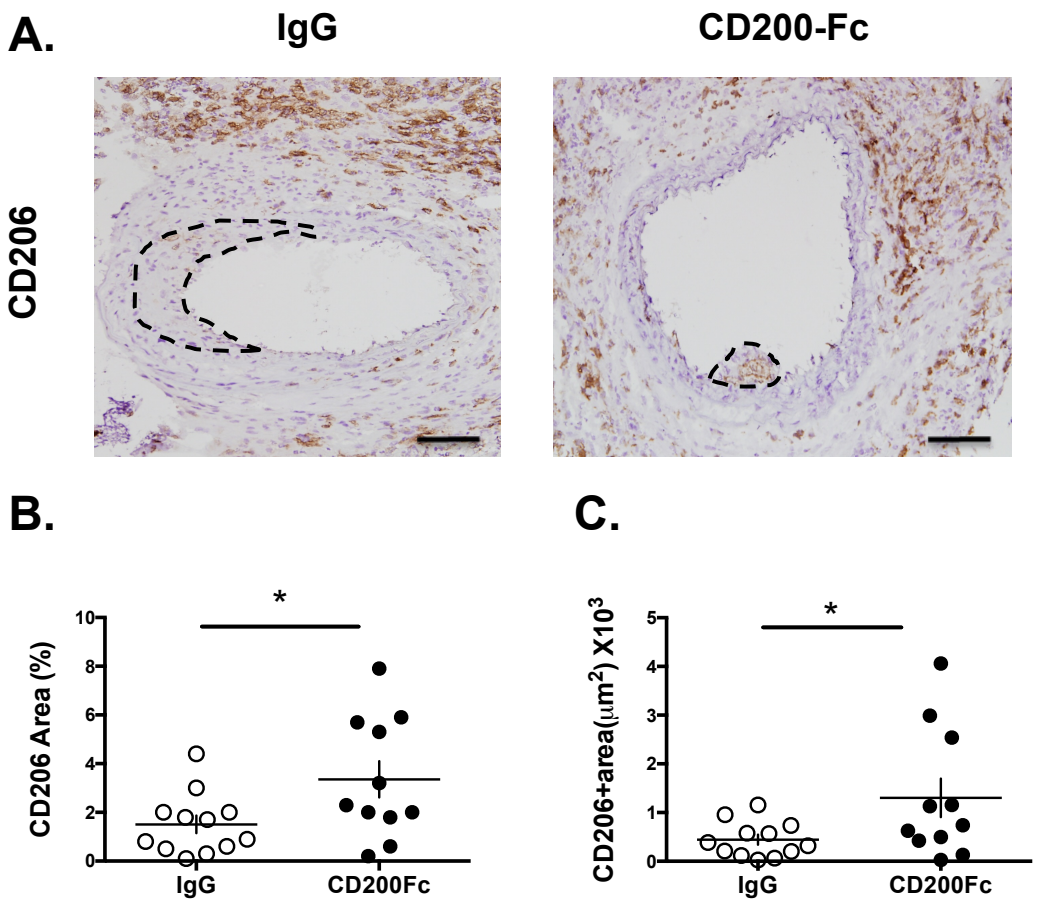


Figure 3.4 CD200-Fc fusion protein treatment increases lesional CD206+ macrophage content in a perivascular carotid collar injury model in ApoE-/- mice. Female ApoE-/- mice aged 22 weeks were anesthetised with isoflurane and a non-occlusive tygon collar was placed around the left carotid artery. Mice received 10mg/kg of CD200-Fc or control (mouse IgG1 kappa, clone MOPC-21) three times a week for three weeks. Carotids were snap frozen in OCT, cryosectioned and stained with an antibody against the macrophage marker CD206. Quantification was performed using Clemex software. (A) Representative photomicrographs of injured carotid arteries from ApoE-/- mice treated with IgG (control) or CD200-Fc fusion protein stained with an antibody against the macrophage marker CD206 and haematoxylin. Dotted lines show lesional areas. Scale bars = 100μm. Graphs show the (B) percentage and (C) absolute lesion area staining positive for CD206 in IgG (control) or CD200Fc -treated carotids. Individual dots represent individual mice. Horizontal line denotes group mean. Graphs show mean ± SEM, * $p<0.05$, n=11-12, unpaired Student's t-test.

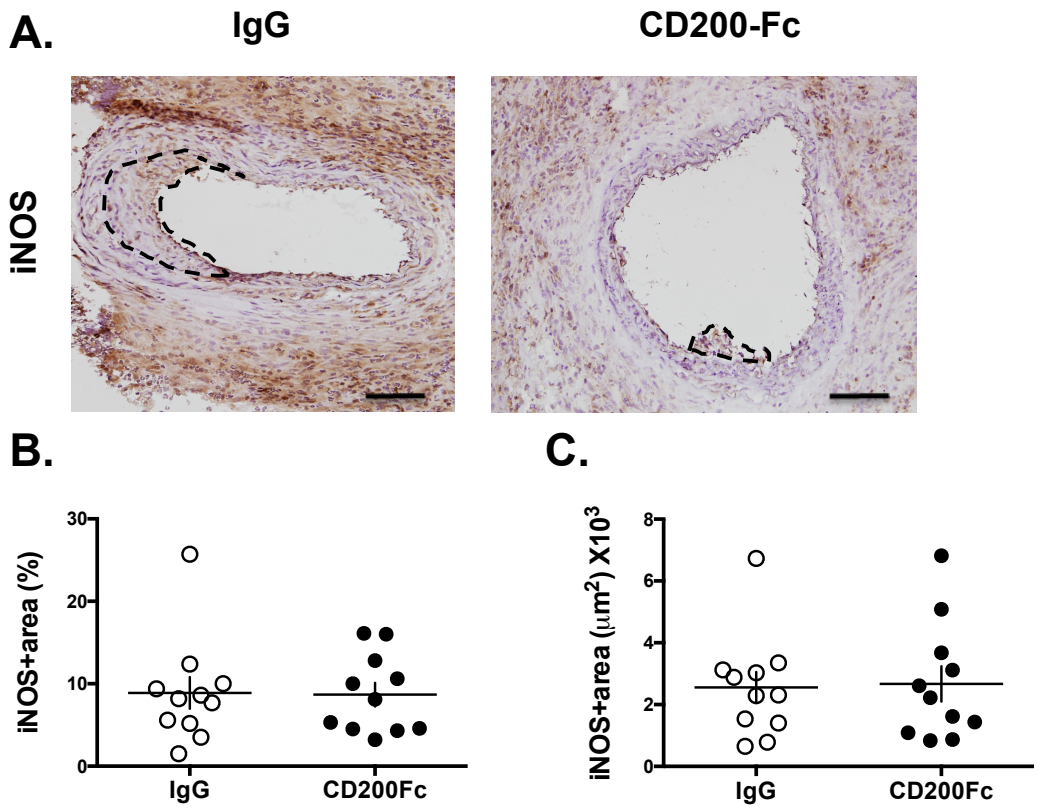


Figure 3.5 CD200-Fc fusion protein treatment does not significantly affect the lesional iNOS+ macrophage content in arterial injury. Female ApoE-/- mice aged 22 weeks were anesthetised with isoflurane and a non-occlusive tygon collar was placed around the left carotid artery. Mice received 10mg/kg of CD200-Fc or control (mouse IgG1 kappa, clone MOPC-21) three times a week for three weeks. Carotids were snap frozen in OCT, cryosectioned and stained with an antibody against iNOS. Quantification was performed using Clemex software. (A) Representative photomicrographs of injured carotid arteries from ApoE-/- mice treated with IgG (control) or CD200-Fc fusion protein stained with an antibody against iNOS and with haematoxylin. Dotted lines show lesional areas. Scale bars = 100μm. Graphs show the (B) percentage and (C) absolute lesion area staining positive for iNOS in IgG (control) or CD200-Fc -treated carotids. Individual dots represent individual mice. Horizontal line denotes group mean. Graphs show mean ± SEM, n=11, unpaired Student's t-test.

3.2.3 CD200-Fc treatment does not affect CD11c expression

To assess the DC content of the lesions, perivascular collar-treated carotids were stained with an antibody against CD11c, a DC marker (Choi et al., 2009). However, CD200-Fc treatment did not significantly affect the lesional CD11c expression (Figure 3.6).

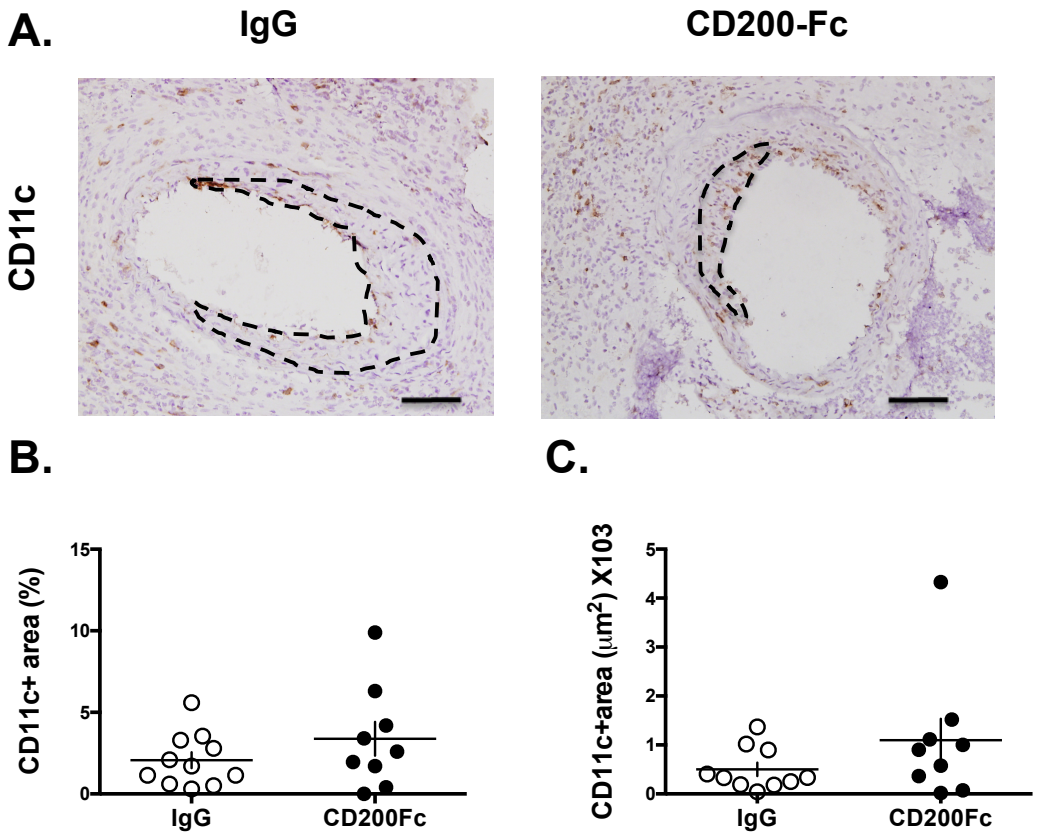


Figure 3.6 CD200-Fc fusion protein treatment does not significantly affect the lesional CD11c expression. Female ApoE-/- mice aged 22 weeks were anesthetised with isoflurane and a non-occlusive tygon collar was placed around the left carotid artery. Mice received 10mg/kg of CD200-Fc or control (mouse IgG1 kappa, clone MOPC-21) three times a week for three weeks. Dotted lines show lesional areas. Carotids were snap frozen in OCT, cryosectioned and stained with an antibody against CD11c. Quantification was performed using Clemex software. (A) Representative photomicrographs of injured carotid arteries from ApoE-/- mice treated with IgG (control) or CD200-Fc fusion protein stained with an antibody against the DC marker CD11c and with haematoxylin. Scale bars = 100μm. Graphs show the (B) percentage and (C) absolute lesion area staining positive for CD11c in IgG (control) or CD200-Fc -treated carotids. Individual dots represent individual mice. Horizontal line denotes group mean. Graphs show mean ± SEM, n=9-11, unpaired Student's t-test.

3.2.4 CD200-Fc treatment does not affect cellular proliferation, necrosis or collagen content but increases lipid content

Next, the injured carotids were stained with haematoxylin and eosin (H&E) and the acellular areas were used for necrosis quantification. Although there was a trend towards decreased necrosis with CD200-Fc treatment, this did not reach statistical significance (Figure 3.7). However, it should be noted that in this model the amount of necrosis induced is minimal and is therefore not ideal for studying the development of the necrotic core. To identify the amount of collagen in the plaques, the carotids were stained with Masson Trichrome (TM) stain. No differences between the two treatment groups were found (Figure 3.8). Nevertheless, lipid content as assessed by Oil red O (ORO) quantification was found to be increased in CD200-Fc treated lesions when expressed as absolute area (1328 ± 305 μm^2 versus 2924 ± 645.3 μm^2, p=0.04) but not as a fraction of lesion (Figure 3.9). To assess cellular proliferation, the carotid sections were stained with an antibody against ki-67. However, no differences were found between CD200-Fc and control treated carotids (Figure 3.10). Finally, CD200-Fc treatment did not significantly affect the lesional CD200 and CD200R+ area (Figures 3.11 and 3.12).

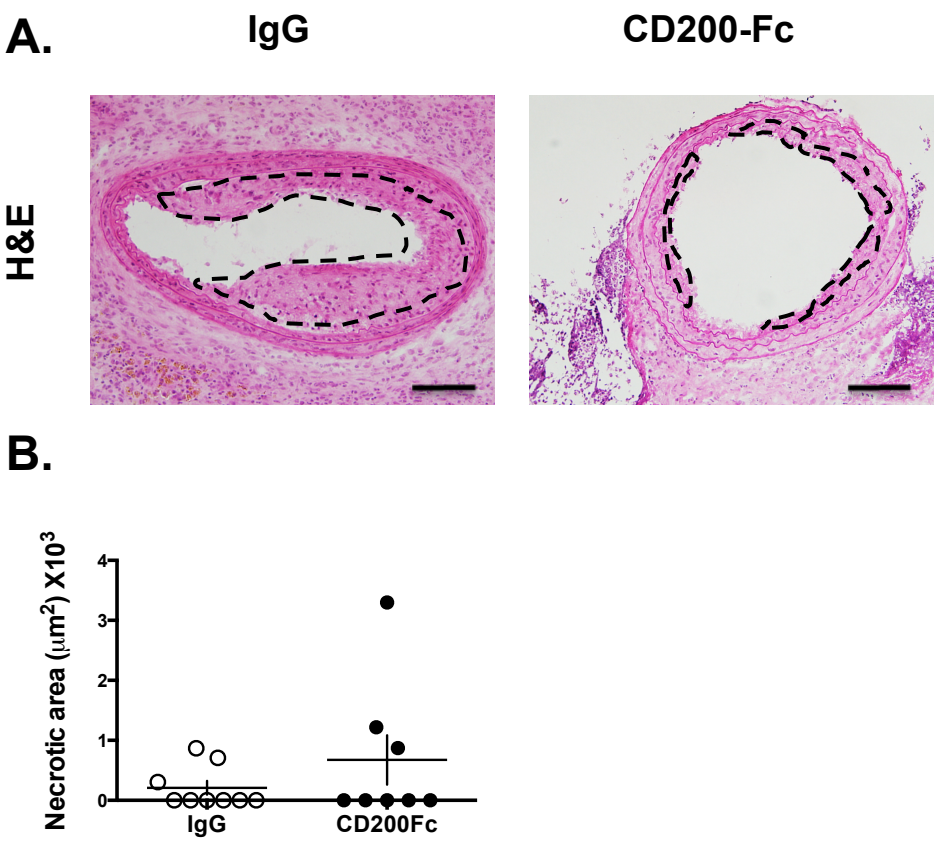


Figure 3.7 CD200-Fc fusion protein treatment does not significantly affect the necrosis in a perivascular carotid collar injury model in ApoE-/- mice. Female ApoE-/- mice aged 22 weeks were anesthetised with isoflurane and a non-occlusive tygon collar was placed around the left carotid artery. Mice received 10mg/kg of CD200-Fc or control (mouse IgG1 kappa,clone MOPC-21) three times a week for three weeks. Carotids were snap frozen in OCT, cryosectioned and stained with H&E stain. Quantification of the necrotic areas (> 300μm^2 threshold) was performed using ProgRes CapturePro image analysis software. (A) Representative photomicrographs of injured carotid arteries from ApoE-/- mice treated with IgG (control) or CD200-Fc fusion protein stained H&E. Dotted lines show lesional areas. Scale bars = 100μm. Graph shows (B) absolute lesion area stained for H&E to assess necrosis in IgG (control) or CD200-Fc -treated carotids. Individual dots represent individual mice. Horizontal line denotes group mean. Graph shows mean ± SEM, n=8-9, unpaired Student's t-test.

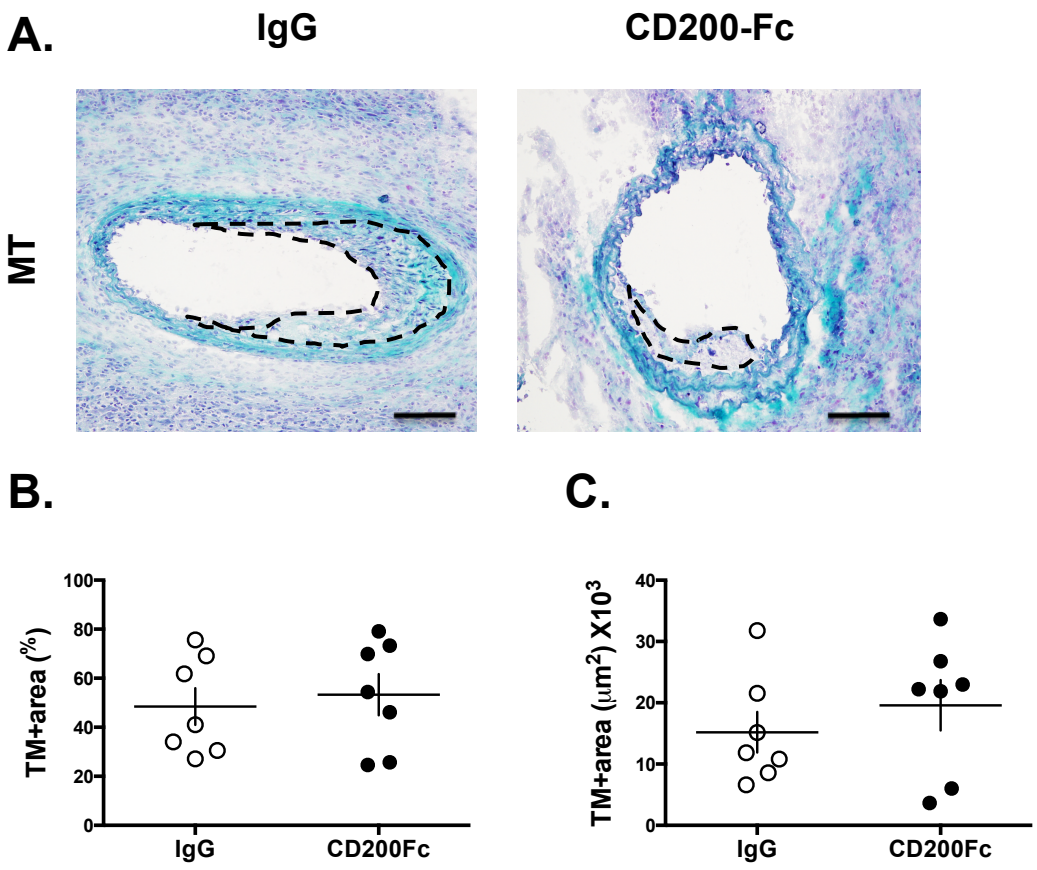


Figure 3.8 CD200-Fc fusion protein treatment does not affect the collagen content within the lesions in a perivascular carotid collar model in ApoE-/- mice. Female ApoE-/- mice aged 22 weeks were anesthetised with isoflurane and a non-occlusive tygon collar was placed around the left carotid artery. Mice received 10mg/kg of CD200-Fc or control (mouse IgG1 kappa, clone MOPC-21) three times per week for three weeks. Carotids were snap frozen in OCT, cryosectioned and stained with Masson Trichrome stain (TM). Quantification was performed using Clemex software. (A) Representative photomicrographs of injured carotid arteries from ApoE-/- mice treated with IgG (control) or CD200-Fc fusion protein stained with MT. Dotted lines show lesional areas. Scale bars = 100μm. Graphs show the (B) percentage and (C) absolute lesion area staining positive for MT to assess collagen content in green in IgG (control) or CD200-Fc -treated carotids. Individual dots represent individual mice. Horizontal line denotes group mean. Graphs show mean ± SEM, n=7, unpaired Student's t-test.

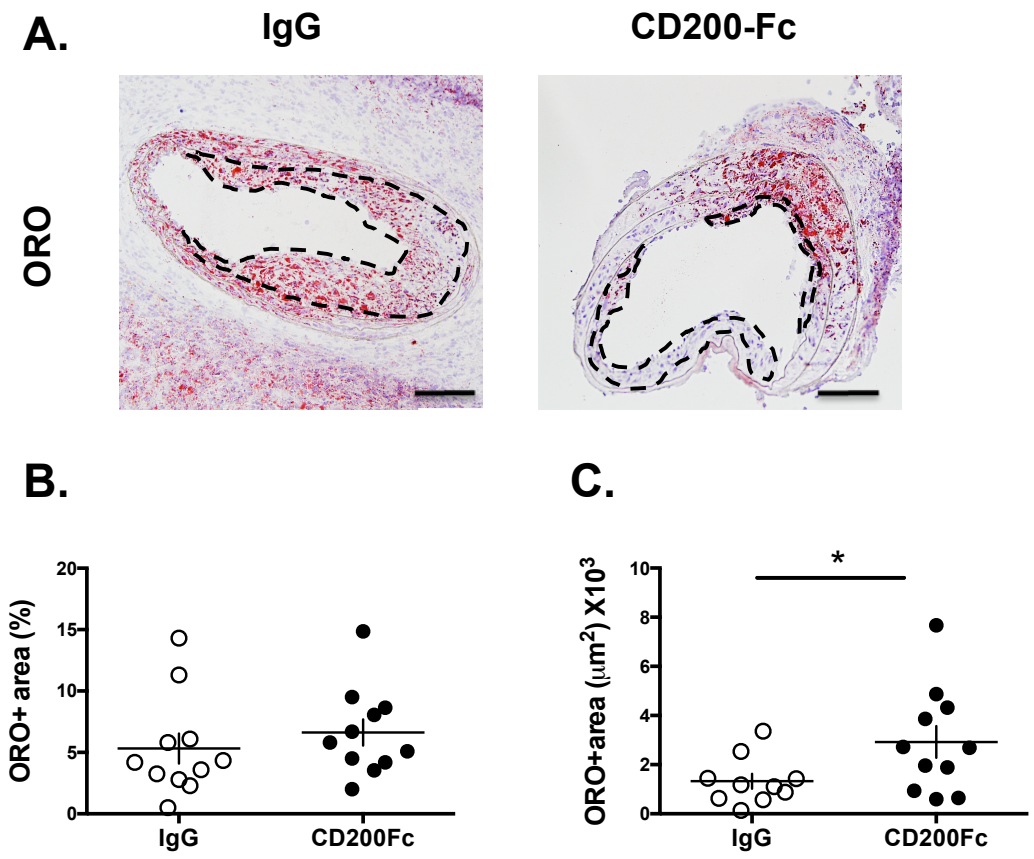


Figure 3.9 CD200-Fc fusion protein treatment affects the lipid content within the lesions in a perivascular carotid collar model in ApoE-/- mice. Female ApoE-/- mice aged 22 weeks were anesthetised with isoflurane and a non-occlusive tygon collar was placed around the left carotid artery. Mice received 10mg/kg of CD200-Fc or control (mouse IgG1 kappa, clone MOPC-21) three times per week for three weeks. Carotids were snap frozen in OCT, cryosectioned and stained with ORO stain. Quantification was performed using Clemex software. **(**A) Representative photomicrographs of injured carotid arteries from ApoE-/- mice treated with IgG (control) or CD200-Fc fusion protein stained ORO. Dotted lines show lesional areas. Scale bars = 100μm. Graphs show the (B) percentage and (C) absolute lesion area staining positive for ORO to assess lipid content in red in IgG (control) or CD200-Fc - treated carotids. Individual dots represent individual mice. Horizontal line denotes group mean. Graphs show mean ± SEM, * $p<0.05$, n=10-11, unpaired Student's t-test.

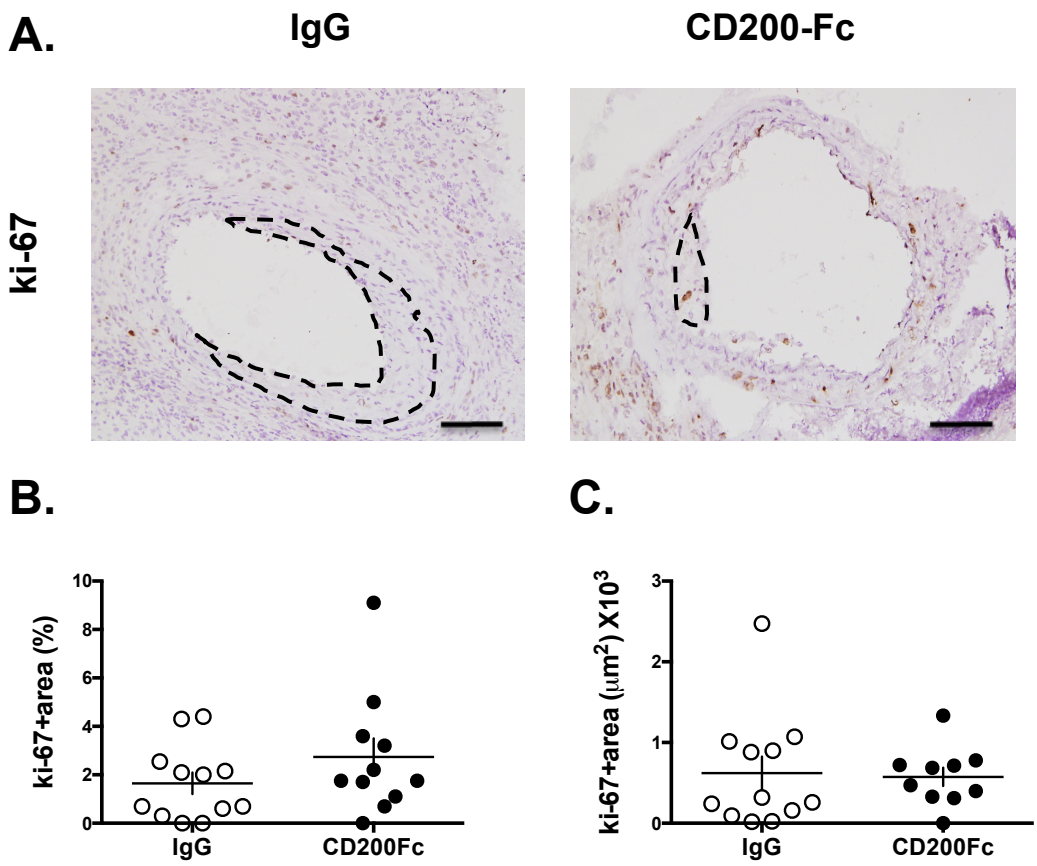


Figure 3.10 CD200-Fc fusion protein treatment does not significantly affect cellular ki-67+ content within the lesions in a perivascular carotid collar model in ApoE-/- mice. Female ApoE-/- mice aged 22 weeks were anesthetised with isoflurane and a non-occlusive tygon collar was placed around the left carotid artery. Mice received 10mg/kg of CD200-Fc or control (mouse IgG1 kappa, clone MOPC-21) three times per week for three weeks. Carotids were snap frozen in OCT, cryosectioned and stained with an antibody against a proliferation marker, ki-67. Quantification was performed using Clemex software. (A) Representative photomicrographs of injured carotid arteries from ApoE-/- mice treated with IgG (control) or CD200-Fc fusion protein stained with an antibody against a proliferation marker, ki-67, and with haematoxylin. Dotted lines show lesional areas. Scale bars = 100μm. Graphs show the (B) percentage and (C) absolute lesion area staining positive for ki-67 in IgG (control) or CD200-Fc -treated carotids. Individual dots represent individual mice. Horizontal line denotes group mean. Graphs show mean ± SEM, n=10-12, unpaired Student's t-test.

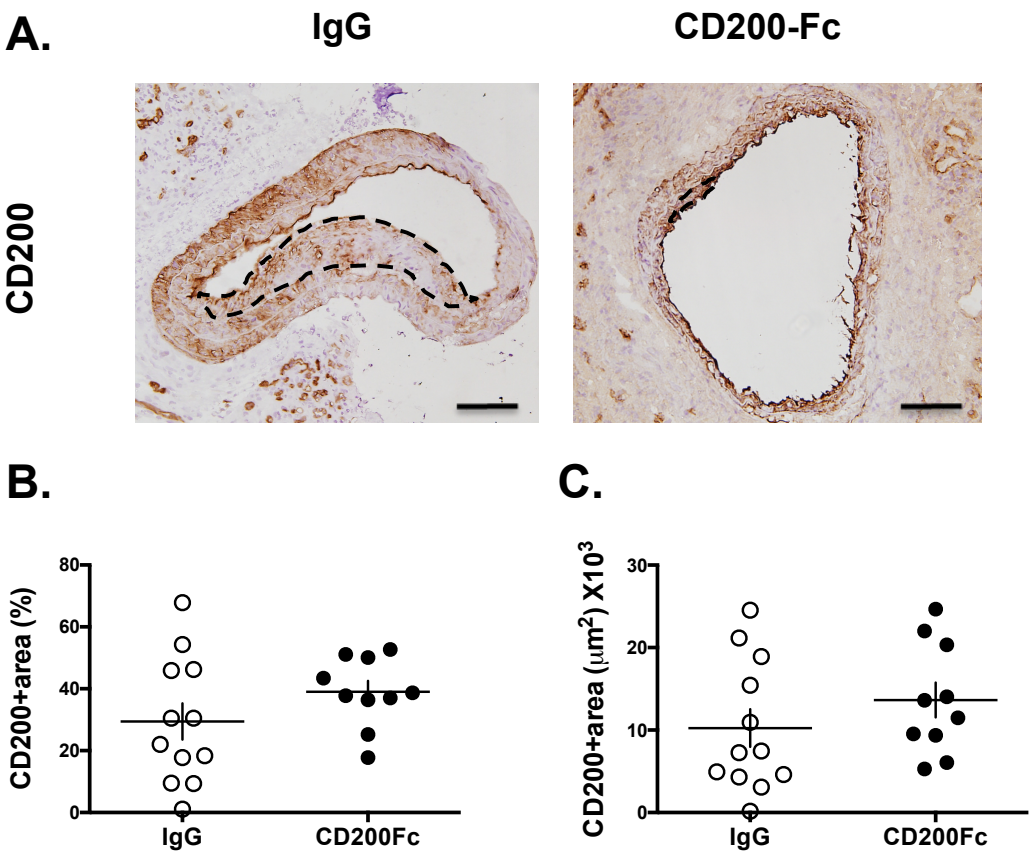


Figure 3.11 CD200-Fc fusion protein treatment does not significantly affect lesional CD200+ content in a perivascular carotid collar model in ApoE-/- mice. Female ApoE-/- mice aged 22 weeks were anesthetised with isoflurane and a non-occlusive tygon collar was placed around the left carotid artery. Mice received 10mg/kg of CD200-Fc or control (mouse IgG1 kappa, clone MOPC-21) three times per week for three weeks. Carotids were snap frozen in OCT, cryosectioned and stained with an antibody against CD200. Quantification was performed using Clemex software. **(**A) Representative photomicrographs of injured carotid arteries from ApoE-/- mice treated with IgG (control) or CD200-Fc fusion protein stained with an antibody against CD200 and with haematoxylin. Dotted lines show lesional areas. Scale bars = 100μm. Graphs show the (B) percentage and (C) absolute lesion area staining positive for CD200 in IgG (control) or CD200-Fc -treated carotids. Individual dots represent individual mice. Horizontal line denotes group mean. Graphs show mean ± SEM, n=10-12, unpaired Student's t-test.

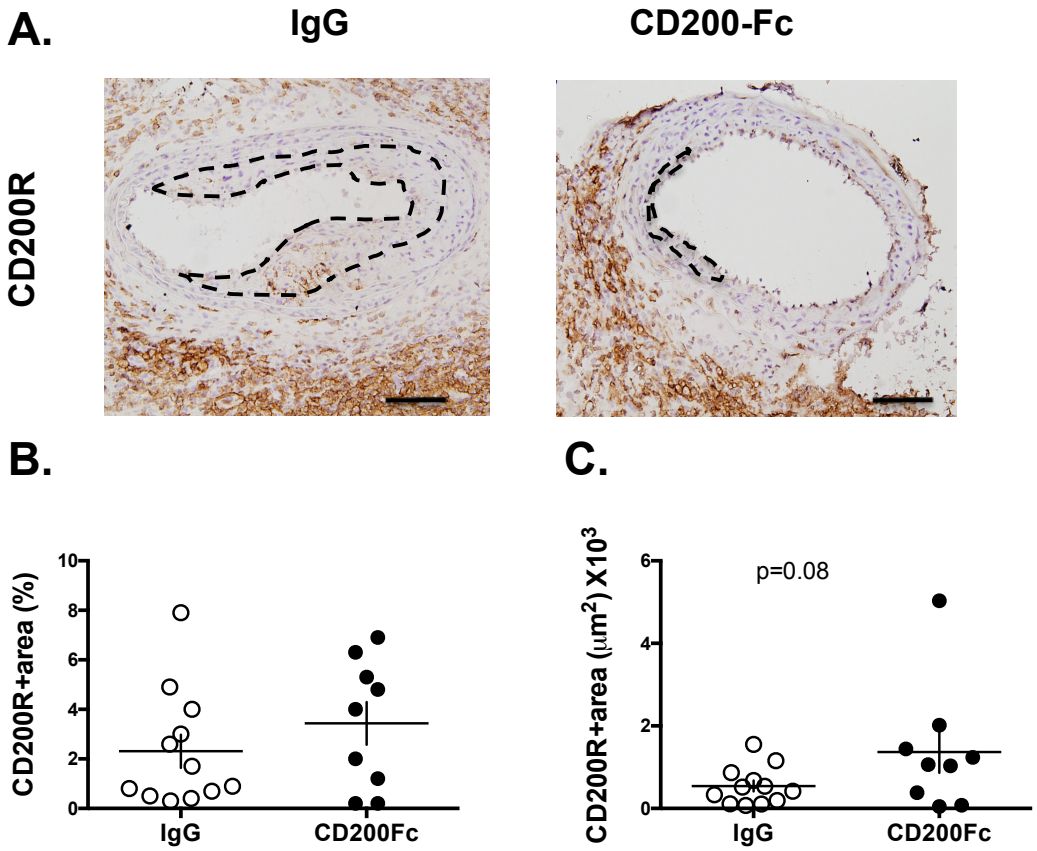


Figure 3.12 CD200-Fc fusion protein treatment does not significantly affect the lesional CD200R+ cell content in a perivascular carotid collar model in ApoE-/- mice. Female ApoE-/- mice aged 22 weeks were anesthetised with isoflurane and a non-occlusive tygon collar was placed around the left carotid artery. Mice received 10mg/kg of CD200-Fc or control (mouse IgG1 kappa, clone MOPC-21) three times per week for three weeks. Carotids were snap frozen in OCT, cryosectioned and stained with an antibody against CD200R. Quantification was performed using Clemex software. (A) Representative photomicrographs of injured carotid arteries from ApoE-/- mice treated with IgG (control) or CD200-Fc fusion protein stained with an antibody against CD200R and haematoxylin. Dotted lines show lesional areas. Scale bars = 100μm. Graphs show the (B) percentage and (C) absolute lesion area staining positive for CD200R in IgG (control) or CD200-Fc -treated carotids. Individual dots represent individual mice. Horizontal line denotes group mean. Graphs show mean ± SEM, n=9-12, unpaired Student's t-test.

3.2.5 CD200-Fc treatment does not affect myeloid populations in the aorta but increases F4/80+ macrophages in the spleen

Myeloid populations, including macrophages and DCs, were assessed in the aorta, spleen and lymph nodes in control and CD200-Fc treated ApoE-/- mice by flow cytometry. The gating strategy is described in Figure 3.13. No differences in the numbers of myeloid cells (assessed by the expression of CD45, CD11b, F4/80, CD11c, CD103, MHCII, and CD68) in the aorta and lymph nodes of IgG and CD200 Fc treated mice were observed (Figures 3.14A,B). F4/80+CD11b+ myeloid cells, expressed as percentage of CD45+cells (IgG: 2.1 ± 0.34% versus CD200 Fc: 3.4 ± 0.32%, p=0.0079) and as an absolute number (0.69 ± 0.19 $x10^6$ versus 1.7 ± 0.5 $x10^6$, p=0.0879) and F4/80+CD11b- myeloid cells as percentages of CD45+ cells (1.046 ± 0.09% versus 2.1 ± 0.3%, p=0.0397) and absolute numbers (0.34 ± 0.058 $x10^6$ versus 1.1 ± 0.31 $x10^6$, p=0.0374) were increased in the spleen of CD200-Fc treated mice compared to the control group (Figures 3.14B,C). Cells gated also on splenic CD68+F4/80+were also significantly increased. No differences in the numbers of splenic CD11b+ or CD103+ DCs were observed.

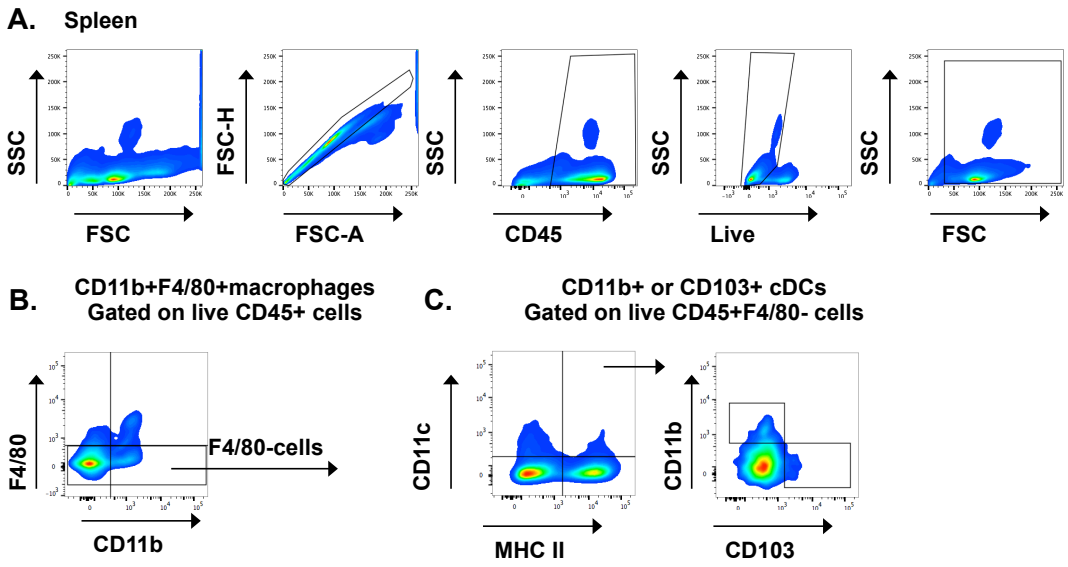


Figure 3.13 Gating strategy applied to detect myeloid cells in the spleen of CD200-Fc-treated ApoE-/- mice. Female ApoE-/- mice aged 22 weeks were anaesthetised with isoflurane and a non-occlusive tygon collar was placed around the left carotid artery. Mice received 10mg/kg of CD200-Fc or control (mouse IgG1 kappa, clone MOPC-21) three times per week for three weeks. Plots are representative for spleens collected from female ApoE-/- mice after three weeks of IgG or CD200-Fc treatment. (A) Dead cells and debris were excluded from the analysis and cells were gated on CD45+live cells. Macrophages were defined as F4/80+CD11b+ (CD68+/-) cells (B and D). Red pulp macrophages were defined as F4/80+CD11b- cells. DCs were gated as F4/80-CD11c+MHCII+ and two cDCs populations were defined as CD11b+ or CD103+(C).

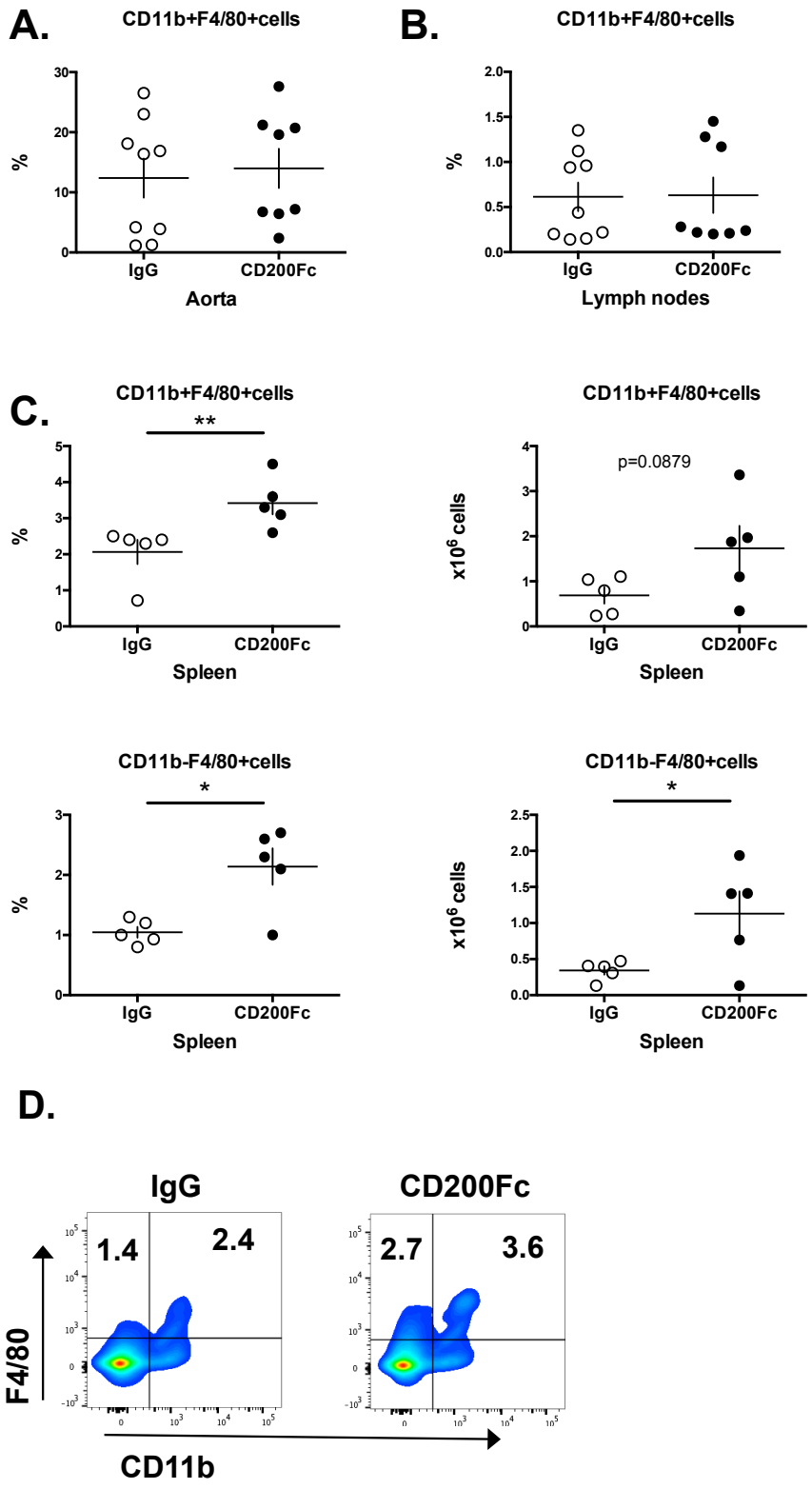


Figure 3.14 CD200-Fc treatment increases the number of macrophages in the spleen but has no effect on myeloid cells in the aorta and lymph nodes in ApoE-/- mice. Female ApoE-/- mice aged 22 weeks were anesthetised with isoflurane and a non-occlusive tygon collar was placed around the left carotid artery. Mice received 10mg/kg of CD200-Fc or control (mouse IgG1 kappa, clone MOPC-21) three times per week for three weeks. Graphs show (A) the number of CD11b+F4/80+macrophages in the aorta and in (B) the lymph nodes of IgG and CD200-Fc-treated mice, expressed as a percentage of CD45+cells, (C) number of

CD11b+F4/80+ and CD11b-F4/80+macrophages in the spleen of IgG and CD200-Fc-treated mice, expressed as a percentage of CD45+ cells and absolute cell numbers. (D) Plots show CD11b+F4/80+ and CD11b-F4/80+macrophages in the spleen of IgG and CD200Fc-treated mice. Individual dots represent individual mice. Data show mean ± SEM, ** $p<0.01$, *$p<0.05$, n=5-9, unpaired Student's t-test.

3.2.6 CD200R treatment inhibits IFN-γ but increases LPS or IL-4/IL-13 mediated IL-6 production in M-CSF treated myeloid cells *in vitro*

To assess the role of CD200R-CD200 in myeloid mediated cytokine production, granulocyte macrophage colony stimulating factor (GM-CSF) and macrophage colony stimulating factor (M-CSF) derived bone marrow (BM) myeloid cells were cultured *in vitro* and stimulated with an agonistic CD200R antibody (Akkaya et al., 2013). GM-CSF-treated cells were stimulated with lipopolysaccharide (LPS). MCSF-treated macrophages were additionally stimulated with IFN-γ and LPS for M1 polarisation, or with IL-4 and IL-13 for M2 polarisation, and the levels of IL-6 in the supernatants of those cultures were assessed by ELISA. No differences were observed in IL-6 production in GM-CSF-treated myeloid cells following CD200R antibody treatment (Figure 15A). M-CSF-treated macrophages had higher IL-6 levels after LPS and IFN-γ stimulation while the lowest IL-6 levels were found after M2 polarisation. Interestingly, CD200R antibody treatment significantly decreased IL-6 production in IFN-γ +LPS compared with LPS only stimulated M-CSF-treated macrophages (9112 ± 1198 pg/mL versus 4468 ± 983.2 pg/mL, $p=0.01$). Surprisingly, agonistic CD200R antibody treatment significantly increased IL-6 production in LPS treated M-CSF derived macrophages (3374 ± 1376 pg/ml versus 9112 ± 1198 pg/ml). Additionally, CD200R increased IL-6 production in IL-4/ IL-13 activated macrophages, although this difference did not reach statistical significance (924.6 ± 908 pg/ml, versus 5450 ± 2310 pg/ml, $p=0.09$) (Figure 3.15B).

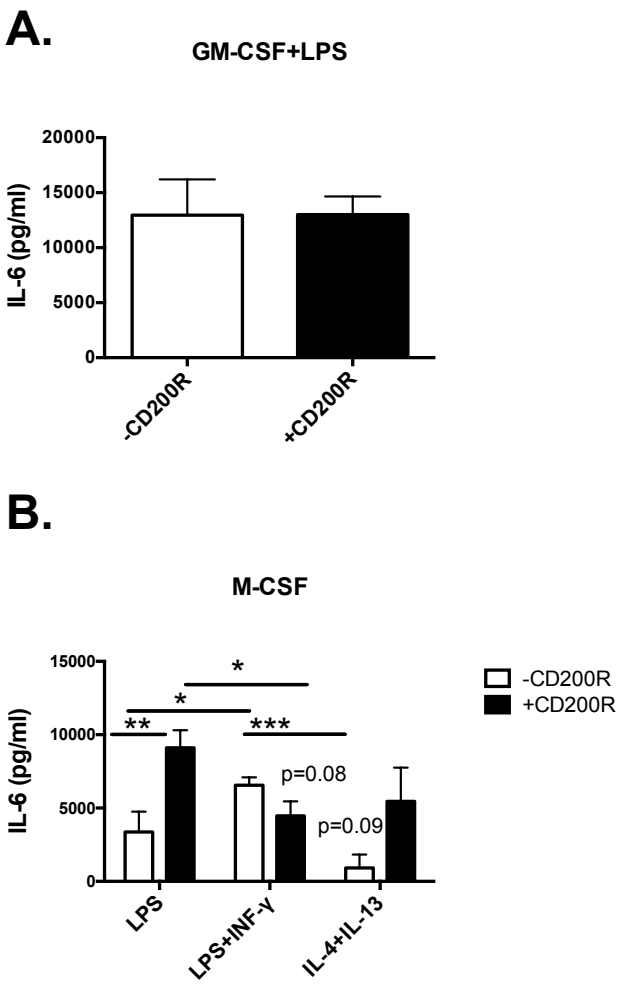


Figure 3.15 IL-6 secretion in GM-CSF and M-CSF treated myeloid cells following an agonistic CD200R antibody treatment. Bone marrow cells were obtained from 22-week old female ApoE-/- mice and cultured with 20ng/ml GM-CSF with 100ng/ml LPS or with 100ng/ml M-CSF with 100ng/ml LPS. For M1 polarisation, M-CSF-treated macrophages were additionally stimulated with 10ng/ml IFN-γ and 100ng/ml LPS while for M2 polarisation, M-CSF treated macrophages were stimulated with 20ng/ml IL-4 and IL-13. IL-6 levels from the supernatants of GM-CSF + LPS (A) and M-CSF + LPS, IFN-γ and LPS-treated (M1), IL-4 and IL-13-treated (M2) treated cells (B) with or without overnight CD200R antibody (10ug/ml) stimulation. Graphs show mean ± SEM, ***p<0.001, ** p<0.01, *p<0.05, n=8, unpaired Student's t-test.

3.3 Discussion

In order to evaluate the effects of CD200R activation during vascular lesion development, a murine model of perivascular collar-induced injury was used. The advantage of this model is the generation of lesions in three weeks compared to the slow lesion development in traditional hypercholesterolemia-based models. The short time frame facilitates the use of injectables. There is a variety of arterial injury mouse models developed so far, including the wire-injury model, carotid artery ligation, the electric injury and the perivascular collar. In perivascular collar model, the lesions are formed in close proximity to the collar, possibly due to haemodynamic factors (Yin et al., 2010, Carmeliet et al., 1997, Xu, 2004, von der Thusen et al., 2001, Sasaki et al., 2004). The real advantage of this model is that it is reproducible and the location of the plaques can be easily identified as after three weeks of collar placement, there is a fibrotic tissue formed close to the collar.

Activation of CD200R signalling by a CD200-Fc fusion protein has been previously shown to exert anti-inflammatory action (Simelyte et al., 2008). In the context of the current study, female ApoE-/- mice were treated intraperitoneally with CD200-Fc or an IgG1 control three times per week for three weeks. CD200-Fc prevented the significant decrease in weight loss seen in control mice during the first week post-surgery, possibly by inhibiting inflammatory responses. No changes in the weight of the mice were observed at the end of the treatment. In accordance to this, Snelgrove *et al.,* showed that mice treated with a CD200-Fc or an agonistic CD200R antibody had less weight loss than the control mice, when infected with influenza virus and that was associated with decreased production of proinflammatory cytokines, IL-6 and IFN-γ and T cell responses in the lung tissue and airways (Snelgrove et al., 2008).

Treatment with CD200-Fc fusion protein significantly decreased lesion size and increased CD206+ M2 macrophage accumulation while it did not affect iNOS+M1 macrophage or CD11c+ cell accumulation in the plaques. At the time of redaction of this thesis, Hayakawa *et al.,* published that treatment with human CD200-Fc upregulates markers of M2 macrophages, including Arg1 and TGM2 and enhances C/EBP-β transcriptional activity while suppresses nuclear factor kappa light polypeptide gene enhancer in B cells (NF-κB) activity in peritoneal macrophages (Hayakawa et al., 2016).

Since CD200-Fc was administered systematically, additional effects of the peripheral immune system were assessed by flow cytometry of the aorta, lymph nodes and spleen. Although, no differences in myeloid cell populations were found in aorta and lymph nodes, there was an increase of F4/80+ macrophages in the spleen. Interestingly, Gorczynski *et al.,* found that administration of CD200-Fc delays graft rejection, and its activity is associated with an immunosuppressive F4/80+ splenic macrophage population in an MHC-restricted fashion (Gorczynski et al., 2000). Theurl *et al.,* recently described two F4/80+ splenic subsets at steady state: F4/80^{hi} CD11b^{int} red pulp macrophages and a small population of F4/80^{hi}CD11b^{hi} transient macrophages. The latter ones are responsible for erythrophagocytosis mainly in the liver and not in the spleen due to the suppressive activity of GM-CSF in the spleen (Theurl et al., 2016). Whether erythrophagocytosis is one of those mechanisms responsible for the increase of the splenic F4/80+ macrophages following CD200-Fc treatment remains to be investigated.

Finally, I was interested to evaluate the effects of CD200R agonism in myeloid activation *in vitro.* As there was limited supply of CD200-Fc; I decided to use an agonistic CD200R antibody (Akkaya et al., 2013). The levels of IL-6 were assessed in

bone marrow derived GM-CSF/M-CSF treated myeloid cells. Those cells were activated with LPS or IFN-γ and LPS for M1 polarisation or IL-4 and IL-13 for M2 polarisation. Although CD200R antibody treatment increased IL-6 levels in LPS and IL-4/IL-13 stimulated macrophages, it decreased IL-6 secretion in M1 polarised macrophages. Those results are in accordance with a study from Copland *et al.,* who used another CD200R agonistic antibody (DX109) and showed it also prevented IFN-γ mediated macrophage activation but did not affect LPS mediated macrophage activation (Copland et al., 2007).

In summary, the findings of this study demonstrate that CD200-Fc has a therapeutic effect on atherosclerosis. CD200-Fc reduces neointima formation potentially by enhancing the lesional content of anti-inflammatory plaque macrophages. The potential link with changes in the spleen macrophages requires further study.

Chapter 4 CD200 deficiency promotes the development of advanced atherosclerotic lesions

Chapter 4: CD200 deficiency promotes the development of advanced atherosclerotic lesions

4.1 Introduction

CD200 deficiency has been linked to increased myeloid activation in various experimental autoimmune disease and neurodegeneration models. The first CD200-/- mice were reported by Hoek *et al.,* (Hoek et al., 2000) and showed increased numbers of activated macrophages in the spleen, lymph nodes and central nervous system (CNS) and increased susceptibility to collagen induced arthritis (CIA) and experimental autoimmune encephalomyelitis (EAE). Additionally, CD200-/- mice have increased bone density, suggesting a role for CD200 in osteoclastogenesis (Cui et al., 2007). Another study demonstrated that CD200-/- mice have increased microglial activation and accelerated onset of experimental autoimmune uveoretinitis (EAU), another autoimmune disease (Broderick et al., 2002). The role of the CD200-CD200R signalling pathway has also been evaluated in immune homeostasis in the respiratory tract, where influenza-infected CD200-/- mice had heightened inflammatory responses, including the expression of the proinflammatory cytokine tumour necrosis factor (TNF)-α (Snelgrove et al., 2008). CD200/band T lymphocyte attenuator (BTLA) deletions have been suggested as a prognostic factor in human B-cell precursor acute lymphoblastic leukemia (Ghazavi et al., 2015). Therefore, I postulated that the CD200-CD200R axis regulates myeloid cell function and aimed to assess the role of CD200 deficiency on myeloid cell phenotypes and atherosclerosis development.

4.2 Results

4.2.1 CD200 deficiency does not affect the body weight of ApoE-/-mice

ApoE-/- and CD200-/- mice were crossed to generate ApoE-/-CD200-/- mice, as described in Materials and Methods. Male ApoE-/- and ApoE-/-CD200- /- mice were fed a chow diet and culled at 15, 20 or 27 weeks of age. At the time of culling all ApoE-/- and ApoE-/-CD200-/- mice were weighed. No statistical differences were found in the weights of the mice (Figure 4.1).

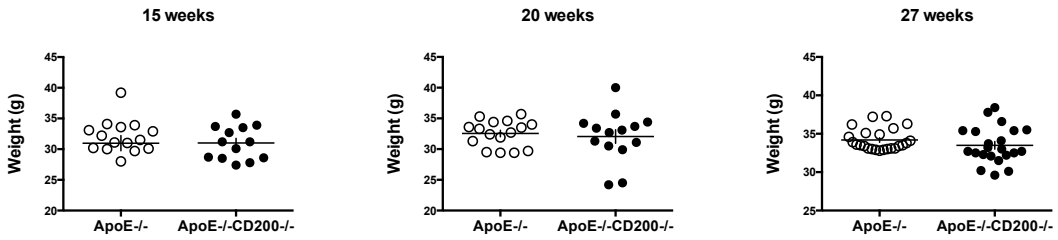


Figure 4.1 Weights of male ApoE-/- and ApoE-/-CD200-/- mice at 15, 20 or 27 weeks of age on chow diet. Male ApoE-/- (littermates) and ApoE-/-CD200-/- mice were fed a chow diet and culled at 15, 20 or 27 weeks of age and their weight was measured in grams. Dots represent individual mice. Horizontal line denotes group mean with error bars, n=13-24, unpaired Student's t-test.

4.2.2 CD200 deficiency does not affect serum cholesterol levels

Cholesterol levels in the serum of ApoE-/- and ApoE-/-CD200-/- mice on a chow diet were measured. No differences between the two groups were observed at 27 weeks of age (Table 4.1).

Table 4-1 Serum cholesterol levels in ApoE-/- and ApoE-/-CD200-/- mice at 27 weeks of age. Male ApoE-/- and ApoE-/-CD200- /- mice were fed a chow diet up to 27 weeks (wks) of age and the serum cholesterol levels were measured as described in Material and Methods. n=7-8, unpaired Student's t-test.

Mouse genotype	Age(wk)	Serum cholesterol ±SEM (mg/dL)	p vs. ApoE-/-
ApoE-/-	27	473.1±23.55	
ApoE-/-CD200-/-	27	464.4±62.13	$p > 0.05$

4.2.3 CD200 deficiency increases the lesion size in 27-week old ApoE-/- mice

The aortic roots of ApoE-/- and ApoE-/-CD200-/- mice fed a chow diet for 15, 20 or 27 weeks of age were harvested and cryosectioned to assess atherosclerotic disease at this site. No difference in lesion size was noticeable between the two groups of mice at 20 weeks of age (Figures 4.2A-D). However, ApoE-/-CD200-/- mice had significantly increased lesion size compared to ApoE-/- mice at 27 weeks of age, when expressed as both a percentage of the cross-sectional area (8.041 ± 0.471% versus 12.94 ± 1.085%, p=0.0013) (Figure 4.2C) and as an absolute area of the aortic root (85216 ± 399 μm^2 versus 140631 ± 16205 μm^2, p=0.0068) (Figure 4.2B). The lesion area was determined at specific distances from the aortic sinus. Interestingly, a significant increase in lesion size was only observed in 27 weeks old ApoE-/-CD200-/-mice at distances 400μm and longer from the start of the aortic sinus (Figure 4.2D).

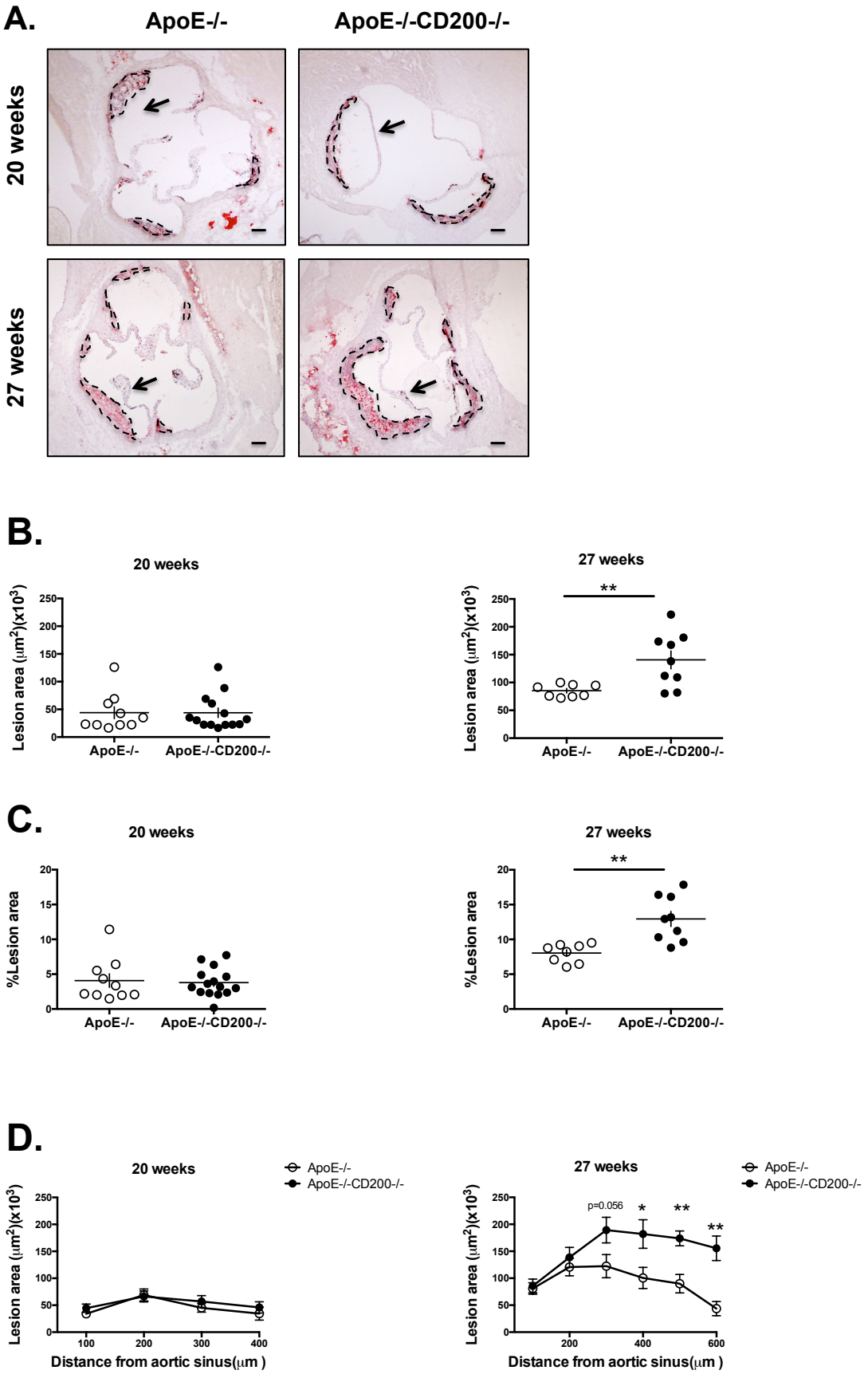

A.
ApoE-/-
ApoE-/-CD200-/-
20 weeks
27 weeks
B.
20 weeks
27 weeks
Lesion area (μm²)(x10³)
**
ApoE-/-
ApoE-/-CD200-/-
C.
20 weeks
27 weeks
%Lesion area
**
ApoE-/-
ApoE-/-CD200-/-
D.
20 weeks
27 weeks
ApoE-/-
ApoE-/-CD200-/-
Lesion area (μm²)(x10³)
p=0.056
*
**
**
Distance from aortic sinus(μm)

Figure 4.2 CD200 deficiency increases atherogenesis in 27-week old ApoE-/- mice. Male ApoE-/- and ApoE-/-CD200- /- mice were fed a chow diet for 20 or 27 weeks of age. A) Representative images of aortic root sections from male ApoE-/- and ApoE-/-CD200-/- mice aged 20 or 27 weeks of age stained with Oil Red-O (ORO) solution and haematoxylin. Dotted lines surround lipid-rich lesion regions of the plaques. Scale bars = 100μm. B) Quantification of lesion area in μm^2 in the aortic root. C) Quantification of lesion area as a percentage of the aortic root cross-sectional area, **p<0.01, n=7-14, unpaired Student's t-test. D) Lesion size measured on serial sections throughout the proximal aorta. Horizontal lines within the data sets represent means with error bars, **p<0.01, *p<0.05, n=7-14, Multiple t-test.

4.2.4 CD200 deficiency affects lesion phenotype in 27-week old ApoE-/- mice

To assess the effect of CD200 deletion on macrophage infiltration, aortic root sections from ApoE-/- and ApoE-/-CD200-/- mice were stained for the pan-macrophage marker CD68. No difference in lesional macrophage content was observed between the two groups of mice in the aortic root at 20 weeks of age. However, ApoE-/-CD200-/- mice had a significant increase in lesional CD68 positive content at 27 weeks of age, when expressed as a percentage (46.06 ± 2.146% versus 53.84 ± 3.034%, p=0.0489) but also as an absolute area (37676 ± 6077 μm^2 versus 93677 ± 16518 μm^2, p=0.0052) of the aortic roots (Figure 4.3).

Next, aortic root sections were stained with haematoxylin and eosin (H&E) to allow quantification of the necrotic core size. In comparison to ApoE-/- mice, ApoE-/-CD200-/- mice had an increase in lesional necrotic core area at 27 weeks of age, when expressed both as a percentage (15.11 ± 2.237% versus 22.95 ± 1.261%, p=0.001) and as an absolute area (14559 ± 2916 μm^2 versus 35041 ± 4361 μm^2, p=0.0012) of the aortic root (Figure 4.4).

Aortic root sections were also stained with a fluorescent anti-smooth muscle cell (SMC) α-actin antibody. CD200 deletion significantly reduced the lesional SMC positive area in ApoE-/- mice at 27 weeks of age, when expressed as a percentage

(4.150 ± 1.034% versus 1.429 ± 0.4893 %, p=0.04) of the cross-sectional area of the aortic root (Figure 4.5).

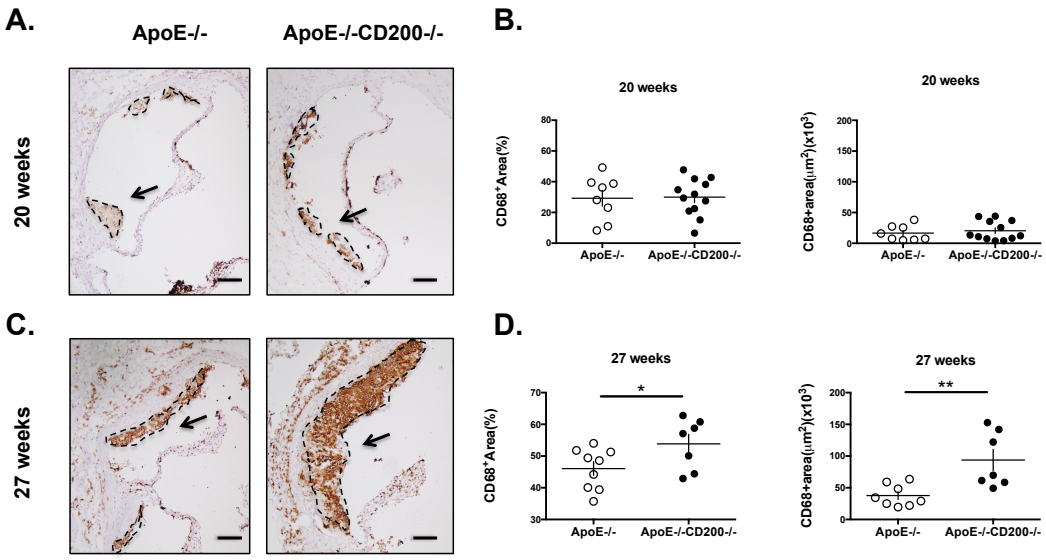


Figure 4.3 CD200 deficiency increases lesional macrophage infiltration in 27-week old ApoE-/- mice. Male ApoE-/- and ApoE-/-CD200- /- mice were fed a chow diet up to 27 weeks of age. A) Representative images of aortic root sections from male ApoE-/- and ApoE-/-CD200-/- mice aged 20 weeks stained with an antibody against CD68 (brown) and haematoxylin. Scale bars = 100μm. B) Lesion area staining positive for CD68 from aortic roots of ApoE-/- and ApoE-/-CD200-/- mice aged 20 weeks. C) Representative images of aortic root sections for CD68 (brown) from male ApoE-/- and ApoE-/-CD200-/- mice aged 27 weeks. D) Lesion area staining positive for CD68 from aortic roots of ApoE-/- and ApoE-/-CD200-/- mice aged 27 weeks. Dotted lines surround lesional areas. Scale bars = 100μm. Horizontal lines within the data sets represent means with error bars, **p<0.01, *p<0.05, n=7-12, unpaired Student's t-test.

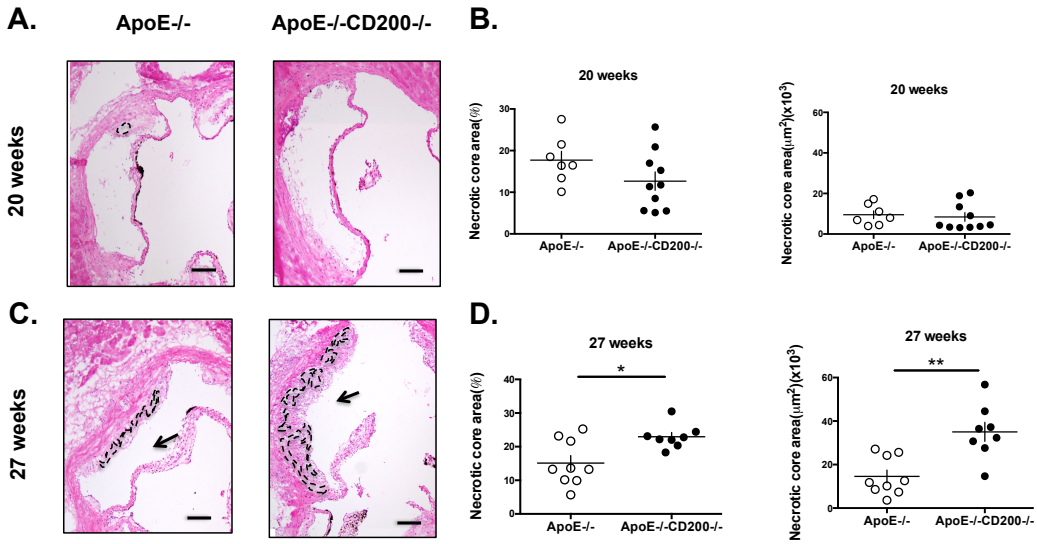


Figure 4.4 CD200 deficiency increases necrotic core size in 27-week old ApoE-/- mice. Male ApoE-/- and ApoE-/-CD200- /- mice were fed a chow diet up to 27 weeks of age. A) Representative images of H&E-stained aortic root sections from male ApoE-/- and ApoE-/-CD200-/- mice aged 20 weeks. B) Quantification of anuclear, afibrotic, and eosin-negative necrotic areas in the aortic root lesions of 20-week old male ApoE-/- and ApoE-/-CD200-/- mice. (C) Representative images of H&E-stained aortic root sections from male ApoE-/- and ApoE-/-CD200-/- mice aged 27 weeks. (D) Quantification of anuclear, afibrotic, and eosin-negative necrotic from aortic roots of male ApoE-/- and ApoE-/-CD200-/- mice aged 27 weeks. Dotted lines surround necrotic regions of the plaques. Scale bars = 100μm. Horizontal lines within the data sets represent means with error bars, **p<0.01, *p<0.05, n=7-10, unpaired Student's t-test.

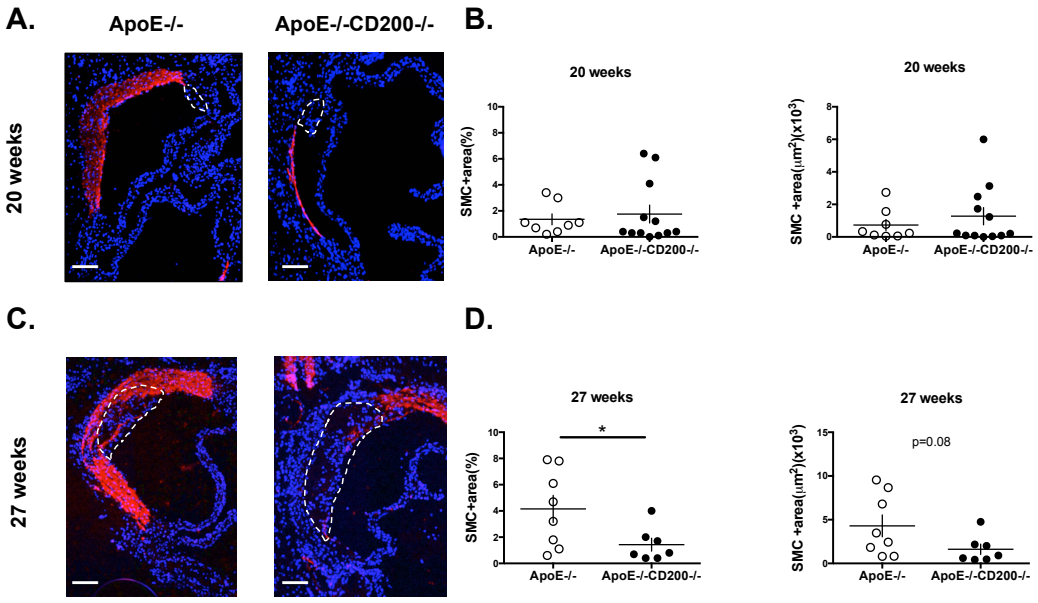


Figure 4.5 CD200 deficiency decreases SMC content within aortic root lesions in 27-week old ApoE-/- mice. Male ApoE-/- and ApoE-/-CD200- /- mice were fed a chow diet up to 27 weeks of age. A) Representative images of aortic root sections stained with an antibody against SMC α-actin (red) and cell nuclei stained with DAPI (blue) from male ApoE-/- and ApoE-/-CD200-/- mice aged 20 weeks. B) Quantification of smooth muscle cell positive areas in μm^2 in the aortic root of ApoE-/- and ApoE-/-CD200-/- mice aged 20 weeks. (C) Representative images aortic root sections stained for smooth muscle cell α-actin (red) and cell nuclei stained with DAPI (blue) from male ApoE-/- and ApoE-/-CD200-/- mice aged 27 weeks. D) Quantification of smooth muscle cell positive areas in the aortic root of ApoE-/- and ApoE-/-CD200-/- mice aged 27 weeks. Dotted lines surround lesional areas. Scale bars = 100μm. Horizontal lines within the data sets represent means with error bars, *$p<0.05$, n=7-10, unpaired Student's t-test.

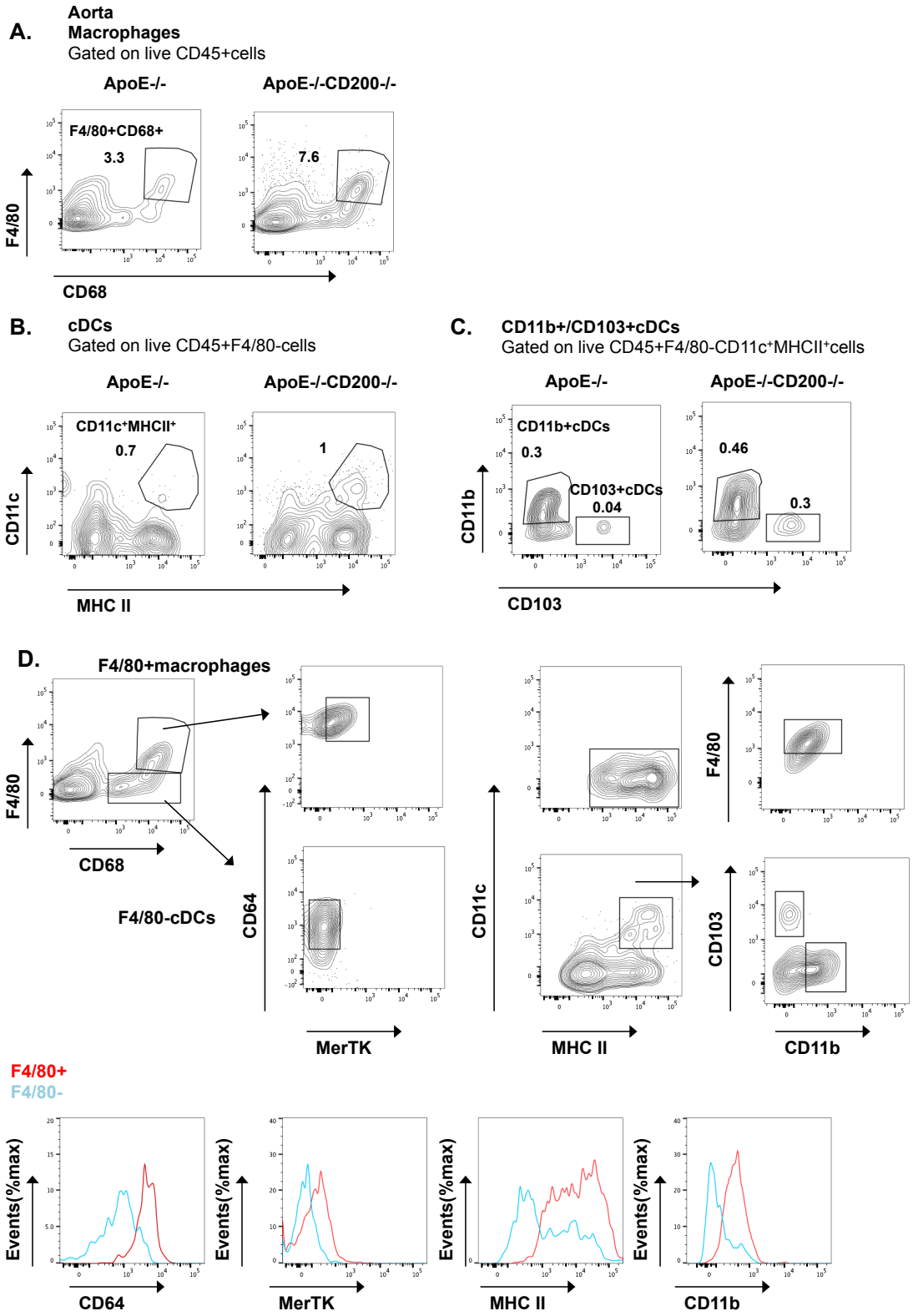
4.2.5 CD200 deficiency enhances arterial myeloid cell accumulation in 27-week old ApoE-/- mice

Aortas from 15, 20 and 27 weeks old ApoE-/- and ApoE-/-CD200-/- mice were harvested, enzymatically digested and single cell suspensions were used for 10-color flow cytometry. Myeloid populations were gated and defined as shown in Figures 4.6 A-D. The numbers of macrophages and cDCs in the aorta of ApoE-/- and ApoE-/-CD200-/- mice at 15, 20 and 27 weeks of age, were determined and expressed as

percentages of CD45+ cells and as absolute numbers. The data is summarised in Tables 4.2-4.3.

The number of macrophages (defined as CD45+F4/80+CD68+cells) (Ensan et al., 2016) was unchanged by CD200 deficiency in the aortas of ApoE-/- mice aged 15 and 20 weeks. However, at 27 weeks of age ApoE-/-CD200-/- mice had a significant increase in macrophages in the aorta, when expressed as a percentage (4.23 ± 1.088% versus 7.92 ± 0.8639% p=0.04) (Figures 4.6A, 4.7A, C). The phenotype of the macrophages was characterised by the expression of CD64, MerTK, MHCII and CD11b (Figures 4.6A, D) (Tables 4.2-3). F4/80-CD68- cells could include other leucocytes such as lymphocytes. F4/80-CD68+cells could include DC populations (Figure 4.6D). Macrophages were significantly increased when gated on other macrophage markers apart from F4/80 such as CD64 (Table 4.3).

Interestingly; the number of cDCs (gated on CD45+CD11c^{+}MHCII^{+}F4/80-cells) (Figure 4.6E) was significantly increased during all time points in ApoE-/-CD200-/- mice (Figures 4.6B, 4.7B, C). cDCs expressed high levels of CD68 (Figure 4.6E) and were characterised by low expression of CD64 and MerTK, and were further gated on CD11b+ and CD103+ cDCs, to identify the two subsets of cDCs (Figure 4.6E) (Choi et al., 2011). CD103+cDCs were consistently increased at all timepoints of atherosclerosis development in ApoE-/-CD200-/-mice. The number of CD11b+cDCs was also increased at all timepoints but this difference did not reach statistical significance (Figures 4.8 A-C).


A.
Aorta
Macrophages
Gated on live CD45+cells
ApoE-/-
ApoE-/-CD200-/-
F4/80+CD68+
3.3
7.6
F4/80
CD68
B.
cDCs
Gated on live CD45+F4/80-cells
ApoE-/-
ApoE-/-CD200-/-
CD11c+MHCII+
0.7
1
CD11c
MHC II
C.
CD11b+/CD103+cDCs
Gated on live CD45+F4/80-CD11c+MHCII+cells
ApoE-/-
ApoE-/-CD200-/-
CD11b+cDCs
0.3
CD103+cDCs
0.04
0.46
0.3
CD11b
CD103
D.
F4/80+macrophages
F4/80
CD68
F4/80-cDCs
CD64
MerTK
CD11c
MHC II
F4/80
CD103
CD11b
F4/80+
F4/80-
Events(%max)
CD64
MerTK
MHC II
CD11b

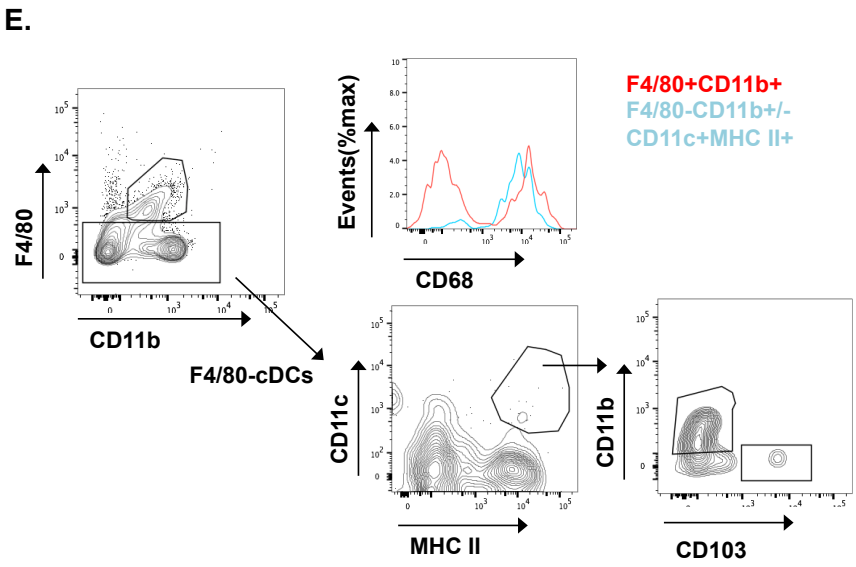


Figure 4.6 Gating strategy for macrophages and DCs in the aorta of ApoE-/- and ApoE-/-CD200-/- mice at 27 weeks of age. Male ApoE-/- and ApoE-/-CD200- /- mice were fed a chow diet up to 27 weeks of age. Single aortas were enzymatically digested as described in Material and Methods and single cell suspensions were used for 10-color flow cytometry. Plots show representative images of (A) F4/80+CD68+macrophages (gated on live CD45+cells) (B) $CD11c^{+}MHCII^{+}$cDCs (gated on live CD45+F4/80-cells) and (C) CD11b+ and CD103+DCs (gated on live CD45+F4/80-$CD11c^{+}MHCII^{+}$cells) in the aorta of ApoE-/- and ApoE-/-CD200-/- at 27 weeks of age. (D) Plots show the expression of CD64, MerTK, MHCII, CD11b, CD103 and CD11c on F4/80+macrophages (CD68+F4/80+ cells, red line) and F4/80-cells (gated on F4/80-CD68+cells, blue line). (E) Plots show the gating strategy for cDCs (gated on F4/80-CD11b+/- cells) and the level of CD68 expression within F4/80+CD11b+ (red line) and F4/80-CD11b+/-CD11c+MHCII+cDCs (blue line).

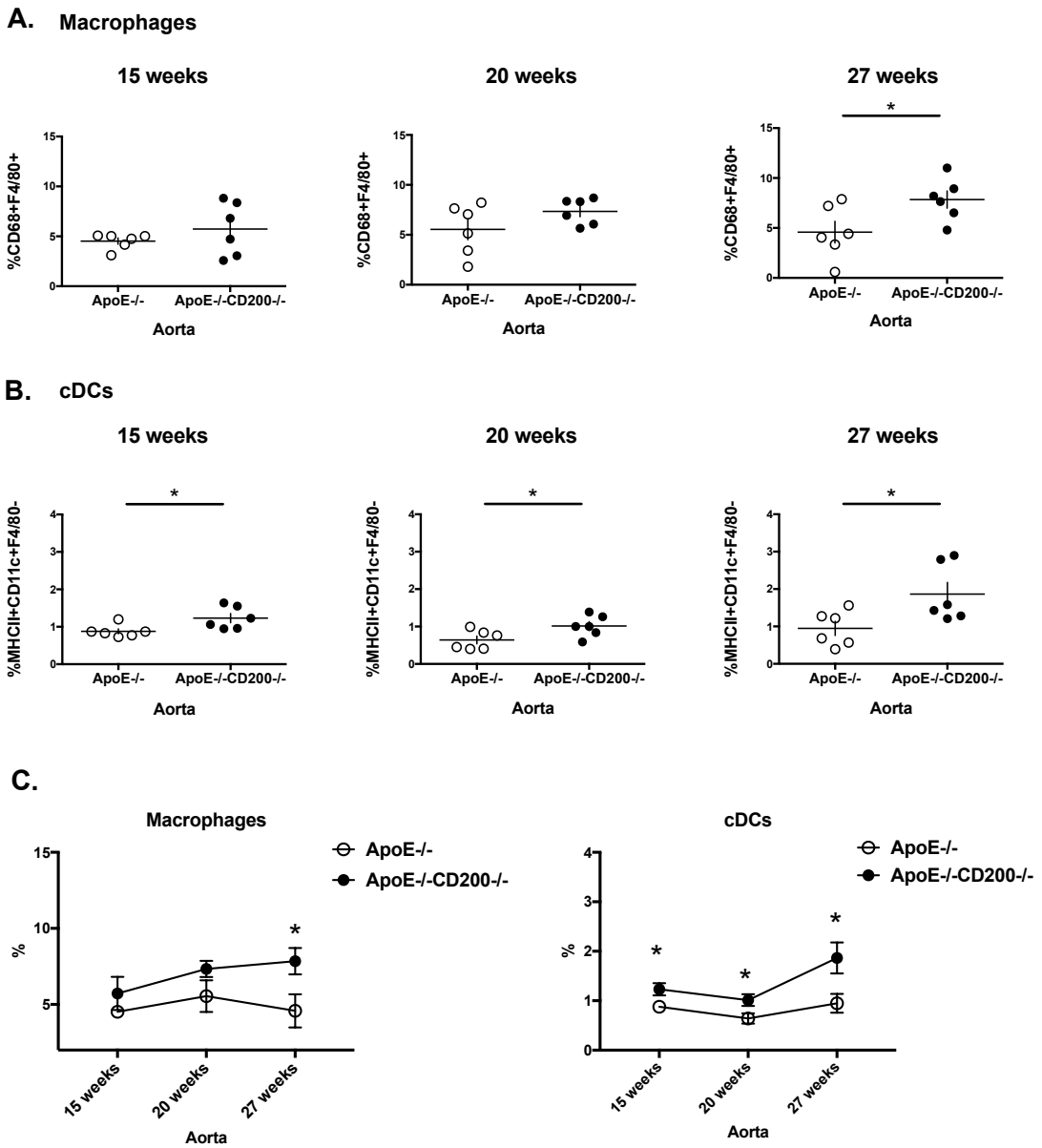


Figure 4.7 Increased numbers of F4/80+ macrophages and CD11c$^+$MHCII$^+$ DCs in the aorta of ApoE-/-CD200-/- mice. Male ApoE-/- (littermates) and ApoE-/-CD200- /- mice were fed a chow diet up to 15, 20 and 27 weeks of age. Single aortas were enzymatically digested as described in Material and Methods and single cell suspensions were used for 10-color flow cytometry. (A) Number of macrophages (gated on live CD45+F4/80+CD68+cells), expressed as a percentage of CD45+cells. (B) Number of DCs (gated on live CD45+F4/80-CD11c$^+$MHCII$^+$cells), expressed as a percentage of CD45+cells, in the aorta of ApoE-/- and ApoE-/-CD200-/- on chow diet at 15, 20 and 27 weeks of age. (C) Plots show the percentages of macrophages and cDCs in the aorta of ApoE-/- and ApoE-/-CD200-/- mice over time. Data show mean ± SEM, *p<0.05, n=6, Mann-Whitney U test.

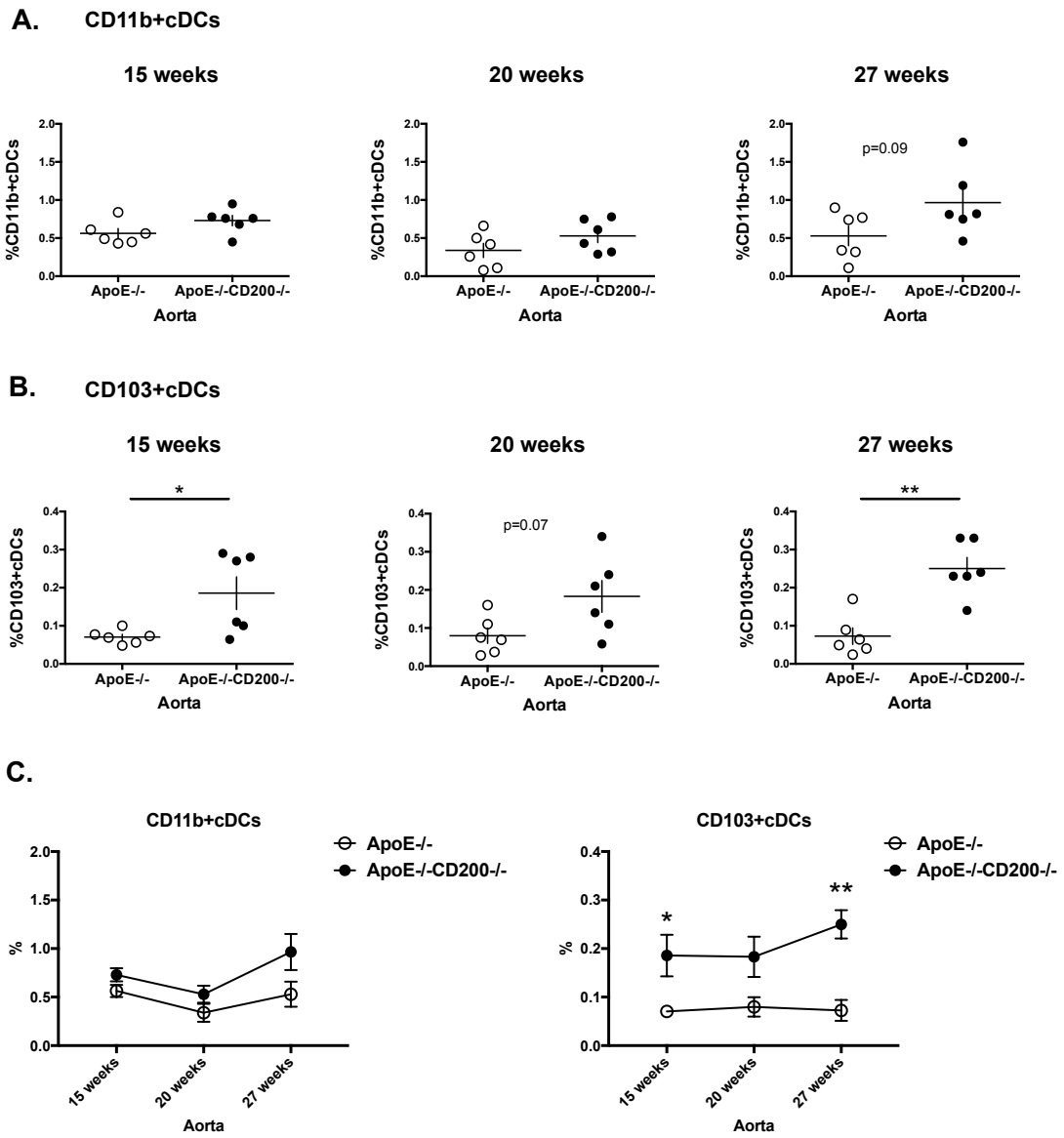


Figure 4.8 CD103+ DCs are increased in the aorta of ApoE-/-CD200-/- mice. Male ApoE-/- (littermates) and ApoE-/-CD200- /- mice were fed a chow diet up to 15, 20 and 27 weeks of age. Single aortas were enzymatically digested as described in Material and Methods and single cell suspensions were used for 10-color flow cytometry. (A) Number of CD11b+cDCs (gated on live CD45+F4/80-CD11c^{+}MHCII^{+}cells), expressed as a percentage of CD45+cells. (B) Number of CD103+cDCs (gated on live CD45+F4/80-CD11c^{+}MHCII^{+}CD11b-cells), expressed as a percentage of CD45+cells, in the aorta of ApoE-/- and ApoE-/-CD200-/- on chow diet at 15, 20 and 27 weeks of age. (C) Plots show the percentages of CD11b+ and CD103+cDCs in the aorta of ApoE-/- and ApoE-/-CD200-/- mice over time. Data show mean ± SEM, **p<0.01, *p<0.05, n=6, Mann-Whitney U test.

Table 4-2 The number of macrophages, cDCs, CD11b+cDCs and CD103+cDCs expressed as percentages of CD45+ cells and absolute numbers, in the aorta of ApoE-/- and ApoE-/-CD200-/- mice at 15, 20 and 27 weeks of age. Male ApoE-/- and ApoE-/-CD200- /- mice were fed a chow diet and culled at 15, 20 and 27 weeks (wks) of age. Single aortas were enzymatically digested as described in Material and Methods and single cell suspensions were used for 10-color flow cytometry. Data show mean ± SEM, **p<0.01, *p<0.05, n=6, Mann-Whitney U test.



	15wks			20wks			27wks		
Arterial Macrophages	**ApoE-/-**	**ApoE-/-CD200-/-**	**p value vs ApoE-/-**	**ApoE-/-**	**ApoE-/-CD200-/-**	**p value vs ApoE-/-**	**ApoE-/-**	**ApoE-/-CD200-/-**	**p value vs ApoE-/-**
%	4.52 ± 0.32	5.73 ± 1.09	p=0.78	5.55 ± 1.04	7.34 ± 0.53	p=0.18	4.58 ± 1.09	7.85 ± 0.86	**p*=0.04**
x103	3 ± 0.001	4 ± 0.002	p=0.82	5 ± 0.002	9 ± 0.002	p=0.18	2.8 ± 0.89	6.9 ± 1.66	**p*=0.017**
Arterial cDCs									
%	0.878 ± 0.068	1.232 ± 0.123	**p*=0.013**	0.642 ± 0.104	1.013 ± 0.117	**p*=0.026**	0.948 ± 0.19	1.865 ± 0.315	**p*=0.04**
x103	1 ± 0.0001	1 ± 0.0003	p=0.72	0.5 ± 0.0002	1 ± 0.0002	**p*=0.03**	1 ± 0.001	2 ± 0.001	p=0.6
Arterial CD11b+cDCs									
%	0.563 ± 0.062	0.730 ± 0.067	p=0.145	0.34 ± 0.09	0.53 ± 0.09	p=0.18	0.53 ± 0.129	0.965 ± 0.185	p=0.09
x103	0.4 ± 0.0001	0.5 ± 0.0002	p=0.79	0.3 ± 0.0001506	0.52 ± 0.00008333	p=0.07	0.7 ± 0.0003	0.9 ± 0.0003	p=0.5
Arterial CD103+cDCs									
%	0.07 ± 0.01	0.19 ± 0.04	**p*=0.03**	0.08 ± 0.02	0.18 ± 0.041	p=0.07	0.073 ± 0.021	0.25 ± 0.029	**p**=0.004**
x103	0.1± 0.00002	0.1 ± 0.00007	p=0.71	0.05± 0.00002	0.2 ± 0.00005	**p*=0.04**	0.1 ± 0.00004	0.2 ± 0.00005	p=0.1

Table 4-3 The numbers of arterial macrophages, characterised by additional markers (such as CD64 and MerTK) and expressed as percentages of single cells, CD45+ cells and absolute numbers in the aorta of ApoE-/- and ApoE-/-CD200-/- mice at 27 weeks of age. Male ApoE-/- and ApoE-/-CD200- /- mice were fed a chow diet and culled at 27 weeks (wks) of age. Single aortas were enzymatically digested as described in Material and Methods and single cell suspensions were used for 10-color flow cytometry. Data show mean ± SEM, **p<0.01, *p<0.05, n=6, Mann-Whitney U test.

	27wks		
Arterial Macrophages	**ApoE-/-**	**ApoE-/-CD200-/-**	**p value vs ApoE-/-**
CD64+ cells			
% (single cells)	0.29 ± 0.055	0.84 ±0.21	**p*=0.017**
%(CD45)	7.06 ± 1.7	11.02 ± 1	p=0.17
x103	4.6 ±0.0013	9.65 ± 0.0023	p=0.08
CD68+cells			
% (single cells)	0.56 ± 0.15	1.4 ± 0.28	**p*=0.03**
%(CD45)	15 ± 4.69	18.68 ± 1.2	p=0.13
x103	8.4 ± 0.002	16 ± 0.004	p=0.24
CD64+CD68+ cells			
% (single cells)	0.25 ± 0.08	0.8 ± 0.2	**p*=0.017**
%(CD45)	3.7 ± 1.16	7.2 ± 0.75	**p*=0.04**
x103	3.6 ± 0.0014	8.9 ± 0.002	p=0.05
CD64+MerTK+ cells			
% (single cells)	0.3 ± 0.13	0.6 ± 0.15	p=0.07
%(CD45)	4.5 ± 1.2	7.9 ± 0.8	p=0.099
x103	2.2 ± 0.0007	5.7 ± 0.001	p=0.08
CD11b+F4/80+ cells			
% (single cells)	0.5 ± 0.19	0.8 ± 0.2	p=0.17
%(CD45)	7.1 ± 1.4	10.6 ± 1.1	p=0.07
x103	7.9 ± 0.0036	9.1 ± 0.002	p=0.3
CD11b+F4/80+CD64+MerTK+ cells			
% (single cells)	0.4 ± 0.2	0.7 ± 0.2	p=0.3
%(CD45)	6 ± 1.5	9 ± 1.5	p=0.19
x103	1.2 ± 0.0004	4 ± 0.0008	**p*=0.017**

4.2.6 The effect of CD200 deficiency in secondary organs

Myeloid populations were also analysed in secondary organs, including spleen and lymph nodes (para-aortic lymph nodes or PALNs, and subiliac lymph nodes or SILNs). No differences in cDCs between the two genotypes of mouse were identified. The numbers of macrophages in the spleen and lymph nodes of ApoE-/- and ApoE-/-CD200-/- mice at 15, 20 and 27 weeks of age are shown in Table 4.4. Macrophages (defined as CD68+F4/80+ cells) were increased in the spleen of ApoE-/-CD200-/- mice at all time points examined (Table 4.4). These CD68+F4/80+ macrophages had increased expression of CD206, CD64 and MerTK but low levels of CD11b (Figure 4.9); suggesting that they are red pulp macrophages (Theurl et al., 2016). Apart from gating on F4/80+CD68+ cells, splenic macrophages were significantly increased when gated on F4/80+CD11b- cells or CD206+ cells. No significant differences in the numbers of CD11b+ macrophages were observed between the 2 groups. In the lymph nodes, there was an increase in CD68+CD64+ macrophages at 15 and 20 weeks of age, whilst there was a trend towards a reduction in these macrophages at 27 weeks of age (Table 4.4). The macrophages in the lymph nodes expressed CD64, MerTK, F4/80, CD11b, MHCII and CD11c (Figure 4.10).

Table 4-4 Numbers of macrophages in the spleen and lymph nodes, expressed as percentages of CD45+ cells and as absolute numbers of ApoE-/- and ApoE-/-CD200-/- mice at 15, 20 and 27 weeks. Male ApoE-/- and ApoE-/-CD200-/- mice were fed a chow diet for 15, 20 or 27 weeks of age. Spleen and lymph nodes (SILNs and PALNs) were isolated, and single cell suspensions were prepared as described in Materials and Methods for 10-color flow cytometry. Data show mean ± SEM, **p<0.01, *p<0.05, n=6, Mann-Whitney U test.

	15wks			20wks			27wks		
Splenic macrophages	**ApoE-/-**	**ApoE-/-CD200-/-**	**p value vs ApoE-/-**	**ApoE-/-**	**ApoE-/-CD200-/-**	**p value vs ApoE-/-**	**ApoE-/-**	**ApoE-/-CD200-/-**	**p value vs ApoE-/-**
%	1.45 ± 0.09	5.68 ± 2.7	p=0.1	2.58 ± 0.45	4.77 ± 0.46	**p*=0.026**	0.82 ± 0.16	3.4 ± 0.71	**p**=0.0043**
x106	0.41 ± 0.02	2.44 ± 1.42	p=0.1	1.3 ± 0.49	3.16 ± 0.35	**p*=0.015**	0.4 ± 0.14	2.1 ± 0.54	**p*=0.026**
Lymph node macrophages	**ApoE-/-**	**ApoE-/-CD200-/-**	**p value vs ApoE-/-**	**ApoE-/-**	**ApoE-/-CD200-/-**	**p value vs ApoE-/-**	**ApoE-/-**	**ApoE-/-CD200-/-**	**p value vs ApoE-/-**
%	0.15 ± 0.03	0.8 ± 0.22	**p**=0.002**	0.32 ± 0.1	0.57 ± 0.2	p=0.39	0.2 ± 0.041	0.09 ± 0.015	p=0.1
x106	0.02 ± 0.01	0.12 ± 0.06	**p*=0.026**	0.08 ± 0.02	0.09 ± 0.02	p=0.7	0.06 ± 0.005	0.03 ± 0.01	p=0.1

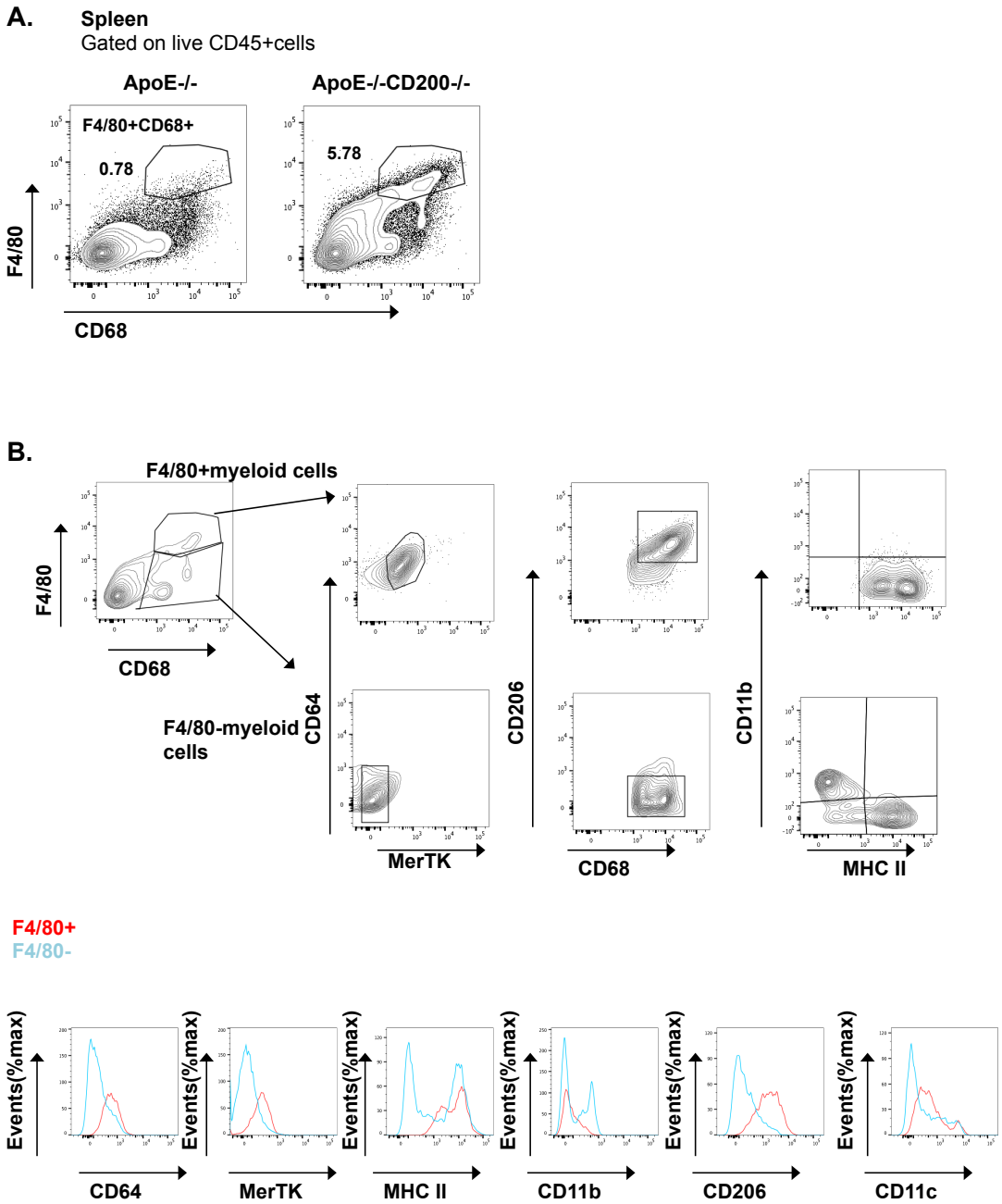


Figure 4.9 Splenic macrophages in ApoE-/- and ApoE-/-CD200-/- mice. Male ApoE-/- and ApoE-/-CD200- /- mice were fed a chow diet for 15, 20 or 27 weeks of age. Spleens were isolated, and single cell suspensions were prepared for 10-color flow cytometry as described in Materials and Methods. (A) Representative plots show F4/80+CD68+ macrophages in the spleen of ApoE-/- and ApoE-/-CD200-/- mice at 27 weeks of age. (B) Plots show the expression of CD64, MerTK, MHCII, CD11b, CD206 and CD11c on F4/80+ CD68+cells (red line) and F4/80- CD68+cells (blue line). F4/80+CD68+ cells express high levels of CD206, CD64, MerTK but low levels of CD11b.

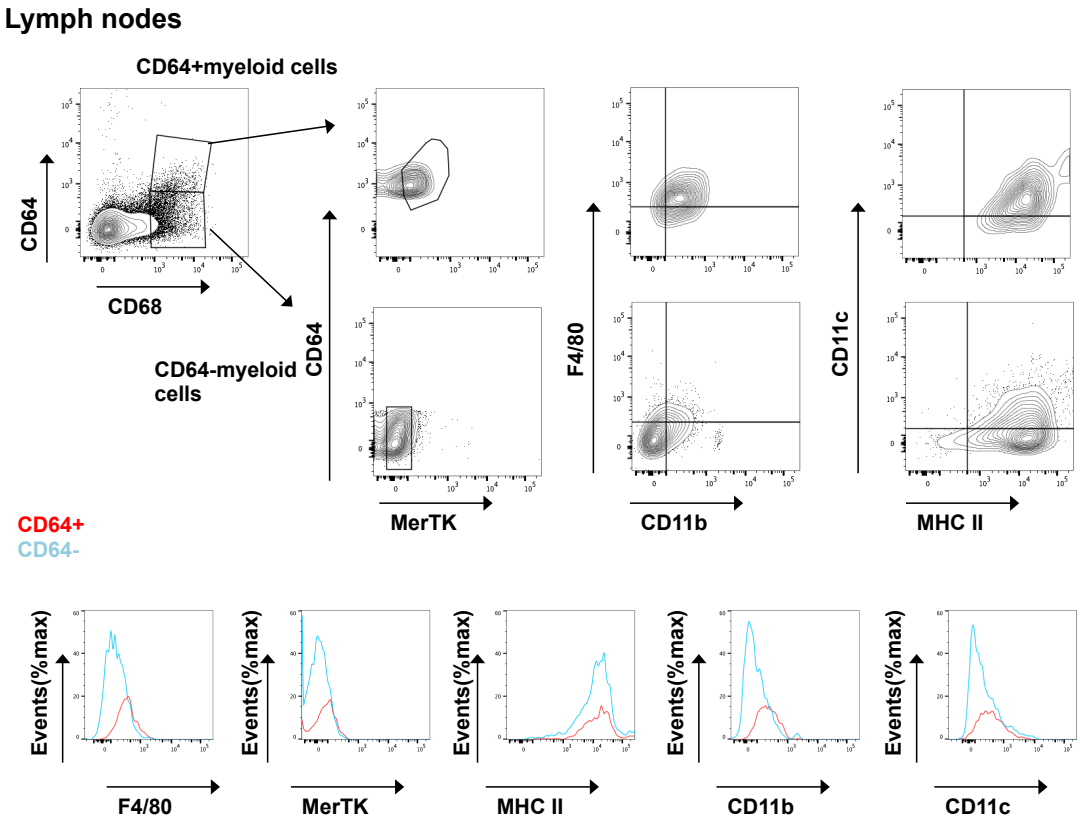


Figure 4.10 Lymph node macrophages in ApoE-/- and ApoE-/-CD200-/- mice. Male ApoE-/- and ApoE-/-CD200- /- mice were fed a chow diet up to 15, 20 and 27 weeks (wks) of age. Lymph nodes (SILNs and PALNs) were isolated, and single cell suspensions were prepared as described in Materials and Methods for 10-color flow cytometry. Representative plots show the expression of F4/80, MerTK, MHCII, CD11b, and CD11c on CD64+CD68+cells (red line) and CD64+CD68+cells (blue line). CD64+CD68+ cells express high levels of CD64, MerTK, F4/80,CD11b, MHCII and CD11c.

4.2.7 CD200 deficiency increases inflammatory blood monocytes in 27-week old ApoE-/- mice

Monocyte and neutrophil cell populations were evaluated in the blood and bone marrow (BM) in ApoE-/- and ApoE-/-CD200-/- mice at 15, 20 and 27 weeks of age by flow cytometry (Table 4.5). Interestingly, monocytes were increased in the blood of ApoE-/-CD200-/-mice at 27 weeks, when expressed as a percentage of CD11b+ cells (14.7 ± 1.6% versus 2 ± 1.7%, p=0.02) (Figure 4.11A). These CD11b+ monocytes had high expression of C-C chemokine receptor (CCR) 2 (Figure 4.12B),

indicating a proinflammatory phenotype. Blood neutrophils were unchanged at all timepoints. However, BM neutrophils were significantly increased at 15 weeks of age, when expressed as a percentage of CD11b+ cells (57 ± 1.3 % versus 61 ± 0.64 %, p=0.017) and absolute cell numbers (22 ± 1.7 $x10^6$ versus 31 ± 2.21 $x10^6$, p=0.0043) (Figure 4.11B).

Table 4-5 The numbers of monocytes and neutrophils in the blood and BM of ApoE-/- and ApoE-/-CD200-/- mice at 15, 20 and 27 weeks of age. Monocytes and neutrophils, expressed as a percentage of CD11b+cells and as absolute numbers. Data show mean ± SEM, **p<0.01, *p<0.05, n=6-15, Mann-Whitney U test.

	15wks			20wks			27wks		
Blood Monocytes	**ApoE-/-**	**ApoE-/-CD200-/-**	**p value vs ApoE-/-**	**ApoE-/-**	**ApoE-/-CD200-/-**	**p value vs ApoE-/-**	**ApoE-/-**	**ApoE-/-CD200-/-**	**p value vs ApoE-/-**
%	21 ± 1.9	19 ± 1.9	p=0.5	18 ± 5.1	16 ± 4.1	p=0.82	14.7 ± 1.6	20 ± 1.7	**p*=0.02**
x10⁶	0.038 ± 0.012	0.058 ± 0.015	p=0.4	0.24 ± 0.10	0.22 ± 0.12	p=0.59	0.046 ± 0.014	0.075 ± 0.026	p=0.4
BM Monocytes	**ApoE-/-**	**ApoE-/-CD200-/-**	**p value vs ApoE-/-**	**ApoE-/-**	**ApoE-/-CD200-/-**	**p value vs ApoE-/-**	**ApoE-/-**	**ApoE-/-CD200-/-**	**p value vs ApoE-/-**
%	28 ± 0.96	28 ± 0.80	p=0.97	17.3 ± 2.9	17.7 ± 2.6	p>0.99	26.20 ± 2.1	26.9 ± 2.5	p=0.7
x10⁶	11 ± 0.96	14 ± 1.45	p=0.065	6.17 ± 0.98	5.4 ± 1.19	p=0.93	9.6 ± 2.2	12.8 ± 4	p=0.80
Blood Neutrophils	**ApoE-/-**	**ApoE-/-CD200-/-**	**p value vs ApoE-/-**	**ApoE-/-**	**ApoE-/-CD200-/-**	**p value vs ApoE-/-**	**ApoE-/-**	**ApoE-/-CD200-/-**	**p value vs ApoE-/-**
%	42.9 ± 2.3	48 ± 3.1	p=0.37	45.8 ± 6.1	54 ± 4	p=0.48	59 ± 5	56 ± 4	p=0.3
x10⁶	0.08 ± 0.028	0.19 ± 0.082	p=0.3	0.48 ± 0.1754	0.5 ± 0.19	p=0.13	0.13 ± 0.04	0.129 ± 0.04	p>0.99
BM Neutrophils	**ApoE-/-**	**ApoE-/-CD200-/-**	**p value vs ApoE-/-**	**ApoE-/-**	**ApoE-/-CD200-/-**	**p value vs ApoE-/-**	**ApoE-/-**	**ApoE-/-CD200-/-**	**p value vs ApoE-/-**
%	57 ± 1.3	61 ± 0.64	**p*=0.017**	73 ± 2.8	69 ± 2.93	p=0.24	52 ± 6.1	48 ± 3.4	p=0.36
x10⁶	22 ± 1.7	31 ± 2.21	**p**=0.0043**	28 ± 3.7	21 ± 2.5	p=0.82	17.8± 3.3	19 ± 3.4	p>0.99

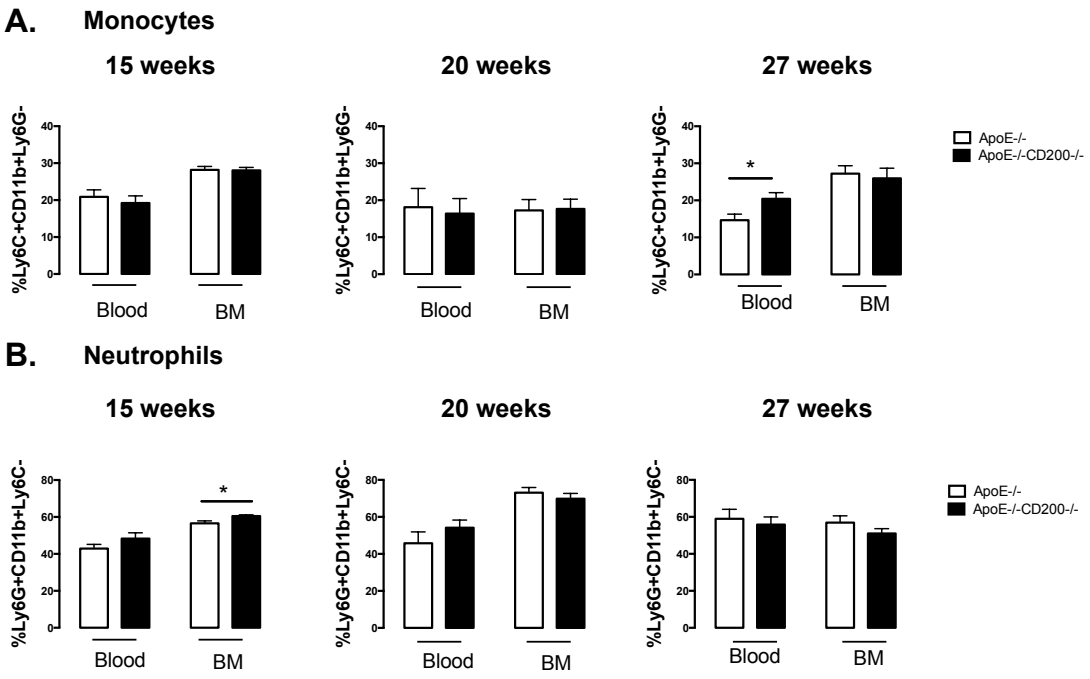


Figure 4.11 The numbers of monocytes and neutrophils in the blood and BM of ApoE-/- and ApoE-/-CD200-/- mice. Male ApoE-/- and ApoE-/-CD200-/- mice were fed a chow diet up to 15, 20 and 27 weeks of age. The blood and the bones were isolated as described in Materials and Methods and single cell suspensions were prepared for flow cytometry. (A) Number of monocytes (gated on live CD11b+Ly6C+Ly6G-cells) and (B) neutrophils (gated on live CD11b+Ly6C-Ly6G+cells) expressed as a percentage of CD11b+ cells in the blood and bones of ApoE-/- and ApoE-/-CD200-/- on chow diet at 15, 20 and 27 weeks of age. Data show mean ± SEM, *$p<0.05$, n=6-15, Mann-Whitney U test.

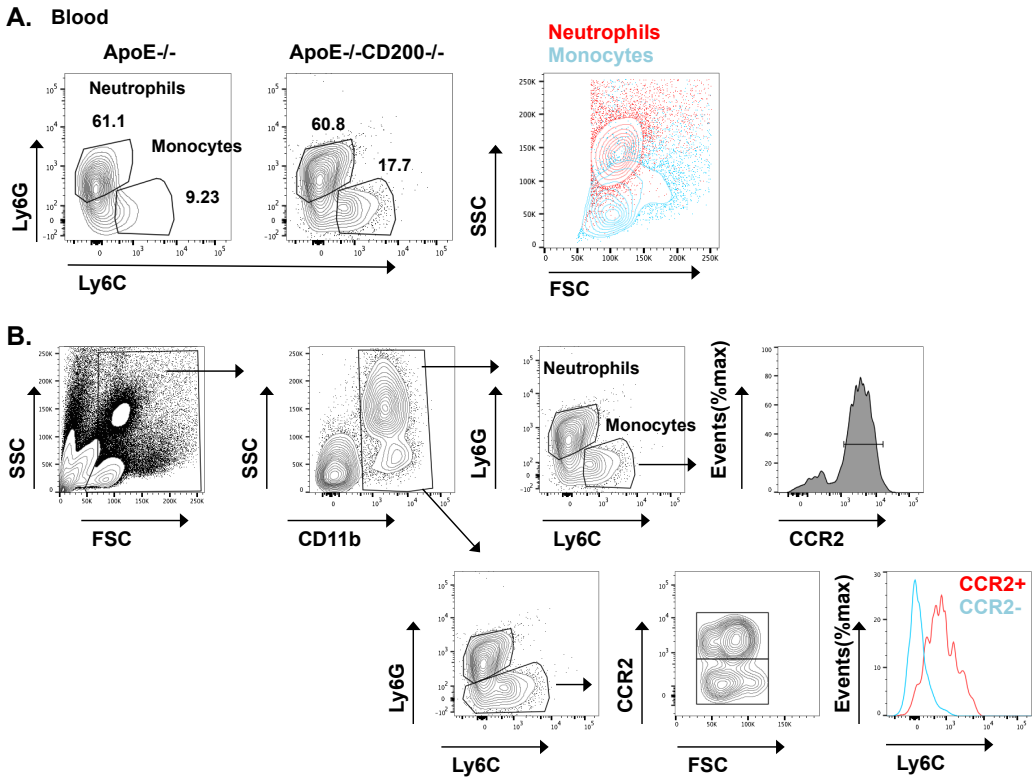


Figure 4.12 Monocytes and neutrophils in the blood of ApoE-/- and ApoE-/-CD200-/- mice. (A) Representative plots show blood neutrophils and monocytes in 27- week old ApoE-/- and ApoE-/-CD200-/- mice. (B) Plots show the gating strategy for blood neutrophils (gated on live CD11b+Ly6G+Ly6C-cells), monocytes (gated on live CD11b+Ly6C+Ly6G-cells) and the level of CCR2 expression on Ly6C+monocytes in ApoE-/- and ApoE-/-CD200-/- mice at 27 weeks of age.

4.3 Discussion

Macrophages are crucial players in atherosclerosis development. In this study I have shown that the CD200-CD200R pathway is a myeloid regulator during advanced stages of atherosclerosis development.

Firstly, ApoE-/-CD200-/- mice have increased lesion development compared to ApoE-/- mice at 27 weeks of age while CD200 deficiency does not affect the development of early atherosclerosis. In particular, at 27 weeks of age, ApoE-/-CD200-/- mice developed plaques, which had high macrophage infiltration and necrotic core areas and low SMC content, which are surrogate markers of vulnerable plaques. The levels of serum cholesterol were unchanged between ApoE-/- and ApoE-/-CD200-/- mice at 27 weeks of age, indicating that cholesterol did not affect the phenotype of these mice.

Since the CD200-CD200R1 axis has been shown to control myeloid regulation (Hoek et al., 2000), I next assessed the number and phenotype of myeloid cells in various organs, including the aorta, spleen, lymph nodes, blood and BM by 10-color flow cytometry. In the aorta, I assessed macrophage and cDCs populations. The discrimination between macrophage and DC populations is challenging, due to the overlap of identification markers. I used several markers including F4/80, CD11b, CD68, CD64 and MerTK and confirmed that F4/80+CD68+ cells expressed CD64 and MerTK. F4/80- cells expressed lower levels of CD64 and MerTK and therefore were considered cDC populations (Busch et al., 2014, Ensan et al., 2016). Although CD64 can distinguish macrophages from DCs in physiological conditions, some studies suggest that it can be expressed by arterial CD11c+CD11b+F4/80+mo-DCs while not detected in CD11c+F4/80-CD11b+cDCs (Busch et al., 2014, Ensan et al., 2016). This study focuses on cDCs and categorises the CD11b+F4/80+ subset

possibly as a macrophage subset, which agrees with more recent studies (Ensan et al., 2016). However, the phenotypic profile of arterial macrophages and DC subsets still need to be fully elucidated.

This study shows that arterial $CD11c^+$ $MHCII^+$-expressing cDCs were increased at all time points of atherosclerosis development in ApoE-/-CD200-/- mice. Choi *et al.,* have recently demonstrated that mouse aorta contains two types of cDCs, CD11b+cDCs, which are macrophage-colony stimulating factor (M-CSF)-dependent and CD103+cDCs which are fms related tyrosine kinase 3 (Flt-3)–dependent (Choi et al., 2011). CD103+ cDCs have an atheroprotective role, while the role of CD11b+cDCs is still unknown. Nevertheless, both subsets are increased during hypercholesterolemic conditions (Choi et al., 2011, Ren et al., 2015). In this study, the numbers of CD103+cDCs were significantly increased at all timepoints of atherosclerosis development in the ApoE-/-CD200-/- mice. Further studies are needed to ascertain whether these cells are increased due to an adaptive mechanism or whether they participate in atherosclerosis development. To the contrary, macrophages were specifically increased at the 27-week time point, suggesting that they may be the main drivers of disease development associated with CD200 deficiency. These results are consistent with the histological data, where I found increased macrophage infiltration in the plaques of 27-week old ApoE-/-CD200-/- mice. However, the underlying mechanisms involved in this macrophage accumulation still need to be investigated.

As well as in the aorta, I found a significant increase in splenic F4/80+ red pulp macrophages at all timepoints (Theurl et al., 2016) and an increase in lymph node macrophages particularly at earlier stages of disease in ApoE-/-CD200-/- mice. This result suggests that the effect of CD200 deficiency does not only affect myeloid

populations in the aorta but also has a systemic effect on the haematopoietic system. Spleen –derived myeloid cells contribute to approximately 30% of plaque macrophages (Robbins et al., 2012) and are mobilised particularly during acute events such as in response to myocardial infarction (MI) (Swirski et al., 2009, Dutta et al., 2015).

In support of this possibility, I found an increase of proinflammatory CCR2-expressing monocytes in the blood of ApoE-/-CD200-/- mice at 27 weeks of age, thus suggesting that CD200 deletion is associated with enhanced hypercholesterolemia-induced monocytosis, a process described by Swirski *et al.,* (Swirski et al., 2007). Genetic deletion of CD200 affects the size and phenotype of advanced lesions in hypercholesterolemic mice without affecting cholesterol levels.

CD200-deficient mice have a significant increase in lesional infiltration of macrophages and DCs. This indicates that CD200 expression is important in resolving athero-inflammation in advanced atherosclerosis disease and that its defect induces more "vulnerable" plaque phenotypes. Impaired resolution of inflammation is a key mechanism that has been recently advocated (Tabas, 2010) to explain the chronicity of athero-inflammation. For instance, Annexin A1, a key mediator of inflammation resolution can induce significant plaque changes (Fredman et al., 2015). CD200 provision, as shown in the previous chapter, would be an additional therapeutic possibility for selective targeting of myeloid populations at advanced stages of atherosclerosis, which are often the clinically relevant stages of the disease.

In conclusion, CD200 deficiency increases macrophages in the lesions, but also leads to an increase in macrophage subsets in the spleen and lymph nodes, and inflammatory monocytes in the circulating blood. This indicates that CD200-mediated

regulation of lesion size and phenotype might be in partly related to systemic changes on the haematopoietic system in CD200-deficient mice.

Chapter 5 High dimensional analysis unravels a role for CD200 in athero-inflammation

Chapter 5: High dimensional analysis unravels a role for CD200 in athero-inflammation

5.1 Introduction

Previously, I demonstrated that CD200 deletion in 27-week old apolipoprotein (ApoE) -/- mice results in an increase in arterial myeloid cells. Myeloid cells are crucial players in atherosclerosis, however their heterogeneity is complex and many phenotypic markers are overlapping, leading to confusing nomenclature (Chinetti-Gbaguidi et al., 2015). Flow cytometric analysis of cells is a far progressed technology; nevertheless, it has several limitations such as autofluorescence, which can lead to erroneous interpretation of data in particular when tissue extracts are involved. In contrast, mass cytometry enables the use of metal isotopes instead of fluorescent tags and allows high-dimensional analysis leading to a deeper understanding of cellular complexity (Bendall et al., 2011). Herein, I aim to use single-cell "mass cytometry" to simultaneously measure 36 parameters and examine myeloid and non-myeloid populations in the aorta, spleen and lymph nodes in ApoE-/- and ApoE-/-CD200-/- mice. Due to time constraints, mice were placed on a high fat diet (HFD) in order to accelerate the development of the disease (Figure 5.1).

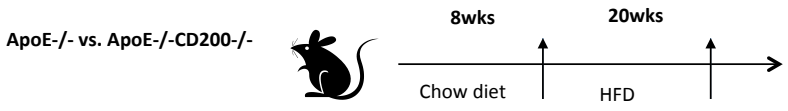
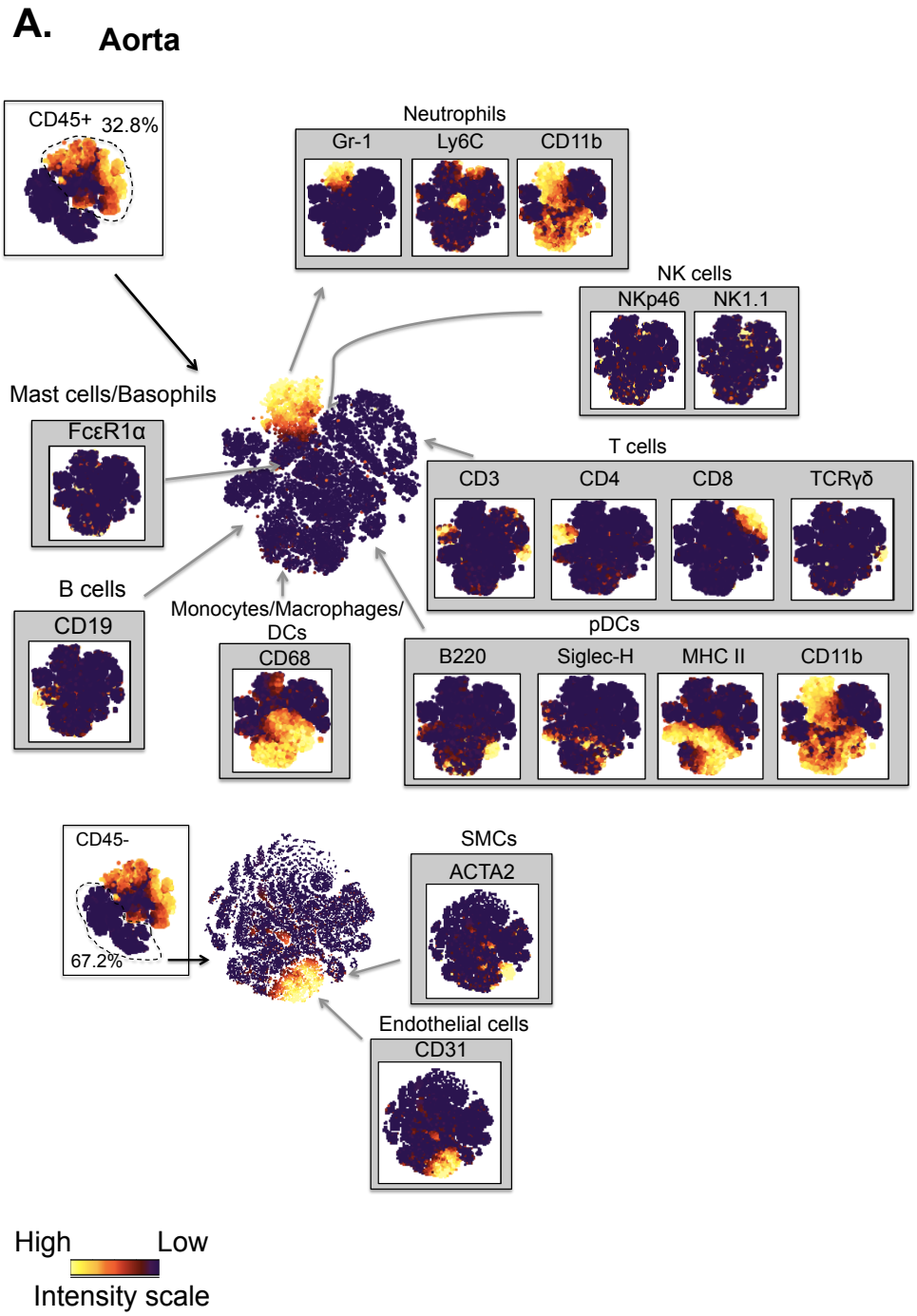


Figure 5.1 Schematic diagram of experimental design showing the time-course of low- and high-cholesterol feeding in ApoE-/- mice. ApoE-/- and ApoE-/-CD200-/- mice were put on HFD at 8 weeks of age for 12 weeks. Tissues, including blood, bones, aortas, lymph nodes and spleen were taken as described in Materials and Methods.

5.2 Results

5.2.1 Immune cell composition in the aorta of ApoE-/-CD200-/- mice

To understand the effect of CD200 deficiency on innate and adaptive immune cells and on stromal cells in the vascular wall, I performed full screening of aortic cells by mass cytometry, whereby cells were stained with 36 metal conjugated antibodies. Within the CD45- population I was able to identify endothelial cells (ECs) and smooth muscle cells (SMCs) (Figures 5.2 A, C). However, these cells only accounted for a fifth of the CD45- cells and I was unable to identify the other CD45- populations with the present marker panel. Nevertheless, using this panel of antibodies, I was able to identify the majority of CD45+ leucocytes which included T cells, B cells, natural killer (NK) cells, mast cells, basophils, dendritic cells (DCs), monocytes, neutrophils and macrophages (Figures 5.2 A, C). The number of these populations of aortic cells, expressed as a percentage of CD45+ or – cells in ApoE-/- and ApoE-/-CD200-/- mice, are illustrated in Table 5.1. The first finding was an increase in CD45+ subsets and a decrease of CD45- cells as a whole in the aortas of CD200-deficient mice (Figure 5.2 C), supporting the previous histology finding of a SMC poor lesion phenotype with a significant infiltration of myeloid cells (Chapter 4). Interestingly, there was a significant increase in T cells (4.6 ± 0.5% versus 8 ± 1%, p=0.016), Fc epsilon receptor (FcεRI) α+Mast cells/Basophils (0.4 ± 0.12% versus 0.3 ± 0.1%, p=0.018) and macrophages (4.4 ± 1.2% versus 8.7 ± 1.3%, p=0.04) in the aorta of ApoE-/-CD200-/- mice compared to ApoE-/- mice.


A.
Aorta
CD45+ 32.8%
Neutrophils
Gr-1
Ly6C
CD11b
NK cells
NKp46
NK1.1
Mast cells/Basophils
FcεR1α
T cells
CD3
CD4
CD8
TCRγδ
B cells
CD19
Monocytes/Macrophages/
DCs
CD68
pDCs
B220
Siglec-H
MHC II
CD11b
CD45-
67.2%
SMCs
ACTA2
Endothelial cells
CD31
High
Low
Intensity scale

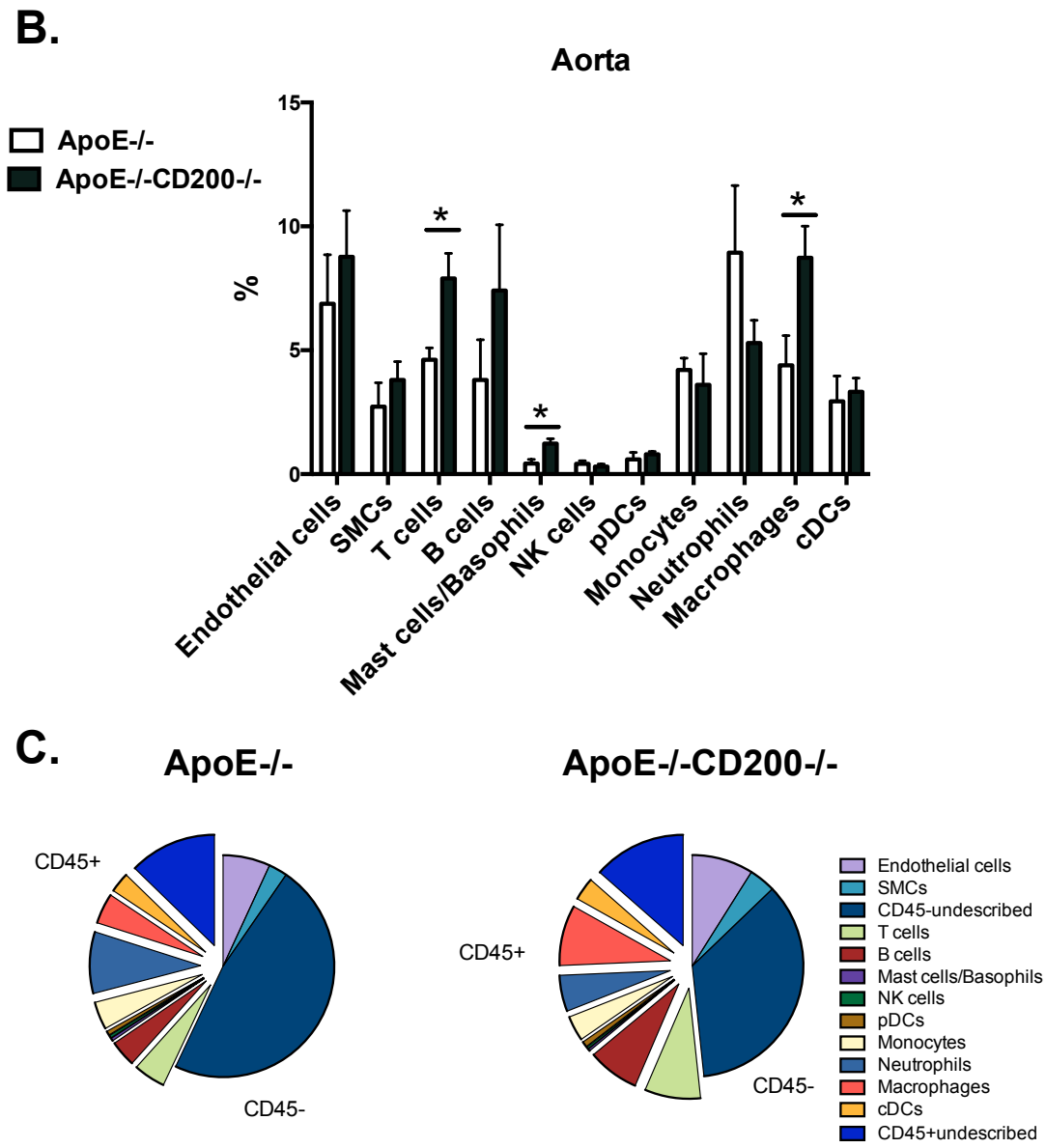


Figure 5.2 Immune and stromal cell composition of the aorta of ApoE-/- and ApoE-/-CD200-/- mice. Male ApoE-/- and ApoE-/-CD200-/- mice were placed on a HFD at 8 weeks of age for 12 weeks. Aortas from two mice were pooled per genotype and were enzymatically digested and used for mass cytometry staining to assess aortic cell populations. Cells were gated on intact live cells. A) viSNE plots illustrate the expression of several markers within CD45- and CD45+ cells. Horizontal color scale represents the median intensity for the markers indicated (yellow=high, black=low). (B) Graph showing the numbers of endothelial cells and SMCs, expressed as a percentage of CD45- cells, and the numbers of T cells, B cells, NK cells, mast cells/basophils, monocytes, neutrophils, pDCs, macrophages and cDCs, expressed as a percentage of CD45+ cells in the aorta of ApoE-/- and ApoE-/-CD200-/- mice. FcεRIα can be expressed both by mast cells and basophils and as I did not have a specific marker to distinguish them, FcεRIα+ cells were considered as mast cells or basophils. (C) Pie charts showing the percentages of endothelial cells and SMCs, expressed as a percentage of CD45- cells, and the numbers of T cells, B cells, NK cells, mast cells/basophils, monocytes, neutrophils, pDCs, macrophages and cDCs, CD45-undescribed cells and CD45+undescribed cells in the aorta of ApoE-/- and ApoE-/-CD200-/- mice. Graphs show mean ± SEM,

*p<0.05, n=4-5, unpaired Student's t-test.

Table 5-1 The numbers of ECs, SMCs, T cells, B cells, NK cells, mast cells, basophils, pDCs, monocytes, neutrophils, macrophages and cDCs in the aortic wall of ApoE-/- and ApoE-/-CD200-/- mice. Male ApoE-/- and ApoE-/-CD200-/- mice were placed on a HFD at 8 weeks of age for 12 weeks. Aortas from two mice were pooled per genotype and were enzymatically digested and used for mass cytometry staining to assess aortic cell populations. Cells were gated on intact live cells. The numbers of endothelial cells and SMCs, expressed as a percentage of CD45- cells, and the numbers of T cells, B cells, NK cells, mast cells/basophils, monocytes, neutrophils, pDCs, macrophages and cDCs, expressed as a percentage of CD45+ cells. FcεRIα can be expressed both by mast cells and basophils and as I did not have a specific marker to distinguish them, FcεRIα+ cells were considered as mast cells or basophils. Data show mean ± SEM, *p<0.05, n=4-5, unpaired Student's t-test.

Cell type	ApoE-/-	ApoE-/-CD200-/-	p vs ApoE-/-
Endothelial cells			
Gated on CD45-CD31+ACTA2-			
%	6.8 ± 2	8.8 ± 1.9	0.5
SMCs			
Gated on CD45-CD31-ACTA2+			
%	2.7 ± 1	3.8 ± 0.7	0.4
T cells			
Gated on CD45+CD3+			
%	4.6 ± 0.5	8 ± 1	**0.016**
B cells			
Gated on CD45+CD3-CD19+CD4-CD8-CD11b-Gr-1-			
%	3.8 ± 1.6	7.4 ± 2.7	0.26
Mast cells/Basophils			
Gated on CD45+CD3-CD19-CD8-CD4-Gr-1-FcεRIα+			
%	0.4 ± 0.12	0.3 ± 0.1	**0.018**
NK cells			
Gated on CD45+CD3-CD19-CD8-CD4-Gr-1-NKp46+NK.1.1+			
%	0.4 ± 0.1	0.3 ± 0.1	0.5
pDCs			
Gated on CD45+CD3-CD19-B220+MHCII+Siglec-H+			
%	0.6 ± 0.3	0.8 ± 0.1	0.5
Monocytes			
Gated on CD45+CD3-CD19-Ly6C+CD11b+Gr-1-			
%	4 ± 0.5	3.6 ± 1.3	0.6
Neutrophils			
Gated on CD45+CD3-CD19-Ly6C-CD11b+Gr-1+			
%	8.9 ± 2.7	5.2 ± 0.9	0.29
Macrophages			
Gated on CD45+CD3-CD19-F4/80+CD68+			
%	4.4 ± 1.2	8.7 ± 1.3	**0.04**
cDCs			
Gated on CD45+CD3-CD19-F4/80-CD11c+MHCII+			
%	2.9 ± 1	3.3 ± 0.5	0.76

5.2.2 Proliferating arterial iNOS+ macrophages are increased in the aorta of ApoE-/-CD200-/- mice

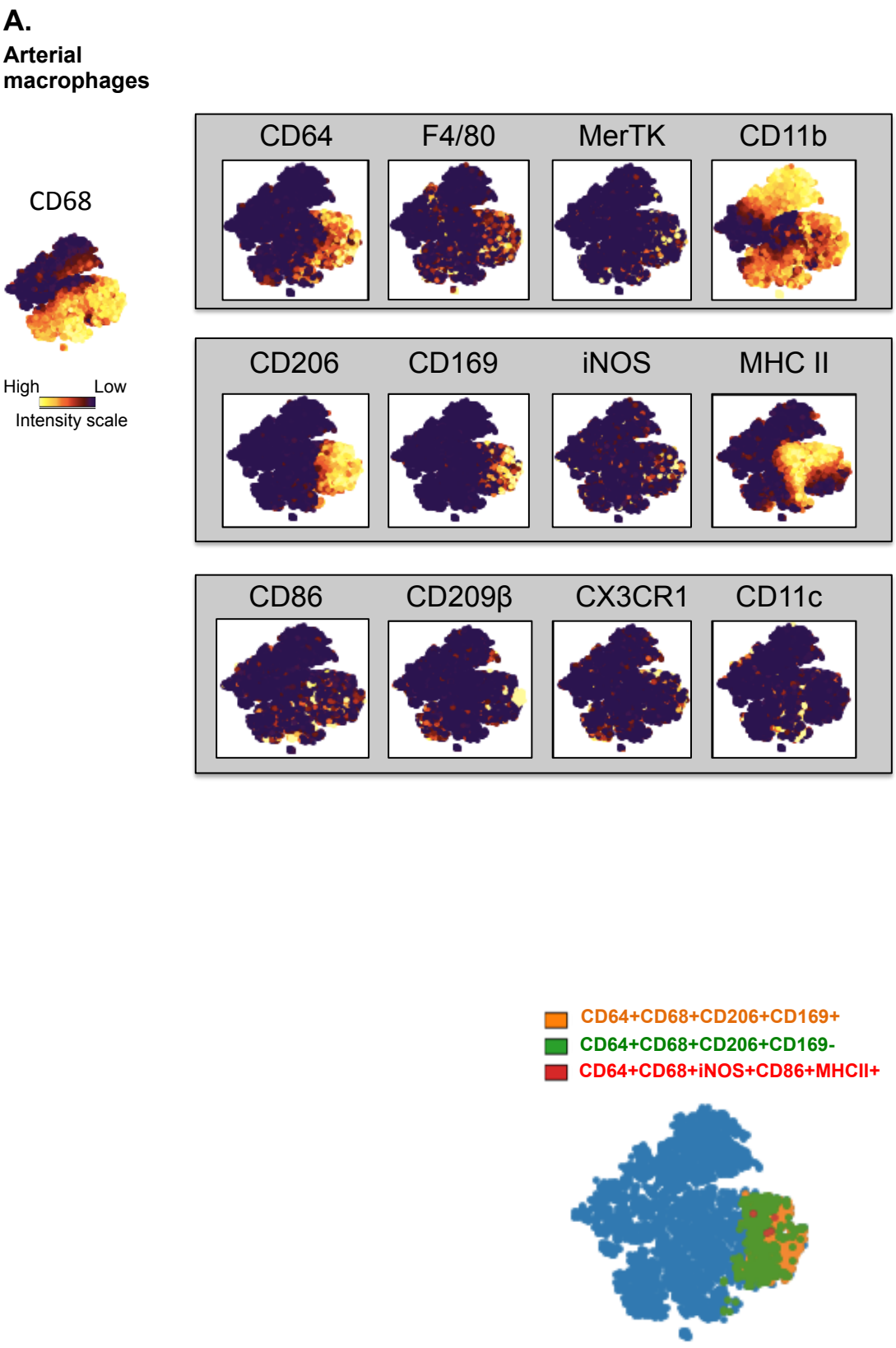
The phenotypic heterogeneity of myeloid cells, including macrophages and DCs, is highly complex as those cells can change their phenotypes depending on tissue microenvironment signals. Since Mantovani *et al.,* proposed the M1/M2 macrophage paradigm; the biology of macrophages (including their ontogeny and functional features) is being constantly revisited (Mantovani et al., 2009, Mantovani et al., 2005, Ginhoux and Jung, 2014).

To assess arterial myeloid populations I first excluded dead cells, T and B cells and I gated on CD68, a common macrophage marker. However, CD68 is not a macrophage-specific marker in the aorta as it was also expressed by DCs (Chapter 4). Therefore, I used additional markers including CD64, CD11b, MerTK and F4/80 to map macrophage populations on viSNE (Figure 5.3 A-D). To identify macrophage subsets I used antibodies against CD206, CD169, iNOS and CD209β. To assess macrophage maturation/activation status I used antibodies against CD86 and MHCII, while their proliferation was examined using ki-67 staining. viSNE analysis of the data revealed that the majority of the CD64+ macrophages express CD206 to some degree. At least three macrophage subsets were identifiable with the current panel: CD206+CD169- macrophages, CD206+CD169+ macrophages and iNOS+CD86+MHCII+ macrophages. A CD206+ CD68+ $CD64^{lo}F4/80^{lo}$CD11c+MHCII+ subset was further identifiable, but more markers will be needed to clarify if they are true macrophages or DCs. Interestingly, all of the CD64+ macrophages expressed CD206. CD206 was also expressed by $CD64^{lo}F4/80^{lo}$CD11c+$MHCII^{+}$ cells, which are possibly DCs. Within CD206+ cells I could identify a cluster of CD169+, iNOS+ and CD209β+ macrophages. The CD169+

macrophages appeared to express high levels of CX3CR1. Additionally, although CD11c has been traditionally considered as a macrophage marker, high levels of CD11c were also found in a $CD64^{lo}$ expressing population. The majority of CD64+ macrophages were CD206+CD169- (CD206+ versus iNOS + versus CD169 = 49.5 ± 2.3% versus 1.7 ± 0.4% versus 29.3 ± 2.6%, p=0.008), while iNOS+ macrophages were a much smaller population (Figures 5.3.A, B).

Interestingly, CD200 deficiency significantly increased the numbers of arterial iNOS+CD86+MHCII+ cells, when expressed as a percentage of macrophages (1.69 ± 0.37% versus 4.6 ± 0.65%, p=0.0049). Arterial CD169+ macrophages appeared to be also increased in ApoE-/-CD200-/- mice, but these differences did not reach statistical significance.

Next, I assessed the level of proliferation by assessing ki-67 expression within the different macrophage subsets. Although, CD206+CD169- macrophages appeared to be able to proliferate more than iNOS+ and CD169+ macrophages, CD200 deficiency significantly increased the mean of ki-67 within iNOS+ (1.69 ± 0.6 versus 7.6 ±1.9, p=0.02) and CD169+ (1.085 ± 0.35 versus 12 ± 2.5, p= 0.05) macrophage subsets (Figure 5.3C).


A.
Arterial macrophages
CD68
High
Low
Intensity scale
CD64
F4/80
MerTK
CD11b
CD206
CD169
iNOS
MHC II
CD86
CD209β
CX3CR1
CD11c
CD64+CD68+CD206+CD169+
CD64+CD68+CD206+CD169-
CD64+CD68+iNOS+CD86+MHCII+

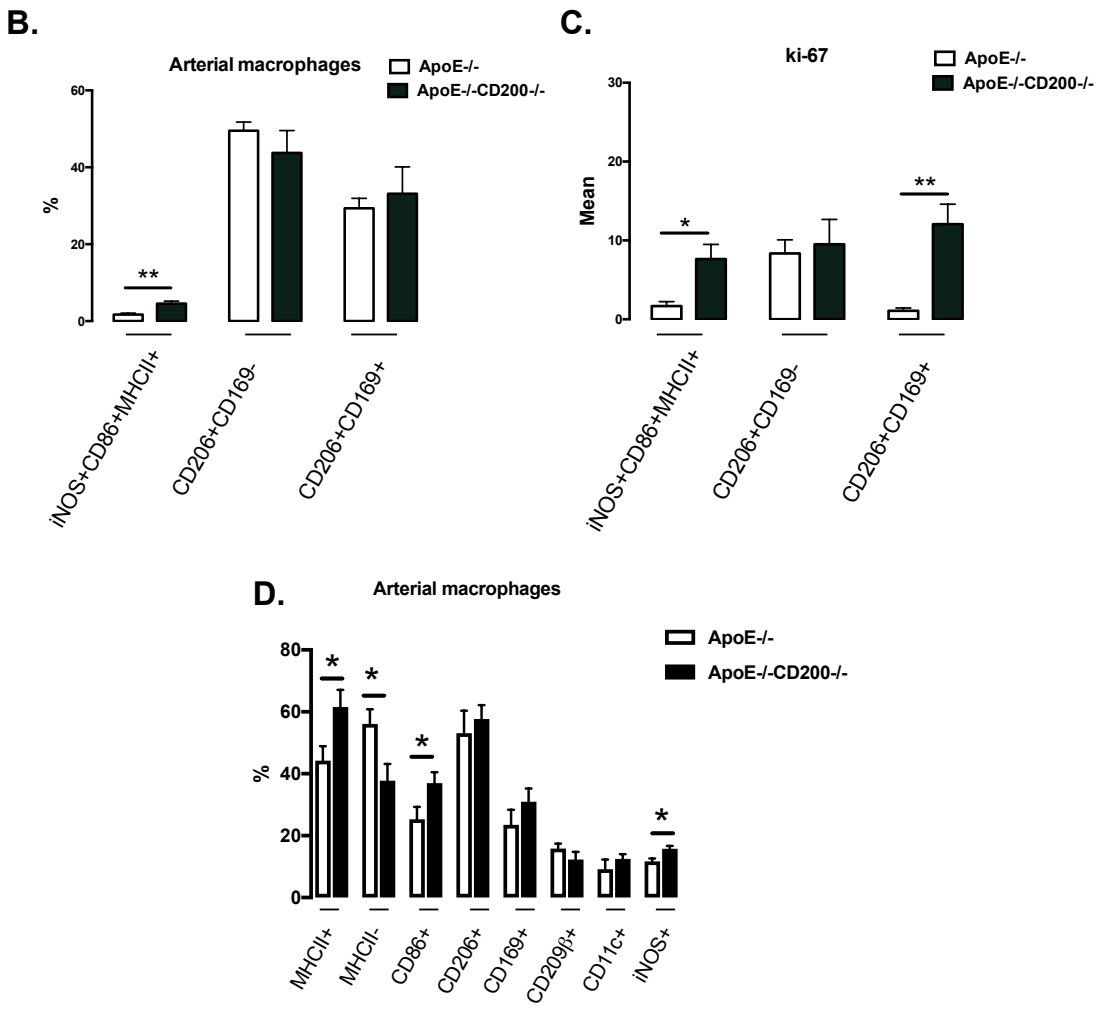


Figure 5.3 Macrophage subsets within the aortic wall of ApoE-/- and ApoE-/-CD200-/- mice. Male ApoE-/- and ApoE-/-CD200-/- mice were placed on HFD at 8 weeks of age for 12 weeks. Aortas from two mice were pooled per genotype and were enzymatically digested and used for mass cytometry staining to assess aortic cell populations. A) viSNE plots show the expression of CD64, F4/80, CD11b, CD206, CD169, iNOS, CD86, CD209β, CX3CR1, CD11c and MHCII within CD68+ cells. Horizontal color scale represents the median intensity for the markers indicated (yellow=high, black=low). (B) Graph showing the numbers of iNOS+CD86+MHCII+, CD206+CD169- and CD206+CD169+ macrophages, expressed as a percentage of macrophages in aorta of ApoE-/- and ApoE-/-CD200-/- mice. (C) Graph showing the mean of ki-67 within iNOS+CD86+MHCII+, CD206+CD169- and CD206+CD169+ macrophages. (D) Graph showing the numbers of MHCII+, MHCII-, CD86+, CD206+, CD169+, CD209β +, CD11c+ and iNOS+ macrophages in aorta of ApoE-/- and ApoE-/-CD200-/- mice. Data show mean ± SEM, **p<0.01, *p<0.05, n=4-5, unpaired Student's t-test.

5.2.3 CD4+T cells are expanded in the aorta of ApoE-/-CD200-/- mice

As a significant increase was identifiable in CD3+ T cells in the aorta of ApoE-/-CD200-/- mice, I next assessed arterial T cell subsets including CD4+, CD8+, ROR-

γ+ and TCRγδ+ T cells (Figure 5.2A). Interestingly, CD200 deficiency significantly expanded CD4+ T cells, when expressed as a percentage of CD3+ T cells (45.5 ± 3.4% versus 58.8 ± 2.8%, p=0.02) (Figure 5.4A). However, this expansion was not due to an increase in Th17 cells (gated on CD4+ROR-γ+) but rather an increase in ROR-γ- cells (40.9 ± 3.34% versus 55.9 ± 2%, p=0.09) (Figure 5.4A). I also assessed T cell proliferation and found an increase in the mean of ki-67 within arterial CD4+ T cells, and particularly CD4+ ROR-γ- T cells, in ApoE-/-CD200-/- mice, albeit this difference did not reach statistical significance (Figure 5.4B).

The accumulating iNOS+ arterial macrophages were expressing co-stimulatory molecules such as CD86 and MHCII (Figure 5.3), which could explain the enhanced arterial T cell activation associated with CD200 deficiency.

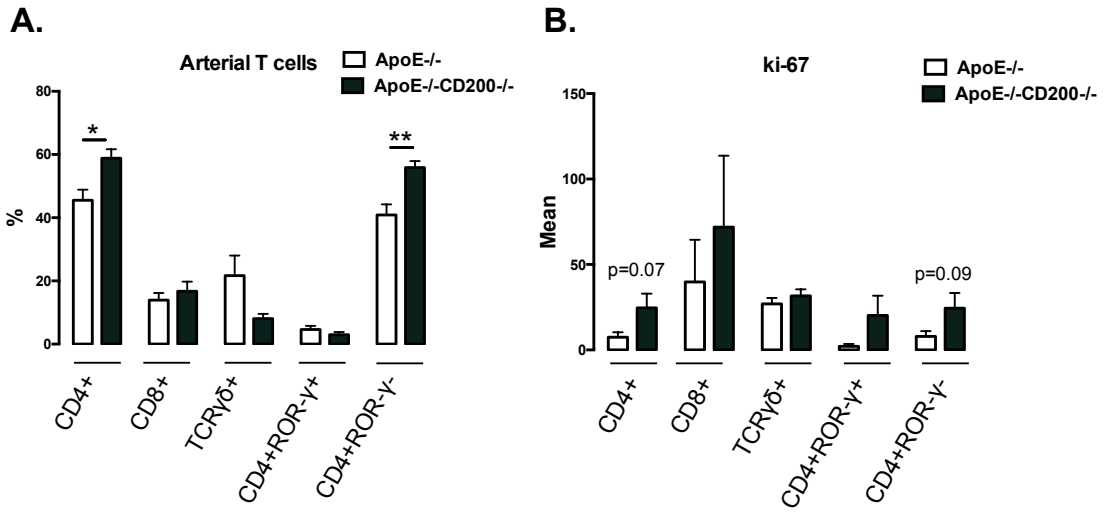
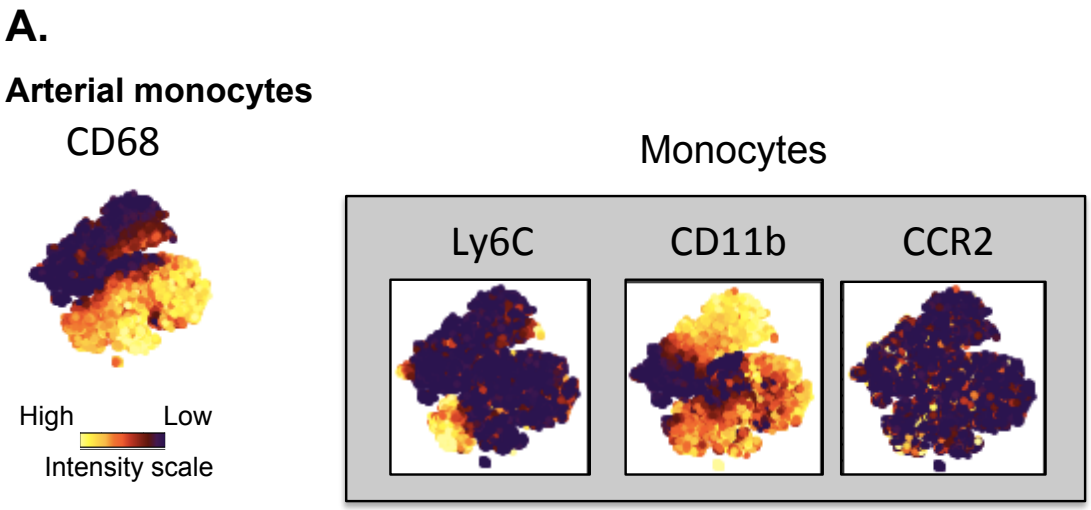


Figure 5.4 T cell subsets within the aortic wall of ApoE-/- and ApoE-/-CD200-/- mice. Male ApoE-/- and ApoE-/-CD200-/- mice were placed on a HFD at 8 weeks of age for 12 weeks. Aortas from two mice were pooled per genotype and were enzymatically digested and used for mass cytometry staining to assess arterial T cell populations. (A) Graph shows the numbers of CD4+, CD8+, TCRγδ+ and CD4+ROR-γ+/- T cells expressed as a percentage of CD3+T cells in aorta of ApoE-/- and ApoE-/-CD200-/- mice. (B) Graph shows the mean expression of ki-67 within CD4+, CD8+, TCRγδ+ and CD4+ROR-γ+/- T cells in aorta of ApoE-/- and ApoE-/-CD200-/- mice. Graphs show mean ± SEM, **p<0.001, p*<0.05, n=4-5, unpaired Student's t-test.

5.2.4 CD200 deficiency increases arterial CCR2+ monocytes in ApoE-/- mice

To assess the role of CD200 in myeloid cells, I also investigated arterial CCR2/CX3CR1+ monocytes in ApoE-/- and ApoE-/-CD200-/- mice (Figure 5.5A). I found that arterial CCR2+ monocytes had higher Ly6C expression than CX3CR1+ monocytes. Interestingly, arterial CCR2+ monocytes were significantly increased in ApoE-/-CD200-/- mice, when expressed as a percentage of monocytes (14.4 ± 2.5% versus 36.7 ± 5%, p=0.003) (Figure 5.5A,B). Arterial CX3CR1+ monocytes were decreased in ApoE-/-CD200-/- mice, but this difference did not reach statistical significance (Figure 5.5B).



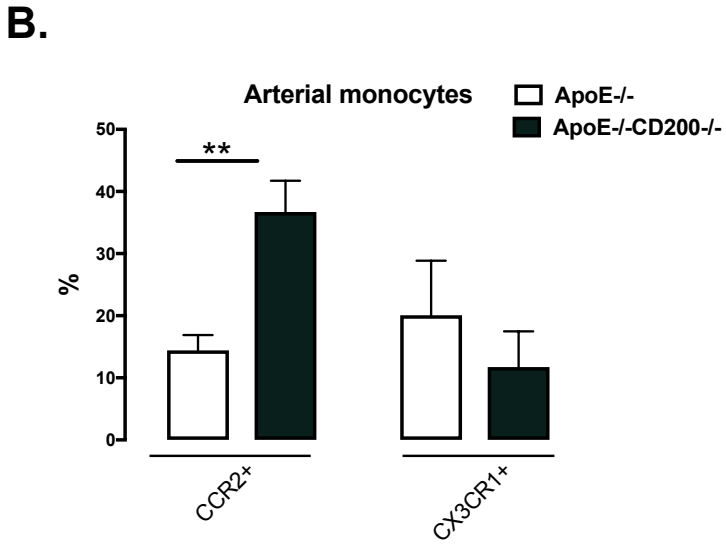


Figure 5.5 CCR2+ and CX3CR1+ monocytes within the aortic wall of ApoE-/- and ApoE-/-CD200-/- mice. Male ApoE-/- and ApoE-/-CD200-/- mice were placed on HFD at 8 weeks of age for 12 weeks. Aortas from two mice were pooled per genotype and were enzymatically digested and used for mass cytometry staining to assess arterial monocyte populations. A) viSNE plots show the expression of Ly6C, CD11b and CCR2 within Ly6C+ monocytes. Horizontal color scale represents the median intensity for the markers indicated (yellow=high, black=low). (B) Graph shows the numbers of CCR2+ and CX3CR1+ monocytes, expressed as a percentage of Ly6C+monocytes in aorta of ApoE-/- and ApoE-/-CD200-/- mice. Graph shows mean ± SEM, p**<0.01, n=4-5, unpaired Student's t-test.

5.2.5 CD200 deficiency affects immune cells in secondary organs

Next, I assessed the role of CD200 deficiency on immune cells in the spleen and lymph nodes in ApoE-/- mice. In the spleen, I found a significant increase in B cells (23.5 ± 2.6% versus 29.6 ± 1.5%, p=0.05) and a decrease in mast cells/basophils (1.9 ± 0.3% versus 1.2 ± 0.1%, p=0.02), NK cells (1.6 ± 0.16% versus 0.97 ± 0.1%, p=0.01), monocytes, (4.7 ± 0.85% versus 1.6 ± 0.26%, p=0.0027) neutrophils, (9.3 ± 2.2% versus 2.9 ± 0.7%, p=0.015), macrophages (4 ± 0.6% versus 1.8 ± 0.25%, p=0.003) and cDCs (0.5 ± 0.08% versus 0.3 ± 0.04%, p=0.014) in ApoE-/-CD200-/- mice (Figures 5.6A, B). To assess macrophage populations and their subsets I used antibodies against CD206, CD169, F4/80, MerTK, CD11b, MHCII, CD11c, CD209β and iNOS. I could identify CD64+, MertK+, F4/80+ and CD206+ macrophages, which were either $CD11b^{lo}$ or $CD11b^{hi}$. The majority of these macrophages expressed high levels of MHCII, possibly indicating their maturation status. On the other hand, CD209β+ macrophages expressed high levels of CD11b but lower levels of F4/80 and MHCII (Figure 5.6A). Additionally, the decrease in CD64+ macrophages was due to a reduction in CD209β+ macrophages (Figure 5.6C). In lymph nodes, there was a significant decrease in neutrophils (0.27 ± 0.024% versus 0.18 ± 0.03%, p=0.048),

while no differences in macrophage populations were observed between ApoE-/- and ApoE-/-CD200-/- mice (Figures 5.6D, E).

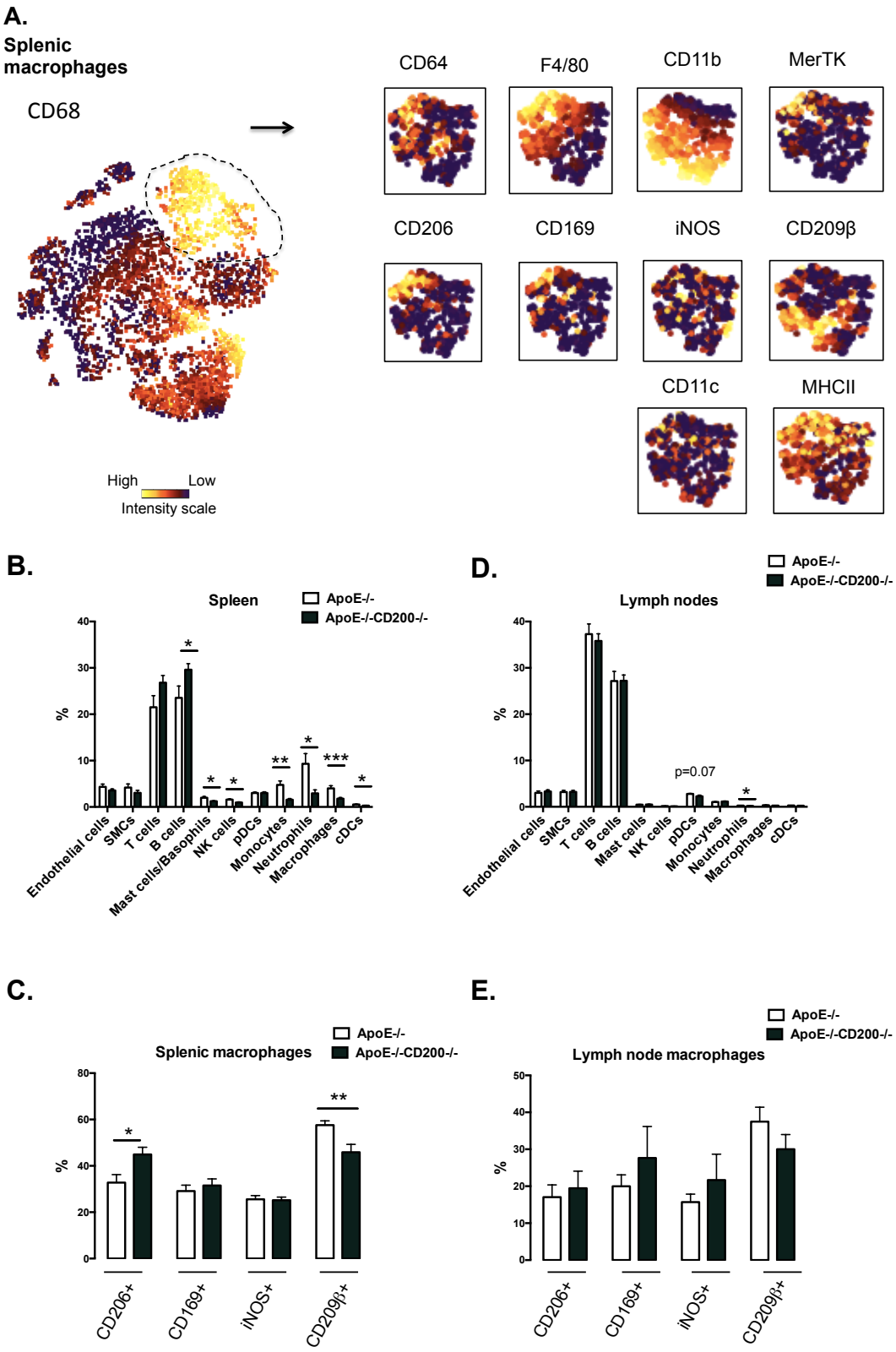


Figure 5.6 Immune cell composition of the spleen and lymph nodes of ApoE-/- and ApoE-/-CD200-/- mice. Male ApoE-/- and ApoE-/-CD200-/- mice were placed on HFD at 8 weeks of age for 12 weeks. Cells were analysed by mass cytometry. Cells were gated on intact live cells. A) viSNE plots show the expression of CD64, F4/80, CD11b, CD206, CD169, iNOS and CD209β within CD68+ cells. Horizontal color scale represents the median intensity for the markers indicated (yellow=high, black=low). (B) Graph shows the numbers of endothelial cells and SMCs, expressed as a percentage of CD45- cells, and the numbers of T cells, B cells, NK cells, mast cells/basophils, monocytes, neutrophils, pDCs, macrophages and cDCs, expressed as a percentage of CD45+ cells, in the spleen of ApoE-/- and ApoE-/-CD200-/- mice. (C) Graph shows the numbers of CD206+, CD169+, iNOS+ and CD209β+ macrophages, expressed as a percentage of macrophages in the spleen of ApoE-/- and ApoE-/-CD200-/- mice. (D) Graph shows the numbers of endothelial cells and SMCs, expressed as a percentage of CD45- cells, and the numbers of T cells, B cells, NK cells, mast cells/basophils, monocytes, neutrophils, pDCs, macrophages and cDCs, expressed as a percentage of CD45+ cells in the lymph nodes of ApoE-/- and ApoE-/-CD200-/- mice. (E) Graph shows the numbers of CD206+, CD169+, iNOS+ and CD209β + macrophages, expressed as a percentage of macrophages in the lymph nodes of ApoE-/- and ApoE-/-CD200-/- mice. Graphs show mean ± SEM, ***p<0.001, **p<0.01, *p<0.05, n=8-10, unpaired Student's t-test.

5.2.6 CD200 and CD200R expression *in vivo* and *in vitro*

In order to understand the role of CD200-CD200R signalling in the immune system I assessed their expression in various tissues, including aorta, spleen and lymph nodes by mass cytometry in ApoE-/- mice. CD200 and CD200R expression on leucocytes and non-leucocytes is shown in Tables 5.2 and 5.3. Both CD200 and CD200R expression were detected in various cell types, including non-leucocytes such as endothelial cells and SMCs but also in leucocytes such as T cells, B cells and myeloid cells (Figures 5.7 A-C). Interestingly, in the aorta, CD200 was mainly expressed by endothelial cells, SMCs and pDCs, while CD200R expression was mainly observed in splenic endothelial cells and lymph node neutrophils in ApoE-/- mice (Figures 5.7 B, C).

To specifically understand the role of CD200 and CD200R in myeloid cells, I also assessed CD200 and CD200R expression in granulocyte macrophage colony stimulating factor (GM-CSF) and macrophage colony stimulating factor (M-CSF)

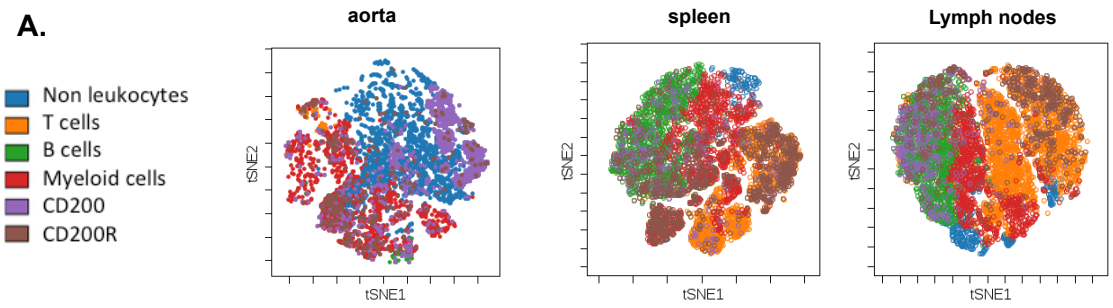
polarised bone marrow (BM)-derived macrophages *in vitro*. I found that CD200 expression was increased by lipopolysaccharide (LPS) treatment both in GM-CSF (117 ± 7 versus 173 ± 13, p= 0.014) and M-CSF (130 ± 9.5% versus 250 ± 42%, p=0.0084) treated cell cultures. Interferon (IFN)-γ addition also increased CD200 expression (130 ± 9.5% versus 242 ± 14%, p<0.0001) while addition of interleukin (IL)-4/IL-13 did not significantly affect CD200 expression (Figure 5.7 D). CD200R expression was also significantly increased by addition of LPS in GM-CSF treated macrophages (170 ± 8% versus 260 ± 20%, p=0.0009). IFN-γ (659 ± 129% versus 1080 ± 68%, p=0.01) and IL-4/IL-13 (659 ± 129% versus 1162 ±202%, p=0.05) treatment in M-CSF treated macrophages (Figure 5.7 D).

Table 5-2 CD200 expression (mean) on T cells, B cells, NK cells, neutrophils, monocytes, macrophages/DCs, pDCs, SMCs and ECs in the aorta, spleen and lymph nodes in ApoE-/- mice. Male ApoE-/- and ApoE-/-CD200-/- mice were placed on HFD at 8 weeks of age for 12 weeks. T cells were gated on CD45+CD3+ cells, B cells were gated on CD45+CD3-CD19+ Gr-1- cells, NK cells were gated on CD45+CD3-CD19-CD335+CD161+ cells, pDCs were gated on CD45+CD3-CD19-B220+MHCII+SiglecH+cells, monocytes were gated on CD45+CD3-CD19-Ly6C+CD11b+Gr-1- cells, neutrophils were gated on CD45+CD3-CD19-Ly6C-CD11b+Gr-1+, macrophages/DCs were gated on CD45+CD3-CD19-CD68+ Gr-1-Ly6C-CD335-CD161-. Data show mean ± SEM, n=5-10.

CD200 expression (mean)	Aorta	Spleen	Lymph nodes
T cells	1.30 ± 0.3	3.8 ± 0.5	3.2 ± 0.1
B cells	2.3 ± 0.6	5.4 ± 0.7	10.3 ± 0.4
NK cells	1.13 ± 0.6	0.9 ± 0.1	2.5 ± 0.6
Neutrophils	0.87 ±0.2	1.3 ± 0.6	1.3 ± 0.8
Monocytes	2.4 ± 1	1.2 ± 0.2	1.98 ± 0.4
Macrophages/DCs	2 ± 0.6	2 ± 0.2	2 ± 0.1
pDCs	5.7 ± 2.9	3 ± 0.3	2.7 ± 0.27
SMCs	43 ± 18	1.3 ± 0.3	1.9 ± 0.4
Endothelial cells	161 ± 35	0.3 ± 0.1	0.9 ± 0.3

Table 5-3 CD200R expression (mean) on T cells, B cells, NK cells, neutrophils, monocytes, macrophages/DCs, pDCs, SMCs and ECs in the aorta, spleen and lymph nodes in ApoE-/- mice. Male ApoE-/- and ApoE-/-CD200-/- mice were placed on HFD at 8 weeks of age for 12 weeks. T cells were gated on CD45+CD3+ cells, B cells were gated on CD45+CD3-CD19+ Gr-1- cells, NK cells were gated on CD45+CD3-CD19-CD335+CD161+ cells, pDCs were gated on CD45+CD3-CD19-B220+MHCII+SiglecH+cells, monocytes were gated on CD45+CD3-CD19-Ly6C+CD11b+Gr-1- cells, neutrophils were gated on CD45+CD3-CD19-Ly6C-CD11b+Gr-1+, macrophages/DCs were gated on CD45+CD3-CD19-CD68+ Gr-1-Ly6C-CD335-CD161- cells. Data show mean ± SEM, n=5-10.

CD200R expression (mean)	Aorta	Spleen	Lymph nodes
T cells	0.67 ± 0.2	3.5 ± 0.3	2 ± 0.05
B cells	0.5 ± 0.1	2 ± 0.3	1.2 ± 0.1
NK cells	0.46 ± 0.1	2.58 ± 0.8	1.6 ± 0.3
Neutrophils	0.2 ± 0.04	6.8 ± 0.4	9.6 ± 4.5
Monocytes	0.5 ± 0.1	3.78 ± 0.4	0.8 ± 0.2
Macrophages/DCs	0.8 ± 0.3	2.9 ± 0.3	0.4 ± 0.04
pDCs	0.45 ± 0.1	1.4 ± 0.1	0.98 ± 0.2
SMCs	1.4 ± 0.15	0.15 ± 0.1	0.4 ± 0.14
Endothelial cells	0.16 ± 0.04	15 ± 6	0.3 ± 0.1



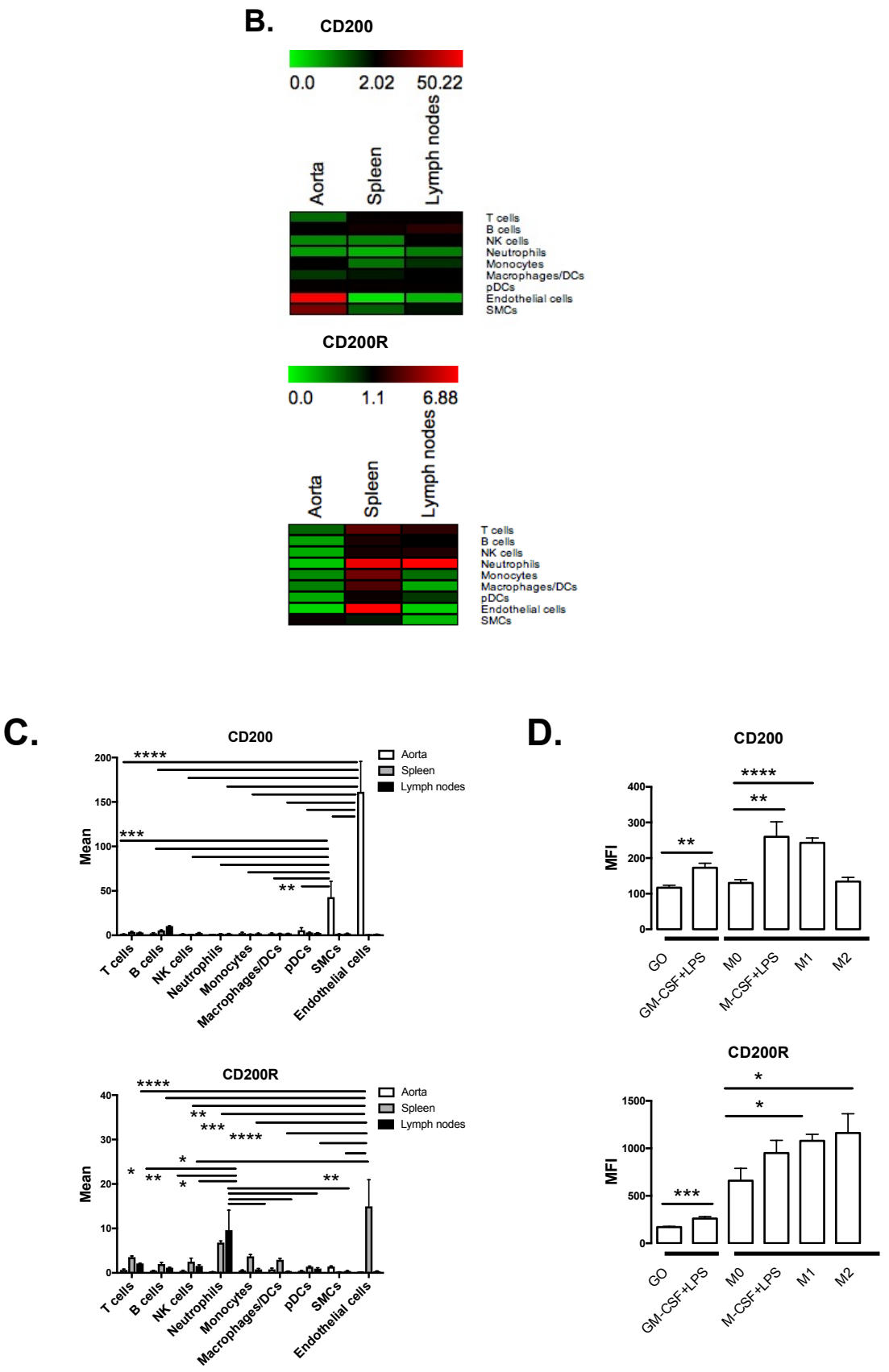


Figure 5.7 The expression of CD200 and CD200R *in vivo* and *in vitro*. Male ApoE-/- mice were placed on HFD at 8 weeks of age for 12 weeks or kept on chow diet for 27 weeks and CD200 and CD200R expression was assessed *in vivo* and *in vitro*. (A) viSNE plots show

CD200 and CD200R expression within T cells, B cells and myeloid cells in the aorta, spleen and lymph nodes. (B) Heat maps show CD200 and CD200R expression within T cells, B cells, NK cells, macrophages/DCs, pDCs, endothelial cells and SMCs in the aorta, spleen and lymph nodes (red=high, green= low). (C) Mean of CD200 and CD200R expression within T cells, B cells, NK cells, macrophages/DCs, pDCs, endothelial cells and SMCs in the aorta, spleen and lymph nodes of ApoE-/- mice on HFD for 12 weeks. Data show mean ± SEM, n=5, Two-way ANOVA. (D) MFI (median) of CD200 and CD200R in 20ng/ml GM-CSF, unstimulated (G0) or 100ng/ml LPS-stimulated and 100ng/ml M-CSF unstimulated (M0) LPS-stimulated, 10ng/ml IFN-γ and 100ng/ml LPS-stimulated (M1) and 20ng/ml IL-4/IL-13-stimulated (M2) cell cultures derived from the bones of 27 week old ApoE-/- mice. Data show mean ± SEM, n=9.

5.3 Discussion

In this chapter I aimed to investigate the effect of CD200-CD200R on leucocytes and non-leucocytes in various tissues, including aorta, spleen and lymph nodes. Therefore, ApoE-/- and ApoE-/-CD200-/- mice were fed a HFD for 12 weeks to accelerate the development of the disease and their tissues were used for single-cell mass cytometry. I explored the expression of CD200 and CD200R in ApoE-/- mice to try to determine the types of cells that may be interacting during atherosclerosis. I mainly detected CD200 expression in arterial ECs and SMCs while CD200R expression was found on various cell types in the aorta of ApoE-/- mice, such as myeloid cells, ECs, SMCs and lymphocytes. CD200 expression was also detected on a non-leucocyte population, which could not be described. CD200R expression was largely found on splenic ECs and lymph node neutrophils. Therefore, it is plausible that the CD200-CD200R interaction is an interaction between a non-leucocyte, possibly EC and a leucocyte. A recent study showed that the endothelial localisation of CD200 is heterogeneous and depends on the tissue microenvironment, such as high shear stress and intraluminal pressure. The physical interaction between an endothelial CD200+ cell and a CD200R+ cell might have an impact on macrophage–endothelium interactions or T cell adhesion (Ko et al., 2009). I also found that CD200 expression is increased by LPS treatment *in vitro*, indicating that the CD200R pathway is induced by toll-like receptor (TLR)- mediated signalling.

Secondly, I assessed the effect of CD200 deletion on arterial monocyte and macrophage/DC cell populations in ApoE-/- mice. Interestingly, CD200 deficiency increased arterial CCR2+ monocytes and iNOS + macrophages. Additionally, the proliferation of iNOS + macrophages appeared to significantly increase with CD200

deficiency. This data is consistent with the literature. Increased iNOS+ cells in CD200-/- mice have been previously reported by other studies (Nathan and Muller, 2001, Cortez et al., 2011, Deckert et al., 2006, Hoek et al., 2000). However, this data is the first to suggest that both monocyte recruitment and macrophage proliferation could possibly contribute to the proinflammatory macrophage accumulation associated with CD200 deficiency. Further studies are needed to elucidate the exact mechanisms of this accumulation.

I also found a significant increase in CD4+T cells in the aorta of ApoE-/-CD200-/- mice, which was not due to Th17 cells. Increased T cell responses have been previously reported in CD200-/- mice in various studies (Li et al., 2012, Caserta et al., 2012). One possible explanation for the increased CD4+ T cells could be the enhanced antigen presentation by the CD86+MHCII+iNOS+ macrophages.

FcεRIα+ cells were also increased in the aorta of ApoE-/-CD200-/- mice. However, since I did not have additional markers, such as c-kit, mast cells and basophils could not be further distinguished. According to the literature there is evidence that associates the CD200R axis with mast cell regulation. Treatment with agonistic CD200R antibodies has been shown to inhibit FcεRIα+ mast cell degranulation *in vitro* (Cherwinski et al., 2005, Zhang et al., 2004). However, the role of mast cells in atherorosclerosis is poorly understood and thus further studies are needed.

Previously I have shown that the effect of CD200 deficiency is systemic as there was a significant increase in splenic and lymph node macrophages in CD200 deficient mice, which were fed on chow diet. Here, ApoE-/- and ApoE-/-CD200-/- mice were put on HFD in order to speed up the development of the disease. Interestingly, ApoE-/-CD200-/- mice had increased numbers of splenic B cells but decreased splenic mast cells/basophils, NK cells, monocytes, neutrophils, and macrophages and cDCs,

indicating that the CD200R pathway might affect the innate and adaptive system differently in the spleen. The decrease within the macrophage subsets was due to a decrease in CD209β+ macrophages while CD206+ red pulp macrophages were significantly increased in the spleen of ApoE-/-CD200-/- mice. CD209β+ macrophages are a specialised splenic tissue resident subset located in the marginal zone and responsible for the clearance of microbes and viruses from the circulation (Davies et al., 2013a). The phenotype of these macrophages was distinct from red pulp CD206+ and CD169+ metallophilic macrophages, as they could express high levels of CD11b and low levels of MHCII, which might indicate that they are immature macrophages (Andreesen et al., 1990). Remarkably, the increase in arterial inflammatory monocytes and macrophages was accompanied by a decrease in splenic monocytes and macrophages, suggesting that CD200 deficiency might promote monocyte mobilisation from the spleen at advanced stages of the disease, which has been previously reported in Angiotensin II studies (Mellak et al., 2015). However, it should be noted that the myeloid distribution is tissue specific and therefore the functional role of each myeloid subset should be investigated in a tissue-specific manner.

ApoE-/-CD200-/- mice also exhibited a decrease in lymph node neutrophils. Interestingly, CD200R is highly expressed in lymph node neutrophils, indicating that CD200 deficiency might lead to changes in CD200R+ cells and therefore the effect of CD200 deletion on various cell types may be tissue specific.

In chapter 4, I have shown that CD200 deficiency was associated with changes in DCs, which were mainly related to the CD103+ subset that could not be interrogated in the CyTOF panel due to unforeseen technical reasons. Further studies are needed to elucidate the role of chow versus HFD diet on CD200 deficiency. Nevertheless, both

27-week old chow-fed and 20 -week old HFD-fed ApoE-/-CD200-/-mice had a significant increase in arterial macrophage numbers.

This study provided an opportunity to appreciate the phenotypic complexity of myeloid cells. According to these results, many phenotypic markers were overlapping, particularly in the aorta, suggesting that discriminating macrophages based on M1/M2 markers is not enough. This data suggests the use of co-stimulatory markers to understand the activation/maturation status of macrophages and proposes new underappreciated markers such as CD169 and CD209β. An additional suggestion would be to understand the specific localisation of the macrophage cell types to explore the phenotypic characteristics of adventitial versus lesional macrophages.

This mass cytometry study indicates that CD200 expression in vascular tissues is particularly abundant on non-myeloid cell types and that is important for regulating myeloid behaviour. The absence of CD200 deletion is associated with the expansion of selected macrophage subsets in the aorta and the spleen. The predominant macrophage subsets affected by CD200 deficiency are the iNOS+CD86+MHCII+ macrophages. These changes in aortic tissue are associated with an increase in proinflammatory monocyte recruitment within the lesions and an increase in T cell content, potentially due to an increase in the expression of co-stimulatory molecules (CD86, MHCII). Further studies are warranted to identify exactly which T cell subsets are affected. Previous literature pointed towards a role for CD200 in Th17 biology (Ren et al., 2015, Li et al., 2012) but other subsets might be involved in atherosclerosis. The effect of CD200 deletion of other cell types such as mast cells would be also of interest.

In summary, CD200 expression on stromal cells is fundamental in resolving athero-inflammation at advanced stages of atherosclerosis in hypercholesterolemic mice.

Chapter 6 CD200 regulates GM-CSF mediated myelopoiesis during atherosclerosis

Chapter 6: CD200 regulates GM-CSF mediated myelopoiesis during atherosclerosis

6.1 Introduction

I have shown that CD200 deficiency affects specific arterial myeloid subsets in 27-week old chow-fed and 20 -week old high fat diet (HFD)-fed apolipoprotein (ApoE)-/- mice (Chapters 4 and 5). To recapitulate this *in vitro,* myeloid cells were generated from granulocyte macrophage colony stimulating factor (GM-CSF) - and macrophage colony stimulating factor (M-CSF)-derived bone marrow (BM) cells. GM-CSF and M-CSF are well known haematopoietic growth factors that differentially control the survival and differentiation of myeloid cells (Wiktor-Jedrzejczak et al., 1990, Lacey et al., 2012). For example, studies demonstrated that GM-CSF-derived cells are able to promote the differentiation of dendritic cells (DCs) (Inaba et al., 1992). However, it has recently been shown that the transcriptome of *in vitro* GM-CSF-derived cells is closer to macrophages rather than DCs (Helft et al., 2015, Mabbott et al., 2010). On the other hand, *in vitro* generation of M-CSF-derived macrophages is often used as a model to study tissue macrophages (Akagawa et al., 2006, Davies et al., 2013b). To study macrophage polarisation, cells are often stimulated with interferon (IFN)-γ and lipopolysaccharide (LPS) for classical activation (Pace et al., 1983) or with interleukin (IL)-4 and IL-13 for alternative activation (Helft et al., 2015, Lacey et al., 2012, Stein et al., 1992). Due to the heterogeneous myeloid populations found in GM-CSF and M-CSF cultures, in this study I will refer to them as GM-BMMs (GM-CSF BM-derived myeloid cells) and M-BMMs (M-CSF BM-derived myeloid cells). The *in vitro* GM-CSF and M-CSF cultures were performed using bones from 27-week old ApoE-/- and ApoE-/-CD200-/- mice.

To explore the role of CD200-CD200R in myelopoiesis/leucocytosis, the effects of CD200 deletion on haematopoietic stem cell (HSC) populations in the BM and the spleen were assessed by flow cytometry. Leucocytosis has been linked with high cardiovascular risk and heightened HSC proliferation in ApoE-/- mice (Murphy et al., 2011). Therefore, I hypothesised that CD200 deficiency controls the proliferation of HSCs and subsequently expands myeloid cells. Due to time constraints, ApoE-/- and ApoE-/-CD200-/- mice were kept on HFD for 12 weeks to accelerate the development of the disease.

6.2 Results

6.2.1 CD200 deficiency affects macrophage regulation in response to GM-CSF *in vitro*

To understand the effect of CD200 deficiency in macrophage differentiation and activation, I cultured GM-CSF (GM-BMMs) and M-CSF (M-BMMs) BM-derived myeloid cells *in vitro*. GM-BMMs were cultured with 20ng/ml GM-CSF without (G0) or with 100ng/ml LPS stimulation for 18 hours, while M-BMMs were cultured with 100ng/ml M-CSF without (M0) or with 100ng/ml LPS stimulation for 18 hours. For M1 polarisation, M-CSF-treated macrophages were additionally stimulated with 10ng/ml IFN-γ and 100ng/ml LPS while for M2 polarisation, M-CSF treated macrophages were stimulated with 20ng/ml IL-4 and IL-13. Following culture, macrophage phenotypes and their inflammatory cytokine expression and signalling pathways were assessed.

6.2.1.1 CD200 deficiency increases cell numbers but decreases IL-6 secretion in LPS-stimulated GM-BMMs

GM-BMMs were cultured from the bones of ApoE-/- and ApoE-/-CD200-/-mice and stimulated with or without LPS for 18 hours before the expression of CD11b, F4/80, CD11c, MHCII, CD200, CD200R, iNOS and CD206 was assessed by flow cytometry. As expected, CD200 expression was diminished in ApoE-/-CD200-/- mice (Figure 6.1A). Interestingly, CD200 deficiency increased the expression of most myeloid markers, but most significantly the numbers of F4/80+ (32 ± 1% vs 41 ± 1%, p=0.0004) and CD200R+ (22 ± 1.7% versus 28 ± 1%, p=0.01) GM-BMMs, while the numbers of CD206+GM-BMMs (19 ± 1.8% versus 15 ± 0.8%, p=0.05) were

decreased. Addition of LPS increased the numbers of CD11b (67 ± 2.7% versus 75 ±1.8%, p=0.02), F4/80 (37 ± 3.9% versus 49 ± 2.8%, p=0.02), CD11c (28 ± 1.7% versus 37 ± 3%, p=0.02), CD68 (64 ± 4% versus 75 ± 2%, p=0.03), CD200R+ (27 ± 2.8% versus 36 ± 1.6%, p=0.01) and CD206+ (21 ± 2% versus 29 ± 2%, p=0.01) GM-BMMS in ApoE-/-CD200-/- compared to ApoE-/- mice (Figure 6.1A). Interestingly, the expression of CD200R was significantly upregulated in all myeloid subsets in ApoE-/-CD200-/- mice (Figure 6.2A). Next IL-6 secretion in the supernatants of LPS-stimulated GM-BMMs was assessed. IL-6 release was significantly decreased in the GM-BMMs from ApoE-/-CD200-/- mice compared to ApoE-/- mice (17196 ± 660 pg/ml versus 12993 ± 882 pg/ml, p=0.002) (Figure 6.1C). Unstimulated GM-BMMs were starved from GM-CSF overnight and then stimulated with GM-CSF for 15 minutes to assess the expression of phospho-signal transducers and activators of transcription (pSTAT) 5 by phospho -flow cytometry. No differences were found in pSTAT5 expression in GM-BMMs from ApoE-/- and ApoE-/-CD200-/- mice (Figure 6.1D).

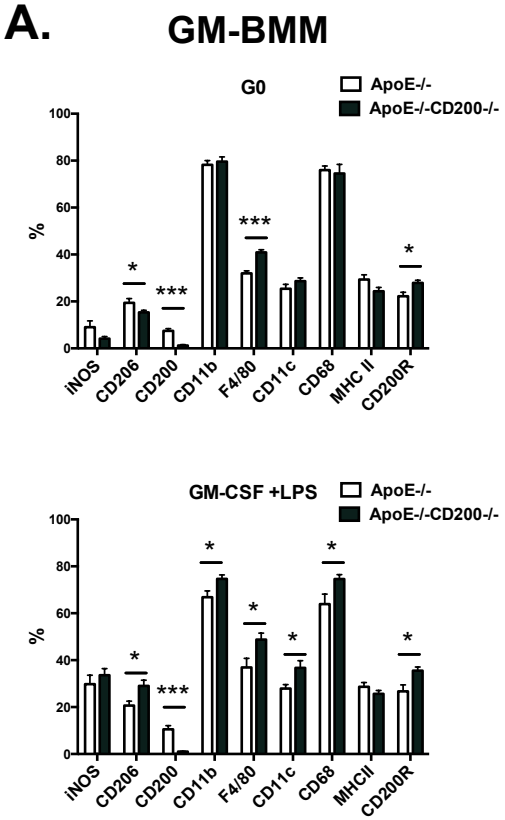
6.2.1.2 CD200 deficiency does not affect cell numbers but increases activation through ERK signalling in M-BMMs

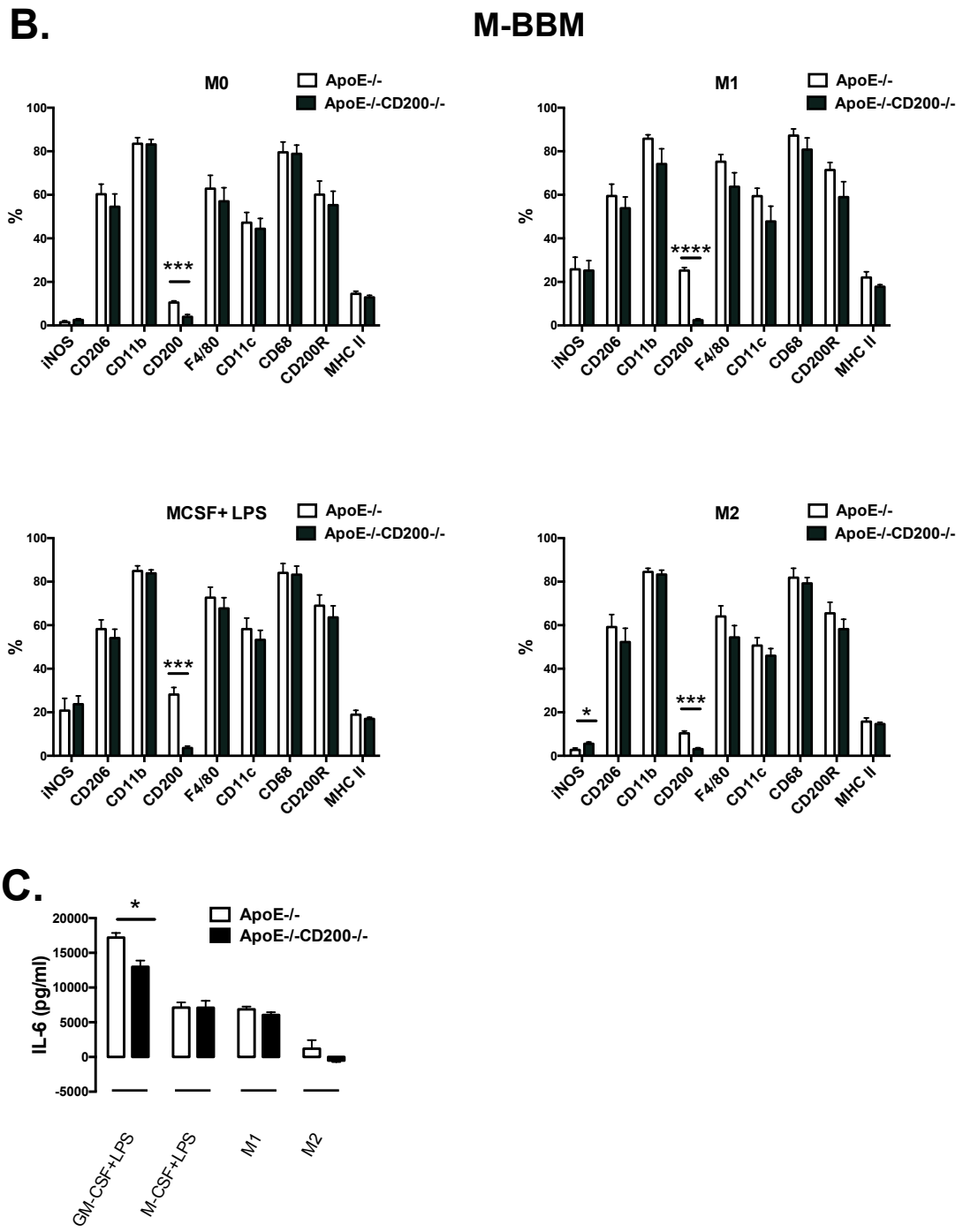
M-BMMs were cultured from the bones of ApoE-/- and ApoE-/-CD200-/-mice, and stimulated with or without LPS. For M1 polarisation, M-CSF-treated macrophages were additionally stimulated with IFN-γ and for M2 polarisation, M-CSF treated macrophages were stimulated with IL-4 and IL-13. Interestingly, CD200 deficiency did not affect the numbers of cells staining positive for each myeloid marker in unstimulated, LPS or M1- stimulated M-BMMs (Figure 6.1B). Additionally, CD200R expression was unchanged in ApoE-/-CD200-/- mice (Figure 6.1B). No differences in

IL-6 secretion were found in LPS-stimulated M-BMMs from ApoE-/- and ApoE-/-CD200-/- mice (Figure 6.1C). M-BMMs were also starved from M-CSF overnight and stimulated with M-CSF for 15 minutes to assess the expression of phospho extracellular signal–regulated kinase (pERK) 1/2 by phopsho-flow cytometry. Interestingly, CD200 deficiency significantly increased the level of expression (MFI) of pERK1/2 in M-BMMs (46 ± 2, versus 56 ± 3, p=0.04) (Figure 6.1D).

6.2.1.3 IL-4 increases iNOS expression, but does not affect pSTAT6 expression in M-BMMs

To assess the role of CD200-CD200R signalling in M2 polarisation, M-BMMs were cultured with IL-4/IL-13. Although, IL-4/IL-13 stimulation did not affect the expression of most of the myeloid markers, it significantly increased the numbers of iNOS expressing cells in ApoE-/-CD200-/- mice (2.7 ± 0.9% versus 5.5 ± 0.8%, p=0.03). There was a decrease in CD206+ M-BMMs, but this difference did not reach statistical significance (Figure 6.1B). M-BMMs were also stimulated with IL-4 for 15 minutes to assess the expression of pSTAT6 by phopsho-flow cytometry. There was no difference in phospho-signal transducers and activators of transcription (pSTAT) 6 expression in M-BMMs between ApoE-/- and ApoE-/-CD200-/- mice (Figure 6.1 D).


A.
GM-BMM
G0
ApoE-/-
ApoE-/-CD200-/-
%
100
80
60
40
20
0
*
***
***
*
iNOS
CD206
CD200
CD11b
F4/80
CD11c
CD68
MHC II
CD200R
GM-CSF +LPS
ApoE-/-
ApoE-/-CD200-/-
%
*
*
*
*
*
***
iNOS
CD206
CD200
CD11b
F4/80
CD11c
CD68
MHCII
CD200R


B.
M-BBM
M0
M1
MCSF+ LPS
M2
ApoE-/-
ApoE-/-CD200-/-
%
iNOS
CD206
CD11b
CD200
F4/80
CD11c
CD68
CD200R
MHC II
C.
IL-6 (pg/ml)
GM-CSF+LPS
M-CSF+LPS
M1
M2

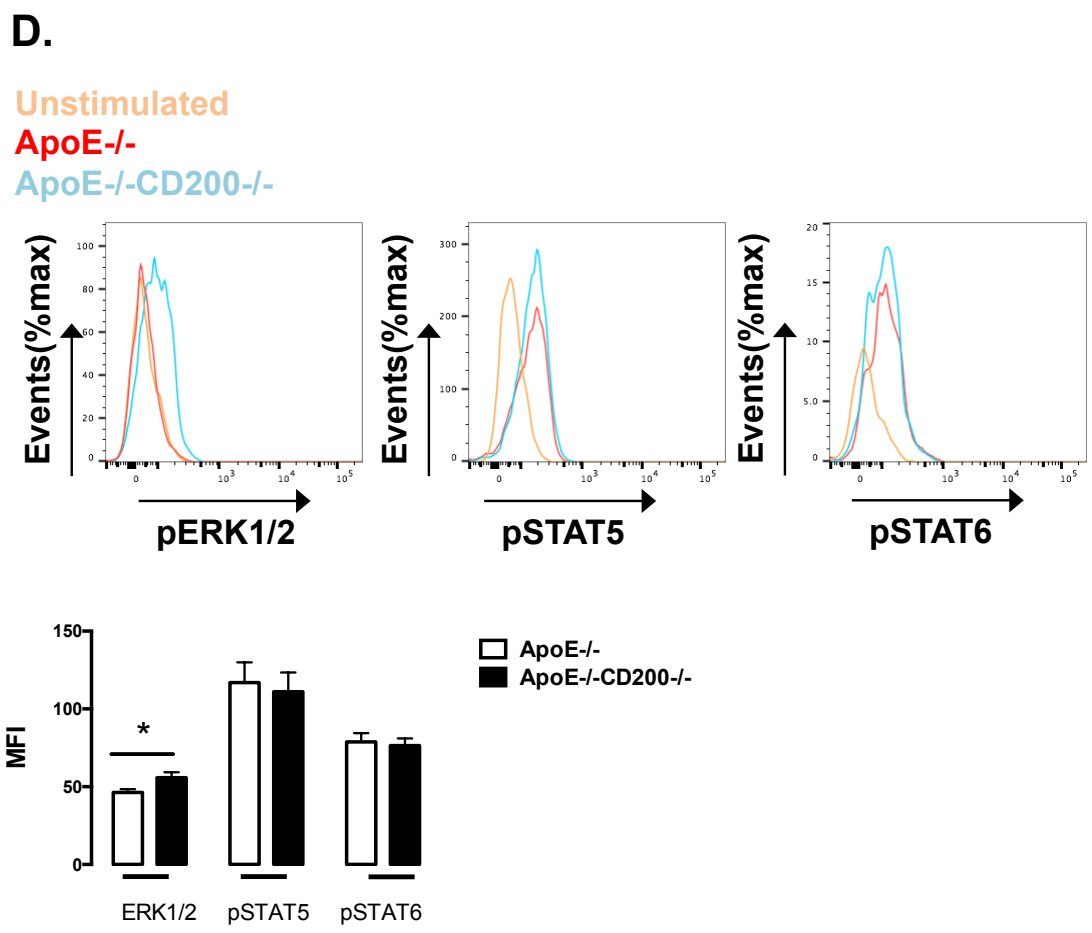


Figure 6.1 CD200 deficiency affects macrophage regulation *in vitro*. Male ApoE-/- and ApoE-/-CD200-/- mice were kept on chow diet for 27 weeks. Bone marrow cells were isolated and the cells were cultured *in vitro*. (A+B) Graphs show the percentages of CD11b+, F4/80+, CD11c+ MHCII+, CD200R+, CD68+, CD200+, CD206+, iNOS+ cells in (A) GM-BMMs in the following conditions: GM-CSF untreated (G0), GM-CSF LPS and (B) in BMMs in the following conditions: M-CSF untreated (M0), M-CSF LPS treated cells, IFN- γ and LPS-treated (M1), IL-4 and IL-13-treated (M2) macrophages. Graphs show mean ± SEM n=8-9, unpaired Student's t-test (C) IL-6 concentration from the supernatants of GM-BMMs: GM-CSF untreated (G0), GM-CSF LPS and in BMMs: M-CSF untreated (M0), M-CSF LPS treated cells, IFN- γ and LPS-treated (M1), IL-4 and IL-13-treated (M2) macrophages. Graphs show mean ± SEM, n=4-8, unpaired Student's t-test (D) Phospho-staining of GM-CSF and M-CSF-treated macrophages with pSTAT5, pERK and pSTA6 after 15minutes of GM-CSF, M-CSF and IL-4/IL-13 incubation. Graphs show the MFI (median) of pERK1/2,pSTAT5 and pSTAT6 within CD11b+cells. Graphs show mean ± SEM n=8-12, unpaired Student's t-test.

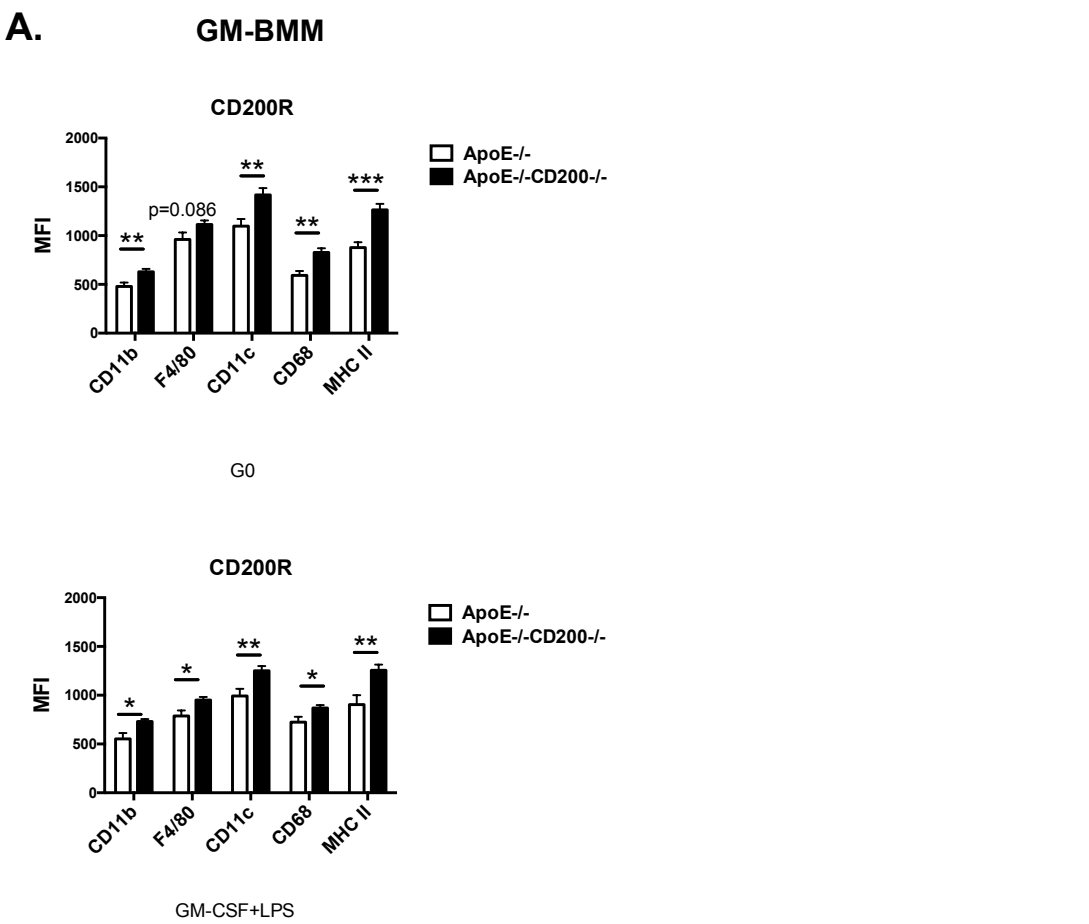

A.
GM-BMM
CD200R
MFI
ApoE-/-
ApoE-/-CD200-/-
p=0.086
CD11b
F4/80
CD11c
CD68
MHC II
G0
GM-CSF+LPS
B.
M-BMM
M0
M1
M-CSF+LPS
M2

Figure 6.2 CD200R expression in *in vitro* differentiated myeloid populations in ApoE-/- and ApoE-/-CD200-/- mice. Male ApoE-/- and ApoE-/-CD200-/- mice were kept on chow diet for 27 weeks. Bone marrow cells were isolated and the cells were cultured *in vitro*. GM-BMMs were cultured with 20ng/ml GM-CSF without (G0) or with 100ng/ml LPS-stimulated while M-BMMs were cultured with 100ng/ml M-CSF without (M0) or with 100ng/ml LPS 10ng/ml. For M1 polarisation, M-CSF-treated macrophages were additionally stimulated with 10ng/ml IFN-γ and 100ng/ml LPS-stimulated while for M2 polarisation, M-CSF treated macrophages were stimulated with 20ng/ml IL-4 and IL-13. Graphs show (A) the MFI (mean) of CD200R expression within CD11b, F4/80, CD11c, MHCII and CD68-expressing GM-BMMs and (B) the MFI (mean) of CD200R within CD11b, F4/80, CD11c, MHCII and CD68-expressing M-BMMs. Graphs show mean ± SEM n=8-12, unpaired Student's t-test.

6.2.1.3 Treatment with a CD200R agonistic antibody does not affect pSTAT6 expression in M-BMMs

M-BMMs were additionally stimulated with 10μg/ml of an agonistic CD200R overnight. The next day, the cells were stimulated with IL-4 and IL-13 for 15 minutes and the expression of pSTAT6 was assessed by phopsho-flow cytometry. CD200R stimulation did not affect pSTAT6 expression in M-BMMs derived from the bones of ApoE-/- mice. Additionally, CD200R stimulation decreased pSTAT6 in M-BMMs in ApoE-/-CD200-/- mice, but this difference did not reach statistical significance (Figure 6.3).

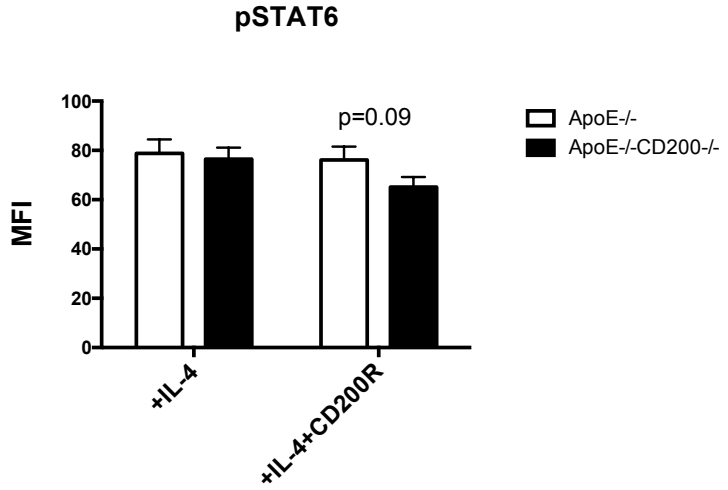


Figure 6.3 Stimulation with agonistic CD200R antibody does not affect pSTAT6 expression *in vitro*. Male ApoE-/- and ApoE-/-CD200-/- mice were placed on HFD at 8 weeks of age for 12 weeks or kept on a chow diet until 27 weeks of age. Bone marrow cells were isolated and the cells cultured *in vitro*. M-BMMs were cultured with 100ng/ml M-CSF. M-BMMs were additionally stimulated with 10 μg/ml of an agonistic CD200R antibody overnight. The next day, the cells were stimulated with 20ng/ml IL4/IL13 for 15 minutes and the expression of pSTAT6 was assessed by phospho-flow cytometry. Graphs show mean ± SEM, n=8-12, unpaired Student's t-test.

6.2.2 CD200 deficiency significantly expands HSCs in the BM of ApoE-/- mice

Given the findings that CD200 deficiency increases myeloid cell numbers in GM-CSF cultures and the known role of GM-CSF in HSCs regulation, I aimed to assess the role of CD200 deficiency in myelopoiesis/leucocytosis. According to the classical paradigm of HSC development, HSCs differentiate into multipotent progenitors (MPPs), which in turn give rise to common lymphoid progenitors (CLPs) and common myeloid progenitors (CMPs). CMPs can then differentiate into megakaryocyte/erythrocyte progenitors (MEPs) and granulocyte/macrophage progenitors (GMPs) (Seita and Weissman, 2010).

HSC populations in the BM and spleen of ApoE-/- and ApoE-/-CD200-/- mice were assessed by flow cytometry. Single cells and debris were excluded and cells were gated on Lin-CD45+c-kit+ cells. Lin−Sca-1+c-Kit+ LSKs were defined as Sca-1+c-kit^{hi}, MPPs as Sca-1+c-kit^{hi} CD34+CD150-, LT-HSCs as Sca-1+c-kit^{hi} CD34-CD150+, GMPs as Sca-1-c-kit^{hi} CD34+CD16/32+, CMPs as Sca-1-c-kit^{hi} CD34+CD16/32- and MEPs as Sca-1-c-kit^{hi}CD34-CD16/32- (Figure 6.4).

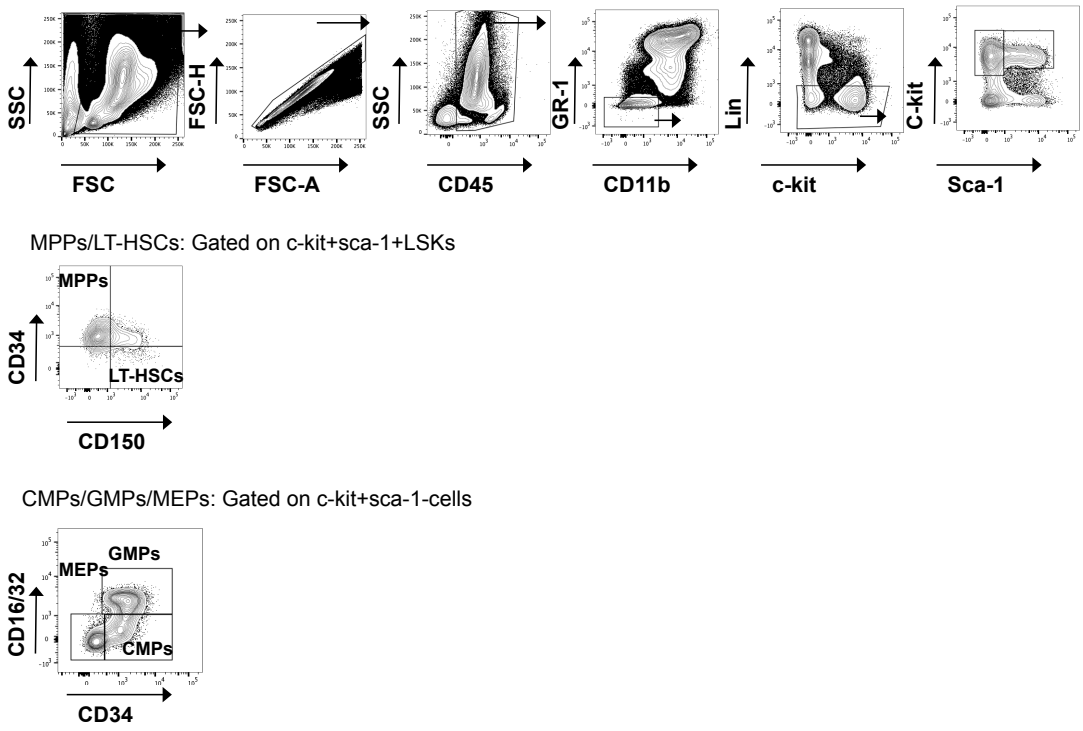


Figure 6.4 Gating strategy for HSCs progenitors in the BM of ApoE-/- mice. Male ApoE-/- and ApoE-/-CD200-/- mice were placed on HFD at 8 weeks of age for 12 weeks and HSC populations, including LSKs, MPPs, LT-HSCs, GMPs, CMPs and MEPs, were assessed by flow cytometry in the BM and spleen. Cells were gated on singlets, CD45+Gr-1-CD11b- and lineage (lin) negative cells which are cells negative for CD3, CD4, B220, Ter-119, NKp46 and FcεR1.

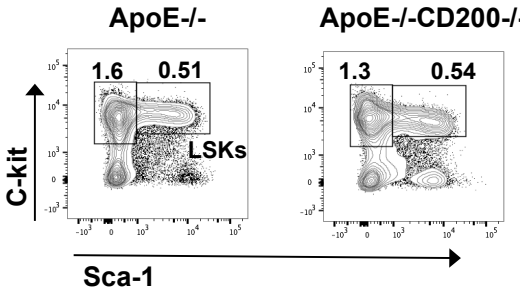
The numbers of HSCs in the BM of ApoE-/- and ApoE-/-CD200-/- mice are shown in Table 6.1. Interestingly, there was a significant increase in MPPs, LSKs, MEPs and CMPs (Figures 6.5A and B), but not LT-HSCs in ApoE-/-CD200-/- mice. There were no significant differences in the numbers of splenic HSCs in ApoE-/- and ApoE-/-CD200-/- mice (Figure 6.5C).

Table 6-1 Numbers of HSCs, including LSKs, MPPs, LT-HSCs, GMPs, CMPs and MEPs, expressed as percentages of single cells and absolute numbers, in the BM of ApoE-/- and ApoE-/-CD200-/- mice fed a HFD for 12 weeks. Data show mean ± SEM, **p<0.01, *p<0.05, n=7-10, Mann-Whitney U test.

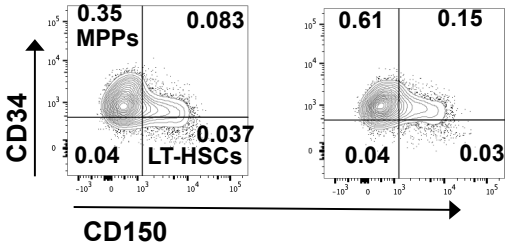
HSC populations	ApoE-/-	ApoE-/-CD200-/-	p vs ApoE-/-
LT-HSCs			
Gated on Lin-CD45+Gr-1-CD11b-sca-1+c-kit high CD34-CD150+			
%	0.017 ± 0.003	0.022 ± 0.005	0.6
10^3	11 ± 2.3	11.9 ± 3.4	0.8
MPPs			
Gated on Lin-CD45+Gr-1-CD11b-sca-1+c-kit high CD34+CD150-			
%	0.28 ± 0.024	0.42 ± 0.05	**0.02**
10^3	169 ± 17	222 ± 22.5	0.07
LSKs			
Gated on Lin-CD45+Gr-1-CD11b-sca-1+c-kit high			
%	0.38 ± 0.035	0.58 ± 0.073	**0.04**
10^3	230 ± 25	306 ± 36	0.087
GMPs			
Gated on Lin-CD45+Gr-1-CD11b-sca-1+c-kit high sca-1-c-kit high CD34+CD16/32+			
%	0.65 ± 0.079	0.62 ± 0.07	0.72
10^3	400 ± 60	335 ± 39	0.67
MEPs			
Gated on Lin-CD45+Gr-1-CD11b-sca-1-c-kit high CD34-CD16/32-			
%	0.22 ± 0.04	0.4 ± 0.047	**0.012**
10^3	133 ± 25	210 ± 23	**0.014**
CMPs			
Gated on Lin-CD45+Gr-1-CD11b-sca-1-c-kit high CD34+CD16/32-			
%	0.33 ± 0.033	0.5 ± 0.052	**0.006**
10^3	204 ± 24	264 ± 19	**0.03**

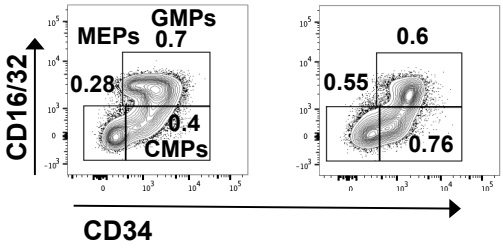
A. **BM HSCs**

LSKs: Gated on Lin-CD11b-CD45+c-kit+cells

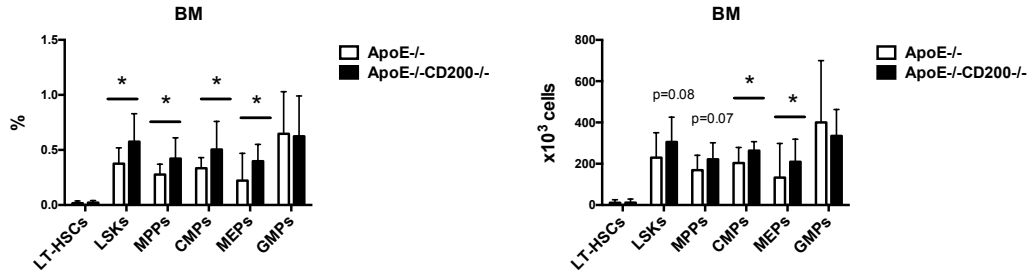


MPPs/LT-HSCs: Gated on c-kit+sca-1+LSKs





B.



C.

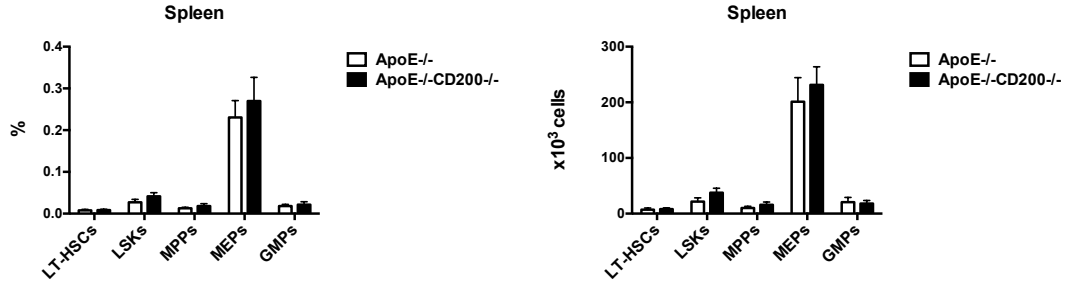


Figure 6.5 CD200 deficiency increases HSCs in the BM but not in the spleen of ApoE-/- mice. Male ApoE-/- and ApoE-/-CD200-/- mice were placed on HFD at 8 weeks of age for 12 weeks and HSC populations, including LSKs, MPPs, LT-HSCs, GMPs, CMPs and MEPs, were assessed by flow cytometry in the BM and spleen. (A) Representative plots show HSC populations in ApoE-/- and ApoE-/-CD200-/- bone marrow. (B+C) Graphs show the numbers of HSCs expressed as a percentage of single cells and absolute numbers, in the (B) BM and (C) spleen of ApoE-/- and ApoE-/-CD200-/- on HFD. Graphs show mean ± SEM, *$p<0.05$, n=7-10, Mann-Whitney U test.

6.2.2.1 CD200 and CD200R expression on HSCs

I also assessed the level of expression (MFI) of CD200 and CD200R on BM progenitor cells and found that both CD200 and CD200R are mainly expressed on c-kit+sca-1+LSKs rather than c-kit+sca-1- cells (CD200: 13 ± 1.7% versus 4.3 ± 0.4%, p= 0.008, CD200R: 225 ± 30.5% versus 129 ± 12%, p=0.008) (Figure 6.6), indicating that this signalling pathway might be involved in the first stages of haematopoiesis. Additionally, the level of CD200R expression is increased in c-kit+ progenitor cells in ApoE-/-CD200-/- mice but this difference did not reach statistical significance (Figure 6.6D).

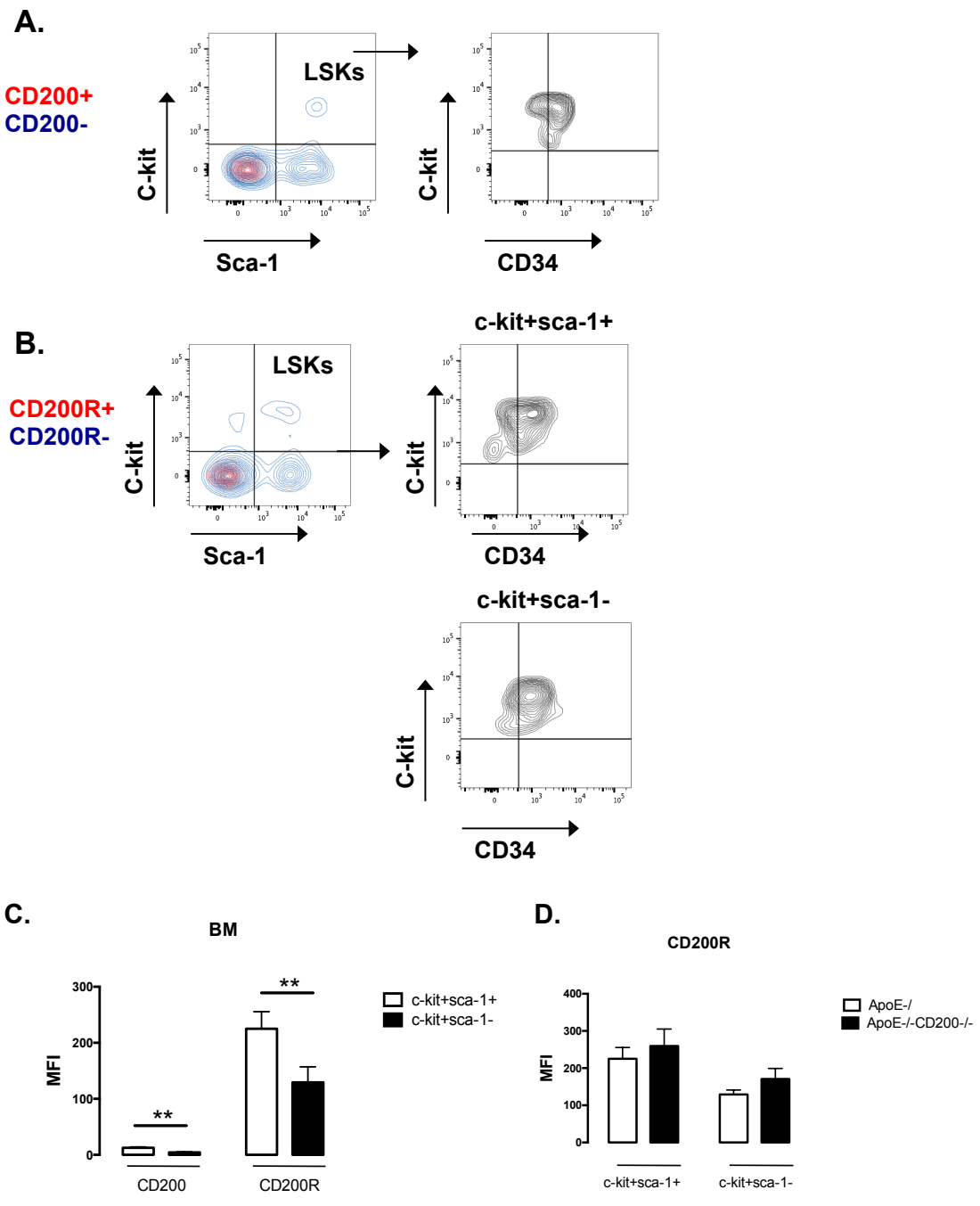


Figure 6.6 CD200 and CD200R expression on BM HSCs in ApoE-/- mice. Male ApoE-/- and ApoE-/-CD200-/- mice were placed on HFD at 8 weeks of age for 12 weeks. (A) Representative plots show CD200 and (B) CD200R expression within c-kit+sca-1+/-HSCs populations. Graphs show the MFI (mean) of CD200 and CD200R expression on (C) c-kit+Sca-1+/- HSCs in the BM of ApoE-/- mice and (D) the MFI (mean) of CD200R on c-kit+Sca-1+/- HSCs in the BM of ApoE-/- and ApoE-/-CD200-/- mice. Data show mean ± SEM, **p<0.01, n=3-5, Mann-Whitney U test.

6.2.2.2 CD200 and CD200R expression on BM and blood monocytes and neutrophils

To understand the role of CD200-CD200R signalling in blood and BM, I assessed BM and blood monocyte and neutrophil populations in ApoE-/- and ApoE-/-CD200-/- mice, which were fed a HFD for 12 weeks, by flow cytometry. Ly6C^{hi} monocytes were increased while neutrophils were decreased in the BM and blood of ApoE-/-CD200-/- mice. However, these differences did not reach statistical significance (Figure 6.7A). Interestingly, the level CD200R expression was higher in monocytes rather than neutrophils in the blood and BM of ApoE-/- mice. However, CD200R expression was significantly increased in neutrophils in the BM and blood of ApoE-/-CD200-/- mice (Figure 6.7B).

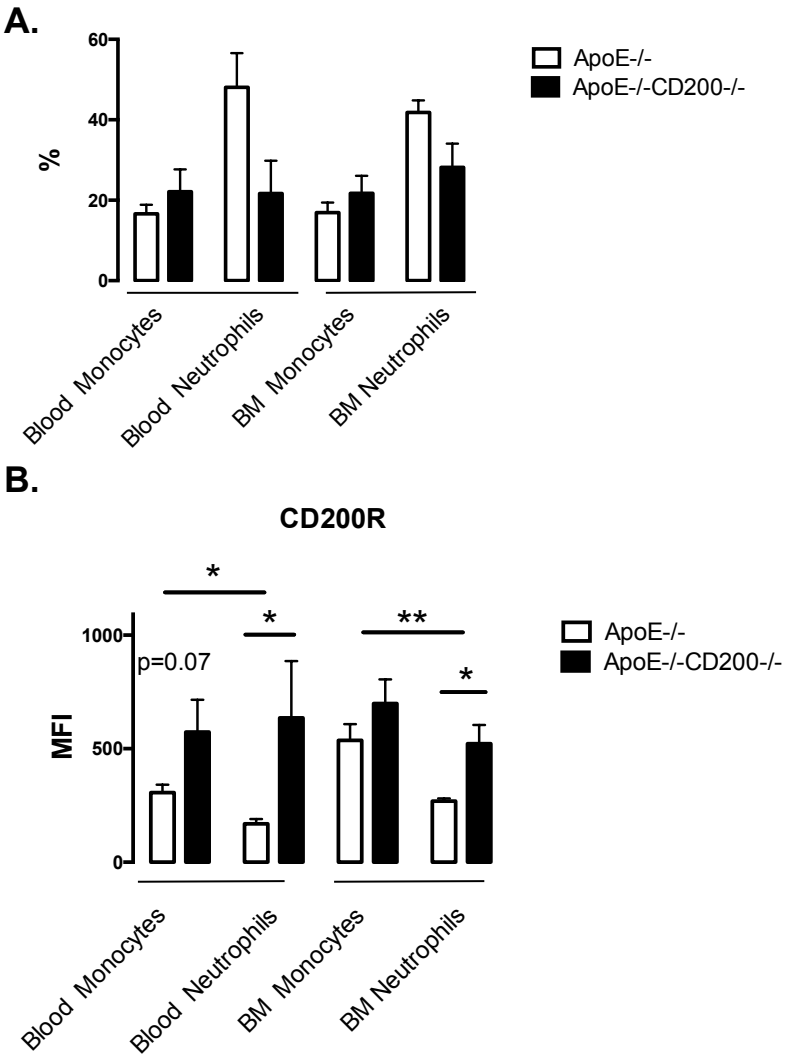


Figure 6.7 The effect of CD200 deficiency on monocytes and neutrophils in the BM and blood of ApoE-/- mice. Male ApoE-/- and ApoE-/-CD200-/- mice were placed on HFD at 8 weeks of age for 12 weeks. Graphs show (A) the numbers Ly6G+CD11b+Ly6C- (neutrophils) and Ly6G-CD11b+Ly6C+(monocytes), expressed as a percentage of CD11b+cells and (B) the level of CD200R expression as MFI (mean) in monocytes and neutrophils in the blood and BM in ApoE-/- and ApoE-/-CD200-/- mice. Graphs show mean ± SEM, **p<0.01, *p<0.05, n=3-5, unpaired Student's t-test.

6.3 Discussion

In the previous chapters I was able to demonstrate that CD200 deletion increases atherosclerotic lesions size and worsens their phenotype and that these changes are associated with the expansion of a iNOS+CD86+MHCII+ macrophage subset within lesions. CD200 deletion was also associated with more systemic changes in circulating monocytes and splenic monocytes. Hence I hypothesised that CD200 might regulate broadly the haematopoietic system and macrophage maturation. In this chapter, I first assessed the role of CD200-CD200R in myeloid regulation *in vitro*. I found that CD200 deficiency increased the expression of most myeloid markers (such as CD11b and F4/80) in GM-CSF but not M-CSF-derived BM macrophages, suggesting a role of CD200 in macrophage maturation. Moreover, CD200 deficiency decreased their IL-6 secretion after LPS stimulation in GM-BMMs, while it increased the pERK1/2 expression of M-BMMs, indicating a differential role for CD200-CD200R in GM-CSF/M-CSF signalling pathways.

There are several studies that suggest a link between CD200-CD200R signalling and growth factor signalling. In particular, a recent study showed that the downstream of tyrosine kinase (Dok) 1 and 2 (the downstream molecules in CD200-CD200R signalling pathway) negatively regulate myeloid cell proliferation upon GM-CSF and M-CSF but not granulocyte-colony stimulating factor (G-CSF) signalling and suppress downstream ERK and AKT activation *in vitro* (Yasuda et al., 2004, Mashima et al., 2010). Specifically, Dok-2 has been found to regulate the induction of c-myc in response to M-CSF (Suzu et al., 2000). In this chapter, I also showed that IL-4 addition increased iNOS expression but did not affect pSTAT6 signalling in ApoE-/-CD200-/- mice. This suggests that the IL-4-pSTAT6 axis may not be

involved in CD200R mediated macrophage regulation but rather secondary modulators are involved. Increased iNOS expression has been associated with a deficiency in IL-4Rα (Deckert et al., 2006). According to a recent study, a role for Dok-2 in down-regulating Ras signalling in the context of the IL-4 receptor has been proposed (Nelms et al., 1998). It would be interesting to assess the role of the suppressor of cytokine signalling (SOCS) protein family in CD200R-Dok-2 mediated signalling pathway, as SOC3 has been found to maintain the activity of the ERK pathway (Cacalano et al., 2001).

Another interesting finding was that although CD200 deficiency significantly decreased the numbers of CD206+ GM-BMMs, LPS treatment significantly increased the numbers of CD206+GM-BMMs, indicating that mature CD206+ GM-BMMs cells were regulated in CD200 deficiency in a TLR4 dependent manner. Additionally, IL-6 secretion in LPS-stimulated GM-BMMs was significantly decreased with CD200 deficiency. CD206 has been traditionally considered as indicative of an M2 anti-inflammatory macrophage phenotype in atherosclerosis. However, the M1/M2 paradigm of macrophage activation appears to be oversimplified and recent studies have tried to explore the great complexity of macrophages' phenotypic and functional properties (Martinez and Gordon, 2014). For example, Wentworth *et al.,* observed a subset of CD11c+CD206+ adipose tissue macrophages (ATMs) that could secrete high levels of proinflammatory cytokines, such as IL-1 and TNF-α, and were associated with deregulated insulin-stimulated glucose uptake in obese women (Wentworth et al., 2010). In support of this study, Moraes-Vieira *et al.,* showed that glucose intolerant RBP4-overexpressing mice have increased numbers of CD206+ATMs in a JNK-dependent manner. Therefore, in the case of CD200 deficiency, LPS-stimulated CD206+GM-BMMs might behave similarly to CD206+

ATMs (Moraes-Vieira et al., 2014). Further studies, in which CD206+GM-BMMs are sorted and their functional properties, such as their cytokine production and antigen presentation abilities are assessed, might help to further the understanding of their functional profile.

However, several limitations of the *in vitro* GM-CSF/M-CSF models should be noted. Firstly, GM-CSF has been traditionally thought to generate DC populations *in vitro*. Indeed, in this study several GM-CSF-derived cells displayed high expression of MHCII and CD11c and intermediate levels of CD11b and F4/80, suggesting a DC-like phenotype. However, recent studies have highlighted the heterogeneity of myeloid cells that are generated from *in vitro* GM-CSF models, thus creating an ambiguity about the ontogenic profile of these myeloid cells. In particular, Helft *et al.,* observed both macrophage and DC populations in GM-CSF cultures and defined them as monocyte derived CD11c+MHCII^{int}CD115(M-CSFR)+MerTK+ GM-Macs and CD11c+MHCII^{+}CD115–CD135 (Flt3)+ GM-DCs. Interestingly, transcriptome analysis revealed that both GM-DCs and GM-Macs did not resemble their *in vivo* counterparts, thus suggesting a need for better refinement of the *in vitro* models. Additionally, culture conditions such as culture medium and serum batch may vary from laboratory to laboratory, which may result in differential generation of myeloid cells (Helft et al., 2015). For example, several studies discard adherent GM-CSF cells and evaluate only non-adherent GM-CSF cells; thereby using cultures where GM-Macs are absent. In this study both adherent and non-adherent GM-CSF cells were evaluated.

Next, due to the increased amount of evidence including my own data that CD200 deficiency increases the numbers of myeloid cells (Hoek et al., 2000), I aimed to investigate the role of this pathway in myelopoiesis. Therefore, I applied flow

cytometry to assess HSC populations, including LSKs, LT-HSCs, MPPs, CMPs, GMPs and MEPs in the BM but also in the spleen to assess the contribution of extramedullary haematopoiesis. Interestingly, there was a significant increase in HSCs in the BM but not in the spleen of ApoE-/-CD200-/- compared to ApoE-/- mice. These results are partly contradictory to another study (Rijkers et al., 2007) that showed that CD200-/- mice have normal myelopoiesis. Nevertheless, those studies were applied to young 8-week old CD200-/- mice, while here 20-week old hypercholesterolemic mice were used. Another study by Coppin *et al.,* showed that Dok-1 and Dok-2, known tyrosines downstream CD200R signalling, regulate HSC quiescence (Coppin et al., 2016). In particular, double Dok-1 and Dok-2 deficient mice have increased numbers of LSKs, similar to this study. Nevertheless, they also found a decrease in CMPs and increase in GMP HSCs, which is contradictory to this study. This could be due to the fact that Dok-2 has been found to have a more essential role than Dok-1 in CD200R signalling and Dok-1 is a negative regulator of Dok-2-mediated CD200R signalling (Mihrshahi et al., 2009, Mihrshahi and Brown, 2010). Therefore, knocking down both Dok-1 and Dok-2 might not help studying CD200R signalling.

A possible limitation of this study is that both ApoE-/- and ApoE-/-CD200-/- mice were fed a HFD, while previous experiments (Chapter 4) were performed on ApoE-/- and ApoE-/-CD200-/- mice fed a chow diet. Although I found similar differences in immune phenotypes between 27-week old chow-fed and 20-week old HFD-fed ApoE-/-CD200-/- mice (e.g. increase in arterial macrophages, increase in blood and BM monocytes, increase in splenic red pulp macrophages), future efforts could concentrate on any additional effects of the HFD on the phenotype of the CD200 deficient mice.

In summary, CD200 is a key regulator of macrophage maturation and polarisation as well as myelopoiesis likely via regulation of growth factor signalling. Although further studies are needed to unravel the role of CD200 in the regulation of signalling of specific growth factors, a strong candidate is GM-SCF.

Chapter 7 Final discussion

Chapter 7: Final discussion

7.1 Hypothesis of the study

Myeloid cells play a pivotal role in numerous chronic inflammatory diseases, through their pro and anti-inflammatory abilities. A century after Metchnikoff's Nobel prize for the discovery of macrophages, the dynamics of myeloid lineage cells have been described in systemic metabolism, haematopoiesis, vasculogenesis, apoptosis and malignancy (Ohashi et al., 2015). Myeloid cell function is thought to be dictated by activating or inhibitory receptors.

Resolution of inflammation is a coordinated and active process that restores tissue integrity and function. This process is orchestrated by immune cells including myeloid and lymphoid cells. Failure of resolution leads to chronic inflammation, which is the underlying mechanism of many human diseases such as atherosclerosis (Tabas, 2010).

The current literature provides strong evidence that the CD200-CD200R axis delivers an inhibitory signal to myeloid cells and, therefore, attracts considerable therapeutic interest. Unlike the majority of immune inhibitory receptors that contain an immunoreceptor tyrosine-based inhibition motif (ITIM) motif, CD200R appears to trigger a different inhibitory pathway (Wright et al., 2000, Hoek et al., 2000, Barclay and Ward, 1982, Gorczynski et al., 2000). In particular, CD200R contains a NPXY motif that contains 3 tyrosine residues in its cytoplasmic tail. CD200-CD200R interaction leads to the phosphorylation of those residues and the recruitment and phosphorylation of downstream of tyrosine kinases (Dok) 1 and 2. Subsequently, those adaptor proteins bind to RasGAP and SH2-domain-containing inositol polyphosphate 5' phosphatase (SHIP) and inhibit the Ras/mitogen-activated protein

kinase (MAPK) pathway (Zhang et al., 2004, Coppin et al., 2016, Mihrshahi and Brown, 2010). However, the exact mechanism by which CD200-CD200R interactions regulate immune responses is not fully understood.

Manipulation of the CD200-CD200R pathway has been shown to have therapeutic promise in experimental models of infection (Snelgrove et al., 2008), autoimmunity (Hoek et al., 2000, Taylor et al., 2005), arthritis (Hoek et al., 2000, Gorczynski et al., 2002, Simelyte et al., 2008) and cancer (Gorczynski et al., 2011b, Kretz-Rommel et al., 2007).

Thus, I hypothesised that the CD200-CD200R axis is important in shaping myeloid cell behaviour during atherosclerosis development.

7.2 Key findings of the study

This study has revealed a new role for the CD200-CD200R pathway in myeloid function during advanced stages of atherosclerosis.

In brief, the key findings are:

1) CD200 expression is almost exclusively confined to non-leucocytes, primarily arterial stromal cells including endothelial cells (ECs) and smooth muscle cells (SMCs) in ApoE-/- mice (Chapter 5).

2) Manipulation of the CD200-CD200R axis has a therapeutic potential in atherosclerosis. Genetic deletion of CD200 induces larger and more "vulnerable" plaque phenotypes at advanced stages of the disease (Chapter 4), characterised by

macrophage accumulation (Chapters 4 and 5), particularly of arterial iNOS +CD86+MHCII+ inflammatory macrophages, with a higher proliferative potential (Chapter 5).

3) CD200 provision (achieved using a CD200-Fc fusion protein) decreases neointima formation in a murine model of perivascular collar-induced injury. This decrease is associated with an enrichment of CD206+anti-inflammatory macrophages. CD200 provision might also regulate interferon (IFN)-γ signalling *in vitro* (Chapter 3).

4) CD200 provides atheroprotection possibly by controlling monocytosis (Chapter 4 and 5) and by regulating myelopoiesis in the bone marrow (BM) at advanced stages of the disease (Chapter 6). ApoE-/-CD200-/- mice have increased numbers of proinflammatory C-C chemokine receptor type 2 (CCR2)+Ly6C^{hi} monocytes in the blood (Chapter 4) and plaques (Chapter 5). This increase is accompanied by an increase in lesion size (Chapter 4) and the accumulation of proinflammatory arterial iNOS+CD86+MHCII+ inflammatory macrophages (Chapter 5) at advanced stages of atherosclerosis.

5) CD200 controls granulocyte-macrophage colony-stimulating factor (GM-CSF) mediated myelopoiesis. CD200 deficiency expands haematopoietic stem cells (HSCs) in the BM and increases the numbers of myeloid cells in response to GM-CSF, but not macrophage colony-stimulating factor (M-CSF) *in vitro* (Chapter 6).

6) CD200 controls CD4+T cell activation (Chapter 5). CD200 deficiency increases the expression of co-stimulatory molecules (such as CD86 and MHCII) in macrophages, which possibly enhances T cell activation (Chapter 5).

Collectively, these findings imply that stromal CD200 expression provides atheroprotection and dampens athero-inflammation at advanced stages of the disease by downregulating macrophage activation; hypercholesterolemia-induced monocytosis and GM-CSF-mediated myelopoiesis.

7.2.1 CD200 mediates hypercholesterolemia-induced monocytosis

I have shown that CD200 deficiency results in increased numbers of proinflammatory CCR2-expressing monocytes in the blood and plaques, which was associated with an increase in lesion size during advanced atherosclerosis (Chapter 4). This result suggests that CD200 may modulate hypercholesterolemia-induced monocytosis, a process described for the first time in atherosclerosis by Swirski *et al.,* (Swirski et al., 2007).

Monocytes are considered to be protagonists in atherosclerosis development. They differentially employ chemokine mediators, such as CCR2, CCR5 and CX3C chemokine receptor 1 (CX3CR1), to enter the plaques. Tacke *et al.,* found elevated numbers of blood monocytes in ApoE-/- mice fed a high fat diet (HFD) whose phenotype was skewed towards CCR2+Ly6C^{hi} monocytes (Tacke et al., 2007). In addition to that, Swirski *et al.,* labelled monocytes in mice either by adoptive transfer of EGFP-expressing monocytes or with the radioactive tracer [111In] oxine and found that their accumulation is increased with plaque size (Swirski et al., 2006). A more sophisticated study by the same group further delineated that the subset of monocytes

that accumulate during hypercholesterolemic conditions is the Ly6C^{hi} monocytes. These monocytes selectively accumulated in atherosclerotic lesions; they adhere to tumour necrosis factor (TNF) activated endothelium and differentiate into macrophages (Swirski et al., 2007).

A mechanism behind monocytosis in atherosclerosis is the expansion of medullary and extramedullary myelopoiesis. Several studies suggest a link between cholesterol efflux and HSC hyperproliferation in atherosclerosis. Yvan-Charvet *et al.,* showed that mice deficient in the adenosine triphosphate–binding cassette (ABC) transporters ABCA1 and ABCG1 (which are important promoters of cholesterol efflux from macrophages) increased HSC proliferation and accelerated atherosclerosis (Yvan-Charvet et al., 2010). This HSC expansion positively correlated with high plasma levels of the IL-3/GM-CSF receptor that, in turn, led to increased downstream Ras/Erk signalling and increased proliferative responses to IL-3 and GM-CSF. Further studies by Murphy *et al.,* highlighted a role for apolipoprotein E (ApoE) in HSC expansion and monocytosis (Murphy et al., 2011). Administration of cholesterol-poor phospholipid/ApoA-I complexes as cholesterol acceptors restored normal HSC proliferation and inhibited monocytosis (Weber and Soehnlein, 2011, Murphy et al., 2011).

CD200-mediated hypercholesterolemia-induced monocytosis might be driven by increased myelopoiesis as CD200 deletion expands BM HSCs (Chapter 6). This expansion was associated with increased markers of lipopolysaccharide (LPS)-induced macrophage maturation in response to GM-CSF in the (bone marrow) BM-derived cells in CD200-/- mice *in vitro* (Chapter 6). This indicates that responses induced by GM-CSF can by regulated by CD200. Further studies are needed to refine the phenotype of HSCs. An additional observation was that CD200 deficiency

expanded megakaryocyte-erythroid progenitor cells (MEPs) in the BM (Chapter 6). The expansion of BM MEPs was associated with an increase in splenic red pulp macrophages, which are known for their ability to clear erythrocytes (Kohyama et al., 2009). This data suggests that CD200 might play a role in controlling erythrocyte and platelet differentiation and clearance. Both cell types have a role in atherosclerosis. Erythrocytes are involved in intraplaque haemorrhage (Kolodgie et al., 2003) while platelets can activate EC (Bombeli et al., 1998, Huo et al., 2003) and myeloid cells (Stokes et al., 2006).

Monocytosis also occurs in extramedullary sites such as in the spleen. I have shown that CD200 deficiency resulted in myeloid cell changes not only in the aorta but also in the spleen and in the blood (Chapters 4 and 5). In particular, CD200 deficiency expanded the numbers of splenic macrophages. Similar effects have been previously observed in other studies (Hoek et al., 2000). However, in those studies, the phenotype of the macrophages was ill defined. The current study applied 10-color flow cytometry and a high multiparametric technique (CyTOF), which enabled a more comprehensive phenotypic characterisation of those splenic macrophages and allowed their identification as red pulp macrophages (Chapter 5). Interestingly, Robbins *et al.,* showed that the red pulp is an important extramedullary site that generates Ly6C^{hi} monocytes that infiltrate atherosclerotic lesions (Robbins et al., 2012). However, no changes in the number of HSC in the spleen in CD200-/- deficient mice were observed (Chapter 6) suggesting that other molecules (Dutta et al., 2015) besides CD200 might have a role. Further studies are needed to clarify the role of CD200 in extramedullary haematopiesis.

Furthermore, the role of growth factors, particularly that of GM-CSF, could be fundamental in CD200-mediated immunoregulation. I have shown that CD200

regulates GM-CSF-mediated myelopoiesis *in vitro* (Chapter 6). GM-CSF has been reported to be involved in HSC hyperproliferation and monocytosis during hypercholesterolemic conditions in atherosclerosis (Murphy et al., 2011). Therefore, CD200 could possibly interact with GM-CSF to down regulate myelopoiesis during atherosclerosis development.

7.2.2 CD200 regulates the balance of inflammatory M1-M2 macrophages

I have shown that CD200 deletion results in macrophage accumulation during late disease. These macrophages are phenotypically characterised by the expression of iNOS, CD86 and MHCII (Chapters 4 and 5), which is indicative of inflammatory macrophages. Conversely, CD200 provision increases CD206+macrophages, and this is associated with a significant decrease in neointima formation in a perivascular collar injury model (Chapter 3). Collectively, this data suggests that CD200 provides athero-protection by affecting macrophage polarisation during advanced stages of the disease.

How does CD200 affect the status of macrophage activation? I have shown that CD200 deficiency increases myeloid cells in response to GM-CSF but not M-CSF *in vitro* (Chapter 6), suggesting that CD200 deficiency enhances GM-CSF signalling. *In vitro* stimulation of monocytes with GM-CSF has been linked with the production of proinflammatory cytokines such as TNFα, IL-6, IL-12p70 and IL-23, whereas culture with M-CSF results in the production of anti-inflammatory cytokines such as IL-10 (Hamilton, 2008, Fleetwood et al., 2007). *In vitro* studies have generated a paradigm of 'M-CSF resistance', whereby when exposed to increased concentrations of GM-CSF or IFN-γ or LPS, macrophages can overcome the M-CSF-driven polarisation, which is responsible for maintaining the anti-inflammatory state of macrophages in

homeostatic conditions (Hamilton, 2008). It is possible to postulate that CD200 deletion enhances the LPS sensitivity of GM-CSF-induced macrophages, privileging the inflammatory programming.

IFN-γ signalling might also be affected by the CD200-CD200R pathway. I have shown that CD200 provision might inhibit IFN-γ signalling *in vitro* and thus promote the M2 macrophage phenotype and induce athero-protection (Chapter 3). This role has been also suggested by other studies (Copland et al., 2007, Gorczynski et al., 2002).

The prevalence of M1 macrophages in plaques associated with CD200 deletion could also be linked to the increase in CCR2-expressing $Ly6C^{hi}$ monocytes. However, there is ongoing debate concerning the origins and the contribution to macrophage populations of $Ly6C^{hi}$ and $Ly6C^{lo}$ monocytes (Hettinger et al., 2013), which needs further validation.

My data as a whole indicates that macrophage phenotype in atherosclerosis is particularly modulated by resolution pathways. The inflammatory macrophage phenotype observed was characterised by enhanced CD86 and MHCII expression (Chapter 5), indicating an increased ability to present antigen. This was associated with enhanced CD4+ T cell representation in the lesions (Chapter 5). Although previous literature reports that CD200 is responsible for the fine-tuning and regulation of the immune response of Th17 cells (Ren et al., 2015, Liu et al., 2010), I have shown that that is not true in this study (Chapter 5). The precise T cell phenotypes need to be better evaluated in the future.

The increased antigen presentation associated with CD200 deficiency could also be confirmed by the increased numbers of DCs, particularly CD103+DCs, in the aorta of

ApoE-/-CD200-/- mice during all stages of the disease (Chapter 4). However, the role of CD200 on DCs needs further evaluation.

This data suggests that CD200 might regulate myeloid deactivation by interacting with GM-CSF, IFN-γ signalling and the antigen presenting abilities of myeloid cells.

CD200 deficiency could also increase the numbers of mast cells in the plaques. A link between CD200 and mast cell regulation has been reported by previous studies (Zhang et al., 2004, Cherwinski et al., 2005). Recent studies have shown that mast cells play an important role not only in Th2 diseases such as asthma and allergy but that they are also involved in the pathogenesis of atherosclerosis, primarily by secreting proinflammatory cytokines such as TNFα, IFN-γ, MCP-1, IL-6 and IL-8 (Lappalainen et al., 2011, Bot et al., 2007). Mast cells can also express receptors for GM-CSF (Dahl et al., 2004). This indicates that the changes in these immune cells in CD200 deficient mice could be due to changes in GM-CSF signalling.

On the basis of *in vitro* studies, GM-CSF may be a possible candidate involved in the mechanism of CD200-CD200R mediated immunoregulation in atherosclerosis. Further studies will be needed to provide proof *in vivo*.

7.2.3 CD200-CD200R: A role for stromal-immune cell interactions in atherosclerosis

I have shown that CD200 expression is mainly confined to stromal cells in the plaques, primarily ECs and SMCs, while CD200R expression is detected in various cell types including myeloid cells (Chapter 5). In particular, CD200R has been proposed as a marker of human M2 alternatively activated macrophages (Jaguin et al., 2013). Loss of CD200 expression enhances lesion size at advanced stages of atherosclerosis (Chapter 4). Therefore, the CD200-CD200R pathway could provide

atheroprotection through interactions between stromal and immune cells. In accordance with this, recent evidence suggests that *in vitro* alveolar macrophage-epithelial cell co-cultures induce cytokine production in macrophages only in the presence of CD200R. This emphasises an important role for epithelial CD200 in regulating alveolar macrophage function (Snelgrove et al., 2008, Hussell and Bell, 2014). Therefore the binding of stromal CD200 expressing cells to CD200R might modulate macrophage function in advanced atherosclerosis and thus act as a mechanism for resolving plaque inflammation.

7.3 Final conclusions

To conclude, this study provides evidence that the CD200-CD200R pathway has emerged as a potential therapeutic target for cardiovascular disease, contributing to the resolution phase of inflammation (Figure 7.1).

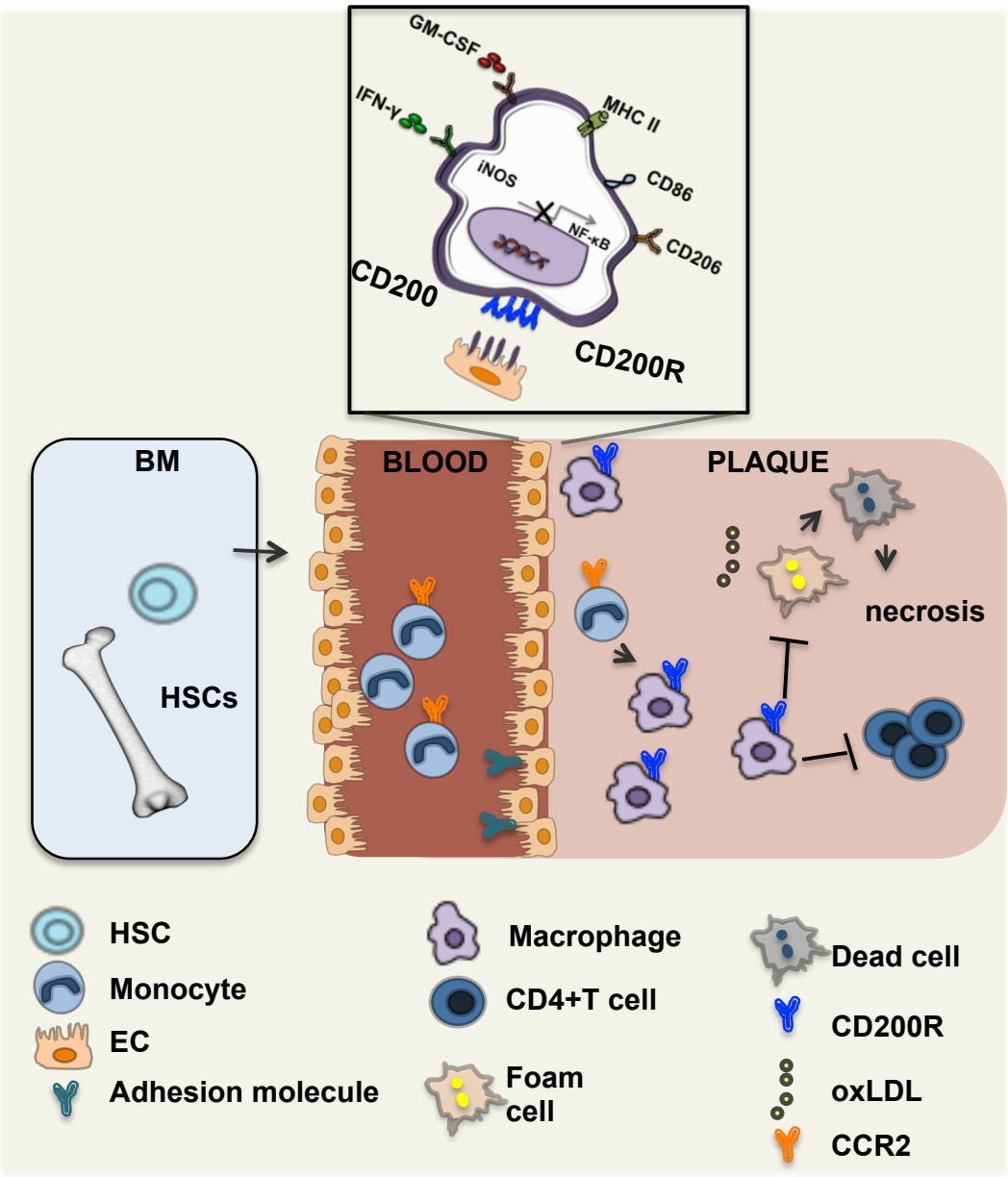


Figure 7.1 The proposed model of CD200 in myeloid function in advanced atherosclerotic lesions. In summary, the proposed model of CD200 in myeloid function in advanced lesions is: 1) HSCs differentiate in the BM during postnatal haematopoiesis. In response to oxLDL and GM-CSF, HSCs are proliferating and expanding. CD200 limits the differentiation of HSCs 2) Myeloid progenitors then give rise to monocytes and neutrophils in the BM. CD200 regulates the levels of CCL2 /CCR2-expressing cells, and thus downregulates proinflammatory monocyte migration in atherosclerotic plaques 3) The expression of CD200 by ECs might also regulate monocyte transmigration into the intima 4) Monocytes differentiate into myeloid cells. Subsequently, myeloid cells accumulate in the arterial wall by proliferation or due to monocyte recruitment. CD200 inhibits GM-CSF and IFN-γ signalling and the expression of co-stimulatory molecules by myeloid cells and also inhibits the proliferation of proinflammatory macrophages 5) This in turn leads to an attenuation of CD4+ T cell responses 6) CD200 enhances anti-inflammatory mediators in the plaque, inhibits foam cell and necrotic core formation and leads to resolution of inflammation.

References

1983. Classics in arteriosclerosis research: On experimental cholesterin steatosis and its significance in the origin of some pathological processes by N. Anitschkow and S. Chalatow, translated by Mary Z. Pelias, 1913. *Arteriosclerosis,* 3**,** 178-82.

AFONSO, C. L., TULMAN, E. R., LU, Z., ZSAK, L., OSORIO, F. A., BALINSKY, C., KUTISH, G. F. & ROCK, D. L. 2002. The genome of swinepox virus. *J Virol,* 76**,** 783-90.

AIT-OUFELLA, H., HERBIN, O., BOUAZIZ, J. D., BINDER, C. J., UYTTENHOVE, C., LAURANS, L., TALEB, S., VAN VRE, E., ESPOSITO, B., VILAR, J., SIRVENT, J., VAN SNICK, J., TEDGUI, A., TEDDER, T. F. & MALLAT, Z. 2010. B cell depletion reduces the development of atherosclerosis in mice. *J Exp Med,* 207**,** 1579-87.

AIT-OUFELLA, H., SALOMON, B. L., POTTEAUX, S., ROBERTSON, A. K., GOURDY, P., ZOLL, J., MERVAL, R., ESPOSITO, B., COHEN, J. L., FISSON, S., FLAVELL, R. A., HANSSON, G. K., KLATZMANN, D., TEDGUI, A. & MALLAT, Z. 2006. Natural regulatory T cells control the development of atherosclerosis in mice. *Nat Med,* 12**,** 178-80.

AKAGAWA, K. S., KOMURO, I., KANAZAWA, H., YAMAZAKI, T., MOCHIDA, K. & KISHI, F. 2006. Functional heterogeneity of colony-stimulating factor-induced human monocyte-derived macrophages. *Respirology,* 11 Suppl**,** S32-6.

AKASHI, K., TRAVER, D., MIYAMOTO, T. & WEISSMAN, I. L. 2000. A clonogenic common myeloid progenitor that gives rise to all myeloid lineages. *Nature,* 404**,** 193-7.

AKIRA, S., UEMATSU, S. & TAKEUCHI, O. 2006. Pathogen recognition and innate immunity. *Cell,* 124**,** 783-801.

AKKAYA, M., AKNIN, M. L., AKKAYA, B. & BARCLAY, A. N. 2013. Dissection of agonistic and blocking effects of CD200 receptor antibodies. *PLoS One,* 8**,** e63325.

ALENGHAT, F. J. 2016. The Prevalence of Atherosclerosis in Those with Inflammatory Connective Tissue Disease by Race, Age, and Traditional Risk Factors. *Sci Rep,* 6**,** 20303.

ALLAN, R. S., WAITHMAN, J., BEDOUI, S., JONES, C. M., VILLADANGOS, J. A., ZHAN, Y., LEW, A. M., SHORTMAN, K., HEATH, W. R. & CARBONE, F. R. 2006. Migratory dendritic cells transfer antigen to a lymph node-resident dendritic cell population for efficient CTL priming. *Immunity,* 25**,** 153-62.

ALLEN, J. E. & WYNN, T. A. 2011. Evolution of Th2 immunity: a rapid repair response to tissue destructive pathogens. *PLoS Pathog,* 7**,** e1002003.

AMENTO, E. P., EHSANI, N., PALMER, H. & LIBBY, P. 1991. Cytokines and growth factors positively and negatively regulate interstitial collagen gene expression in human vascular smooth muscle cells. *Arterioscler Thromb,* 11**,** 1223-30.

ANBER, V., GRIFFIN, B. A., MCCONNELL, M., PACKARD, C. J. & SHEPHERD, J. 1996. Influence of plasma lipid and LDL-subfraction profile on the interaction between low density lipoprotein with human arterial wall proteoglycans. *Atherosclerosis,* 124**,** 261-71.

ANDREESEN, R., BRUGGER, W., SCHEIBENBOGEN, C., KREUTZ, M., LESER, H. G., REHM, A. & LOHR, G. W. 1990. Surface phenotype analysis of human monocyte to macrophage maturation. *J Leukoc Biol,* 47**,** 490-7.

ANDREEVA, E. R., PUGACH, I. M. & OREKHOV, A. N. 1997. Subendothelial smooth muscle cells of human aorta express macrophage antigen in situ and in vitro. *Atherosclerosis,* 135**,** 19-27.

ANITSCHKOW, N. N., WOLKOFF, K. G., KIKAION, E. E. & POZHARISSKI, K. M. 1964. Compensatory Adjustments in the Structure of Coronary Arteries of the Heart with Stenotic Atherosclerosis. *Circulation,* 29**,** 447-55.

BANERJEE, D. & DICK, A. D. 2004. Blocking CD200-CD200 receptor axis augments NOS-2 expression and aggravates experimental autoimmune uveoretinitis in Lewis rats. *Ocul Immunol Inflamm,* 12**,** 115-25.

BARATH, P., FISHBEIN, M. C., CAO, J., BERENSON, J., HELFANT, R. H. & FORRESTER, J. S. 1990. Detection and localization of tumor necrosis factor in human atheroma. *Am J Cardiol,* 65**,** 297-302.

BARCLAY, A. N. & WARD, H. A. 1982. Purification and chemical characterisation of membrane glycoproteins from rat thymocytes and brain, recognised by monoclonal antibody MRC OX 2. *Eur J Biochem,* 129**,** 447-58.

BARCLAY, A. N., WRIGHT, G. J., BROOKE, G. & BROWN, M. H. 2002. CD200 and membrane protein interactions in the control of myeloid cells. *Trends Immunol,* 23**,** 285-90.

BATES, E. E., FOURNIER, N., GARCIA, E., VALLADEAU, J., DURAND, I., PIN, J. J., ZURAWSKI, S. M., PATEL, S., ABRAMS, J. S., LEBECQUE, S., GARRONE, P. & SAELAND, S. 1999. APCs express DCIR, a novel C-type lectin surface receptor containing an immunoreceptor tyrosine-based inhibitory motif. *J Immunol,* 163**,** 1973-83.

BECHER, B., SCHLITZER, A., CHEN, J., MAIR, F., SUMATOH, H. R., TENG, K. W., LOW, D., RUEDL, C., RICCARDI-CASTAGNOLI, P., POIDINGER, M., GRETER, M., GINHOUX, F. & NEWELL, E. W. 2014. High-dimensional analysis of the murine myeloid cell system. *Nat Immunol,* 15**,** 1181-9.

BENDALL, S. C., SIMONDS, E. F., QIU, P., AMIR EL, A. D., KRUTZIK, P. O., FINCK, R., BRUGGNER, R. V., MELAMED, R., TREJO, A., ORNATSKY, O. I., BALDERAS, R. S., PLEVRITIS, S. K., SACHS, K., PE'ER, D., TANNER, S. D. & NOLAN, G. P. 2011. Single-cell mass cytometry of differential immune and drug responses across a human hematopoietic continuum. *Science,* 332**,** 687-96.

BENTZON, J. F., OTSUKA, F., VIRMANI, R. & FALK, E. 2014. Mechanisms of plaque formation and rupture. *Circ Res,* 114**,** 1852-66.

BOMBELI, T., SCHWARTZ, B. R. & HARLAN, J. M. 1998. Adhesion of activated platelets to endothelial cells: evidence for a GPIIbIIIa-dependent bridging mechanism and novel roles for endothelial intercellular adhesion molecule 1 (ICAM-1), alphavbeta3 integrin, and GPIbalpha. *J Exp Med,* 187**,** 329-39.

BOOTH, R. F., MARTIN, J. F., HONEY, A. C., HASSALL, D. G., BEESLEY, J. E. & MONCADA, S. 1989. Rapid development of atherosclerotic lesions in the

rabbit carotid artery induced by perivascular manipulation. *Atherosclerosis,* 76**,** 257-68.

BORRIELLO, F., LEDERER, J., SCOTT, S. & SHARPE, A. H. 1997. MRC OX-2 defines a novel T cell costimulatory pathway. *J Immunol,* 158**,** 4548-54.

BOT, I., DE JAGER, S. C., ZERNECKE, A., LINDSTEDT, K. A., VAN BERKEL, T. J., WEBER, C. & BIESSEN, E. A. 2007. Perivascular mast cells promote atherogenesis and induce plaque destabilization in apolipoprotein E-deficient mice. *Circulation,* 115**,** 2516-25.

BOUDAKOV, I., LIU, J., FAN, N., GULAY, P., WONG, K. & GORCZYNSKI, R. M. 2007. Mice lacking CD200R1 show absence of suppression of lipopolysaccharide-induced tumor necrosis factor-alpha and mixed leukocyte culture responses by CD200. *Transplantation,* 84**,** 251-7.

BOUHLEL, M. A., DERUDAS, B., RIGAMONTI, E., DIEVART, R., BROZEK, J., HAULON, S., ZAWADZKI, C., JUDE, B., TORPIER, G., MARX, N., STAELS, B. & CHINETTI-GBAGUIDI, G. 2007. PPARgamma activation primes human monocytes into alternative M2 macrophages with anti-inflammatory properties. *Cell Metab,* 6**,** 137-43.

BOYLE, J. J., HARRINGTON, H. A., PIPER, E., ELDERFIELD, K., STARK, J., LANDIS, R. C. & HASKARD, D. O. 2009. Coronary intraplaque hemorrhage evokes a novel atheroprotective macrophage phenotype. *Am J Pathol,* 174**,** 1097-108.

BOYLE, J. J., JOHNS, M., LO, J., CHIODINI, A., AMBROSE, N., EVANS, P. C., MASON, J. C. & HASKARD, D. O. 2011. Heme induces heme oxygenase 1 via Nrf2: role in the homeostatic macrophage response to intraplaque hemorrhage. *Arterioscler Thromb Vasc Biol,* 31**,** 2685-91.

BRODERICK, C., HOEK, R. M., FORRESTER, J. V., LIVERSIDGE, J., SEDGWICK, J. D. & DICK, A. D. 2002. Constitutive retinal CD200 expression regulates resident microglia and activation state of inflammatory cells during experimental autoimmune uveoretinitis. *Am J Pathol,* 161**,** 1669-77.

BROWN, A. J., MANDER, E. L., GELISSEN, I. C., KRITHARIDES, L., DEAN, R. T. & JESSUP, W. 2000. Cholesterol and oxysterol metabolism and subcellular distribution in macrophage foam cells. Accumulation of oxidized esters in lysosomes. *J Lipid Res,* 41**,** 226-37.

BUCHANAN, C. F., VERBRIDGE, S. S., VLACHOS, P. P. & RYLANDER, M. N. 2014. Flow shear stress regulates endothelial barrier function and expression of angiogenic factors in a 3D microfluidic tumor vascular model. *Cell Adh Migr,* 8**,** 517-24.

BUSCH, M., WESTHOFEN, T. C., KOCH, M., LUTZ, M. B. & ZERNECKE, A. 2014. Dendritic cell subset distributions in the aorta in healthy and atherosclerotic mice. *PLoS One,* 9**,** e88452.

CACALANO, N. A., SANDEN, D. & JOHNSTON, J. A. 2001. Tyrosine-phosphorylated SOCS-3 inhibits STAT activation but binds to p120 RasGAP and activates Ras. *Nat Cell Biol,* 3**,** 460-5.

CAI, Q., LANTING, L. & NATARAJAN, R. 2004a. Growth factors induce monocyte binding to vascular smooth muscle cells: implications for monocyte retention in atherosclerosis. *Am J Physiol Cell Physiol,* 287**,** C707-14.

CAI, Q., LANTING, L. & NATARAJAN, R. 2004b. Interaction of monocytes with vascular smooth muscle cells regulates monocyte survival and differentiation through distinct pathways. *Arterioscler Thromb Vasc Biol,* 24**,** 2263-70.

CALIGIURI, G., RUDLING, M., OLLIVIER, V., JACOB, M. P., MICHEL, J. B., HANSSON, G. K. & NICOLETTI, A. 2003. Interleukin-10 deficiency increases atherosclerosis, thrombosis, and low-density lipoproteins in apolipoprotein E knockout mice. *Mol Med,* 9**,** 10-7.

CAMEJO, G., FAGER, G., ROSENGREN, B., HURT-CAMEJO, E. & BONDJERS, G. 1993. Binding of low density lipoproteins by proteoglycans synthesized by proliferating and quiescent human arterial smooth muscle cells. *J Biol Chem,* 268**,** 14131-7.

CARMELIET, P., MOONS, L., STASSEN, J. M., DE MOL, M., BOUCHE, A., VAN DEN OORD, J. J., KOCKX, M. & COLLEN, D. 1997. Vascular wound healing and neointima formation induced by perivascular electric injury in mice. *Am J Pathol,* 150**,** 761-76.

CARO, C. G., FITZ-GERALD, J. M. & SCHROTER, R. C. 1971. Atheroma and arterial wall shear. Observation, correlation and proposal of a shear dependent mass transfer mechanism for atherogenesis. *Proc R Soc Lond B Biol Sci,* 177**,** 109-59.

CASERTA, S., NAUSCH, N., SAWTELL, A., DRUMMOND, R., BARR, T., MACDONALD, A. S., MUTAPI, F. & ZAMOYSKA, R. 2012. Chronic infection drives expression of the inhibitory receptor CD200R, and its ligand CD200, by mouse and human CD4 T cells. *PLoS One,* 7**,** e35466.

CHAPLIN, D. D. 2003. 1. Overview of the immune response. *J Allergy Clin Immunol,* 111**,** S442-59.

CHAUDHRY, A., SAMSTEIN, R. M., TREUTING, P., LIANG, Y., PILS, M. C., HEINRICH, J. M., JACK, R. S., WUNDERLICH, F. T., BRUNING, J. C., MULLER, W. & RUDENSKY, A. Y. 2011. Interleukin-10 signaling in regulatory T cells is required for suppression of Th17 cell-mediated inflammation. *Immunity,* 34**,** 566-78.

CHELLADURAI, P., SEEGER, W. & PULLAMSETTI, S. S. 2012. Matrix metalloproteinases and their inhibitors in pulmonary hypertension. *Eur Respir J,* 40**,** 766-82.

CHENG, C., TEMPEL, D., VAN HAPEREN, R., VAN DER BAAN, A., GROSVELD, F., DAEMEN, M. J., KRAMS, R. & DE CROM, R. 2006. Atherosclerotic lesion size and vulnerability are determined by patterns of fluid shear stress. *Circulation,* 113**,** 2744-53.

CHERWINSKI, H. M., MURPHY, C. A., JOYCE, B. L., BIGLER, M. E., SONG, Y. S., ZURAWSKI, S. M., MOSHREFI, M. M., GORMAN, D. M., MILLER, K. L., ZHANG, S., SEDGWICK, J. D. & PHILLIPS, J. H. 2005. The CD200 receptor is a novel and potent regulator of murine and human mast cell function. *J Immunol,* 174**,** 1348-56.

CHINETTI-GBAGUIDI, G., COLIN, S. & STAELS, B. 2015. Macrophage subsets in atherosclerosis. *Nat Rev Cardiol,* 12**,** 10-7.

CHISTIAKOV, D. A., OREKHOV, A. N. & BOBRYSHEV, Y. V. 2015. Endothelial Barrier and Its Abnormalities in Cardiovascular Disease. *Front Physiol,* 6**,** 365.

CHO, K. Y., MIYOSHI, H., KURODA, S., YASUDA, H., KAMIYAMA, K., NAKAGAWARA, J., TAKIGAMI, M., KONDO, T. & ATSUMI, T. 2013. The phenotype of infiltrating macrophages influences arteriosclerotic plaque vulnerability in the carotid artery. *J Stroke Cerebrovasc Dis,* 22**,** 910-8.

CHOI, J. H., CHEONG, C., DANDAMUDI, D. B., PARK, C. G., RODRIGUEZ, A., MEHANDRU, S., VELINZON, K., JUNG, I. H., YOO, J. Y., OH, G. T. &

STEINMAN, R. M. 2011. Flt3 signaling-dependent dendritic cells protect against atherosclerosis. *Immunity,* 35**,** 819-31.

CHOI, J. H., DO, Y., CHEONG, C., KOH, H., BOSCARDIN, S. B., OH, Y. S., BOZZACCO, L., TRUMPFHELLER, C., PARK, C. G. & STEINMAN, R. M. 2009. Identification of antigen-presenting dendritic cells in mouse aorta and cardiac valves. *J Exp Med,* 206**,** 497-505.

CLARK, M. J., GAGNON, J., WILLIAMS, A. F. & BARCLAY, A. N. 1985. MRC OX-2 antigen: a lymphoid/neuronal membrane glycoprotein with a structure like a single immunoglobulin light chain. *EMBO J,* 4**,** 113-8.

COCHAIN, C., KOCH, M., CHAUDHARI, S. M., BUSCH, M., PELISEK, J., BOON, L. & ZERNECKE, A. 2015. CD8+ T Cells Regulate Monopoiesis and Circulating Ly6C-high Monocyte Levels in Atherosclerosis in Mice. *Circ Res,* 117**,** 244-53.

COEN, M., GABBIANI, G. & BOCHATON-PIALLAT, M. L. 2011. Myofibroblast-mediated adventitial remodeling: an underestimated player in arterial pathology. *Arterioscler Thromb Vasc Biol,* 31**,** 2391-6.

COLE, J. E., NAVIN, T. J., CROSS, A. J., GODDARD, M. E., ALEXOPOULOU, L., MITRA, A. T., DAVIES, A. H., FLAVELL, R. A., FELDMANN, M. & MONACO, C. 2011. Unexpected protective role for Toll-like receptor 3 in the arterial wall. *Proc Natl Acad Sci U S A,* 108**,** 2372-7.

COLLINS, A. R., GUPTE, A. A., JI, R., RAMIREZ, M. R., MINZE, L. J., LIU, J. Z., ARREDONDO, M., REN, Y., DENG, T., WANG, J., LYON, C. J. & HSUEH, W. A. 2012. Myeloid deletion of nuclear factor erythroid 2-related factor 2 increases atherosclerosis and liver injury. *Arterioscler Thromb Vasc Biol,* 32**,** 2839-46.

COMBADIERE, C., POTTEAUX, S., RODERO, M., SIMON, T., PEZARD, A., ESPOSITO, B., MERVAL, R., PROUDFOOT, A., TEDGUI, A. & MALLAT, Z. 2008. Combined inhibition of CCL2, CX3CR1, and CCR5 abrogates Ly6C(hi) and Ly6C(lo) monocytosis and almost abolishes atherosclerosis in hypercholesterolemic mice. *Circulation,* 117**,** 1649-57.

COPLAND, D. A., CALDER, C. J., RAVENEY, B. J., NICHOLSON, L. B., PHILLIPS, J., CHERWINSKI, H., JENMALM, M., SEDGWICK, J. D. & DICK, A. D. 2007. Monoclonal antibody-mediated CD200 receptor signaling suppresses macrophage activation and tissue damage in experimental autoimmune uveoretinitis. *Am J Pathol,* 171**,** 580-8.

COPPIN, E., DE GRANDIS, M., PANDOLFI, P. P., ARCANGELI, M. L., AURRAND-LIONS, M. & NUNES, J. A. 2016. Dok1 and Dok2 Proteins Regulate Cell Cycle in Hematopoietic Stem and Progenitor Cells. *J Immunol,* 196**,** 4110-21.

CORTEZ, M., HUYNH, C., FERNANDES, M. C., KENNEDY, K. A., ADEREM, A. & ANDREWS, N. W. 2011. Leishmania promotes its own virulence by inducing expression of the host immune inhibitory ligand CD200. *Cell Host Microbe,* 9**,** 463-71.

COSMAN, D., FANGER, N., BORGES, L., KUBIN, M., CHIN, W., PETERSON, L. & HSU, M. L. 1997. A novel immunoglobulin superfamily receptor for cellular and viral MHC class I molecules. *Immunity,* 7**,** 273-82.

CUI, W., CUARTAS, E., KE, J., ZHANG, Q., EINARSSON, H. B., SEDGWICK, J. D., LI, J. & VIGNERY, A. 2007. CD200 and its receptor, CD200R, modulate bone mass via the differentiation of osteoclasts. *Proc Natl Acad Sci U S A,* 104**,** 14436-41.

CYBULSKY, M. I. & GIMBRONE, M. A., JR. 1991. Endothelial expression of a mononuclear leukocyte adhesion molecule during atherogenesis. *Science,* 251**,** 788-91.

CYBULSKY, M. I., IIYAMA, K., LI, H., ZHU, S., CHEN, M., IIYAMA, M., DAVIS, V., GUTIERREZ-RAMOS, J. C., CONNELLY, P. W. & MILSTONE, D. S. 2001. A major role for VCAM-1, but not ICAM-1, in early atherosclerosis. *J Clin Invest,* 107**,** 1255-62.

DAHL, C., HOFFMANN, H. J., SAITO, H. & SCHIOTZ, P. O. 2004. Human mast cells express receptors for IL-3, IL-5 and GM-CSF; a partial map of receptors on human mast cells cultured in vitro. *Allergy,* 59**,** 1087-96.

DAI, X. M., RYAN, G. R., HAPEL, A. J., DOMINGUEZ, M. G., RUSSELL, R. G., KAPP, S., SYLVESTRE, V. & STANLEY, E. R. 2002. Targeted disruption of the mouse colony-stimulating factor 1 receptor gene results in osteopetrosis, mononuclear phagocyte deficiency, increased primitive progenitor cell frequencies, and reproductive defects. *Blood,* 99**,** 111-20.

DAISSORMONT, I. T., CHRIST, A., TEMMERMAN, L., SAMPEDRO MILLARES, S., SEIJKENS, T., MANCA, M., ROUSCH, M., POGGI, M., BOON, L., VAN DER LOOS, C., DAEMEN, M., LUTGENS, E., HALVORSEN, B., AUKRUST, P., JANSSEN, E. & BIESSEN, E. A. 2011. Plasmacytoid dendritic cells protect against atherosclerosis by tuning T-cell proliferation and activity. *Circ Res,* 109**,** 1387-95.

DAUGHERTY, A. 2002. Mouse models of atherosclerosis. *Am J Med Sci,* 323**,** 3-10.

DAVIES, L. C., JENKINS, S. J., ALLEN, J. E. & TAYLOR, P. R. 2013a. Tissue-resident macrophages. *Nat Immunol,* 14**,** 986-95.

DAVIES, L. C., ROSAS, M., JENKINS, S. J., LIAO, C. T., SCURR, M. J., BROMBACHER, F., FRASER, D. J., ALLEN, J. E., JONES, S. A. & TAYLOR, P. R. 2013b. Distinct bone marrow-derived and tissue-resident macrophage lineages proliferate at key stages during inflammation. *Nat Commun,* 4**,** 1886.

DAVIES, L. C., ROSAS, M., SMITH, P. J., FRASER, D. J., JONES, S. A. & TAYLOR, P. R. 2011. A quantifiable proliferative burst of tissue macrophages restores homeostatic macrophage populations after acute inflammation. *Eur J Immunol,* 41**,** 2155-64.

DAWS, M. R., LANIER, L. L., SEAMAN, W. E. & RYAN, J. C. 2001. Cloning and characterization of a novel mouse myeloid DAP12-associated receptor family. *Eur J Immunol,* 31**,** 783-91.

DEBELLE, L. & TAMBURRO, A. M. 1999. Elastin: molecular description and function. *Int J Biochem Cell Biol,* 31**,** 261-72.

DECKERT, M., SEDGWICK, J. D., FISCHER, E. & SCHLUTER, D. 2006. Regulation of microglial cell responses in murine Toxoplasma encephalitis by CD200/CD200 receptor interaction. *Acta Neuropathol,* 111**,** 548-58.

DIMAYUGA, P., CERCEK, B., OGUCHI, S., FREDRIKSON, G. N., YANO, J., SHAH, P. K., JOVINGE, S. & NILSSON, J. 2002. Inhibitory effect on arterial injury-induced neointimal formation by adoptive B-cell transfer in Rag-1 knockout mice. *Arterioscler Thromb Vasc Biol,* 22**,** 644-9.

DOUGLAS, J., ALBERTSON, D. G., BARCLAY, A. N., DAVIS, M. & RABBITTS, P. H. 1988. RFLP and mapping of human MOX-1 gene on chromosome 3. *Nucleic Acids Res,* 16**,** 9067.

DUTTA, P., HOYER, F. F., GRIGORYEVA, L. S., SAGER, H. B., LEUSCHNER, F., COURTIES, G., BORODOVSKY, A., NOVOBRANTSEVA, T., RUDA,

V. M., FITZGERALD, K., IWAMOTO, Y., WOJTKIEWICZ, G., SUN, Y., DA SILVA, N., LIBBY, P., ANDERSON, D. G., SWIRSKI, F. K., WEISSLEDER, R. & NAHRENDORF, M. 2015. Macrophages retain hematopoietic stem cells in the spleen via VCAM-1. *J Exp Med,* 212**,** 497-512.

ENSAN, S., LI, A., BESLA, R., DEGOUSEE, N., COSME, J., ROUFAIEL, M., SHIKATANI, E. A., EL-MAKLIZI, M., WILLIAMS, J. W., ROBINS, L., LI, C., LEWIS, B., YUN, T. J., LEE, J. S., WIEGHOFER, P., KHATTAR, R., FARROKHI, K., BYRNE, J., OUZOUNIAN, M., ZAVITZ, C. C., LEVY, G. A., BAUER, C. M., LIBBY, P., HUSAIN, M., SWIRSKI, F. K., CHEONG, C., PRINZ, M., HILGENDORF, I., RANDOLPH, G. J., EPELMAN, S., GRAMOLINI, A. O., CYBULSKY, M. I., RUBIN, B. B. & ROBBINS, C. S. 2016. Self-renewing resident arterial macrophages arise from embryonic CX3CR1(+) precursors and circulating monocytes immediately after birth. *Nat Immunol,* 17**,** 159-68.

FLEETWOOD, A. J., LAWRENCE, T., HAMILTON, J. A. & COOK, A. D. 2007. Granulocyte-macrophage colony-stimulating factor (CSF) and macrophage CSF-dependent macrophage phenotypes display differences in cytokine profiles and transcription factor activities: implications for CSF blockade in inflammation. *J Immunol,* 178**,** 5245-52.

FOGELSTRAND, P. & BOREN, J. 2012. Retention of atherogenic lipoproteins in the artery wall and its role in atherogenesis. *Nutr Metab Cardiovasc Dis,* 22**,** 1-7.

FOGG, D. K., SIBON, C., MILED, C., JUNG, S., AUCOUTURIER, P., LITTMAN, D. R., CUMANO, A. & GEISSMANN, F. 2006. A clonogenic bone marrow progenitor specific for macrophages and dendritic cells. *Science,* 311**,** 83-7.

FOURNIER, N., CHALUS, L., DURAND, I., GARCIA, E., PIN, J. J., CHURAKOVA, T., PATEL, S., ZLOT, C., GORMAN, D., ZURAWSKI, S., ABRAMS, J., BATES, E. E. & GARRONE, P. 2000. FDF03, a novel inhibitory receptor of the immunoglobulin superfamily, is expressed by human dendritic and myeloid cells. *J Immunol,* 165**,** 1197-209.

FRANK, M. G., BARRIENTOS, R. M., BIEDENKAPP, J. C., RUDY, J. W., WATKINS, L. R. & MAIER, S. F. 2006. mRNA up-regulation of MHC II and pivotal pro-inflammatory genes in normal brain aging. *Neurobiol Aging,* 27**,** 717-22.

FREDMAN, G., KAMALY, N., SPOLITU, S., MILTON, J., GHORPADE, D., CHIASSON, R., KURIAKOSE, G., PERRETTI, M., FAROKHZAD, O. & TABAS, I. 2015. Targeted nanoparticles containing the proresolving peptide Ac2-26 protect against advanced atherosclerosis in hypercholesterolemic mice. *Sci Transl Med,* 7**,** 275ra20.

FROSTEGARD, J., ULFGREN, A. K., NYBERG, P., HEDIN, U., SWEDENBORG, J., ANDERSSON, U. & HANSSON, G. K. 1999. Cytokine expression in advanced human atherosclerotic plaques: dominance of pro-inflammatory (Th1) and macrophage-stimulating cytokines. *Atherosclerosis,* 145**,** 33-43.

FUJIKADO, N., SAIJO, S., YONEZAWA, T., SHIMAMORI, K., ISHII, A., SUGAI, S., KOTAKI, H., SUDO, K., NOSE, M. & IWAKURA, Y. 2008. Dcir deficiency causes development of autoimmune diseases in mice due to excess expansion of dendritic cells. *Nat Med,* 14**,** 176-80.

FURNKRANZ, A., SCHOBER, A., BOCHKOV, V. N., BASHTRYKOV, P., KRONKE, G., KADL, A., BINDER, B. R., WEBER, C. & LEITINGER, N.

2005. Oxidized phospholipids trigger atherogenic inflammation in murine arteries. *Arterioscler Thromb Vasc Biol,* 25**,** 633-8.

GAUTIER, E. L., SHAY, T., MILLER, J., GRETER, M., JAKUBZICK, C., IVANOV, S., HELFT, J., CHOW, A., ELPEK, K. G., GORDONOV, S., MAZLOOM, A. R., MA'AYAN, A., CHUA, W. J., HANSEN, T. H., TURLEY, S. J., MERAD, M., RANDOLPH, G. J. & IMMUNOLOGICAL GENOME, C. 2012. Gene-expression profiles and transcriptional regulatory pathways that underlie the identity and diversity of mouse tissue macrophages. *Nat Immunol,* 13**,** 1118-28.

GEBUHRER, V., MURPHY, J. F., BORDET, J. C., RECK, M. P. & MCGREGOR, J. L. 1995. Oxidized low-density lipoprotein induces the expression of P-selectin (GMP140/PADGEM/CD62) on human endothelial cells. *Biochem J,* 306 (Pt 1)**,** 293-8.

GEISSMANN, F., JUNG, S. & LITTMAN, D. R. 2003. Blood monocytes consist of two principal subsets with distinct migratory properties. *Immunity,* 19**,** 71-82.

GEISSMANN, F., MANZ, M. G., JUNG, S., SIEWEKE, M. H., MERAD, M. & LEY, K. 2010. Development of monocytes, macrophages, and dendritic cells. *Science,* 327**,** 656-61.

GHAZAVI, F., CLAPPIER, E., LAMMENS, T., SUCIU, S., CAYE, A., ZEGRARI, S., BAKKUS, M., GRARDEL, N., BENOIT, Y., BERTRAND, Y., MINCKES, O., COSTA, V., FERSTER, A., MAZINGUE, F., PLAT, G., PLOUVIER, E., POIREE, M., UYTTEBROECK, A., VAN DER WERFF-TEN BOSCH, J., YAKOUBEN, K., HELSMOORTEL, H., MEUL, M., VAN ROY, N., PHILIPPE, J., SPELEMAN, F., CAVE, H., VAN VLIERBERGHE, P. & DE MOERLOOSE, B. 2015. CD200/BTLA deletions in pediatric precursor B-cell acute lymphoblastic leukemia treated according to the EORTC-CLG 58951 protocol. *Haematologica,* 100**,** 1311-9.

GINHOUX, F., GRETER, M., LEBOEUF, M., NANDI, S., SEE, P., GOKHAN, S., MEHLER, M. F., CONWAY, S. J., NG, L. G., STANLEY, E. R., SAMOKHVALOV, I. M. & MERAD, M. 2010. Fate mapping analysis reveals that adult microglia derive from primitive macrophages. *Science,* 330**,** 841-5.

GINHOUX, F. & JUNG, S. 2014. Monocytes and macrophages: developmental pathways and tissue homeostasis. *Nat Rev Immunol,* 14**,** 392-404.

GLEISSNER, C. A., SHAKED, I., LITTLE, K. M. & LEY, K. 2010. CXC chemokine ligand 4 induces a unique transcriptome in monocyte-derived macrophages. *J Immunol,* 184**,** 4810-8.

GOJOVA, A., BRUN, V., ESPOSITO, B., COTTREZ, F., GOURDY, P., ARDOUIN, P., TEDGUI, A., MALLAT, Z. & GROUX, H. 2003. Specific abrogation of transforming growth factor-beta signaling in T cells alters atherosclerotic lesion size and composition in mice. *Blood,* 102**,** 4052-8.

GOLDSTEIN, J. L. & BROWN, M. S. 2009. The LDL receptor. *Arterioscler Thromb Vasc Biol,* 29**,** 431-8.

GOLDSTEIN, J. L., SOBHANI, M. K., FAUST, J. R. & BROWN, M. S. 1976. Heterozygous familial hypercholesterolemia: failure of normal allele to compensate for mutant allele at a regulated genetic locus. *Cell,* 9**,** 195-203.

GOMEZ, D. & OWENS, G. K. 2012. Smooth muscle cell phenotypic switching in atherosclerosis. *Cardiovasc Res,* 95**,** 156-64.

GORCZYNSKI, R., CHEN, Z., KAI, Y., LEE, L., WONG, S. & MARSDEN, P. A. 2004. CD200 is a ligand for all members of the CD200R family of immunoregulatory molecules. *J Immunol,* 172**,** 7744-9.

GORCZYNSKI, R., CHEN, Z., KHATRI, I. & YU, K. 2013. sCD200 present in mice receiving cardiac and skin allografts causes immunosuppression in vitro and induces Tregs. *Transplantation,* 95**,** 442-7.

GORCZYNSKI, R., KHATRI, I., LEE, L. & BOUDAKOV, I. 2008. An interaction between CD200 and monoclonal antibody agonists to CD200R2 in development of dendritic cells that preferentially induce populations of CD4+CD25+ T regulatory cells. *J Immunol,* 180**,** 5946-55.

GORCZYNSKI, R. M., CHEN, Z., DIAO, J., KHATRI, I., WONG, K., YU, K. & BEHNKE, J. 2010. Breast cancer cell CD200 expression regulates immune response to EMT6 tumor cells in mice. *Breast Cancer Res Treat,* 123**,** 405-15.

GORCZYNSKI, R. M., CHEN, Z., KHATRI, I. & YU, K. 2011a. Graft-infiltrating cells expressing a CD200 transgene prolong allogeneic skin graft survival in association with local increases in Foxp3(+)Treg and mast cells. *Transpl Immunol,* 25**,** 187-93.

GORCZYNSKI, R. M., CHEN, Z., LEE, L., YU, K. & HU, J. 2002. Anti-CD200R ameliorates collagen-induced arthritis in mice. *Clin Immunol,* 104**,** 256-64.

GORCZYNSKI, R. M., CHEN, Z., YU, K. & HU, J. 2001. CD200 immunoadhesin suppresses collagen-induced arthritis in mice. *Clin Immunol,* 101**,** 328-34.

GORCZYNSKI, R. M., CLARK, D. A., ERIN, N. & KHATRI, I. 2011b. Role of CD200 expression in regulation of metastasis of EMT6 tumor cells in mice. *Breast Cancer Res Treat,* 130**,** 49-60.

GORCZYNSKI, R. M., YU, K. & CLARK, D. 2000. Receptor engagement on cells expressing a ligand for the tolerance-inducing molecule OX2 induces an immunoregulatory population that inhibits alloreactivity in vitro and in vivo. *J Immunol,* 165**,** 4854-60.

GREEN, B. J., CLARK, G. J. & HART, D. N. 1998. The CMRF-35 mAb recognizes a second leukocyte membrane molecule with a domain similar to the poly Ig receptor. *Int Immunol,* 10**,** 891-9.

GUILLIAMS, M., GINHOUX, F., JAKUBZICK, C., NAIK, S. H., ONAI, N., SCHRAML, B. U., SEGURA, E., TUSSIWAND, R. & YONA, S. 2014. Dendritic cells, monocytes and macrophages: a unified nomenclature based on ontogeny. *Nat Rev Immunol,* 14**,** 571-8.

HAMILTON, J. A. 2008. Colony-stimulating factors in inflammation and autoimmunity. *Nat Rev Immunol,* 8**,** 533-44.

HAN, K. H., HAN, K. O., GREEN, S. R. & QUEHENBERGER, O. 1999. Expression of the monocyte chemoattractant protein-1 receptor CCR2 is increased in hypercholesterolemia. Differential effects of plasma lipoproteins on monocyte function. *J Lipid Res,* 40**,** 1053-63.

HANSSON, G. K., HOLM, J. & JONASSON, L. 1989. Detection of activated T lymphocytes in the human atherosclerotic plaque. *Am J Pathol,* 135**,** 169-75.

HASHIMOTO, D., CHOW, A., NOIZAT, C., TEO, P., BEASLEY, M. B., LEBOEUF, M., BECKER, C. D., SEE, P., PRICE, J., LUCAS, D., GRETER, M., MORTHA, A., BOYER, S. W., FORSBERG, E. C., TANAKA, M., VAN ROOIJEN, N., GARCIA-SASTRE, A., STANLEY, E. R., GINHOUX, F., FRENETTE, P. S. & MERAD, M. 2013. Tissue-resident macrophages self-maintain locally throughout adult life with minimal contribution from circulating monocytes. *Immunity,* 38**,** 792-804.

HATHERLEY, D. & BARCLAY, A. N. 2004. The CD200 and CD200 receptor cell surface proteins interact through their N-terminal immunoglobulin-like domains. *Eur J Immunol,* 34**,** 1688-94.

HATHERLEY, D., CHERWINSKI, H. M., MOSHREF, M. & BARCLAY, A. N. 2005. Recombinant CD200 protein does not bind activating proteins closely related to CD200 receptor. *J Immunol,* 175**,** 2469-74.

HAYAKAWA, K., WANG, X. & LO, E. H. 2016. CD200 increases alternatively activated macrophages through cAMP-response element binding protein - C/EBP-beta signaling. *J Neurochem,* 136**,** 900-6.

HELFT, J., BOTTCHER, J., CHAKRAVARTY, P., ZELENAY, S., HUOTARI, J., SCHRAML, B. U., GOUBAU, D. & REIS E SOUSA, C. 2015. GM-CSF Mouse Bone Marrow Cultures Comprise a Heterogeneous Population of CD11c(+)MHCII(+) Macrophages and Dendritic Cells. *Immunity,* 42**,** 1197-211.

HETTINGER, J., RICHARDS, D. M., HANSSON, J., BARRA, M. M., JOSCHKO, A. C., KRIJGSVELD, J. & FEUERER, M. 2013. Origin of monocytes and macrophages in a committed progenitor. *Nat Immunol,* 14**,** 821-30.

HIRAGA, S., KAJI, T., UEDA, Y., ZISAKI, F., IWATA, K., KOIZUMI, F., OKADA, Y., KATSUDA, S. & NAKANISHI, I. 2000. Modulation of collagen synthesis by tumor necrosis factor alpha in cultured vascular smooth muscle cells. *Life Sci,* 66**,** 235-44.

HOEK, R. M., RUULS, S. R., MURPHY, C. A., WRIGHT, G. J., GODDARD, R., ZURAWSKI, S. M., BLOM, B., HOMOLA, M. E., STREIT, W. J., BROWN, M. H., BARCLAY, A. N. & SEDGWICK, J. D. 2000. Down-regulation of the macrophage lineage through interaction with OX2 (CD200). *Science,* 290**,** 1768-71.

HUO, Y., SCHOBER, A., FORLOW, S. B., SMITH, D. F., HYMAN, M. C., JUNG, S., LITTMAN, D. R., WEBER, C. & LEY, K. 2003. Circulating activated platelets exacerbate atherosclerosis in mice deficient in apolipoprotein E. *Nat Med,* 9**,** 61-7.

HUSSELL, T. & BELL, T. J. 2014. Alveolar macrophages: plasticity in a tissue-specific context. *Nat Rev Immunol,* 14**,** 81-93.

IMAKITA, M., YUTANI, C., STRONG, J. P., SAKURAI, I., SUMIYOSHI, A., WATANABE, T., MITSUMATA, M., KUSUMI, Y., KATAYAMA, S., MANO, M., BABA, S., MANNAMI, T., MASUDA, J., SUEISHI, K. & TANAKA, K. 2001. Second nation-wide study of atherosclerosis in infants, children and young adults in Japan. *Atherosclerosis,* 155**,** 487-97.

INABA, K., INABA, M., ROMANI, N., AYA, H., DEGUCHI, M., IKEHARA, S., MURAMATSU, S. & STEINMAN, R. M. 1992. Generation of large numbers of dendritic cells from mouse bone marrow cultures supplemented with granulocyte/macrophage colony-stimulating factor. *J Exp Med,* 176**,** 1693-702.

INABA, K., TURLEY, S., YAMAIDE, F., IYODA, T., MAHNKE, K., INABA, M., PACK, M., SUBKLEWE, M., SAUTER, B., SHEFF, D., ALBERT, M., BHARDWAJ, N., MELLMAN, I. & STEINMAN, R. M. 1998. Efficient presentation of phagocytosed cellular fragments on the major histocompatibility complex class II products of dendritic cells. *J Exp Med,* 188**,** 2163-73.

INOUE, S., EGASHIRA, K., NI, W., KITAMOTO, S., USUI, M., OTANI, K., ISHIBASHI, M., HIASA, K., NISHIDA, K. & TAKESHITA, A. 2002. Anti-

monocyte chemoattractant protein-1 gene therapy limits progression and destabilization of established atherosclerosis in apolipoprotein E-knockout mice. *Circulation,* 106**,** 2700-6.

ISHIBASHI, S., BROWN, M. S., GOLDSTEIN, J. L., GERARD, R. D., HAMMER, R. E. & HERZ, J. 1993. Hypercholesterolemia in low density lipoprotein receptor knockout mice and its reversal by adenovirus-mediated gene delivery. *J Clin Invest,* 92**,** 883-93.

IWASAKI, H. & AKASHI, K. 2007. Myeloid lineage commitment from the hematopoietic stem cell. *Immunity,* 26**,** 726-40.

JAGUIN, M., HOULBERT, N., FARDEL, O. & LECUREUR, V. 2013. Polarization profiles of human M-CSF-generated macrophages and comparison of M1-markers in classically activated macrophages from GM-CSF and M-CSF origin. *Cell Immunol,* 281**,** 51-61.

JAKUBZICK, C., GAUTIER, E. L., GIBBINGS, S. L., SOJKA, D. K., SCHLITZER, A., JOHNSON, T. E., IVANOV, S., DUAN, Q., BALA, S., CONDON, T., VAN ROOIJEN, N., GRAINGER, J. R., BELKAID, Y., MA'AYAN, A., RICHES, D. W., YOKOYAMA, W. M., GINHOUX, F., HENSON, P. M. & RANDOLPH, G. J. 2013. Minimal differentiation of classical monocytes as they survey steady-state tissues and transport antigen to lymph nodes. *Immunity,* 39**,** 599-610.

JENKINS, S. J., RUCKERL, D., COOK, P. C., JONES, L. H., FINKELMAN, F. D., VAN ROOIJEN, N., MACDONALD, A. S. & ALLEN, J. E. 2011. Local macrophage proliferation, rather than recruitment from the blood, is a signature of TH2 inflammation. *Science,* 332**,** 1284-8.

JUNG, S., ALIBERTI, J., GRAEMMEL, P., SUNSHINE, M. J., KREUTZBERG, G. W., SHER, A. & LITTMAN, D. R. 2000. Analysis of fractalkine receptor CX(3)CR1 function by targeted deletion and green fluorescent protein reporter gene insertion. *Mol Cell Biol,* 20**,** 4106-14.

KADL, A., MEHER, A. K., SHARMA, P. R., LEE, M. Y., DORAN, A. C., JOHNSTONE, S. R., ELLIOTT, M. R., GRUBER, F., HAN, J., CHEN, W., KENSLER, T., RAVICHANDRAN, K. S., ISAKSON, B. E., WAMHOFF, B. R. & LEITINGER, N. 2010. Identification of a novel macrophage phenotype that develops in response to atherogenic phospholipids via Nrf2. *Circ Res,* 107**,** 737-46.

KASSITERIDI, C. & MONACO, C. 2015. Macrophages and dendritic cells: the usual suspects in atherogenesis. *Curr Drug Targets,* 16**,** 373-82.

KATSUDA, S., OKADA, Y., MINAMOTO, T., ODA, Y., MATSUI, Y. & NAKANISHI, I. 1992. Collagens in human atherosclerosis. Immunohistochemical analysis using collagen type-specific antibodies. *Arterioscler Thromb,* 12**,** 494-502.

KHARITONENKOV, A., CHEN, Z., SURES, I., WANG, H., SCHILLING, J. & ULLRICH, A. 1997. A family of proteins that inhibit signalling through tyrosine kinase receptors. *Nature,* 386**,** 181-6.

KIM, C. H. 2010. Homeostatic and pathogenic extramedullary hematopoiesis. *J Blood Med,* 1**,** 13-9.

KLAPPROTH, K., LASITSCHKA, F. & RODEWALD, H. R. 2016. Multilayered ancestry of arterial macrophages. *Nat Immunol,* 17**,** 117-8.

KO, Y. C., CHIEN, H. F., JIANG-SHIEH, Y. F., CHANG, C. Y., PAI, M. H., HUANG, J. P., CHEN, H. M. & WU, C. H. 2009. Endothelial CD200 is

heterogeneously distributed, regulated and involved in immune cell-endothelium interactions. *J Anat,* 214**,** 183-95.

KOCKX, M. M., DE MEYER, G. R., JACOB, W. A., BULT, H. & HERMAN, A. G. 1992. Triphasic sequence of neointimal formation in the cuffed carotid artery of the rabbit. *Arterioscler Thromb,* 12**,** 1447-57.

KOHYAMA, M., ISE, W., EDELSON, B. T., WILKER, P. R., HILDNER, K., MEJIA, C., FRAZIER, W. A., MURPHY, T. L. & MURPHY, K. M. 2009. Role for Spi-C in the development of red pulp macrophages and splenic iron homeostasis. *Nature,* 457**,** 318-21.

KOJIMA, T., OBATA, K., MUKAI, K., SATO, S., TAKAI, T., MINEGISHI, Y. & KARASUYAMA, H. 2007. Mast cells and basophils are selectively activated in vitro and in vivo through CD200R3 in an IgE-independent manner. *J Immunol,* 179**,** 7093-100.

KOLODGIE, F. D., GOLD, H. K., BURKE, A. P., FOWLER, D. R., KRUTH, H. S., WEBER, D. K., FARB, A., GUERRERO, L. J., HAYASE, M., KUTYS, R., NARULA, J., FINN, A. V. & VIRMANI, R. 2003. Intraplaque hemorrhage and progression of coronary atheroma. *N Engl J Med,* 349**,** 2316-25.

KOO, A., DEWEY, C. F., JR. & GARCIA-CARDENA, G. 2013. Hemodynamic shear stress characteristic of atherosclerosis-resistant regions promotes glycocalyx formation in cultured endothelial cells. *Am J Physiol Cell Physiol,* 304**,** C137-46.

KRETTEK, A., SUKHOVA, G. K. & LIBBY, P. 2003. Elastogenesis in human arterial disease: a role for macrophages in disordered elastin synthesis. *Arterioscler Thromb Vasc Biol,* 23**,** 582-7.

KRETZ-ROMMEL, A., QIN, F., DAKAPPAGARI, N., RAVEY, E. P., MCWHIRTER, J., OLTEAN, D., FREDERICKSON, S., MARUYAMA, T., WILD, M. A., NOLAN, M. J., WU, D., SPRINGHORN, J. & BOWDISH, K. S. 2007. CD200 expression on tumor cells suppresses antitumor immunity: new approaches to cancer immunotherapy. *J Immunol,* 178**,** 5595-605.

KUMAR, A., HOOVER, J. L., SIMMONS, C. A., LINDNER, V. & SHEBUSKI, R. J. 1997. Remodeling and neointimal formation in the carotid artery of normal and P-selectin-deficient mice. *Circulation,* 96**,** 4333-42.

KYAW, T., TAY, C., KHAN, A., DUMOUCHEL, V., CAO, A., TO, K., KEHRY, M., DUNN, R., AGROTIS, A., TIPPING, P., BOBIK, A. & TOH, B. H. 2010. Conventional B2 B cell depletion ameliorates whereas its adoptive transfer aggravates atherosclerosis. *J Immunol,* 185**,** 4410-9.

KYAW, T., WINSHIP, A., TAY, C., KANELLAKIS, P., HOSSEINI, H., CAO, A., LI, P., TIPPING, P., BOBIK, A. & TOH, B. H. 2013. Cytotoxic and proinflammatory CD8+ T lymphocytes promote development of vulnerable atherosclerotic plaques in apoE-deficient mice. *Circulation,* 127**,** 1028-39.

LACEY, D. C., ACHUTHAN, A., FLEETWOOD, A. J., DINH, H., ROINIOTIS, J., SCHOLZ, G. M., CHANG, M. W., BECKMAN, S. K., COOK, A. D. & HAMILTON, J. A. 2012. Defining GM-CSF- and macrophage-CSF-dependent macrophage responses by in vitro models. *J Immunol,* 188**,** 5752-65.

LANDSMAN, L., BAR-ON, L., ZERNECKE, A., KIM, K. W., KRAUTHGAMER, R., SHAGDARSUREN, E., LIRA, S. A., WEISSMAN, I. L., WEBER, C. & JUNG, S. 2009. CX3CR1 is required for monocyte homeostasis and atherogenesis by promoting cell survival. *Blood,* 113**,** 963-72.

LAPPALAINEN, J., LINDSTEDT, K. A., OKSJOKI, R. & KOVANEN, P. T. 2011. OxLDL-IgG immune complexes induce expression and secretion of proatherogenic cytokines by cultured human mast cells. *Atherosclerosis,* 214**,** 357-63.

LAUDER, S. N., TAYLOR, P. R., CLARK, S. R., EVANS, R. L., HINDLEY, J. P., SMART, K., LEACH, H., KIDD, E. J., BROADLEY, K. J., JONES, S. A., WISE, M. P., GODKIN, A. J., O'DONNELL, V. & GALLIMORE, A. M. 2011. Paracetamol reduces influenza-induced immunopathology in a mouse model of infection without compromising virus clearance or the generation of protective immunity. *Thorax,* 66**,** 368-74.

LEBBINK, R. J., DE RUITER, T., KAPTIJN, G. J., BIHAN, D. G., JANSEN, C. A., LENTING, P. J. & MEYAARD, L. 2007. Mouse leukocyte-associated Ig-like receptor-1 (mLAIR-1) functions as an inhibitory collagen-binding receptor on immune cells. *Int Immunol,* 19**,** 1011-9.

LEE, T. S., YEN, H. C., PAN, C. C. & CHAU, L. Y. 1999. The role of interleukin 12 in the development of atherosclerosis in ApoE-deficient mice. *Arterioscler Thromb Vasc Biol,* 19**,** 734-42.

LEITINGER, N. & SCHULMAN, I. G. 2013. Phenotypic polarization of macrophages in atherosclerosis. *Arterioscler Thromb Vasc Biol,* 33**,** 1120-6.

LEY, K., MILLER, Y. I. & HEDRICK, C. C. 2011. Monocyte and macrophage dynamics during atherogenesis. *Arterioscler Thromb Vasc Biol,* 31**,** 1506-16.

LI, Y., ZHAO, L. D., TONG, L. S., QIAN, S. N., REN, Y., ZHANG, L., DING, X., CHEN, Y., WANG, Y. X., ZHANG, W., ZENG, X. F., ZHANG, F. C., TANG, F. L., ZHANG, X., BA, D. N., HE, W., CAO, X. T. & LIPSKY, P. E. 2012. Aberrant CD200/CD200R1 expression and function in systemic lupus erythematosus contributes to abnormal T-cell responsiveness and dendritic cell activity. *Arthritis Res Ther,* 14**,** R123.

LIBBY, P. & HANSSON, G. K. 1991. Involvement of the immune system in human atherogenesis: current knowledge and unanswered questions. *Lab Invest,* 64**,** 5-15.

LIBBY, P., RIDKER, P. M. & MASERI, A. 2002. Inflammation and atherosclerosis. *Circulation,* 105**,** 1135-43.

LIBBY, P., TABAS, I., FREDMAN, G. & FISHER, E. A. 2014. Inflammation and its resolution as determinants of acute coronary syndromes. *Circ Res,* 114**,** 1867-79.

LINDNER, V., FINGERLE, J. & REIDY, M. A. 1993. Mouse model of arterial injury. *Circ Res,* 73**,** 792-6.

LIU, Y., BANDO, Y., VARGAS-LOWY, D., ELYAMAN, W., KHOURY, S. J., HUANG, T., REIF, K. & CHITNIS, T. 2010. CD200R1 agonist attenuates mechanisms of chronic disease in a murine model of multiple sclerosis. *J Neurosci,* 30**,** 2025-38.

LUM, H. & MALIK, A. B. 1994. Regulation of vascular endothelial barrier function. *Am J Physiol,* 267**,** L223-41.

LUTGENS, E., LIEVENS, D., BECKERS, L., DONNERS, M. & DAEMEN, M. 2007. CD40 and its ligand in atherosclerosis. *Trends Cardiovasc Med,* 17**,** 118-23.

MABBOTT, N. A., KENNETH BAILLIE, J., HUME, D. A. & FREEMAN, T. C. 2010. Meta-analysis of lineage-specific gene expression signatures in mouse leukocyte populations. *Immunobiology,* 215**,** 724-36.

MAJOR, A. S., FAZIO, S. & LINTON, M. F. 2002. B-lymphocyte deficiency increases atherosclerosis in LDL receptor-null mice. *Arterioscler Thromb Vasc Biol,* 22**,** 1892-8.

MANTOVANI, A., GARLANDA, C. & LOCATI, M. 2009. Macrophage diversity and polarization in atherosclerosis: a question of balance. *Arterioscler Thromb Vasc Biol,* 29**,** 1419-23.

MANTOVANI, A., SICA, A. & LOCATI, M. 2005. Macrophage polarization comes of age. *Immunity,* 23**,** 344-6.

MARTINEZ, F. O. & GORDON, S. 2014. The M1 and M2 paradigm of macrophage activation: time for reassessment. *F1000Prime Rep,* 6**,** 13.

MASHIMA, R., HONDA, K., YANG, Y., MORITA, Y., INOUE, A., ARIMURA, S., NISHINA, H., EMA, H., NAKAUCHI, H., SEED, B., ODA, H. & YAMANASHI, Y. 2010. Mice lacking Dok-1, Dok-2, and Dok-3 succumb to aggressive histiocytic sarcoma. *Lab Invest,* 90**,** 1357-64.

MAYADAS, T. N., CULLERE, X. & LOWELL, C. A. 2014. The multifaceted functions of neutrophils. *Annu Rev Pathol,* 9**,** 181-218.

MEIR, K. S. & LEITERSDORF, E. 2004. Atherosclerosis in the apolipoprotein-E-deficient mouse: a decade of progress. *Arterioscler Thromb Vasc Biol,* 24**,** 1006-14.

MELLAK, S., AIT-OUFELLA, H., ESPOSITO, B., LOYER, X., POIRIER, M., TEDDER, T. F., TEDGUI, A., MALLAT, Z. & POTTEAUX, S. 2015. Angiotensin II mobilizes spleen monocytes to promote the development of abdominal aortic aneurysm in Apoe-/- mice. *Arterioscler Thromb Vasc Biol,* 35**,** 378-88.

MERAD, M., SATHE, P., HELFT, J., MILLER, J. & MORTHA, A. 2013. The dendritic cell lineage: ontogeny and function of dendritic cells and their subsets in the steady state and the inflamed setting. *Annu Rev Immunol,* 31**,** 563-604.

MEYAARD, L. 2008. The inhibitory collagen receptor LAIR-1 (CD305). *J Leukoc Biol,* 83**,** 799-803.

MICHELSEN, K. S., WONG, M. H., SHAH, P. K., ZHANG, W., YANO, J., DOHERTY, T. M., AKIRA, S., RAJAVASHISTH, T. B. & ARDITI, M. 2004. Lack of Toll-like receptor 4 or myeloid differentiation factor 88 reduces atherosclerosis and alters plaque phenotype in mice deficient in apolipoprotein E. *Proc Natl Acad Sci U S A,* 101**,** 10679-84.

MIHRSHAHI, R., BARCLAY, A. N. & BROWN, M. H. 2009. Essential roles for Dok2 and RasGAP in CD200 receptor-mediated regulation of human myeloid cells. *J Immunol,* 183**,** 4879-86.

MIHRSHAHI, R. & BROWN, M. H. 2010. Downstream of tyrosine kinase 1 and 2 play opposing roles in CD200 receptor signaling. *J Immunol,* 185**,** 7216-22.

MILLER, J. C., BROWN, B. D., SHAY, T., GAUTIER, E. L., JOJIC, V., COHAIN, A., PANDEY, G., LEBOEUF, M., ELPEK, K. G., HELFT, J., HASHIMOTO, D., CHOW, A., PRICE, J., GRETER, M., BOGUNOVIC, M., BELLEMARE-PELLETIER, A., FRENETTE, P. S., RANDOLPH, G. J., TURLEY, S. J., MERAD, M. & IMMUNOLOGICAL GENOME, C. 2012. Deciphering the transcriptional network of the dendritic cell lineage. *Nat Immunol,* 13**,** 888-99.

MILNER, J. D., SANDLER, N. G. & DOUEK, D. C. 2010. Th17 cells, Job's syndrome and HIV: opportunities for bacterial and fungal infections. *Curr Opin HIV AIDS,* 5**,** 179-83.

MONACO, C., GREGAN, S. M., NAVIN, T. J., FOXWELL, B. M., DAVIES, A. H. & FELDMANN, M. 2009. Toll-like receptor-2 mediates inflammation and matrix degradation in human atherosclerosis. *Circulation,* 120**,** 2462-9.

MOR, A., PLANER, D., LUBOSHITS, G., AFEK, A., METZGER, S., CHAJEK-SHAUL, T., KEREN, G. & GEORGE, J. 2007. Role of naturally occurring CD4+ CD25+ regulatory T cells in experimental atherosclerosis. *Arterioscler Thromb Vasc Biol,* 27**,** 893-900.

MORAES-VIEIRA, P. M., YORE, M. M., DWYER, P. M., SYED, I., ARYAL, P. & KAHN, B. B. 2014. RBP4 activates antigen-presenting cells, leading to adipose tissue inflammation and systemic insulin resistance. *Cell Metab,* 19**,** 512-26.

MOREAUX, J., HOSE, D., REME, T., JOURDAN, E., HUNDEMER, M., LEGOUFFE, E., MOINE, P., BOURIN, P., MOOS, M., CORRE, J., MOHLER, T., DE VOS, J., ROSSI, J. F., GOLDSCHMIDT, H. & KLEIN, B. 2006. CD200 is a new prognostic factor in multiple myeloma. *Blood,* 108**,** 4194-7.

MORRISON, S. J. & WEISSMAN, I. L. 1994. The long-term repopulating subset of hematopoietic stem cells is deterministic and isolatable by phenotype. *Immunity,* 1**,** 661-73.

MOSES, H. L., YANG, E. Y. & PIETENPOL, J. A. 1990. TGF-beta stimulation and inhibition of cell proliferation: new mechanistic insights. *Cell,* 63**,** 245-7.

MOUSSEAU, D. D., BANVILLE, D., L'ABBE, D., BOUCHARD, P. & SHEN, S. H. 2000. PILRalpha, a novel immunoreceptor tyrosine-based inhibitory motif-bearing protein, recruits SHP-1 upon tyrosine phosphorylation and is paired with the truncated counterpart PILRbeta. *J Biol Chem,* 275**,** 4467-74.

MULLICK, A. E., SOLDAU, K., KIOSSES, W. B., BELL, T. A., 3RD, TOBIAS, P. S. & CURTISS, L. K. 2008. Increased endothelial expression of Toll-like receptor 2 at sites of disturbed blood flow exacerbates early atherogenic events. *J Exp Med,* 205**,** 373-83.

MULLICK, A. E., TOBIAS, P. S. & CURTISS, L. K. 2005. Modulation of atherosclerosis in mice by Toll-like receptor 2. *J Clin Invest,* 115**,** 3149-56.

MURPHY, A. J., AKHTARI, M., TOLANI, S., PAGLER, T., BIJL, N., KUO, C. L., WANG, M., SANSON, M., ABRAMOWICZ, S., WELCH, C., BOCHEM, A. E., KUIVENHOVEN, J. A., YVAN-CHARVET, L. & TALL, A. R. 2011. ApoE regulates hematopoietic stem cell proliferation, monocytosis, and monocyte accumulation in atherosclerotic lesions in mice. *J Clin Invest,* 121**,** 4138-49.

NAGEH, M. F., SANDBERG, E. T., MAROTTI, K. R., LIN, A. H., MELCHIOR, E. P., BULLARD, D. C. & BEAUDET, A. L. 1997. Deficiency of inflammatory cell adhesion molecules protects against atherosclerosis in mice. *Arterioscler Thromb Vasc Biol,* 17**,** 1517-20.

NAKAJIMA, H., SAMARIDIS, J., ANGMAN, L. & COLONNA, M. 1999. Human myeloid cells express an activating ILT receptor (ILT1) that associates with Fc receptor gamma-chain. *J Immunol,* 162**,** 5-8.

NAKASHIMA, Y., PLUMP, A. S., RAINES, E. W., BRESLOW, J. L. & ROSS, R. 1994. ApoE-deficient mice develop lesions of all phases of atherosclerosis throughout the arterial tree. *Arterioscler Thromb,* 14**,** 133-40.

NAKASHIMA, Y., RAINES, E. W., PLUMP, A. S., BRESLOW, J. L. & ROSS, R. 1998. Upregulation of VCAM-1 and ICAM-1 at atherosclerosis-prone sites on

the endothelium in the ApoE-deficient mouse. *Arterioscler Thromb Vasc Biol,* 18**,** 842-51.

NAKASHIMA, Y., WIGHT, T. N. & SUEISHI, K. 2008. Early atherosclerosis in humans: role of diffuse intimal thickening and extracellular matrix proteoglycans. *Cardiovasc Res,* 79**,** 14-23.

NATHAN, C. & MULLER, W. A. 2001. Putting the brakes on innate immunity: a regulatory role for CD200? *Nat Immunol,* 2**,** 17-9.

NELMS, K., SNOW, A. L., HU-LI, J. & PAUL, W. E. 1998. FRIP, a hematopoietic cell-specific rasGAP-interacting protein phosphorylated in response to cytokine stimulation. *Immunity,* 9**,** 13-24.

NIESSNER, A., SATO, K., CHAIKOF, E. L., COLMEGNA, I., GORONZY, J. J. & WEYAND, C. M. 2006. Pathogen-sensing plasmacytoid dendritic cells stimulate cytotoxic T-cell function in the atherosclerotic plaque through interferon-alpha. *Circulation,* 114**,** 2482-9.

O'LEARY, D. H., POLAK, J. F., KRONMAL, R. A., KITTNER, S. J., BOND, M. G., WOLFSON, S. K., JR., BOMMER, W., PRICE, T. R., GARDIN, J. M. & SAVAGE, P. J. 1992. Distribution and correlates of sonographically detected carotid artery disease in the Cardiovascular Health Study. The CHS Collaborative Research Group. *Stroke,* 23**,** 1752-60.

OHASHI, W., HATTORI, K. & HATTORI, Y. 2015. Control of Macrophage Dynamics as a Potential Therapeutic Approach for Clinical Disorders Involving Chronic Inflammation. *J Pharmacol Exp Ther,* 354**,** 240-50.

OLDENBORG, P. A., ZHELEZNYAK, A., FANG, Y. F., LAGENAUR, C. F., GRESHAM, H. D. & LINDBERG, F. P. 2000. Role of CD47 as a marker of self on red blood cells. *Science,* 288**,** 2051-4.

ONAI, N., KURABAYASHI, K., HOSOI-AMAIKE, M., TOYAMA-SORIMACHI, N., MATSUSHIMA, K., INABA, K. & OHTEKI, T. 2013. A clonogenic progenitor with prominent plasmacytoid dendritic cell developmental potential. *Immunity,* 38**,** 943-57.

ONAI, N., OBATA-ONAI, A., SCHMID, M. A., OHTEKI, T., JARROSSAY, D. & MANZ, M. G. 2007. Identification of clonogenic common Flt3+M-CSFR+ plasmacytoid and conventional dendritic cell progenitors in mouse bone marrow. *Nat Immunol,* 8**,** 1207-16.

PACE, J. L., RUSSELL, S. W., SCHREIBER, R. D., ALTMAN, A. & KATZ, D. H. 1983. Macrophage activation: priming activity from a T-cell hybridoma is attributable to interferon-gamma. *Proc Natl Acad Sci U S A,* 80**,** 3782-6.

PARMAR, K. M., LARMAN, H. B., DAI, G., ZHANG, Y., WANG, E. T., MOORTHY, S. N., KRATZ, J. R., LIN, Z., JAIN, M. K., GIMBRONE, M. A., JR. & GARCIA-CARDENA, G. 2006. Integration of flow-dependent endothelial phenotypes by Kruppel-like factor 2. *J Clin Invest,* 116**,** 49-58.

PESCHON, J. J., MORRISSEY, P. J., GRABSTEIN, K. H., RAMSDELL, F. J., MARASKOVSKY, E., GLINIAK, B. C., PARK, L. S., ZIEGLER, S. F., WILLIAMS, D. E., WARE, C. B., MEYER, J. D. & DAVISON, B. L. 1994. Early lymphocyte expansion is severely impaired in interleukin 7 receptor-deficient mice. *J Exp Med,* 180**,** 1955-60.

PIEDRAHITA, J. A., ZHANG, S. H., HAGAMAN, J. R., OLIVER, P. M. & MAEDA, N. 1992. Generation of mice carrying a mutant apolipoprotein E gene inactivated by gene targeting in embryonic stem cells. *Proc Natl Acad Sci U S A,* 89**,** 4471-5.

PLUMP, A. S., SMITH, J. D., HAYEK, T., AALTO-SETALA, K., WALSH, A., VERSTUYFT, J. G., RUBIN, E. M. & BRESLOW, J. L. 1992. Severe hypercholesterolemia and atherosclerosis in apolipoprotein E-deficient mice created by homologous recombination in ES cells. *Cell,* 71**,** 343-53.

PROCKOP, D. J. & KIVIRIKKO, K. I. 1995. Collagens: molecular biology, diseases, and potentials for therapy. *Annu Rev Biochem,* 64**,** 403-34.

QIAO, J. H., TRIPATHI, J., MISHRA, N. K., CAI, Y., TRIPATHI, S., WANG, X. P., IMES, S., FISHBEIN, M. C., CLINTON, S. K., LIBBY, P., LUSIS, A. J. & RAJAVASHISTH, T. B. 1997. Role of macrophage colony-stimulating factor in atherosclerosis: studies of osteopetrotic mice. *Am J Pathol,* 150**,** 1687-99.

RAINES, E. W. & FERRI, N. 2005. Thematic review series: The immune system and atherogenesis. Cytokines affecting endothelial and smooth muscle cells in vascular disease. *J Lipid Res,* 46**,** 1081-92.

RAJAVASHISTH, T. B., ANDALIBI, A., TERRITO, M. C., BERLINER, J. A., NAVAB, M., FOGELMAN, A. M. & LUSIS, A. J. 1990. Induction of endothelial cell expression of granulocyte and macrophage colony-stimulating factors by modified low-density lipoproteins. *Nature,* 344**,** 254-7.

REDDICK, R. L., ZHANG, S. H. & MAEDA, N. 1994. Atherosclerosis in mice lacking apo E. Evaluation of lesional development and progression. *Arterioscler Thromb,* 14**,** 141-7.

REN, Y., YANG, B., YIN, Y., LENG, X., JIANG, Y., ZHANG, L., LI, Y., LI, X., ZHANG, F., HE, W., ZHANG, X. & CAO, X. 2015. Aberrant CD200/CD200R1 expression and its potential role in Th17 cell differentiation, chemotaxis and osteoclastogenesis in rheumatoid arthritis. *Rheumatology (Oxford),* 54**,** 712-21.

RIJKERS, E. S., DE RUITER, T., BUITENHUIS, M., VENINGA, H., HOEK, R. M. & MEYAARD, L. 2007. Ligation of CD200R by CD200 is not required for normal murine myelopoiesis. *Eur J Haematol,* 79**,** 410-6.

ROBBINS, C. S., CHUDNOVSKIY, A., RAUCH, P. J., FIGUEIREDO, J. L., IWAMOTO, Y., GORBATOV, R., ETZRODT, M., WEBER, G. F., UENO, T., VAN ROOIJEN, N., MULLIGAN-KEHOE, M. J., LIBBY, P., NAHRENDORF, M., PITTET, M. J., WEISSLEDER, R. & SWIRSKI, F. K. 2012. Extramedullary hematopoiesis generates Ly-6C(high) monocytes that infiltrate atherosclerotic lesions. *Circulation,* 125**,** 364-74.

ROBBINS, C. S., HILGENDORF, I., WEBER, G. F., THEURL, I., IWAMOTO, Y., FIGUEIREDO, J. L., GORBATOV, R., SUKHOVA, G. K., GERHARDT, L. M., SMYTH, D., ZAVITZ, C. C., SHIKATANI, E. A., PARSONS, M., VAN ROOIJEN, N., LIN, H. Y., HUSAIN, M., LIBBY, P., NAHRENDORF, M., WEISSLEDER, R. & SWIRSKI, F. K. 2013. Local proliferation dominates lesional macrophage accumulation in atherosclerosis. *Nat Med,* 19**,** 1166-72.

ROSENBLUM, M. D., OLASZ, E., WOODLIFF, J. E., JOHNSON, B. D., KONKOL, M. C., GERBER, K. A., ORENTAS, R. J., SANDFORD, G. & TRUITT, R. L. 2004a. CD200 is a novel p53-target gene involved in apoptosis-associated immune tolerance. *Blood,* 103**,** 2691-8.

ROSENBLUM, M. D., OLASZ, E. B., YANCEY, K. B., WOODLIFF, J. E., LAZAROVA, Z., GERBER, K. A. & TRUITT, R. L. 2004b. Expression of CD200 on epithelial cells of the murine hair follicle: a role in tissue-specific immune tolerance? *J Invest Dermatol,* 123**,** 880-7.

ROSS, R. 1999. Atherosclerosis--an inflammatory disease. *N Engl J Med,* 340**,** 115-26.

ROTZIUS, P., THAMS, S., SOEHNLEIN, O., KENNE, E., TSENG, C. N., BJORKSTROM, N. K., MALMBERG, K. J., LINDBOM, L. & ERIKSSON, E. E. 2010. Distinct infiltration of neutrophils in lesion shoulders in ApoE-/- mice. *Am J Pathol,* 177**,** 493-500.

SAGE, A. P., TSIANTOULAS, D., BAKER, L., HARRISON, J., MASTERS, L., MURPHY, D., LOINARD, C., BINDER, C. J. & MALLAT, Z. 2012. BAFF receptor deficiency reduces the development of atherosclerosis in mice--brief report. *Arterioscler Thromb Vasc Biol,* 32**,** 1573-6.

SALAGIANNI, M., GALANI, I. E., LUNDBERG, A. M., DAVOS, C. H., VARELA, A., GAVRIIL, A., LYYTIKAINEN, L. P., LEHTIMAKI, T., SIGALA, F., FOLKERSEN, L., GORGOULIS, V., LENGLET, S., MONTECUCCO, F., MACH, F., HEDIN, U., HANSSON, G. K., MONACO, C. & ANDREAKOS, E. 2012. Toll-like receptor 7 protects from atherosclerosis by constraining "inflammatory" macrophage activation. *Circulation,* 126**,** 952-62.

SAMARIDIS, J. & COLONNA, M. 1997. Cloning of novel immunoglobulin superfamily receptors expressed on human myeloid and lymphoid cells: structural evidence for new stimulatory and inhibitory pathways. *Eur J Immunol,* 27**,** 660-5.

SASAKI, T., KUZUYA, M., CHENG, X. W., NAKAMURA, K., TAMAYA-MORI, N., MAEDA, K., KANDA, S., KOIKE, T., SATO, K. & IGUCHI, A. 2004. A novel model of occlusive thrombus formation in mice. *Lab Invest,* 84**,** 1526-32.

SASAWATARI, S., YOSHIZAKI, M., TAYA, C., TAZAWA, A., FURUYAMA-TANAKA, K., YONEKAWA, H., DOHI, T., MAKRIGIANNIS, A. P., SASAZUKI, T., INABA, K. & TOYAMA-SORIMACHI, N. 2010. The Ly49Q receptor plays a crucial role in neutrophil polarization and migration by regulating raft trafficking. *Immunity,* 32**,** 200-13.

SATPATHY, A. T., BRISENO, C. G., LEE, J. S., NG, D., MANIERI, N. A., KC, W., WU, X., THOMAS, S. R., LEE, W. L., TURKOZ, M., MCDONALD, K. G., MEREDITH, M. M., SONG, C., GUIDOS, C. J., NEWBERRY, R. D., OUYANG, W., MURPHY, T. L., STAPPENBECK, T. S., GOMMERMAN, J. L., NUSSENZWEIG, M. C., COLONNA, M., KOPAN, R. & MURPHY, K. M. 2013. Notch2-dependent classical dendritic cells orchestrate intestinal immunity to attaching-and-effacing bacterial pathogens. *Nat Immunol,* 14**,** 937-48.

SEITA, J. & WEISSMAN, I. L. 2010. Hematopoietic stem cell: self-renewal versus differentiation. *Wiley Interdiscip Rev Syst Biol Med,* 2**,** 640-53.

SHARMA, N., LU, Y., ZHOU, G., LIAO, X., KAPIL, P., ANAND, P., MAHABELESHWAR, G. H., STAMLER, J. S. & JAIN, M. K. 2012. Myeloid Kruppel-like factor 4 deficiency augments atherogenesis in ApoE-/- mice--brief report. *Arterioscler Thromb Vasc Biol,* 32**,** 2836-8.

SIMELYTE, E., ALZABIN, S., BOUDAKOV, I. & WILLIAMS, R. 2010. CD200R1 regulates the severity of arthritis but has minimal impact on the adaptive immune response. *Clin Exp Immunol,* 162**,** 163-8.

SIMELYTE, E., CRIADO, G., ESSEX, D., UGER, R. A., FELDMANN, M. & WILLIAMS, R. O. 2008. CD200-Fc, a novel antiarthritic biologic agent that targets proinflammatory cytokine expression in the joints of mice with collagen-induced arthritis. *Arthritis Rheum,* 58**,** 1038-43.

SKALEN, K., GUSTAFSSON, M., RYDBERG, E. K., HULTEN, L. M., WIKLUND, O., INNERARITY, T. L. & BOREN, J. 2002. Subendothelial retention of atherogenic lipoproteins in early atherosclerosis. *Nature,* 417**,** 750-4.

SMITH, E., PRASAD, K. M., BUTCHER, M., DOBRIAN, A., KOLLS, J. K., LEY, K. & GALKINA, E. 2010. Blockade of interleukin-17A results in reduced atherosclerosis in apolipoprotein E-deficient mice. *Circulation,* 121**,** 1746-55.

SNELGROVE, R. J., GOULDING, J., DIDIERLAURENT, A. M., LYONGA, D., VEKARIA, S., EDWARDS, L., GWYER, E., SEDGWICK, J. D., BARCLAY, A. N. & HUSSELL, T. 2008. A critical function for CD200 in lung immune homeostasis and the severity of influenza infection. *Nat Immunol,* 9**,** 1074-83.

SORG, R. V., KOGLER, G. & WERNET, P. 1999. Identification of cord blood dendritic cells as an immature CD11c- population. *Blood,* 93**,** 2302-7.

STARY, H. C., CHANDLER, A. B., DINSMORE, R. E., FUSTER, V., GLAGOV, S., INSULL, W., JR., ROSENFELD, M. E., SCHWARTZ, C. J., WAGNER, W. D. & WISSLER, R. W. 1995. A definition of advanced types of atherosclerotic lesions and a histological classification of atherosclerosis. A report from the Committee on Vascular Lesions of the Council on Arteriosclerosis, American Heart Association. *Circulation,* 92**,** 1355-74.

STEEVELS, T. A. & MEYAARD, L. 2011. Immune inhibitory receptors: essential regulators of phagocyte function. *Eur J Immunol,* 41**,** 575-87.

STEFATER, J. A., 3RD, REN, S., LANG, R. A. & DUFFIELD, J. S. 2011. Metchnikoff's policemen: macrophages in development, homeostasis and regeneration. *Trends Mol Med,* 17**,** 743-52.

STEIN, M., KESHAV, S., HARRIS, N. & GORDON, S. 1992. Interleukin 4 potently enhances murine macrophage mannose receptor activity: a marker of alternative immunologic macrophage activation. *J Exp Med,* 176**,** 287-92.

STEINMAN, R. M. & COHN, Z. A. 1973. Identification of a novel cell type in peripheral lymphoid organs of mice. I. Morphology, quantitation, tissue distribution. *J Exp Med,* 137**,** 1142-62.

STOKES, K. Y., CALAHAN, L., RUSSELL, J. M., GURWARA, S. & GRANGER, D. N. 2006. Role of platelets in hypercholesterolemia-induced leukocyte recruitment and arteriolar dysfunction. *Microcirculation,* 13**,** 377-88.

STROM, A. C., CROSS, A. J., COLE, J. E., BLAIR, P. A., LEIB, C., GODDARD, M. E., ROSSER, E. C., PARK, I., HULTGARDH NILSSON, A., NILSSON, J., MAURI, C. & MONACO, C. 2015. B regulatory cells are increased in hypercholesterolaemic mice and protect from lesion development via IL-10. *Thromb Haemost,* 114**,** 835-47.

SUBRAMANIAN, M., THORP, E., HANSSON, G. K. & TABAS, I. 2013. Treg-mediated suppression of atherosclerosis requires MYD88 signaling in DCs. *J Clin Invest,* 123**,** 179-88.

SUZU, S., TANAKA-DOUZONO, M., NOMAGUCHI, K., YAMADA, M., HAYASAWA, H., KIMURA, F. & MOTOYOSHI, K. 2000. p56(dok-2) as a cytokine-inducible inhibitor of cell proliferation and signal transduction. *EMBO J,* 19**,** 5114-22.

SWIRSKI, F. K., LIBBY, P., AIKAWA, E., ALCAIDE, P., LUSCINSKAS, F. W., WEISSLEDER, R. & PITTET, M. J. 2007. Ly-6Chi monocytes dominate hypercholesterolemia-associated monocytosis and give rise to macrophages in atheromata. *J Clin Invest,* 117**,** 195-205.

SWIRSKI, F. K., NAHRENDORF, M., ETZRODT, M., WILDGRUBER, M., CORTEZ-RETAMOZO, V., PANIZZI, P., FIGUEIREDO, J. L., KOHLER, R. H., CHUDNOVSKIY, A., WATERMAN, P., AIKAWA, E., MEMPEL, T. R., LIBBY, P., WEISSLEDER, R. & PITTET, M. J. 2009. Identification of splenic reservoir monocytes and their deployment to inflammatory sites. *Science,* 325**,** 612-6.

SWIRSKI, F. K., PITTET, M. J., KIRCHER, M. F., AIKAWA, E., JAFFER, F. A., LIBBY, P. & WEISSLEDER, R. 2006. Monocyte accumulation in mouse atherogenesis is progressive and proportional to extent of disease. *Proc Natl Acad Sci U S A,* 103**,** 10340-5.

TABAS, I. 2010. Macrophage death and defective inflammation resolution in atherosclerosis. *Nat Rev Immunol,* 10**,** 36-46.

TABAS, I., GARCIA-CARDENA, G. & OWENS, G. K. 2015. Recent insights into the cellular biology of atherosclerosis. *J Cell Biol,* 209**,** 13-22.

TABAS, I., LI, Y., BROCIA, R. W., XU, S. W., SWENSON, T. L. & WILLIAMS, K. J. 1993. Lipoprotein lipase and sphingomyelinase synergistically enhance the association of atherogenic lipoproteins with smooth muscle cells and extracellular matrix. A possible mechanism for low density lipoprotein and lipoprotein(a) retention and macrophage foam cell formation. *J Biol Chem,* 268**,** 20419-32.

TACKE, F., ALVAREZ, D., KAPLAN, T. J., JAKUBZICK, C., SPANBROEK, R., LLODRA, J., GARIN, A., LIU, J., MACK, M., VAN ROOIJEN, N., LIRA, S. A., HABENICHT, A. J. & RANDOLPH, G. J. 2007. Monocyte subsets differentially employ CCR2, CCR5, and CX3CR1 to accumulate within atherosclerotic plaques. *J Clin Invest,* 117**,** 185-94.

TAI, L. H., GOULET, M. L., BELANGER, S., TOYAMA-SORIMACHI, N., FODIL-CORNU, N., VIDAL, S. M., TROKE, A. D., MCVICAR, D. W. & MAKRIGIANNIS, A. P. 2008. Positive regulation of plasmacytoid dendritic cell function via Ly49Q recognition of class I MHC. *J Exp Med,* 205**,** 3187-99.

TAKAHASHI, K. & NAITO, M. 1993. Development, differentiation, and proliferation of macrophages in the rat yolk sac. *Tissue Cell,* 25**,** 351-62.

TAKAHASHI, K., YAMAMURA, F. & NAITO, M. 1989. Differentiation, maturation, and proliferation of macrophages in the mouse yolk sac: a light-microscopic, enzyme-cytochemical, immunohistochemical, and ultrastructural study. *J Leukoc Biol,* 45**,** 87-96.

TALEB, S., ROMAIN, M., RAMKHELAWON, B., UYTTENHOVE, C., PASTERKAMP, G., HERBIN, O., ESPOSITO, B., PEREZ, N., YASUKAWA, H., VAN SNICK, J., YOSHIMURA, A., TEDGUI, A. & MALLAT, Z. 2009. Loss of SOCS3 expression in T cells reveals a regulatory role for interleukin-17 in atherosclerosis. *J Exp Med,* 206**,** 2067-77.

TANG, J., LOBATTO, M. E., HASSING, L., VAN DER STAAY, S., VAN RIJS, S. M., CALCAGNO, C., BRAZA, M. S., BAXTER, S., FAY, F., SANCHEZ-GAYTAN, B. L., DUIVENVOORDEN, R., SAGER, H., ASTUDILLO, Y. M., LEONG, W., RAMACHANDRAN, S., STORM, G., PEREZ-MEDINA, C., REINER, T., CORMODE, D. P., STRIJKERS, G. J., STROES, E. S., SWIRSKI, F. K., NAHRENDORF, M., FISHER, E. A., FAYAD, Z. A. & MULDER, W. J. 2015. Inhibiting macrophage proliferation suppresses atherosclerotic plaque inflammation. *Sci Adv,* 1.

TAYLOR, N., MCCONACHIE, K., CALDER, C., DAWSON, R., DICK, A., SEDGWICK, J. D. & LIVERSIDGE, J. 2005. Enhanced tolerance to autoimmune uveitis in CD200-deficient mice correlates with a pronounced Th2 switch in response to antigen challenge. *J Immunol,* 174**,** 143-54.

THEURL, I., HILGENDORF, I., NAIRZ, M., TYMOSZUK, P., HASCHKA, D., ASSHOFF, M., HE, S., GERHARDT, L. M., HOLDERRIED, T. A., SEIFERT, M., SOPPER, S., FENN, A. M., ANZAI, A., RATTIK, S., MCALPINE, C., THEURL, M., WIEGHOFER, P., IWAMOTO, Y., WEBER, G. F., HARDER, N. K., CHOUSTERMAN, B. G., ARVEDSON, T. L., MCKEE, M., WANG, F., LUTZ, O. M., REZOAGLI, E., BABITT, J. L., BERRA, L., PRINZ, M., NAHRENDORF, M., WEISS, G., WEISSLEDER, R., LIN, H. Y. & SWIRSKI, F. K. 2016. On-demand erythrocyte disposal and iron recycling requires transient macrophages in the liver. *Nat Med,* 22**,** 945-51.

TOMASELLO, E., CANT, C., BUHRING, H. J., VELY, F., ANDRE, P., SEIFFERT, M., ULLRICH, A. & VIVIER, E. 2000. Association of signal-regulatory proteins beta with KARAP/DAP-12. *Eur J Immunol,* 30**,** 2147-56.

TOYAMA-SORIMACHI, N., TSUJIMURA, Y., MARUYA, M., ONODA, A., KUBOTA, T., KOYASU, S., INABA, K. & KARASUYAMA, H. 2004. Ly49Q, a member of the Ly49 family that is selectively expressed on myeloid lineage cells and involved in regulation of cytoskeletal architecture. *Proc Natl Acad Sci U S A,* 101**,** 1016-21.

TSE, K., TSE, H., SIDNEY, J., SETTE, A. & LEY, K. 2013. T cells in atherosclerosis. *Int Immunol,* 25**,** 615-22.

TSIANTOULAS, D., DIEHL, C. J., WITZTUM, J. L. & BINDER, C. J. 2014. B cells and humoral immunity in atherosclerosis. *Circ Res,* 114**,** 1743-56.

TSOU, C. L., PETERS, W., SI, Y., SLAYMAKER, S., ASLANIAN, A. M., WEISBERG, S. P., MACK, M. & CHARO, I. F. 2007. Critical roles for CCR2 and MCP-3 in monocyte mobilization from bone marrow and recruitment to inflammatory sites. *J Clin Invest,* 117**,** 902-9.

TUSSIWAND, R., EVERTS, B., GRAJALES-REYES, G. E., KRETZER, N. M., IWATA, A., BAGAITKAR, J., WU, X., WONG, R., ANDERSON, D. A., MURPHY, T. L., PEARCE, E. J. & MURPHY, K. M. 2015. Klf4 expression in conventional dendritic cells is required for T helper 2 cell responses. *Immunity,* 42**,** 916-28.

UNKELESS, J. C. & JIN, J. 1997. Inhibitory receptors, ITIM sequences and phosphatases. *Curr Opin Immunol,* 9**,** 338-43.

UYEMURA, K., DEMER, L. L., CASTLE, S. C., JULLIEN, D., BERLINER, J. A., GATELY, M. K., WARRIER, R. R., PHAM, N., FOGELMAN, A. M. & MODLIN, R. L. 1996. Cross-regulatory roles of interleukin (IL)-12 and IL-10 in atherosclerosis. *J Clin Invest,* 97**,** 2130-8.

VAN DER MERWE, P. A. & BARCLAY, A. N. 1996. Analysis of cell-adhesion molecule interactions using surface plasmon resonance. *Curr Opin Immunol,* 8**,** 257-61.

VAN ES, T., VAN PUIJVELDE, G. H., RAMOS, O. H., SEGERS, F. M., JOOSTEN, L. A., VAN DEN BERG, W. B., MICHON, I. M., DE VOS, P., VAN BERKEL, T. J. & KUIPER, J. 2009. Attenuated atherosclerosis upon IL-17R signaling disruption in LDLr deficient mice. *Biochem Biophys Res Commun,* 388**,** 261-5.

VELICAN, D. & VELICAN, C. 1980. Atherosclerotic involvement of the coronary arteries of adolescents and young adults. *Atherosclerosis,* 36**,** 449-60.

VILLARREAL, G., JR., ZHANG, Y., LARMAN, H. B., GRACIA-SANCHO, J., KOO, A. & GARCIA-CARDENA, G. 2010. Defining the regulation of KLF4 expression and its downstream transcriptional targets in vascular endothelial cells. *Biochem Biophys Res Commun,* 391**,** 984-9.

VIRMANI, R., KOLODGIE, F. D., BURKE, A. P., FARB, A. & SCHWARTZ, S. M. 2000. Lessons from sudden coronary death: a comprehensive morphological classification scheme for atherosclerotic lesions. *Arterioscler Thromb Vasc Biol,* 20**,** 1262-75.

VITALE, C., ROMAGNANI, C., FALCO, M., PONTE, M., VITALE, M., MORETTA, A., BACIGALUPO, A., MORETTA, L. & MINGARI, M. C. 1999. Engagement of p75/AIRM1 or CD33 inhibits the proliferation of normal or leukemic myeloid cells. *Proc Natl Acad Sci U S A,* 96**,** 15091-6.

VITALE, C., ROMAGNANI, C., PUCCETTI, A., OLIVE, D., COSTELLO, R., CHIOSSONE, L., PITTO, A., BACIGALUPO, A., MORETTA, L. & MINGARI, M. C. 2001. Surface expression and function of p75/AIRM-1 or CD33 in acute myeloid leukemias: engagement of CD33 induces apoptosis of leukemic cells. *Proc Natl Acad Sci U S A,* 98**,** 5764-9.

VOEHRINGER, D., ROSEN, D. B., LANIER, L. L. & LOCKSLEY, R. M. 2004. CD200 receptor family members represent novel DAP12-associated activating receptors on basophils and mast cells. *J Biol Chem,* 279**,** 54117-23.

VON DER THUSEN, J. H., VAN BERKEL, T. J. & BIESSEN, E. A. 2001. Induction of rapid atherogenesis by perivascular carotid collar placement in apolipoprotein E-deficient and low-density lipoprotein receptor-deficient mice. *Circulation,* 103**,** 1164-70.

WALKER, D. G., DALSING-HERNANDEZ, J. E., CAMPBELL, N. A. & LUE, L. F. 2009. Decreased expression of CD200 and CD200 receptor in Alzheimer's disease: a potential mechanism leading to chronic inflammation. *Exp Neurol,* 215**,** 5-19.

WASKOW, C., LIU, K., DARRASSE-JEZE, G., GUERMONPREZ, P., GINHOUX, F., MERAD, M., SHENGELIA, T., YAO, K. & NUSSENZWEIG, M. 2008. The receptor tyrosine kinase Flt3 is required for dendritic cell development in peripheral lymphoid tissues. *Nat Immunol,* 9**,** 676-83.

WATSON, A. A., LEBEDEV, A. A., HALL, B. A., FENTON-MAY, A. E., VAGIN, A. A., DEJNIRATTISAI, W., FELCE, J., MONGKOLSAPAYA, J., PALMA, A. S., LIU, Y., FEIZI, T., SCREATON, G. R., MURSHUDOV, G. N. & O'CALLAGHAN, C. A. 2011. Structural flexibility of the macrophage dengue virus receptor CLEC5A: implications for ligand binding and signaling. *J Biol Chem,* 286**,** 24208-18.

WEBER, C., MEILER, S., DORING, Y., KOCH, M., DRECHSLER, M., MEGENS, R. T., ROWINSKA, Z., BIDZHEKOV, K., FECHER, C., RIBECHINI, E., VAN ZANDVOORT, M. A., BINDER, C. J., JELINEK, I., HRISTOV, M., BOON, L., JUNG, S., KORN, T., LUTZ, M. B., FORSTER, I., ZENKE, M., HIERONYMUS, T., JUNT, T. & ZERNECKE, A. 2011. CCL17-expressing dendritic cells drive atherosclerosis by restraining regulatory T cell homeostasis in mice. *J Clin Invest,* 121**,** 2898-910.

WEBER, C. & SOEHNLEIN, O. 2011. ApoE controls the interface linking lipids and inflammation in atherosclerosis. *J Clin Invest,* 121**,** 3825-7.

WENTWORTH, J. M., NASELLI, G., BROWN, W. A., DOYLE, L., PHIPSON, B., SMYTH, G. K., WABITSCH, M., O'BRIEN, P. E. & HARRISON, L. C. 2010. Pro-inflammatory CD11c+CD206+ adipose tissue macrophages are associated with insulin resistance in human obesity. *Diabetes,* 59**,** 1648-56.

WIKTOR-JEDRZEJCZAK, W., BARTOCCI, A., FERRANTE, A. W., JR., AHMED-ANSARI, A., SELL, K. W., POLLARD, J. W. & STANLEY, E. R. 1990. Total absence of colony-stimulating factor 1 in the macrophage-deficient osteopetrotic (op/op) mouse. *Proc Natl Acad Sci U S A,* 87**,** 4828-32.

WIKTOR-JEDRZEJCZAK, W. & GORDON, S. 1996. Cytokine regulation of the macrophage (M phi) system studied using the colony stimulating factor-1-deficient op/op mouse. *Physiol Rev,* 76**,** 927-47.

WILCOX, J. N., SMITH, K. M., WILLIAMS, L. T., SCHWARTZ, S. M. & GORDON, D. 1988. Platelet-derived growth factor mRNA detection in human atherosclerotic plaques by in situ hybridization. *J Clin Invest,* 82**,** 1134-43.

WOLINSKY, H. & GLAGOV, S. 1967. A lamellar unit of aortic medial structure and function in mammals. *Circ Res,* 20**,** 99-111.

WONG, N. D. 2014. Epidemiological studies of CHD and the evolution of preventive cardiology. *Nat Rev Cardiol,* 11**,** 276-89.

WRIGHT, G. J., CHERWINSKI, H., FOSTER-CUEVAS, M., BROOKE, G., PUKLAVEC, M. J., BIGLER, M., SONG, Y., JENMALM, M., GORMAN, D., MCCLANAHAN, T., LIU, M. R., BROWN, M. H., SEDGWICK, J. D., PHILLIPS, J. H. & BARCLAY, A. N. 2003. Characterization of the CD200 receptor family in mice and humans and their interactions with CD200. *J Immunol,* 171**,** 3034-46.

WRIGHT, G. J., PUKLAVEC, M. J., WILLIS, A. C., HOEK, R. M., SEDGWICK, J. D., BROWN, M. H. & BARCLAY, A. N. 2000. Lymphoid/neuronal cell surface OX2 glycoprotein recognizes a novel receptor on macrophages implicated in the control of their function. *Immunity,* 13**,** 233-42.

WU, J., CHERWINSKI, H., SPIES, T., PHILLIPS, J. H. & LANIER, L. L. 2000. DAP10 and DAP12 form distinct, but functionally cooperative, receptor complexes in natural killer cells. *J Exp Med,* 192**,** 1059-68.

XU, D., CHAN, W. L., LEUNG, B. P., HUANG, F., WHEELER, R., PIEDRAFITA, D., ROBINSON, J. H. & LIEW, F. Y. 1998. Selective expression of a stable cell surface molecule on type 2 but not type 1 helper T cells. *J Exp Med,* 187**,** 787-94.

XU, Q. 2004. Mouse models of arteriosclerosis: from arterial injuries to vascular grafts. *Am J Pathol,* 165**,** 1-10.

XU, Q. B., OBERHUBER, G., GRUSCHWITZ, M. & WICK, G. 1990. Immunology of atherosclerosis: cellular composition and major histocompatibility complex class II antigen expression in aortic intima, fatty streaks, and atherosclerotic plaques in young and aged human specimens. *Clin Immunol Immunopathol,* 56**,** 344-59.

YASUDA, T., SHIRAKATA, M., IWAMA, A., ISHII, A., EBIHARA, Y., OSAWA, M., HONDA, K., SHINOHARA, H., SUDO, K., TSUJI, K., NAKAUCHI, H., IWAKURA, Y., HIRAI, H., ODA, H., YAMAMOTO, T. & YAMANASHI, Y. 2004. Role of Dok-1 and Dok-2 in myeloid homeostasis and suppression of leukemia. *J Exp Med,* 200**,** 1681-7.

YIN, Y., ZHAO, L., ZHANG, F. & ZHANG, X. 2016. Impact of CD200-Fc on dendritic cells in lupus-prone NZB/WF1 mice. *Sci Rep,* 6**,** 31874.

YIN, Y., ZHAO, X., FANG, Y. & HUANG, L. 2010. Carotid artery wire injury mouse model with a nonmicrosurgical procedure. *Vascular,* 18**,** 221-6.

YLA-HERTTUALA, S., LIPTON, B. A., ROSENFELD, M. E., SARKIOJA, T., YOSHIMURA, T., LEONARD, E. J., WITZTUM, J. L. & STEINBERG, D. 1991. Expression of monocyte chemoattractant protein 1 in macrophage-rich areas of human and rabbit atherosclerotic lesions. *Proc Natl Acad Sci U S A,* 88**,** 5252-6.

YVAN-CHARVET, L., PAGLER, T., GAUTIER, E. L., AVAGYAN, S., SIRY, R. L., HAN, S., WELCH, C. L., WANG, N., RANDOLPH, G. J., SNOECK, H. W. & TALL, A. R. 2010. ATP-binding cassette transporters and HDL suppress hematopoietic stem cell proliferation. *Science,* 328**,** 1689-93.

YVAN-CHARVET, L., RANALLETTA, M., WANG, N., HAN, S., TERASAKA, N., LI, R., WELCH, C. & TALL, A. R. 2007. Combined deficiency of ABCA1 and ABCG1 promotes foam cell accumulation and accelerates atherosclerosis in mice. *J Clin Invest,* 117**,** 3900-8.

YVAN-CHARVET, L., WELCH, C., PAGLER, T. A., RANALLETTA, M., LAMKANFI, M., HAN, S., ISHIBASHI, M., LI, R., WANG, N. & TALL, A. R. 2008. Increased inflammatory gene expression in ABC transporter-deficient macrophages: free cholesterol accumulation, increased signaling via toll-like receptors, and neutrophil infiltration of atherosclerotic lesions. *Circulation,* 118**,** 1837-47.

ZARINS, C. K., GIDDENS, D. P., BHARADVAJ, B. K., SOTTIURAI, V. S., MABON, R. F. & GLAGOV, S. 1983. Carotid bifurcation atherosclerosis. Quantitative correlation of plaque localization with flow velocity profiles and wall shear stress. *Circ Res,* 53**,** 502-14.

ZHANG, S., CHERWINSKI, H., SEDGWICK, J. D. & PHILLIPS, J. H. 2004. Molecular mechanisms of CD200 inhibition of mast cell activation. *J Immunol,* 173**,** 6786-93.

ZHOU, X., PAULSSON, G., STEMME, S. & HANSSON, G. K. 1998. Hypercholesterolemia is associated with a T helper (Th) 1/Th2 switch of the autoimmune response in atherosclerotic apo E-knockout mice. *J Clin Invest,* 101**,** 1717-25.

ZOCCHI, M. R., PELLEGATTA, F., PIERRI, I., GOBBI, M. & POGGI, A. 2001. Leukocyte-associated Ig-like receptor-1 prevents granulocyte-monocyte colony stimulating factor-dependent proliferation and Akt1/PKB alpha activation in primary acute myeloid leukemia cells. *Eur J Immunol,* 31**,** 3667-75.

Appendices

Abstracts presented at scientific conferences

Keystone symposia_ Myeloid(D3)
Oral and Poster Presentation
Christina Kassiteridi, Jennifer Cole, Michael Goddard, Patricia Green, Inhye Park, Claudia Monaco: *Myeloid cell regulation by CD200 signalling in atherosclerosis*

Frontiers in CardioVascular Biology 2016
Oral and Poster Presentation
Christina Kassiteridi, Jennifer Cole, Michael Goddard, Patricia Green, Inhye Park, Claudia Monaco: *Myeloid cell regulation by CD200 signalling in atherosclerosis*

American Society of Immunology 2016
Poster Presentation
Christina Kassiteridi, Jennifer Cole, Michael Goddard, Patricia Green, Inhye Park, Claudia Monaco: *Myeloid cell regulation by CD200 signalling in atherosclerosis*

Oxford Immunology Group 2016
Poster Presentation
Christina Kassiteridi, Jennifer Cole, Michael Goddard, Patricia Green, Inhye Park, Claudia Monaco: *Myeloid cell regulation by CD200 signalling in atherosclerosis*

British Atherosclerosis Society 2016
Poster Presentation
Christina Kassiteridi, Jennifer Cole, Michael Goddard, Patricia Green, Inhye Park, Claudia Monaco: *Myeloid cell regulation by CD200 signalling in atherosclerosis*

Papers and reviews

Kassiteridi C, Monaco C. Macrophages and dendritic cells: the usual suspects in atherogenesis. Current drug targets. 2015;16(4):373-82. PubMed PMID: 25808566.

Cole JE, **Kassiteridi** C, Monaco C. Toll-like receptors in atherosclerosis: a 'Pandora's box' of advances and controversies. Trends in pharmacological sciences. 2013;34(11):629-36. doi: 10.1016/j.tips.2013.09.008. PubMed PMID: 24139612.

Falck-Hansen M, **Kassiteridi** C, Monaco C. Toll-like receptors in atherosclerosis. International journal of molecular sciences. 2013;14(7):14008-23. doi: 10.3390/ijms140714008. PubMed PMID: 23880853; PubMed Central PMCID: PMC3742229